Chapter 1 Introduction

1.1 Preamble

Characterising myocardial function in preterm infants, particularly those less than 29 weeks gestation has gained considerable interest. Hemodynamic compromise in the early neonatal period, although common, is poorly defined and may contribute to adverse neurodevelopmental outcome later in life (Hunt et al., 2004). A thorough understanding of the physiology of the cardiovascular system in preterm infants is essential for their management during this early critical phase.

Currently used measures of cardiovascular wellbeing include the use of clinical signs (such as capillary refill, blood pressure, heart rate and urine output) with or without conventional echocardiography. However, clinical indicators of systemic perfusion have poor reliability, and conventional echocardiography (such as shortening fraction (SF) and ejection fraction (EF)) maybe relatively insensitive in assessing myocardial function, especially in the preterm infant (Lee et al., 1992, Amoozgar et al., 2011).

Moreover, data on the assessment of right ventricular (RV) function in preterm infants are still limited. RV function plays an important role in predicting morbidity and mortality in preterm and term infants with cardio-pulmonary pathology (Egan et al., 2012, Villafane et al., 2013, Motoji et al., 2013). Alterations in RV function following preterm birth, and its influence on outcomes warrant further study with objective methods of assessments

Recent advances in echocardiography have led to the development of techniques that directly measure global and regional myocardial function, rather than depend on changes in cavity dimensions. Tissue Doppler Imaging (TDI) and myocardial deformation measurements (myocardial strain rate and strain) may provide more detailed information on both systolic and

diastolic myocardial function. Tissue Doppler velocity indices and myocardial deformation imaging based on tissue Doppler derived strain and strain rate (SR) are emergent techniques. These techniques may detect early myocardial compromise before it becomes evident using conventional echocardiographic means. Quantitative assessment of RV function can be obtained using TDI, strain and strain rate, in addition to RV specific markers of performance including tricuspid annular plane systolic excursion (TAPSE) and fractional area change (FAC). These modalities may possess better sensitivity for detecting changes in myocardial performance during the early preterm neonatal period, and provide more insight into the adaptations that occur during the transitional period. In addition, those parameters may identify differences in myocardial function between infants with and without various disease states including patent ductus arteriosus (PDA) and chronic lung disease (CLD).

We aimed to assess the feasibility and reproducibility of measuring myocardial performance in preterm infants less than 29 weeks gestation using the newer echocardiography techniques mentioned above, the longitudinal changes that occur for these measurements over the first week of life and at 36 weeks post menstrual age, the influence of early antenatal and neonatal factors, and the effect of patent ductus arteriosus (PDA) and chronic lung disease (CLD) on those function parameters.

1.2 Cardiovascular physiology of preterm infants

The physiology and haemodynamics of the preterm myocardium, and its post-natal adaptation is unique and shows different characteristics to both the term infants and older children. The myocardial contractile unit of the preterm infant possesses different properties to that of a more mature term infant. Contractility of myocytes in the adult myocardium is largely determined by the release of intracellular calcium ions which are regulated by surface L-type calcium channels. Following depolarisation, a small amount of extracellular calcium enters the myocyte leading to intracellular calcium release from intrinsic stores in the sarcoplasmic reticulum allowing myofibril shortening and muscle contraction. The sarcoplasmic reticulum system lies in close proximity to L-type calcium channels and thus responds to calcium influx with ease. In addition, the T-tubule system which is a network of invaginations of the myocyte wall into the cell allows the extracellular calcium to reach these internal cellular structures(Beard et al., 2004).

In contrast in the preterm heart the myocytes are immature, with a higher surface area to volume ratio to compensate for the lack of the T-tubule system necessary for effective calcium entry into the cell. The myocardium of the preterm infant is stiffer than that of term infants and adults. This is a result of the presence of stiff collagen fibres in the early preterm period and this stiffness will have an impact on diastolic function. There is a lack of Endoplasmic Reticulum (ER) stores within the preterm myocytes and thus they rely on L-type calcium channels as a source of contraction with influx of extracellular calcium to a much greater extent(Noori and Seri, 2005).

Figure 1.1: Diagram of a myocyte in the term and preterm infants.

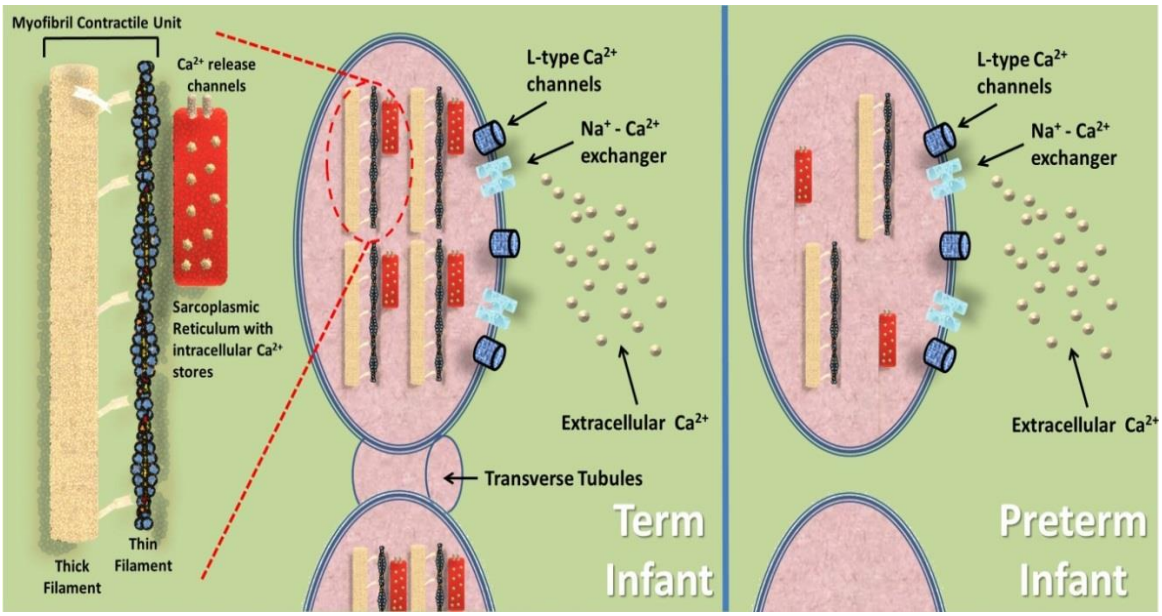

In normal term myocytes, extra cellular calcium (white circles) enters the cell via L-type calcium channels. This in turn activates the release of large amounts intracellular calcium stored in the sarcoplasmic reticulum (SR) into the cytosol. This results in contraction of the myofilament. This whole process is facilitated by the proximity of the SR to the L-type Ca channels and by the presence of transverse tubules, which are invaginations of the myocyte cell wall into the cytosol. Relaxation is a result of active reuptake of cytosolic calcium into the SR. The small amount of calcium that entered the cell via L-type calcium channels is transported back to the extracellular compartment via Na^{+}-Ca^{2+} exchanger. In preterm infants, the SR is physically separated from L-type Ca channels, the transverse tubules are absent, and the myocyte has a greater surface area to volume ratio. Consequently, contraction is more dependent on extracellular calcium influx into the cells.

These developmental differences reduce the functional reserve of the preterm heart when exposed to postnatal stress of extra-uterine life, including the acute changes in loading conditions. The preterm myocardium is very sensitive to increases in afterload associated with the loss of the low pressure system of the placenta, with evidence demonstrating an inverse relationship between afterload and function (Figure 1.2) (Igarashi et al., 1994). This is compounded further by the possible stresses of hypoxia or mechanical ventilation, which the preterm infant is more commonly exposed to (Noori and Seri, 2005, El-Khuffash et al., 2012, Gebauer et al., 2006).

Figure1.2: Graphic depiction of the relationship between ventricular function and afterload.

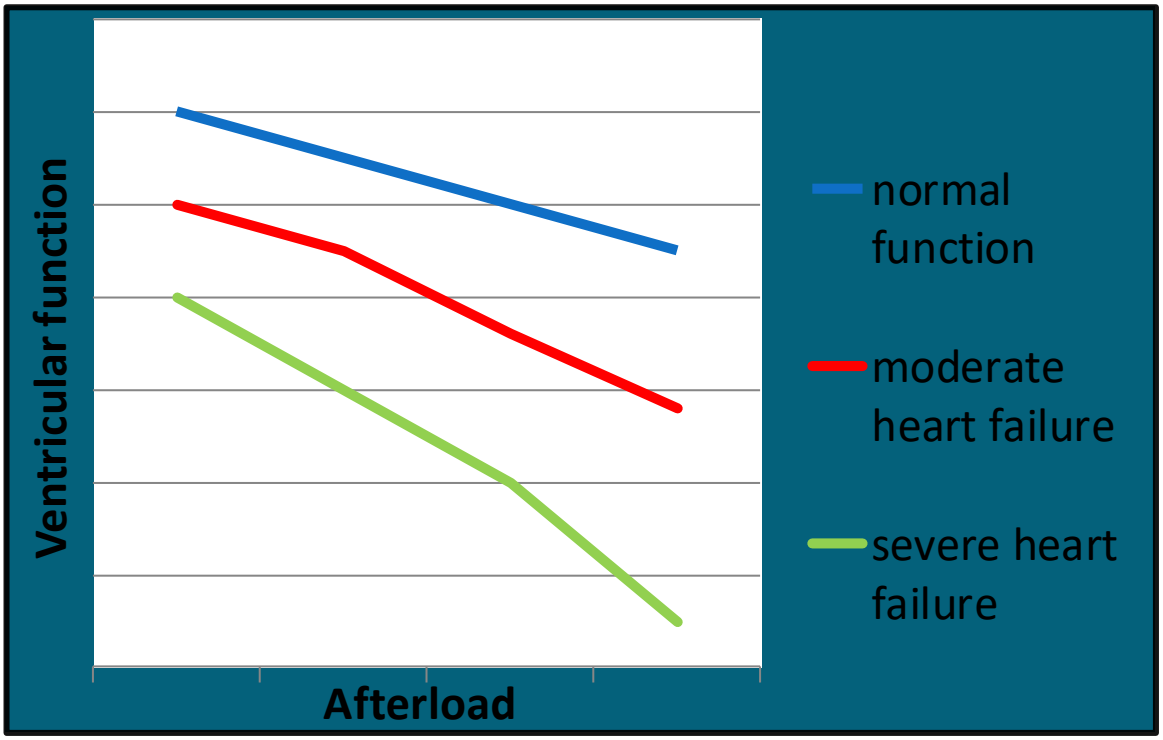

Figure 1.2 shows the varying affects that increased afterload can have on stroke volume and ventricular function. As heart failure worsens (depicted by the red and green lines) increasing afterload results in a dramatic reduction in ventricular function. (Adapted from Maron and Rocco 2011.)

1.3 Transitional Circulation

Foetal cardiac output rises from 50ml/kg/min at 18 weeks gestation to 1200ml/kg/min at term gestation reflecting the increasing need the myocardium has to generate an adequate cardiac output for the developing organs within the growing foetus. Cardiac function is dependent on a variety of factors including preload, afterload, contractility and heart rate.

Preload is characterised by the amount of blood present in the ventricles at the end of diastole and is dependent on hydration status of the infant, pulmonary blood flow (which in turn is partly determined by pulmonary vascular resistance) and diastolic compliance of the ventricles. Afterload is characterised by the resistance against which the ventricle muscle must contract and depends on systemic vascular resistance, blood viscosity and ventricular outflow tract integrity. Myocardial performance or the intrinsic ability of the myocardium to contract and heart rate are the other two important determinants of cardiac function. The foetal heart is usually subjected to a low afterload due to the low pressure placental system and so the foetal myocardium is subjected to very little wall stress. This low pressure system suits the immature myocardium as it is unable to adapt when subjected to additional stresses.

The major source of preload to the left ventricle (LV) during foetal life is derived from the placenta through the umbilical circulation across the foramen ovale (FO). This results in the left ventricular output (LVO) being comprised of oxygenated blood and directed to vital organs such as the brain. The right ventricle receives the majority of blood draining from the superior vena cava, and a proportionately lower amount of oxygenated blood from the umbilical venous system. The majority of right ventricular output (RVO), up to ninety percent, during foetal life is shunted from the pulmonary arteries to the

descending aorta via ductus arteriosus (DA), due to the high pulmonary vascular resistance (PVR) that occurs during foetal life. Pulmonary venous return into the left atrium is low and as mentioned above, LV preload depends primarily on umbilical venous supply through the foramen ovale. The DA serves as a bypass channel to avoid subjecting the right ventricle (RV) to a high afterload due to the high PVR.

Following birth and as a result of the loss of the placenta, the sudden increase in systemic vascular resistance (SVR) immediately after birth poses a major afterload challenge for the preterm infant, which may limit its ability to support cardiac output and result in compromise to organ blood flow. The simultaneous fall in PVR results in the redirection of right ventricular output (RVO) from the lower systemic circulation through the DA to the pulmonary vasculature leading to the increase in pulmonary blood flow. The drop in PVR also results in the DA changing from a right to left direction to a left to right direction leading to some of the left ventricular blood flow being directed to the pulmonary vascular bed.

The above changes that occur during the transitioning period result in pulmonary and systemic circulations that are working in parallel to each other. At this stage the LV preload is solely dependent on pulmonary venous return. Thus adequate pulmonary blood flow is essential to maintain the necessary LVO in the face of increasing LV afterload. This emphasises the importance that changes occurring in the lungs and pulmonary vasculature have for maintaining postnatal life. RV preload now becomes dependent on systemic venous return from the upper and lower body. The fall in PVR occurring soon after birth enables the RV to continue to be exposed to a low afterload.

Figure 1.3: Foetal and Postnatal circulations

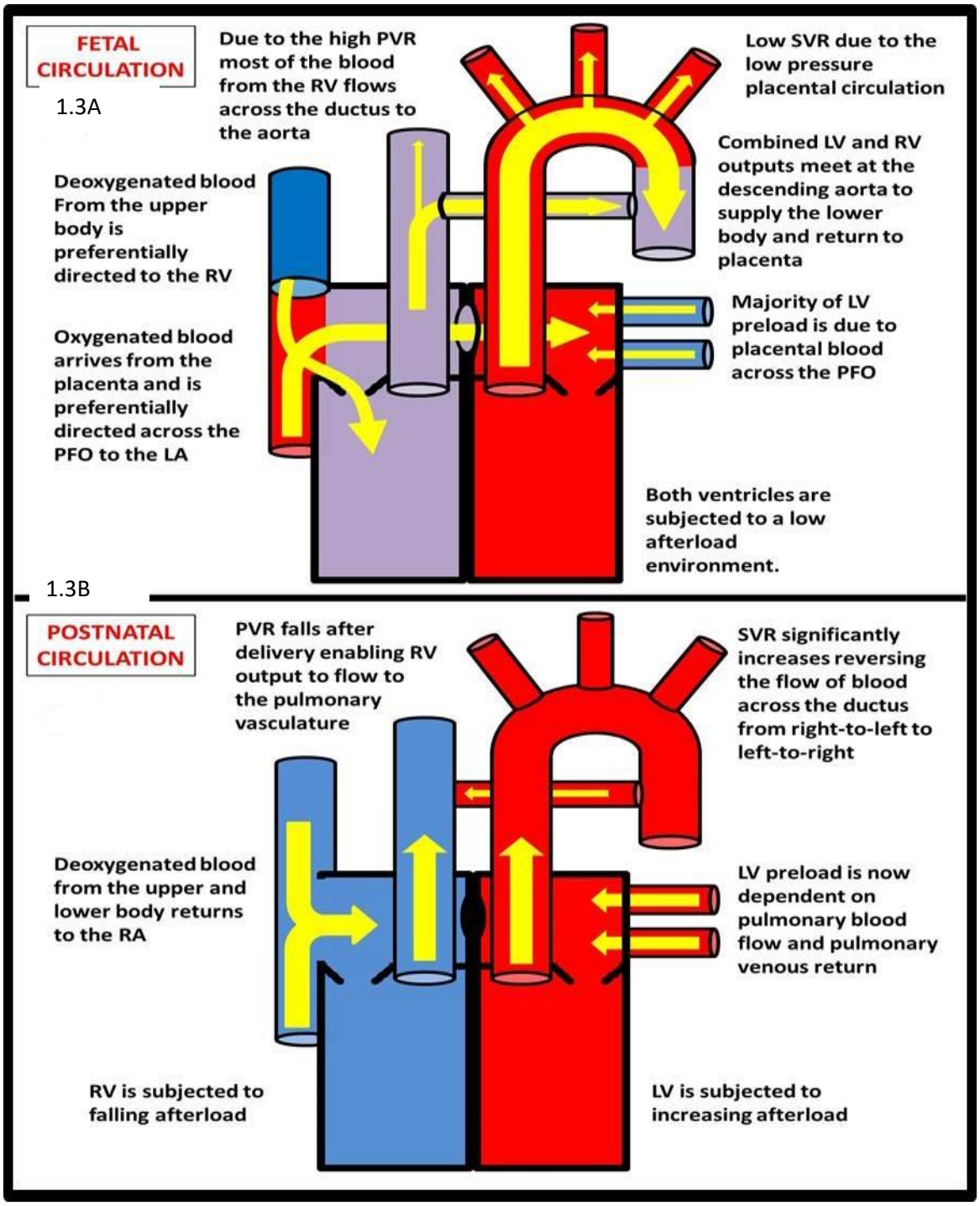

Figure 1.3 is a description of the change that occurs from foetal to postnatal circulation. Figure 1.3A describes the foetal circulation. The circulation incorporates the PFO, PDA as well as the high pulmonary vascular resistance. Figure 1.3B demonstrates the postnatal circulation with the systemic and pulmonary circulation in parallel after the drop in pulmonary vascular resistance.

1.4 Clinical assessment of haemodynamics in preterm infants

Clinical evaluation of the haemodynamic circulation and its impact on the preterm infant is a challenge faced by neonatologists and clinicians relying on relatively inaccurate methods for assessment. In routine clinical practice, neonatologists assess the integrity of the cardiovascular system by examining parameters such as heart rate, blood pressure, urine output, capillary refill and metabolic acidosis all of which have poor reliability in correlating with the perfusion status of the infant (Seri and Evans, 2001, Kluckow and Evans, 2001, Sehgal and McNamara, 2008).

Blood pressure- Hypotension has been associated with intraventricular haemorrhage, periventricular leukomalacia and adverse neurodevelopmental outcome (Hall et al., 2005, Evans et al., 2006). Hypotension is a common problem in preterm infants with up to 40% showing a low blood pressure. However there has been conflicting studies on whether the hypotension is the cause of these poor outcomes or simply reflects the sick nature of these infants with subsequent neurological compromise (Martens et al., 2003, Alderliesten et al., 2014). Clinicians often use arterial blood pressure as a surrogate for systemic blood flow, implying that a normal mean arterial pressure equates to adequate perfusion of vital organs. However this concept does not take into account peripheral vascular resistance (Dempsey and Barrington, 2009). Blood pressure is a product of cardiac output (CO) and SVR (BP = CO X SVR). We use blood pressure as a surrogate for tissue perfusion, however if a physiological state occurs where there is high peripheral vascular resistance then this may result in a normal or high blood pressure reading despite having a low cardiac output reflecting poor blood flow to the tissue. Conversely a low systemic

vascular resistance state can lead to a low blood pressure reading instigating treatment despite the fact that there may be adequate cardiac output and tissue blood flow.

There are no set criteria at present to define what true hypotension is in neonates with many centres using a mean blood pressure less than the gestational age of the baby as a guide to hypotension (Kluckow, 2005). However there are no current trials or outcome measurements to show that this is a robust means of defining hypotension. Furthermore this definition does not take into account the systolic and diastolic components of the arterial blood pressure when looking for appropriate management. Systolic arterial pressure is a useful surrogate of the adequacy of cardiac output whereas diastolic arterial pressure reflects vascular integrity and systemic vascular resistance.

Heart rate and Capillary Refill - Other clinical markers often relied upon by the neonatologist is heart rate and capillary refill time to determine adequacy of perfusion and myocardial performance. Tachycardia or a heart rate of greater than 160 beats per minute can be a physiological response to poor perfusion. However there are several other causes of tachycardia in the neonate, namely pain, sepsis, hyperthermia, hyperthyroidism, catecholamine excess, anaemia, hypoglycaemia, medication (caffeine) and neonatal arrhythmias. These factors confound the use of heart rate as a reliable marker for tissue perfusion. Similarly capillary refill time of greater than 5 seconds correlates weakly with low flow states (Osborn et al., 2002). When used as a clinical marker of perfusion, capillary refill time shows poor reliability in the sick child when being used to assess cardiac output and peripheral perfusion (Lobos et al., 2012, Pickard et al., 2011, Osborn et al., 2004). These commonly used surrogates for systemic blood flow have a very low sensitivity for detecting haemodynamic compromise, whilst also having a high false positive rate.

Urine output, colour, metabolic acidosis- A reduced urine output in the absence of interstitial renal disease or obstructive uropathies can indicate reduced renal perfusion secondary to a low systemic blood flow state. Renal perfusion and glomerular filtration is dependent on renal blood flow thus, below a critical threshold, glomerular filtration and renal output can decrease proportionately. In preterm infants with renal tubular immaturity, urine output can be in the normal range even in the presence of a reduced renal perfusion (Koren et al., 1985).

Lactate and lactic acidosis: At a cellular level when there is a lack of oxygenation, metabolism can change from aerobic to anaerobic. This can be a result of hypoxemia, anaemia, inadequate systemic blood flow or a combination of the above factors. During anaerobic metabolism a rise in lactic acid occurs and as such lactate levels in the blood can be a marker of low cardiac output. Interpreting a high lactate must be interpreted whilst considering other markers of reduced perfusion and other causes of anaerobic metabolism. As an elevated lactate in isolation can be a consequence of increased glycogenolysis and inborn errors of metabolism or other forms of hypoxia other than reduced perfusion. It must also be noted that the lactate level may be reflective of local tissue metabolism and not necessarily reflect global tissue perfusion and metabolism. Similarly, poorly perfused tissue undergoing anaerobic metabolism may not mobilise lactate into the blood stream until perfusion improves with the rise of lactate occurring after restoration of an adequate systemic blood flow (de Boode, 2010)

1.5.1 Current techniques of assessing systolic and diastolic function

Due to the small size of the heart and the sick nature of the patients who are premature, the use of either invasive evaluation or cardiac magnetic resonance imaging (MRI) is impractical and these methods are usually not performed. Cardiac MRI has been studied in infants greater than 34 weeks gestation (Broadhouse et al., 2014) but no data currently exists on those less than 29 weeks gestation. Furthermore many centres involved in the care of extremely preterm infants do not have access to cardiac MRI or are unable to transport these fragile patients to a MRI scanner. Assessment of reponse to treatment is also impractical and is unlikely to come int clinical practice in the near future. Echocardiography is the only method that has been used for repeated non-invasive measurements of the neonatal and preterm heart (Lopez et al., 2010, Mertens et al., 2011b, El-Khuffash et al., 2013a). Despite the increasing use of echocardiography for identifying significant Patent ductus arteriosus (PDA), assessing myocardial function and systemic blood flow, the echocardiographic methods used to date, lack accuracy and validation (Mertens et al., 2011b).

1.5.2 Assessment of Systolic function

Systolic function has traditionally been measured by using echocardiography methods such as ejection fraction (EF), shortening fraction (SF) and velocity of circumferential fibre shortening (VCFc). Shortening fraction has gained in popularity in assessing left myocardial function due to its ease and rapidity (Lee et al., 1992, Rowland and Gutgesell, 1995). Although this parameter only measures a change in LV cavity dimension in one plane, it is used to determine global function in clinical practice and a surrogate for myocardial contractility. It is measured by M-mode assessment of the long axis view or the

short axis of the left ventricle at the tips of the mitral valve leaflets. This measurement becomes inaccurate in the presence of paradoxical septal wall motion which may occur in the first few days of life in preterm infants due to the elevated right sided pressure (Lee et al., 1992). This measurement is also limited by the fact that it is heavily dependent on preload. In addition, the same M-mode method is used to derive EF in one plane only. This has the disadvantage of assuming the LV is cylindrical in shape. In addition, any errors in deriving the LV cavity diameter in diastolic and systole are cubed when deriving EF using this method thereby decreasing its accuracy.

VCFc is a preload independent, afterload adjusted measure of LV function. Although this method is a relatively load-independent measure of myocardial contractility its measurement has not entered into mainstream use due to its cumbersome calculation and the limited data on the applicability of the preterm population (Mertens et al., 2011b).

1.5.3 Assessment of diastolic function

Diastolic function of the heart can be measured indirectly by examining the trans-mitral flow pattern. The usual flow pattern of the mitral valve in diastole is biphasic with and early E wave resulting from early blood flow across the atrioventricular valve in diastole followed by a late A wave resulting from the atrial contraction occurring at late diastole. The maximum velocity of the E and A wave can be measured and compared as a ratio. In the normal setting with good diastolic function the majority of blood flow occurs during the early diastolic phase (E wave) making the E wave higher than the A wave (Figure 1.4). When expressed as a ratio this results in a E:A wave ratio being greater than 1. In poor ventricular relaxation there is a dependence on the atrial contraction to provide ventricular filling. This results in an increased A wave and so an E:A ratio less than 1 indicates diastolic dysfunction. However both E, A wave and E:A wave ratio are indirect measures of diastolic function and

give little information on muscle contraction and relaxation velocities. Furthermore these parameters are dependent on loading conditions and therefore the volume status of the infant and the use of inotropes may play contributing factors.

Figure 1.4: Doppler imaging of the Mitral valve showing the E and A waves

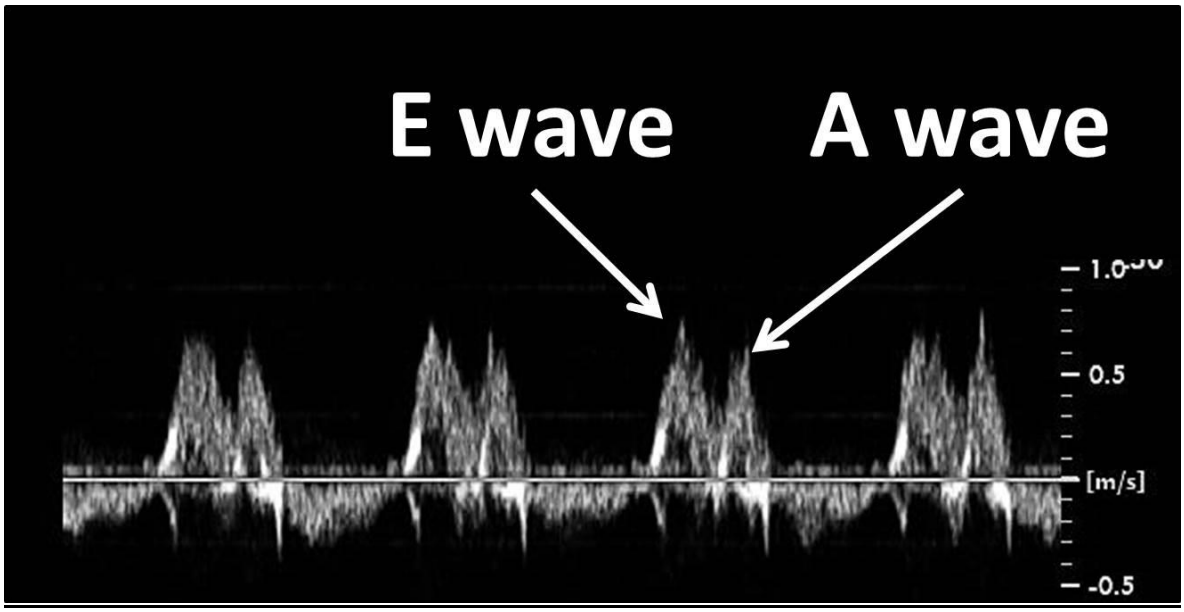

Using Pulsed Wave Doppler we can see the flow through the mitral valve showing the early (E) and late (A) waves

1.6.1 New Methods of Assessment of Myocardial Performance

Newer techniques have recently become available for assessment of cardiac function. These newer techniques have been studied mainly in adults with some research occurring in the paediatric population. The area of term and preterm functional assessment is one which warrants further study. Furthermore despite echocardiography being present for the last 4 decades very little normative data is present on preterm functional parameters despite its growing use in this setting often with small datasets being presented in various disease states without reference to a normative dataset (Groves et al., 2008, Murase and Ishida, 2006). The use of large datasets with normative values is essential for both the clinical and research setting.

Recent advances in echocardiography have led to the development of techniques that measure regional myocardial function. Tissue Doppler imaging (TDI) and myocardial deformation measurements (myocardial strain rate and strain) provide assessment of both systolic and diastolic regional myocardial function. These techniques are relatively less dependent on preload in adults and evaluate myocardial deformation in all relevant dimensions (e.g. longitudinal, radial and circumferential direction). These techniques may prove useful in evaluating myocardial function in the preterm population. Speckle tracking echocardiography (STE) and rotational mechanics are further techniques used to provide information on both regional and global myocardial function. In addition the emergence of RV-specific functional parameters has been increasingly recognised as important when assessing myocardial function and should be incorporated into a comprehensive echocardiogram (Levy et al., 2015, Jain et al., 2014).

1.6.2 Tissue Doppler Velocities

Tissue Doppler velocity Imaging (TDI) is a relatively new ultrasound modality that measures the velocity of movement of muscle tissue in systole and diastole directly from the myocardium. This offers a quantitative assessment of both systolic and diastolic function by assessing the velocity of displacement of the mitral and tricuspid annuli, and base of the septum during the cardiac cycle (Hiarada et al., 2000).

Initially it was thought that tissue Doppler velocity imaging was relatively independent of preload (Frommelt et al., 2002, Nagueh et al., 1997). Nagueth in his study looked at tissue Doppler velocities of the mitral annulus in different loading conditions (normal function, impaired relaxation, and heart failure patients). He found that both impaired relaxation and heart failure patients had lower TDI values compared to normal subjects inferring that it may be a preload-independent marker of LV relaxation. This study uses the mitral E/A ratio as the marker of failure/filing and presuming loading conditions based on these values. More recent studies have shown that TDI is still dependent on loading conditions and is affected by both preload and afterload (El-Khuffash et al., 2012). El-Khuffash and colleagues showed that in preterm infants, the mitral valve systolic and diastolic tissue Doppler velocities decreased significantly after PDA ligation when measured immediately before and immediately after the procedure. A PDA ligation is associated with a sudden fall in preload and, by removing LV exposure to the lower resistance pulmonary circulation, a sharp rise in afterload. The sudden change in those markers in this setting is unlikely to be due to a true change in contractility.

Tissue Doppler velocities can be used to assess regional myocardial function by examining the velocity of various segments of the myocardium (Nikitin et al., 2003). Various studies have looked at TDI and its usage in disease states such as cardiomyopathy

(Mohammed et al., 2009) , chemotherapy-induced dysfunction (Ganame et al., 2007a) and post Kawasaki disease dysfunction (Arnold et al., 2007). Often in these situations, dysfunction is seen by using TDI where it is not detected by conventional markers of cardiac performance such as ejection fraction, shortening fraction and wall stress.

While TDI has been investigated and validated in adults and children and is becoming a routine use for echocardiographic assessment (Pauliks, 2013), in the preterm population, few investigators have reported the clinical use of TDI for early management of circulatory dysfunction.

1.6.3 Strain imaging

The objective quantification of myocardial function remains a challenge despite the advancing use of echocardiography. The use of visual assessment and conventional M-mode imaging has many limiting factors as mentioned above. Tissue Doppler-derived deformation imaging along the long axis of the ventricle is being used more commonly and has shown to be valid and reproducible (Eriksen et al., 2013a, Helfer et al., 2013, Murase et al., 2013). The recent introduction of tissue Doppler derived deformation has allowed regional myocardial deformation assessment by using ultrasound based myocardial strain (S) and strain rate (SR).

Sacromere shortening occurs during systole due to electro-mechanical activation. This results in a reduction in intra-cavity size and ejection of blood from the ventricle. Active relaxation occurs during diastole resulting in the restoration of the ventricular geometry and filling of blood following atrial contraction. The deformation of the ventricular wall occurs in three dimensions which can be expressed in systole as longitudinal shortening, circumferential shortening and radial thickening.

It is important to distinguish between myocardial deformation and myocardial wall motion. Myocardial wall motion is the change in position of a particular region of myocardium over a particular time period and can be measured by velocity and displacement. In this it is assumed that all parts of that region move with the same velocity. In contrast myocardial wall deformation is the change in shape of this particular region which occurs due to different parts of the region moving with different velocities over a certain time point. Myocardial deformation is termed strain and the speed at which this deformation occurs is termed strain rate. Measuring myocardial wall velocity does not differentiate between active and passive movement of the myocardial segment whereas deformation analysis can discriminate between these two factors.

The myocardial strain is a measure of absolute tissue deformation (shortening in long and circumferential planes, thickening in radial plane) by using two reference points along the ventricular wall during the cardiac cycle. Strain is an analogue of regional ejection fraction, and therefore is influenced by preload (which increases wall strain) and afterload (which reduces wall strain). Systolic strain rate measures the time course of deformation (velocity of shortening/time unit).

Strain can be defined by the formula

$$\epsilon = \frac{L - L_0}{L_0} = \frac{\Delta L}{L_0}$$

where ε is strain, L_0= baseline length and L = length at time of measurement.

Systolic strain is represented graphically by a negative deflection for shortening and a positive deflection for lengthening (Figure 1.5). Longitudinal and circumferential shortening are represented as a negative strain while radial thickening is represented as a

positive strain. Once the initial length of the regional myocardium is known at a certain point in the cardiac cycle, the relative length change or strain can be calculated relative to this for the rest of the cardiac cycle in that particular dimension.

Figure 1.5: Tissue Doppler derived Strain of the intraventricular septum showing the peak systolic Strain (S)

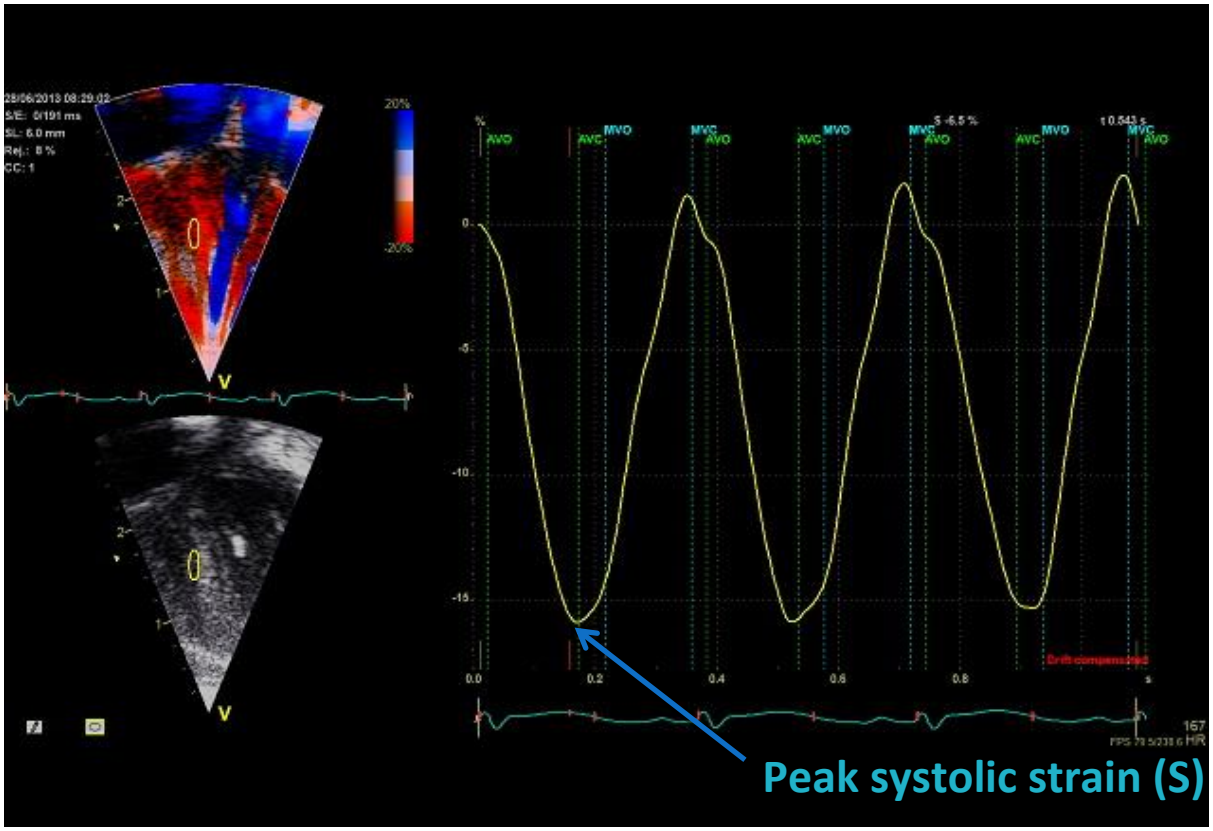

Figure 1.5 gives an indication of the longitudinal strain values observed during the cardiac cycle and by matching these with time points on the electrocardiogram we can see that there is a peak negative strain during systole (peak systolic strain)

Strain rate (SR) is the rate by which the deformation occurs and the unit of strain rate is $s^{-1.}$ SR can be defined by the equation

$$\frac{\Delta \epsilon}{\Delta t}$$

where $\Delta \epsilon$ is the change in strain and Δt is the change in time.

SR has the same direction as strain (that is negative for shortening and positive for elongation). Diastolic strain rate measures the time course of returning to baseline shape. SR correlates with the rate of change of pressure and reflects contractility. Strain rate is thought to be less preload and afterload dependent (Sutherland et al., 2004, Ferferieva et

al., 2012). By measuring both strain and strain rate during different loading conditions, Ferferieva and his colleagues found that strain was influenced by afterload, however strain rate is a more robust measure of contractility and less influenced by loading conditions of the heart. These two parameters complement each other in their evaluation of myocardial performance. SR depicts 3 distinct peaks (Figure 1.6) with a peak negative deflection correlating with peak systolic strain rate and 2 positive deflections correlating with early (E-wave) and late (A-wave) diastasis. When assessing regional myocardial function both strain and SR need to be calculated together as they give complementary information for that region.

Figure 1.6: Tissue Doppler derived strain rate of the septal wall

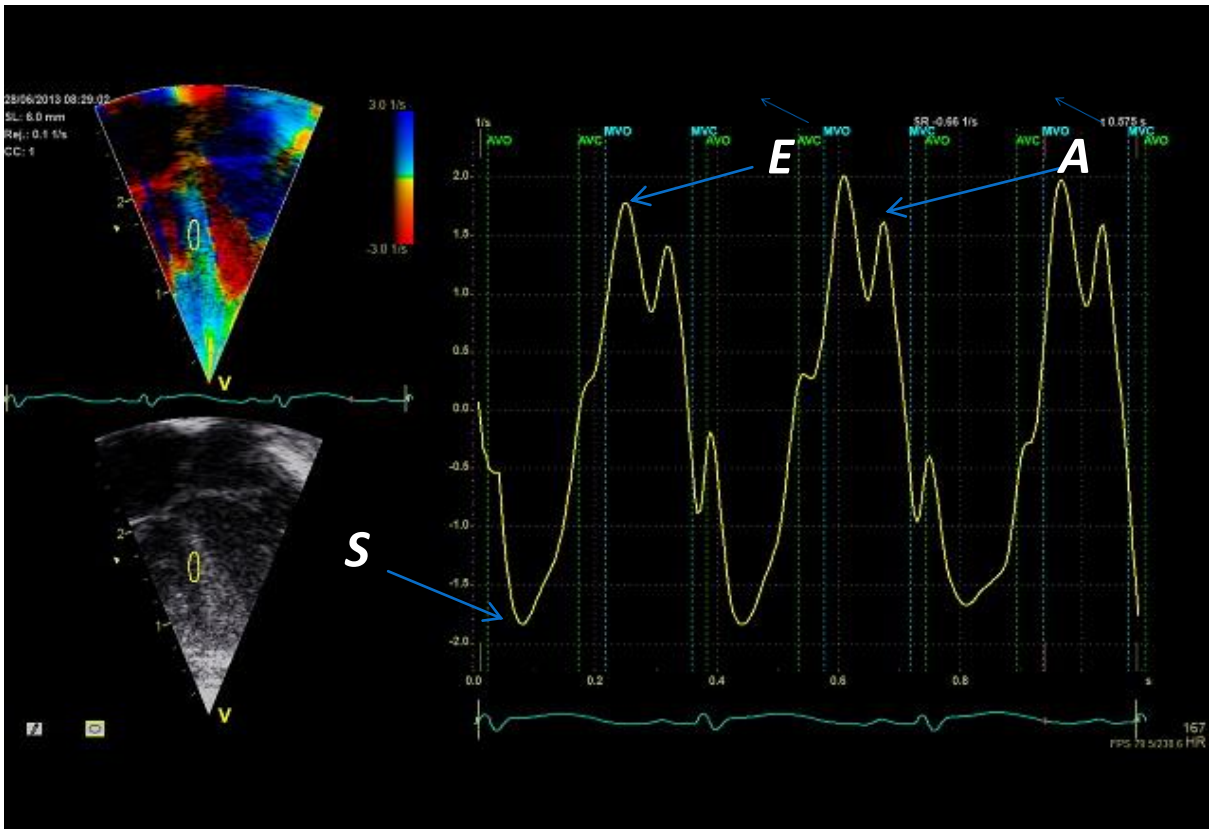

Figure 1.6 depicts the Tissue Doppler derived strain rate of the septal wall during 3 cardiac cycles. The figure shows the peak systolic (S) early diastolic (e) and late diastolic (a) markers.

Contractility is best reflected by measuring the stress/strain relationship, however at present there is no mechanism to measure the stress of the myocardium. Despite this by measuring strain and SR a valuable marker of myocardial function can be achieved.

Strain and SR may be used to assess global and/or regional function in both left and right ventricles (Weidemann et al., 2002). Conventional wall motion measurements cannot differentiate between active and passive movement of a myocardial segment, whereas deformation analysis (strain and strain rate) can discriminate between these.

Deformation imaging has been used previously in cardiac MRI before the current capabilities of echocardiography were present. This involved tissue tagging and three-dimensional magnetic resonance imaging. This method was deemed the gold standard for evaluating strain and strain rate. Although giving accurate values it remained a cumbersome and expensive tool to use and is routinely not available.

Over the last decade, strain and strain rate measured using echocardiography has been validated against MRI techniques (Edvardsen et al., 2002, Amundsen et al., 2006, Tee et al., 2013, Herbots et al., 2004) using both tissue Doppler and speckle tracking methods. This has been achieved using both normal myocardial segments and infarcted areas with excellent agreement in both groups. These results have paved the way for deformation imaging to be used as a valuable tool for echocardiographic assessment of myocardial function. This data has been validated in both adult and paediatricpediatric populations but very little data is available in the preterm population with no data available comparing tissue Doppler and cardiac MRI.

1.6.4 Tissue Doppler Derived deformation imaging

There are two different methods of measuring deformation within the heart: The Tissue Doppler-derived technique or the Speckle tracking echocardiography technique. These modalities and measurements are novel at present and have only been used mainly in the setting of research. One of the factors which is delaying their use in the clinical setting is the fact that the post-processing software is often vendor specific thus contributing to a lack of reproducibility between different groups. Furthermore as using these techniques can allow one to measure regional myocardial function this increases the variability in values based on where the region of interest is located. Finally because tissue Doppler and speckle tracking both have separate advantages and disadvantages there may arise circumstances where one form of deformation imaging would be better than the other.

Acquisition and limitations of tissue Doppler derived strain.

The validity of measurements of tissue derived strain and strain rate has been assessed in-vitro and in vivo models. In the in vitro model gelatine blocks were used to mimic tissue and velocities were measured using commercially available ultrasound systems (Korinek et al., 2005). They found a high degree of accuracy in velocity measurements.

Despite is possible use, tissue Doppler derived strain and strain rate does have some limitations which are important to note. One of the main limitations is that when using tissue Doppler, the measurements are angle dependent. The angle between the myocardium and the ultrasound beam is important when deriving these values. For example, when measuring longitudinal strain in the 4 chamber view if the beam is parallel to myocardial wall, we assume that the transverse strain which is perpendicular to the ultrasound beam is 0 and so does not contribute to the longitudinal strain value. However if

the angle changes then the transverse velocities contribute to the measured velocities giving an inaccurate representation of the longitudinal strain. For acceptable calculations, an angle of insonation less than 20 degrees is deemed acceptable (van Dalen et al., 2009). Another issue to recognise is movement artefact which can occur with all tissue Doppler imaging. It is important to limit movement artefact when acquiring images. It is also important to be aware that assessing tissue movement in relation to the transducer rather than relative to adjacent segments is a fundamental limitation of tissue velocity imaging which will also affect tissue Doppler derived strain and strain rate. Accurate image acquisition with image optimisation and tracking through three cardiac cycles can help to confine these limitations and in the hands of experienced and trained operators this method can be a valuable non-invasive tool for clinical evaluation of myocardial contractile function.

1.6.5 Speckle tracking imaging

Non- Doppler 2D-strain imaging can be derived from speckle tracking echocardiography (STE). It works by following the speckle pattern present on the muscle wall frame by frame. Speckles are the acoustic backscatter generated by the reflected ultrasound beam. These acoustic markers are equally distributed throughout the myocardium but the speckle pattern is unique to each region. Displacement of the speckle pattern represents local tissue movement and the change between speckles represents myocardial deformation. This is performed by vendor specific software and gives values of strain, strain rate and velocity of a defined myocardial segment. STE is based on B-mode grey scale tracking of 2D speckles within the myocardium. The original length is referenced by using the point at end-diastole and from this, the speckles can be tracked as they move

through the cardiac cycle and the degree of deformation can be determined (Figure 1.7) (Teske et al., 2007).

The advantage of using this technique is that it is angle independent as it follows the movement of the speckles in any direction. Speckle tracking measures the deformation in two dimensions which means that in the apical view it can calculate not only the longitudinal strain but also the transverse strain. Similarly in the short axis view both the circumferential and radial strain can be calculated from the same image.

Speckle tracking derived strain and strain rate also has limitations. Optimal speckle tracking can only be produced at a certain frame rate 50 to 70 frames per second (FPS). This is much lower than that seen in TDI which is (>180FPS). This could result in the under sampling especially in patients with a fast heart rate. This becomes an even more relevant problem when considering premature infants who all have heart rates between 120 to 180 beats per minute as a baseline. If the frame rate is increased to reduce the under sampling issue, this will result in a reduction in the spatial resolution and less sampling of the optimal region of interest. When the frame rate is reduced this will increase the spatial resolution. However as the speckle tracking software tracks the speckle frame by frame, the low frame rate can lead to the speckle being outside the software's search area and result in poor tracking and temporal resolution. This compromise between spatial and temporal resolution is one of the difficulties with using speckle tracking.

This issue of what ideal frame rate should be used has been looked at previously by Sanchez et al when they looked at the reliability and reproducibility of various frame rates on strain and strain rate in premature infants(Sanchez et al., 2014). By looking at the inter and intraobserver variability of various frame rates, they found that reproducibility is most robust when cine loops are obtained with frame rate to heart rate ratio's of 0.7 to 0.9

frames/sec per bpm. This frame rate likely results in optimal myocardial speckle tracking and gets the balance between spatial and temporal resolution.

Figure 1.7: Speckle Tracking derived Strain of the Left Ventricle

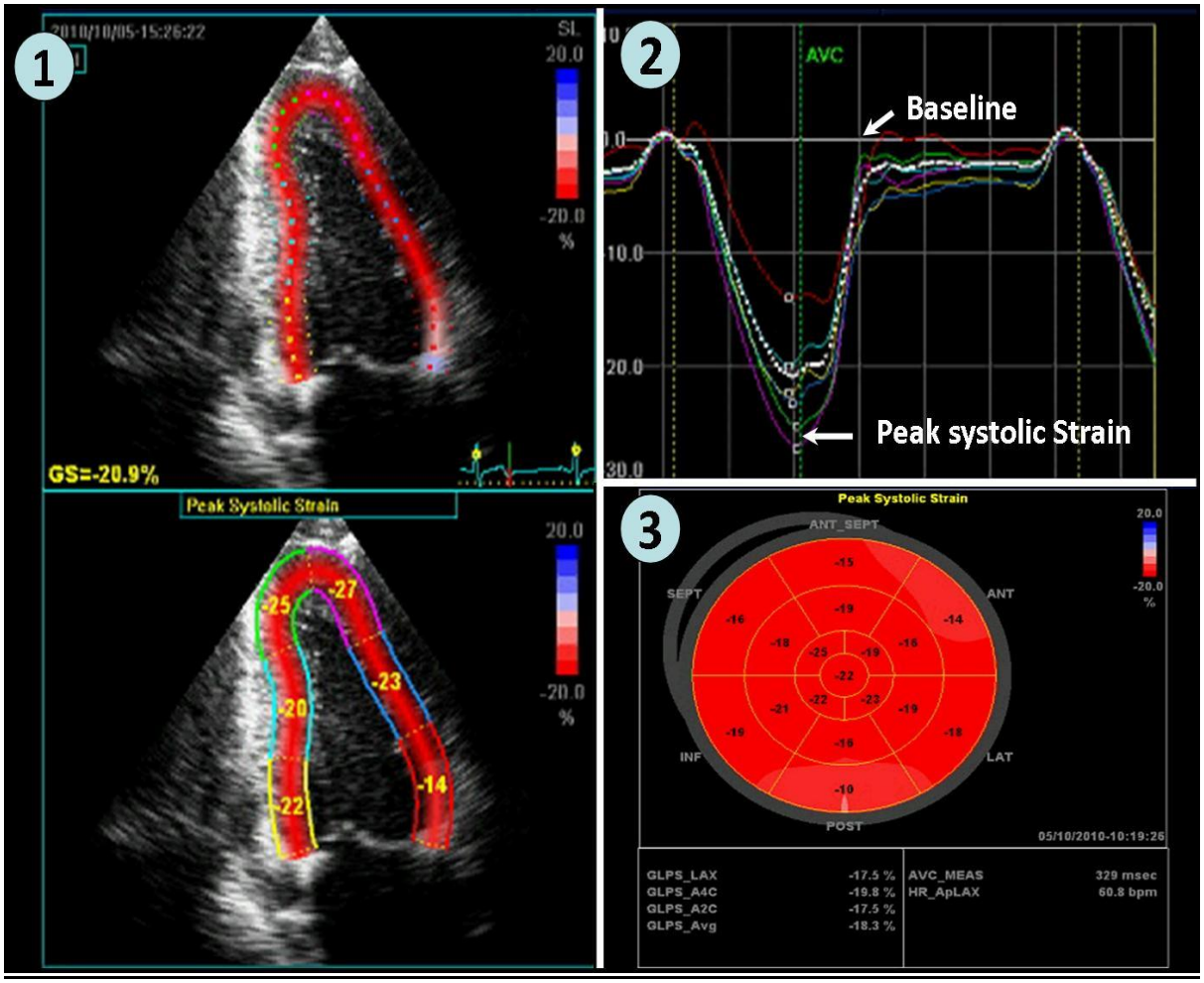

Figure 1.7 shows the image acquisition and post processing software for speckle tracking derived deformation imaging. Figure 1.7 (1) shows the 4 chamber view with the myocardial wall defined to derive an average strain value for each segment. Figure 1.7 (2) shows a graphic representation of the strain values over a cardiac cycle with each segment being depicted by a different colour and global strain being depicted by the white dotted line. From this the peak systolic strain can be calculated. Figure 1.7 (3) shows the bullet view of strain values derived by combining the 2, 4 and 3 chamber views of the left ventricle to represent regional strain values.

1.7 Twist/torsion

Left ventricular (LV) twist describes the wringing motion of the LV during systole, and is the net result of the rotation of the apex and the base in opposite directions along the long axis (Figures 1.8, 1.9, 1.10). LV torsion describes normalised twist to LV length at the end of diastole. Effective ventricular torsion and twist is an essential component of normal ventricular function at rest and during exercise.

This wringing motion improves the ejection of blood from the LV cavity during systole. LV untwist describes the recoiling of the twisted LV during early diastole thereby generating a suction force for LV filling. LV twist is facilitated by the helical arrangement of the subepicardial (left handed) and subendocardial (right handed) fibres (Buckberg et al., 2011) within the myocardium. The magnitude of LV twist and untwist is determined by the contractile force of the myocardium in addition to muscle fibre compliance and elastic recoil properties. As a result, those parameters may be used as surrogates for global LV function (Burns et al., 2008, Buckberg et al., 2011, Russel et al., 2009, Huang and Orde, 2013).

Left ventricular twist can be assessed by speckle tracking echocardiography (STE) which measures apical and basal rotation from the parasternal short axis views and demonstrates acceptable agreements with twist measured by Magnetic Resonance Imaging (MRI) (Notomi et al., 2006b). Recent studies have established twist values in the healthy paediatric population (Takahashi et al., 2010, Al-Naami, 2010, Kaku et al., 2014).

Figure 1.8: Apical rotation of the Left Ventricle (LV) using Speckle tracking echocardiography

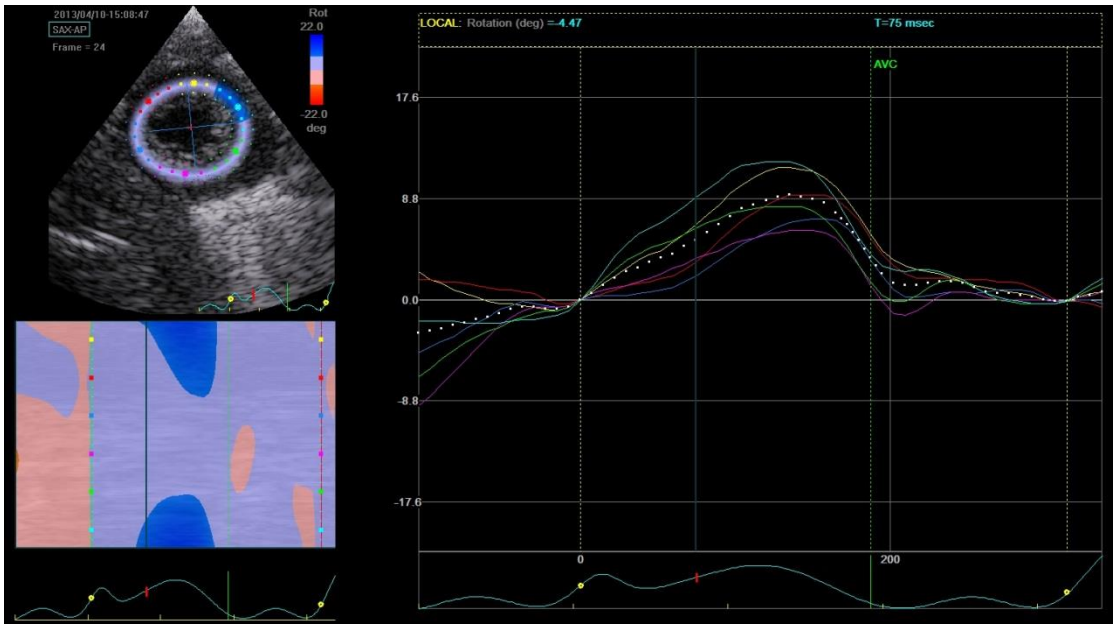

Speckle tracking of the Left ventricle in the short axis plane at the level of the apex showing the positive counter-clockwise rotation of the left ventricle around the ventricular axis.

Figure 1.9: Basal rotation of the Left Ventricle (LV) using Speckle tracking echocardiography

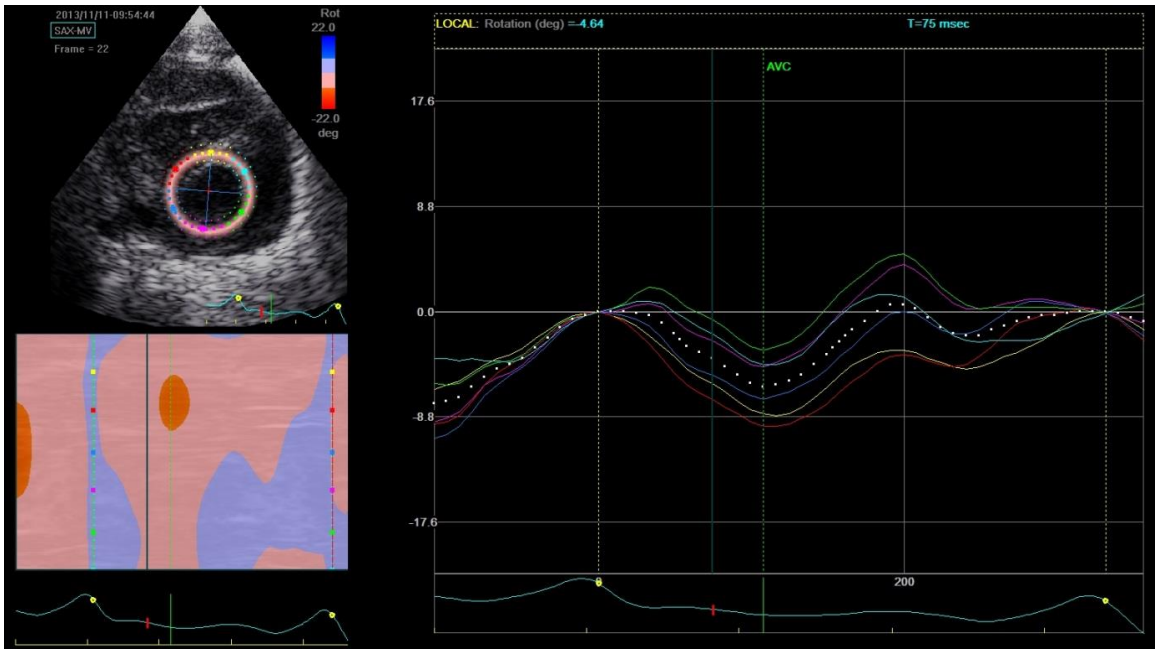

Speckle tracking of the left ventricle in the short axis plane at the level of the mitral valve showing the negative clockwise rotation of the ventricle around the ventricular axis

Figure 1.10: Graphical representation of the net twist of the Left Ventricle (LV)

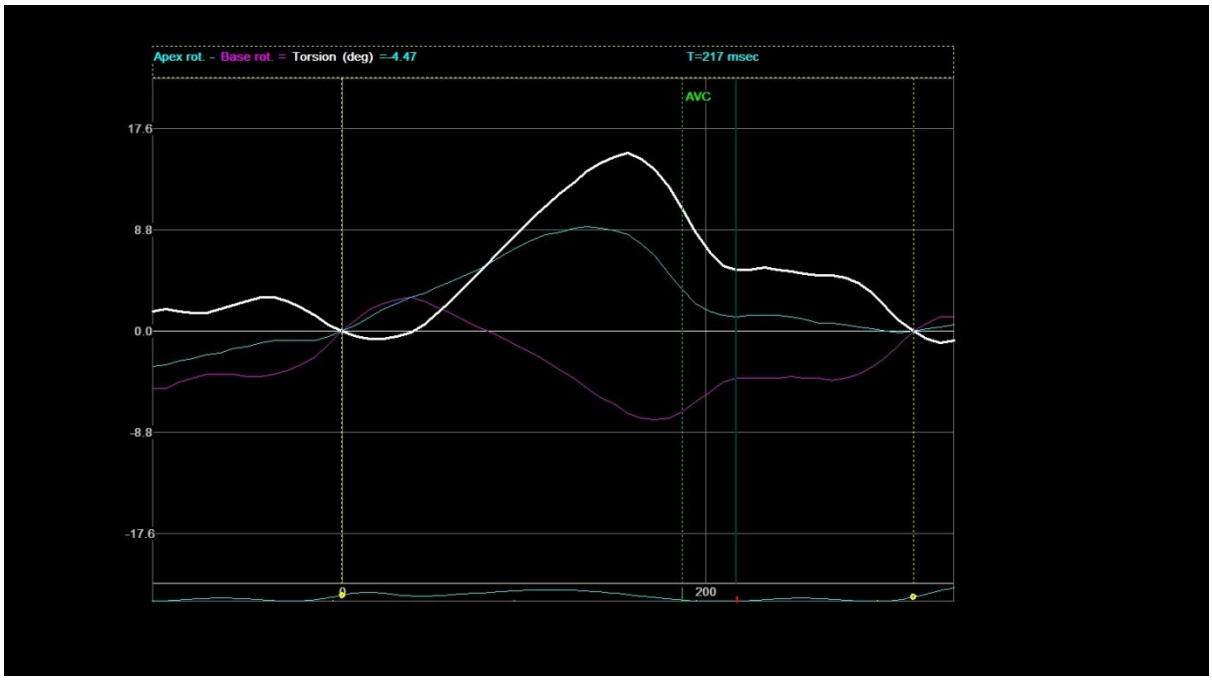

Twist of the left ventricle (LV). The blue line representing the positive apical rotation, the magenta line representing the negative basal rotation and the white line representing the resultant twist of the left ventricle.

Al-Naami and colleagues findings suggest that when LV twist is normalised to LV length, the heart maintains a constant LV rotation profile (Al-Naami, 2010). However they found that the infant heart is somewhat different in that it deforms, twists and untwists at a faster rate than the other groups. When looking at disease states such as congenital heart disease and childhood malignancies (Laser et al., 2013, Cheung et al., 2011b) it was found that using LV twist and torsion may be a valuable tool in assessing early myocardial disease even in those children who have preserved LV ejection fraction. Laser and his group found that using twist and torsion in children with coarctation or aortic stenosis showed a higher initial value to matched controls due to the increase in loading conditions. After successful intervention in these lesions there was a significant reduction in the torsion values showing that twist/torsion may be a valuable tool for assessing changes in loading conditions. Cheung and his colleagues used twist and untwist to assess LV function in childhood cancer patients who were undergoing anthracycline treatment. They found that compared with controls there was a significant reduction in torsion, twist and untwist velocities in those patients who received anthracycline. They found this remained the case even in those patients with preserved ejection fraction suggesting that this may be a more sensitive marker for LV function.

LV twist in the preterm population has not been investigated to date. The use of STE to assess various functional parameters such as strain and strain rate in preterm infants is gaining considerable interest, with recent studies demonstrating acceptable reliability of those techniques (Levy et al., 2013, Helfer et al., 2013, El-Khuffash et al., 2012). Assessment of LV twist using STE in extremely low birth weight infants during the early post-natal period

may provide novel insights into myocardial performance (Noori and Seri, 2005) and enable study of this novel functional marker in disease states associated with prematurity.

1.8.1 Right Ventricular dysfunction and its role in prematurity

Ventricular function plays an important role in the morbidity and mortality of preterm infants(Seri and Evans, 2001). Very little data is available on how right ventricle (RV) function is measured and its impact on the circulation and haemodynamics. It is known that RV dysfunction plays an important role in outcomes of many adult and paediatric diseases being a strong predictive factor for morbidity and playing a role in both a cause and effect of different cardiac and non-cardiac pathologies (Voelkel et al., 2006). In the new-born period the relatively high pulmonary pressures that occur during transition due to the initial high pulmonary vascular resistance may impact on the initial RV function and play a vital role in determining the haemodynamic stability of the infant. The major circulatory changes that occur include decrease in the pulmonary vascular resistance, increase in pulmonary blood flow and closure of foetal shunts such as the PFO and PDA. Complete transition occurs over a number of weeks after birth but the main change is in the first few days of life. In the preterm infant this can be further affected by the haemodynamic effects of a patent ductus arteriosus, the immature contractility of the preterm heart and co-morbid conditions such as respiratory distress syndrome which can impact the circulation.

Newer methods of quantitative measurements of RV function have gained interest in recent times such as Tricuspid Annular Plane Systolic Excursion (TAPSE), Fractional area change (FAC) and RV strain and strain rates.

1.8.2 RV specific functional parameters

As discussed previously, RV function can play an important role during the transitional period of the preterm circulation. Due to the complex geometry of the RV there are very few objective echocardiographic parameters to assess RV function. At present RV function is assessed qualitatively and objective functional measurements are needed. Although some newer RV functional measurements have been used in the adult population (Motoji et al., 2013) there is a lack of normative data available in the preterm population making this an area of research at present.

Jain et al recently published data looking at these parameters in the term population (Jain et al., 2014). The group examined fifty healthy term infants during the first 2 days of life and studied RV dimensions and functional indices as recommended by the American Society of Echocardiography for older populations (Lopez et al., 2010). Additionally they applied novel echocardiographic parameters such as fractional area change (FAC) using both the 4-chamber (4-C) and 3-chamber (3-C) views, RV longitudinal strain from the RV lateral and inferior walls and Tricuspid Annular Plane Systolic Excursion (TAPSE). Having applied these measurements they found that both the conventional and novel RV measurements were both feasible and reproducible for the term neonates and have published normative data based on these results (Jain et al., 2014).

1.8.3 Fractional Area Change (FAC) and Tricuspid annular plane systolic excursion (TAPSE)

RV Fractional areal change (FAC) measures the change in area of the RV in the 4C and 3C view between end diastole and end-systole. The endocardial border is traced in a RV focussed 4C and 3C view, the RV 4C-FAC and the RV 3C-FAC can be calculated (Figure 1.11). From this global RV FAC can be derived (Jain et al., 2014).

TAPSE has been recognised as a good marker of global RV function. Its role as an echocardiographic tool to analyse systolic RV function has been established in adults (Lang et al., 2005, Gupta et al., 2008). Poor RV systolic function is associated with a reduction in the TAPSE value achieved. TAPSE is obtained by either m-mode imaging or tissue Doppler imaging of the tricuspid annulus and evaluating the slope that is seen from diastole to systole as shown in figure 1.12. Koestenberger and his group looked at how TAPSE could be applied to term and preterm infants (Koestenberger et al., 2011). They evaluated 258 patients ranging from 25 to 41 weeks gestation and calculated Z score values within 48 hours of birth. Based on this they found that TAPSE values ranged from 0.44cm in preterm infants to 1.03cm in term infants. This echocardiographic quantification was simple to use and was found to be reliable and reproducible in the neonatal population in a similar way to its use in the adult and paediatric population. This paves the way for TAPSE to be used as part of an echocardiographic assessment for RV functional assessment.

Figure 1.11: RV focussed 4 chamber view showing measurement of right ventricular fractional area change.

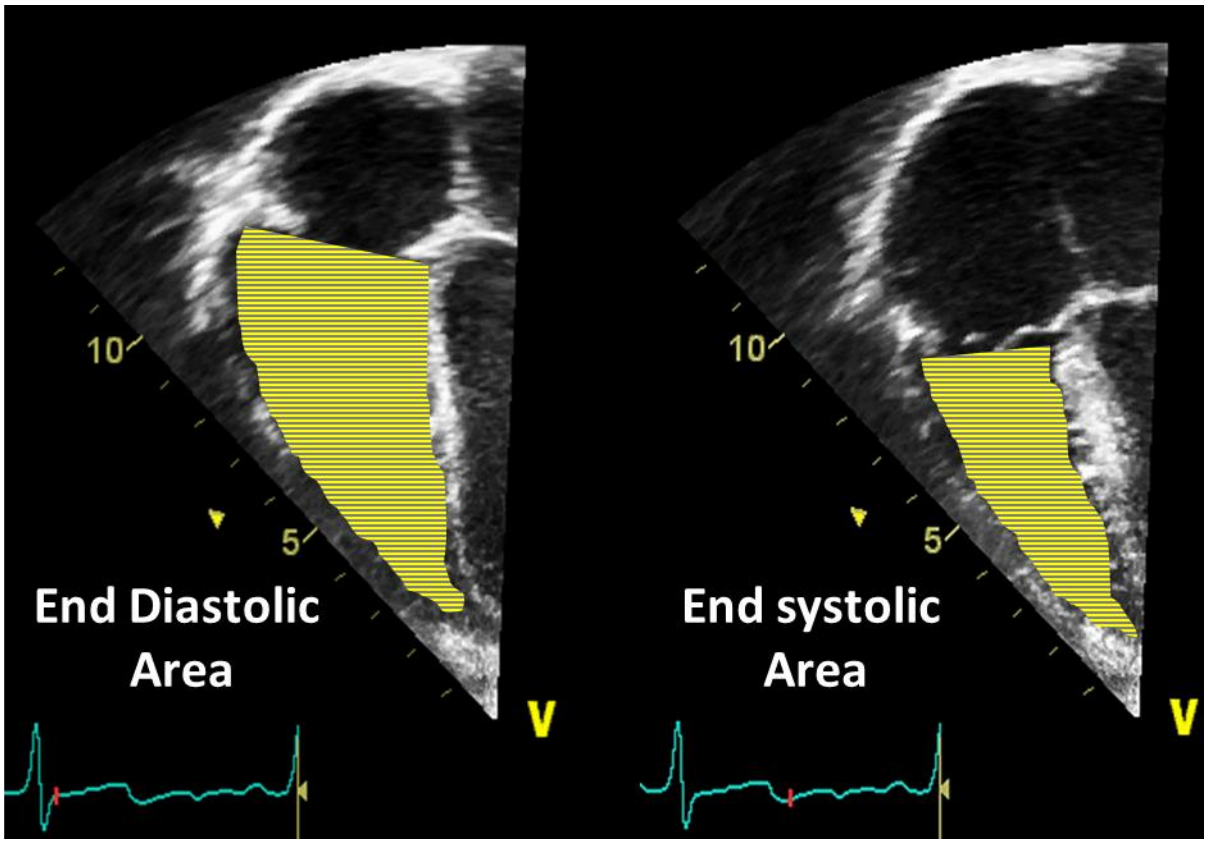

Figure 1.11 shows the graphic representation of the RV cavity end diastolic area (RVEDA) and RV cavity end systolic area (RVESA). After manually tracing these areas the RV FAC can then be calculated using the following formula: RV FAC (%) = [RVEDA(cm^2) – RVESA (cm^2)] ÷ RVEDA(cm^2).

Figure 1.12: M-mode imaging of the tricuspid valve to give the Tricuspid Annular Plane Systolic Excursion (TAPSE)

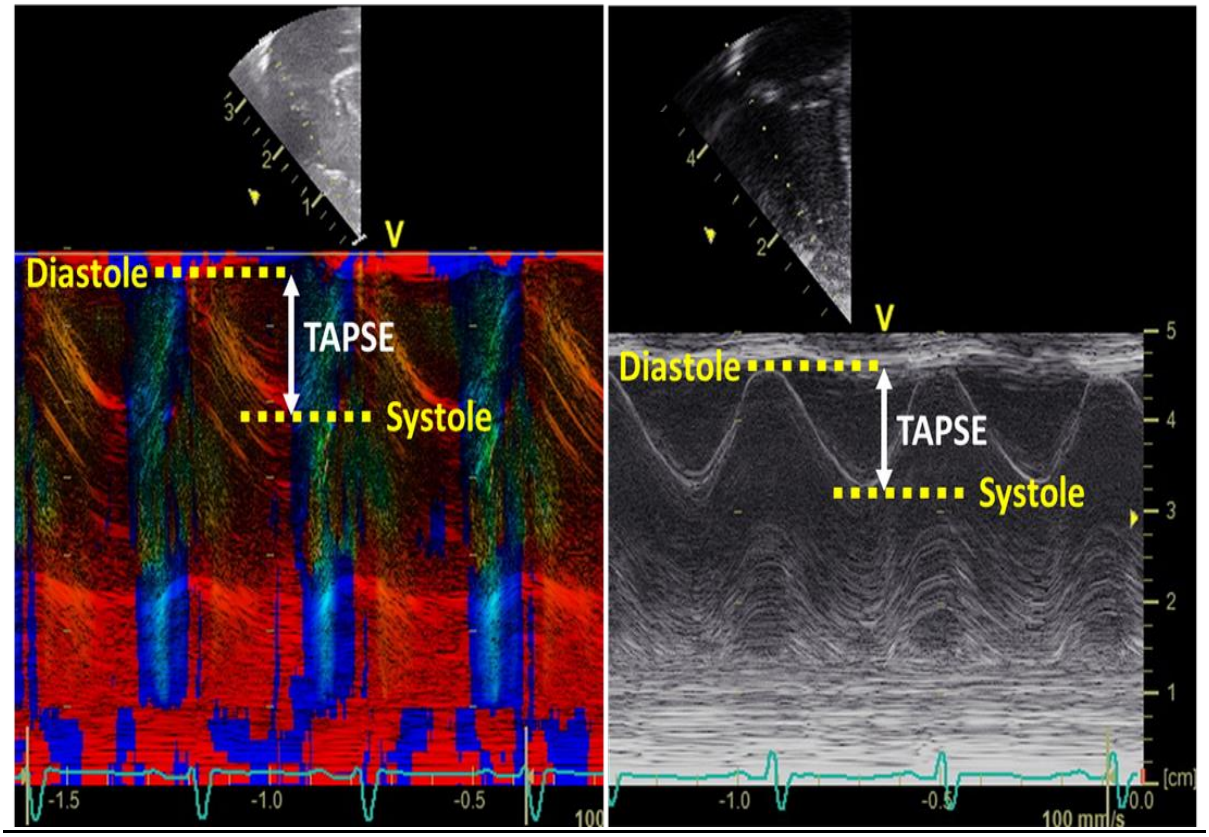

TAPSE is achieved by M mode assessment through the tricuspid annulus of the Right Ventricular free wall. This can be achieved by 2D grey scale (figure 1.12B) or tissue Doppler Imaging (figure 1.12A). TAPSE is the slope calculation between diastole and systole.

1.9 Use in Paediatrics

The use of tissue Doppler velocities and deformation imaging in the paediatric population is relatively recent. The drive to generate reference ranges for those parameters in the paediatric population stems from the inability to extrapolate data already in existence from the adult population due to the smaller heart sizes resulting in lower velocities and the higher variability of those parameters in children. (Pauliks, 2013). The use of those parameters has been explored in conditions such as Duchenne's muscular dystrophy (DMD) (Mertens et al., 2008), post chemotherapy (Biswas et al., 2013) and post cardiac transplant (Kailin et al., 2012). It is well recognised that patients with DMD exhibit subclinical cardiac dysfunction detectable by cardiac MRI before clinical symptoms arise. Mertens and his group demonstrated that despite normal global systolic function values measured using SF, LV deformation parameters were reduced in this cohort. Transplanted patients had deformation assessment one year post transplant and values were compared to age matched controls. The peak global left ventricular longitudinal strain was lower in the transplant group than in the control group suggesting reduced LV function (Kailin et al., 2012).

Normative values of strain and strain rate have been published by various authors to define this novel echo marker for neonates and paediatrics (Takahashi et al., 2010, Kaku et al., 2014, Jain et al., 2014, Elkiran et al., 2013). This basis allows us to use a potentially more sensitive tool for assessing function which has been validated and reproduced in various disease states and populations.

1.9.2 Role in neonates

Researchers have examined both tissue Doppler velocities (TDI) as well as tissue Doppler derived strain and SR in the preterm population. Helfer et al looked at TDI derived strain and strain rate during the first 28 days of life in very low birth weight infants and found that peak systolic strain and SR rose significantly in the RV over that time period (Helfer et al., 2014). They also looked at the reproducibility of measuring TDI derived strain and strain rate in infants less than 1500g and assessed both the feasibility and reproducibility of tissue Doppler-derived S and SR as well as the region of interest size and strain length. By looking at 60 good quality images of the LV free wall, interventricular septum and RV free wall they found that analysis in this patient population was both feasible and reliable (Helfer et al., 2013).

Murase et al looked at LV function in preterm infants over the first 7 days of life by using tissue Doppler velocities (Murase et al., 2013). They assessed 101 VLBW infants with serial echocardiography at 3, 12,24,36,48,72 and 96 hours of age as well as 5-7 days of life. They found that the peak systolic velocity and early diastolic velocity was reduced initially at 3 to 12 hours of age but then gradually increased.

More recently the same group examined tissue Doppler velocities of the right ventricle in the same cohort of patients and again found there was a drop in these values from 3 to 12 hours of age which recovered gradually (Murase et al., 2015a). These studies were interesting in that they looked at a large number of VLBW infants in the transitional period assessing tissue Doppler. However they did not assess deformation imaging as part of the study and very little data was available on loading conditions, clinical factors and conventional echocardiographic values. Furthermore their data of these serial data were

represented mainly in graphical form with broad or absent standard deviation values making it difficult to interpret these results

Joshi et al looked at the reproducibility of tissue Doppler derived deformation imaging in both term and preterm infants (Joshi et al., 2010) which was followed up by a study from the same research group looking at optimisation of deformation imaging in this population (Poon et al., 2011). To assess reproducibility they looked at 16 random echocardiographic studies out of a possible 55 patients (30 term and 25 preterm). Similar to the protocol which we instituted they performed echocardiograms with the Vivid GE system and then performed offline analysis using the EchoPAC system to measure inter and intra-observer variability for tissue Doppler velocities, strain and strain rate. Their definition of preterm infants was those infants born less than 34 weeks gestation which differs from our cohort of infants born less than 29 weeks. In their results, they found that there was good feasibility of performing tissue Doppler derived strain with 90% of infants having images analysed. The LV apical strain was the most difficult image to analyse with only 75% of images suitable for analysis. Variability was assessed by measuring coefficients of variation. Overall they found that intra-observer variability was adequate for these parameters but there was a sub-optimal inter-observer variability suggesting that these indices should be used with caution.

When looking at the optimisation Poon et al demonstrated that the best reproducibility was achieved when a strain length of 10mm was used for term infants while a 6mm strain length was used for preterm infants (Poon et al., 2011). They also noted that the reproducibility of using tissue Doppler derived deformation imaging improved with

higher frame rates with a frame rate of < 180 per second from a coefficient of variation of 17.3% to a coefficient of variation of 11.7% (Poon et al., 2011)

1.10 Reference values

Longitudinal, radial and circumferential strain values derived using speckle tracking echocardiography (STE) in healthy children and adults are recently published by Marcus et al (Marcus et al., 2011b). They divided their subjects into 8 groups up to 40 years of age with the youngest age group being 3 months of age. They found that there was a significant second-order polynomial relation between global peak systolic strain and age with lowest values seen in the youngest and oldest age groups however their cohort did not incorporate infants less than 1 month of age.

Jain and his group analysed healthy term new-borns and assessed RV strain as part of their assessment of RV function during the transition period (Jain et al., 2014). They studied both tissue Doppler velocities and STE derived strain as part of their protocol in 50 infants. They found that the RV basal peak systolic strain had a value of around 21% with good reproducibility by using STE.

A further recent study by Eriksen and his group (Eriksen et al., 2013b) similarly looked at tissue Doppler derived strain but their cohort consisted of older preterm infants with a gestation of 31 to 35 weeks with daily echocardiograms for the first 3 days of life and at term corrected gestational age. They found all velocity indices increased from day one to term corrected gestational age. They also found there was a significant correlation between gestational age and velocities particularly right sided S, E and A velocities.

1.11 Knowledge gap

There is still a lack of data examining tissue Doppler derived strain and strain rate in the preterm population within a large group of infants. In addition, reference ranges for RV dimensions and RV specific functional measurements which include TAPSE and FAC warrant further study. The initial focus of our research is to establish reference ranges for those newer measurements in the preterm population (infants < 29 weeks gestation) and assess their reproducibility and reliability, paving the way for these echocardiographic markers to be used in various disease states and clinical scenarios to aid in the management of preterm infants. The impact of various perinatal characteristics on those markers will also be examined. we also wanted to examine the impact of various disease states on these parameters such as the patent ductus arteriosus (PDA), pulmonary hypertension and chronic lung disease (CLD).

1.12 Pulmonary Hypertension

Term and preterm infants can develop persistent pulmonary hypertension of the newborn (PPHN) due to failure of transitioning from foetal to postnatal circulation and is becoming an increasingly recognised cause of poor oxygenation despite adequate ventilation and surfactant therapy. Often, pulmonary hypertension is associated with RV dysfunction and a better understanding of this along with treatment responses may improve patient management.

Different inotropic agents are currently used in the critically ill preterm infant including dopamine, dobutamine, adrenaline, noradrenaline, vasopressin, hydrocortisone, milrinone (Dempsey and Barrington, 2006, Sehgal et al., 2012a, Seri and Noori, 2005). The evidence for the use in some cases is limited and based on experience and tradition. The use of

echocardiography can allow a better understanding of the pathophysiology contributing to the circulatory compromise and assist in evaluating treatment options. A thorough echocardiogram can allow for assessment of systolic and diastolic function, evaluate for pulmonary hypertension as well as estimate left and right ventricular outflow volumes and function. It also allows for evaluation of structural congenital heart defects that might be contributing to neonatal compromise. By using this tool, a more targeted inotropic agent can be utilised to target the specific conditions.

Milrinone is an inotropic agent which has gained interest in the adult and paediatric population for the treatment of pulmonary hypertension and poor cardiac function. (Patel, 2012, Meyer et al., 2011, Hoffman et al., 2003). Its use in the preterm infant is limited but recent studies have shown that in isolated cases it may be of benefit (A et al., 2013, Danhaive et al., 2005, Sehgal et al., 2011) especially in the setting of pulmonary hypertension and right ventricular dysfunction. For the preterm infant with poor oxygenation often respiratory distress syndromesyndrome is attributed as the cause but in a select few increased pulmonary pressures with pulmonary hypertension may be a contributing factor and should be suspected especially in those in whom surfactant does not improve symptoms. Further delineation of left and right myocardial function in those infants may improve our understanding of those conditions and aid in their management.

1.13 Patent Ductus Arteriosus (PDA)

A PDA is associated with morbidities which include Intraventricular haemorrhage (IVH), Necrotizing Enterocolitis (NEC), chronic lung disease (CLD), death, and poor neurodevelopmental outcome (El-Khuffash et al., 2011, Cunha et al., 2005, Shortland et al., 1990). Recently, the relationship between the severity and duration of the ductal shunt and

the evolution of CLD in preterm infants has been established (Schena et al., 2015). This group showed that a haemodynamically significant PDA was associated with development of CLD and each week exposed to a haemodynamically significant PDA conferred a further added risk of CLD. However, defining haemodynamic significance in the early neonatal period remains a challenge with several methods being employed using clinical criteria, echocardiography, or both (Zonnenberg and de Waal, 2012).The ductus is a normal physiological connection between the pulmonary artery and aorta which is essential to foetal circulation. Normally this vessel closes within the first few days of life as the infant adapts to extra-uterine circulation. In preterm infants there is an increased propensity for the PDA to remain open. As the pulmonary vascular resistance drops in the first few days of life the PDA usually shows shunting of blood from left to right. A PDA with its resultant left to right shunt causes an increase in pulmonary circulation and pulmonary venous return to the left heart. This in turn results in an increase in the preload of the left ventricle. Using a comprehensive echocardiogram we aim to assess the impact a PDA and its resultant change in loading conditions has on both conventional echocardiography markers and more novel functional parameters during the early neonatal period. We will also assess how these changes impact our clinical outcomes

1.14 Chronic Lung Disease

Chronic Lung Disease (CLD) is defined as the need for oxygen or respiratory support at 36 weeks corrected gestational age (Kinsella et al., 2006).CLD is one of the common morbidities seen in preterm infants especially in those that are extremely low birth weight.

CLD is associated with increased right pulmonary pressures and pulmonary hypertension which can cause an increase in the afterload of the right ventricle. This can result in a negative impact on the right ventricular function. Some studies have looked at tissue Doppler velocities, tissue Doppler derived strain and speckle tracking at different time points in children with CLD comparing values to children without CLD (Yates et al., 2008, Czernik et al., 2014, Helfer et al., 2013). Yates and colleagues found that increasing right ventricle E/E' ratio correlates with clinical severity of CLD and infants with CLD had a reduced peak systolic strain of the RV free wall on day 14 and 28 possibly due to an increased afterload of the RV. Very little data exists assessing longitudinal changes of RV functional parameters on infants who develop CLD.

1.15 Desirable Qualities of the measurement

There is some emerging literature describing the clinical utility of those newer markers of function in various disease states and physiological conditions in the preterm population.

One study analysed 30 infants post PDA ligation and divided the group into those with a low (< 200ml/kg/min) or normal (> 200ml/kg/min) Left Ventricular Output (El-Khuffash et al., 2014). Those infants with a low LVO had a significantly lower global longitudinal strain (-10.3% vs -14.4%). Those infants in the Low LVO state who received milrinone as a treatment showed global longitudinal strain values comparable to the high output group at 18 hours of age. This highlights the value that using strain can have in the clinical setting.

Saleemi and colleagues used tissue Doppler velocities in preterm infants before and after red blood cell transfusion (Saleemi et al., 2013). By performing echocardiograms before and after RBC transfusions and comparing them to echocardiograms in control subjects at similar time intervals, they found that there was a significant increase in the LV systolic and diastolic velocities in the transfusion group which was not seen in the control group. What was also interesting was that the change in myocardial performance seen correlated with the degree of severity of anaemia pre-transfusion.

These studies show the applicability of using TDI and deformation in the clinical setting in preterm infants and its advantage outside the clinical setting which has also been seen in the adult and paediatric populations.

1.16 Conclusion

Establishing reference ranges of these new echocardiographic markers of ventricular function in the preterm population will pave the way for further research and clinical care in this field. Knowing the expected measurements in preterm infants in a relatively steady state will allow further research into the effects of diseases (such as sepsis, asphyxia, and respiratory distress) and the impact of therapeutic interventions (such as mechanical ventilation, inotropes and surfactant administration) on myocardial function. In addition, these markers may be used in the future to detect early myocardial compromise, determine the appropriate treatment strategy, and monitor treatment response.

1.17 Aim

We aimed to perform serial echocardiograms on preterm infants from day 1 of life to 36 post menstrual age (PMA) to establish these reference ranges. We then hope to assess how these functional parameters are affected by disease states, namely the patent ductus arteriosus, chronic lung disease and certain inotrope use in the setting of pulmonary hypertension.

1.18 Study Objectives

1) Assess the reliability of myocardial performance assessment by echocardiography in the preterm population (< 29 weeks)
2) Determine reference ranges of echocardiographic parameters of myocardial function in the preterm population
3) Obtain data on serial changes in myocardial function and performance in preterm infants.
4) Assess the influence of specific disease states on parameters of myocardial function: namely: patent ductus arteriosus, the use of inotropes in pulmonary hypertension, and chronic lung disease.

1.19 Hypothesis to be examined

- The use of novel echocardiography markers of left and right myocardial function is feasible and reproducible in preterm infants.
- Myocardial function increases over the first days of age and by 36 weeks PMA.
- Preterm measures of myocardial performance are influenced by PDA, RV pressures, inotropes and chronic lung disease

Chapter 2 Materials and Methods

2.1 Patient population and study setting

This was a prospective observational study carried out in the neonatal intensive care unit (NICU) of the Rotunda Hospital Dublin, Ireland (a tertiary maternity unit which caters for over 9000 deliveries per annum). Infants were excluded if they: had a suspected or definite chromosomal abnormality or congenital heart disease other than a PDA and patent foramen ovale (PFO) identified antenatally or on the initial echocardiogram.

There is currently no consensus in the literature on the best treatment modality for a PDA. Both aggressive treatment with prophylactic NSAID use or early NSAID use as well as early surgical duct ligation have been used in some institutions as well as conservative treatment with close observation of clinical status. Our unit currently adopts a conservative approach to PDA treatment. Prophylactic indomethacin is not used at this institution and medical treatment of the PDA with non-steroidal anti-inflammatory drugs is not provided in the first 7 days of life. High frequency oscillation (HFO) is only used as a rescue mode of ventilation. PDA treatment is attempted at a later stage in infants who are ventilator dependent (beyond the first two weeks of age). The first treatment option is using ibuprofen with a second course of ibuprofen being used if a haemodynamically significant PDA is seen after the first course and it is deemed safe to use without any significant contra-indications. PDA ligation is reserved for infants failing late medical therapy who remain on invasive ventilation beyond three weeks of age and have a significant PDA in accordance

with recently published triaging criteria(El-Khuffash et al., 2013b) . Hypotension is treated with inotropes if the blood pressure is lower than the 3rd centile for any given gestation in addition to clinical and laboratory signs of hemodynamic compromise such as metabolic acidosis or increasing lactate values. The results of the research scans were not communicated to the medical team caring for the infants unless they specifically requested a clinically indicated echocardiographic assessment or if congenital heart disease was identified. Written parental informed consent was obtained from all participants and ethical approval was obtained from the Hospital Ethics Committee prior to recruitment. All infants less than 27^{+0} weeks receive prophylactic surfactant at birth. Infants greater than 27 weeks receive early surfactant if they require greater than 30% oxygen to maintain an oxygen saturation between 90 to 95%.

2.2 Clinical parameters

During the course of the infants stay in the Neonatal unit, outcome measures were recorded until time of discharge. This was obtained from the patients' clinical notes:

The following conditions were monitored:

1. Respiratory Distress Syndrome (RDS): The condition was defined based on clinical signs of respiratory distress include tachypnoea, nasal flaring, grunting, intercostal and subxiphoid retractions, cyanosis, hypoxaemia and a rising pCO_2 on an arterial blood gas sample. In addition, radiological diagnosis was used to further support clinical evidence (Moss, 2006).
2. Chronic Lung Disease (CLD): The need for oxygen supplementation or respiratory support at 36 weeks corrected gestational age with typical chest radiograph changes

was documented. We also noted the previous definition of CLD by regarding infants with oxygen supplementation or respiratory support at 28 days of age (Bancalari and Claure, 2006, Kinsella et al., 2006).

3. Neonatal Sepsis: This was diagnosed based on positive neonatal blood cultures (Holzman et al., 2007). We note that this definition will miss those infants with blood culture negative sepsis which occurs in the preterm neonatal population. However we feel culture positive sepsis will allow for a more defined criteria which can be used for this group. The majority of blood culture positive sepsis will be those infants with late onset sepsis.
4. Intraventricular Haemorrhage defined and graded with the Papile classification (Papile et al., 1978). A single consultant radiologist performs all the scans in out unit. The first scan is performed with in the first 24 hours of life followed by a repeat scan at 48 hours and at day 7 of life. We grouped the infants to those who developed grades I/II (moderate IVH) and those with grades III/IV (severe IVH). We also noted whether there was early IVH defined as IVH within the first 2 days of life or late IVH.
5. Periventricular Leukomalacia (PVL): refers to necrosis of cerebral white matter in a specific distribution, dorsolateral to the external angles of the lateral ventricles and involving the region adjacent to the trigones and to the frontal horn and body of the lateral ventricles. The descending corticospinal tracts, optic radiations in the area of the trigone and occipital horn, the acoustic radiations in the temporal horn, and frontal white matter near the foramen of Monro commonly are affected (Inder and Volpe, 2000). We assessed for PVL on the 28 day cranial ultrasound scan and the ultrasound scan at time of discharge.

6. Necrotizing Enterocolitis (NEC): the diagnosis was based on Bell's criteria (Bell, 1978). Both whether the child had a diagnosis of NEC and the Bells staging of NEC were documented.
7. Retinopathy of prematurity (ROP): Infants are assessed by a consultant paediatric ophthalmologist as part of a screening tool for retinopathy of prematurity if born less than 1500g. We documented if a child had a clinical diagnosis of ROP based on these assessments and whether the infant received treatment for ROP, either laser treatment or bevacizumab treatment.
8. Ventilation: The duration of invasive ventilation (conventional ventilation, high frequency oscillation ventilation) the duration of non-invasive ventilation (Continuous positive pressure ventilation) and the duration of oxygen requirement were noted. We also documented the maximum Mean Airway Pressure (MAP) the infant used during their stay in NICU. The number of times the infant failed extubation was noted, Failed extubation was classed into respiratory causes and non-respiratory causes such as NEC, sepsis etc.
9. Nutritional status. The total number of days the child received Total Parenteral Nutrition TPN and the number of days for the child to reach full feeds were noted. We defined full feeds as the point at which the child was receiving 120ml/kg/day of enteral feeds.
10. Death: Both early death, defined as death with seven days after birth, and death before discharge data was collected.
11. Inotrope use. We documented if inotropes were used at any point and if used, how many and for what duration.
12. Pulmonary haemorrhage

13. Diuretic use: We noted if diuretics were used at any point for the treatment of chronic lung disease or respiratory distress. The diuretics used in our institution for CLD was a combination of furosemide, chlorothiazide and spironolactone. The duration of diuretic use was also recorded. We did not take diuretic use given at the time of a blood transfusion as a valid use of diuretics for this clinical setting.
14. Length of stay in hospital.
15. Transfusion: The number of blood transfusions, number of platelet transfusions and the number of transfusions with fresh frozen plasma

2.3 Antenatal History

We collected the following antenatal information on all infants enrolled in this study:

1. Antenatal steroid administration: timing, dose, type. We defined a complete course as 12.5mg of betamethasone given 12 hours apart. A partial course was defined as 1 dose administered prior to delivery or a course of betamethasone given less than 12 hours before delivery.
2. Presence or absence of pre-eclampsia (PET): pre-eclampsia is defined as a disorder of pregnancy associated with hypertension and proteinuria (Redman and Jefferies, 1988).
3. Presence or absence of clinical and/or histological chorioamnionitis.
4. Antepartum haemorrhage (APH).
5. Absent or reversed end-diastolic flow in the umbilical artery (AEDF / REDF): The normal Doppler signal seen in the umbilical artery is one with continuous positive flow seen in both systole and diastole. (Isalm et al., 2015).

6. Use of Magnesium sulphate ($MgSO_4$) In the Rotunda Hospital, mothers with pregnancies less than 32 weeks gestation who are likely to deliver within 12 – 24 hours are given a 4g loading dose of $MgSO_4$ over a 20 minute period for foetal neuroprotection. No subsequent infusion of $MgSO_4$ is given.
7. Presence of any septic risk factors: Maternal fever > $38^{o}C$; Maternal Group B streptococcus (GBS) bacteraemia on high vaginal swab, or previous infant with invasive GBS infection; Prolonged rupture of membranes > 18hours.

2.4 Delivery details

Delivery details were collected including

a) Gestational age at time of delivery
b) Birth weight, with documentation on whether the child was below the 10^{th} or the 3^{rd} percentile for weight at time of birth
c) Gender
d) Mode of delivery Spontaneous vaginal delivery vs low segmental caesarean section)
e) Apgar scores (recorded at 1 and 5 minutes of age)
f) Resuscitation required (including need for cardiopulmonary resuscitation (CPR) and use of adrenaline)
g) Singleton delivery versus or multiparous delivery
h) Cord gas if available
i) Surfactant administration within the first 6 hours of life and number of doses if multiple doses were used.

2.5 Measurements at time of Echo

Clinical measurements were collected at the time of echocardiogram. These included weight, heart rate, systolic, mean and diastolic blood pressure, mode of ventilation, mean airway pressure, oxygen requirement (FiO_2), ionotropic support, oxygen saturation, fluid intake and pH based on the closest blood gas analysis at the time of the scan.

BP was measured invasively from an intra-arterial catheters placed via the umbilical artery or in the peripheral radial artery or noninvasively from an appropriately sized blood pressure cuff. Peripheral and central measurements were analysed together as they have been shown to correlate with each other (Butt and Whyte, 1984, Nuntnarumit et al., 1999). This correlation is best seen at normotensive levels but the discrepancy in readings occurs at hypotensive and hypertensive levels. We invariably try to use invasive BP monitoring in the haemodynamically unstable preterm infant and non-invasive measurements when the child is haemodynamically stable. The indwelling catheters were attached to a Data Medics Transducer. A continuous blood pressure signal was displayed on a Philips Neonatal Monitor. Systolic, diastolic and mean blood pressure was recorded.

2.6 Echocardiography parameters

Echocardiography scans were performed on these infants at 4 separate time intervals

- 6 to 12 hours of age
- 36 to 48 hours of age
- 5 to 7 days of age
- 36 weeks corrected post gestational age.

A Vivid S6 or Vivid I ultrasound machine was used for all image acquisition using a 12 MHz or 10MHz multi-frequency probe for the first three scans and a 7MHz probe for the 36 week PMA scan (GE Medical, Milwaukee, USA). All scans were acquired in accordance with the most recent neonatal echocardiography guidelines (Mertens et al., 2011a). All infants were in a supine position at the time of the scan. Standard neonatal windows were obtained in addition to some novel RV views described later. All initial scans were reviewed to exclude any structural congenital heart disease other than a PFO or PDA. If such a defect existed the infant was excluded from the study and appropriate follow up was conducted by the Paediatric Cardiology service.

We obtained the following echocardiography parameters

Measures of myocardial performance and dimensions:

1) Shortening fraction.
2) Left ventricular dimensions.
3) Ejection fraction measured by Simpson's biplane method.
4) Tissue Doppler velocities of the mitral, septal and tricuspid annuli.
5) Tissue Doppler-derived Left, septal and right ventricular strain and strain rate.
6) Left and Right ventricular outputs.
7) Left ventricular rotation, twist and untwist mechanics using speckle tracking echocardiography.
8) Right ventricular TAPSE.
9) Right ventricular dimensions.
10) Right ventricular fractional area change.

Assessment of PDA parameters

1) PDA size in 2D measured at the pulmonary end.
2) The direction and peak velocity of flow across the shunt through the duct.
3) Pressure gradient across the shunt.

Assessment of Pulmonary Hypertension:

1) PDA Shunt Direction.
2) Pulmonary artery acceleration time (PAAT).
3) Right ventricular ejection time (RVET).
4) PAAT: RVET ratio.
5) Interventricular septum motion and morphology in systole.
6) Tricuspid regurgitant jet pressure gradient.

Markers of pulmonary over-circulation:

1) Left atrial to aortic root ratio (LA:Ao).
2) Pulmonary vein peak systolic and diastolic velocity.
3) Mitral valve E and A velocities, E:A ratio, and mitral value VTI, IVRT.
4) Left ventricular output.
5) The presence of PFO/ASD and the velocity of the shunt across it.

Markers of systemic hypoperfusion

1) Abdominal aortic peak systolic velocity and diastolic flow direction and velocity.
2) Celiac artery peak systolic velocity and diastolic flow direction and velocity.
3) Middle cerebral artery peak systolic velocity and diastolic flow direction and velocity.

2.6.1 Conventional Echocardiographic parameters

Shortening fraction

We calculated shortening fraction by using M mode imaging in the parasternal long axis view using the calculation:

$$SF\% = \frac{(LVEDD-LVESD)}{LVEDD} \times 100$$

Where LVEDD is the LV end diastolic diameter and LVESD is the LV end systolic diameter.

Normal values of neonatal SF% range from 26 to 40% (Charles S. Kleinman, 2012).

Figure2.1: M mode imaging through the parasternal long axis of the heart giving Left Ventricle cavity dimensions from which the shortening fraction can be calculated

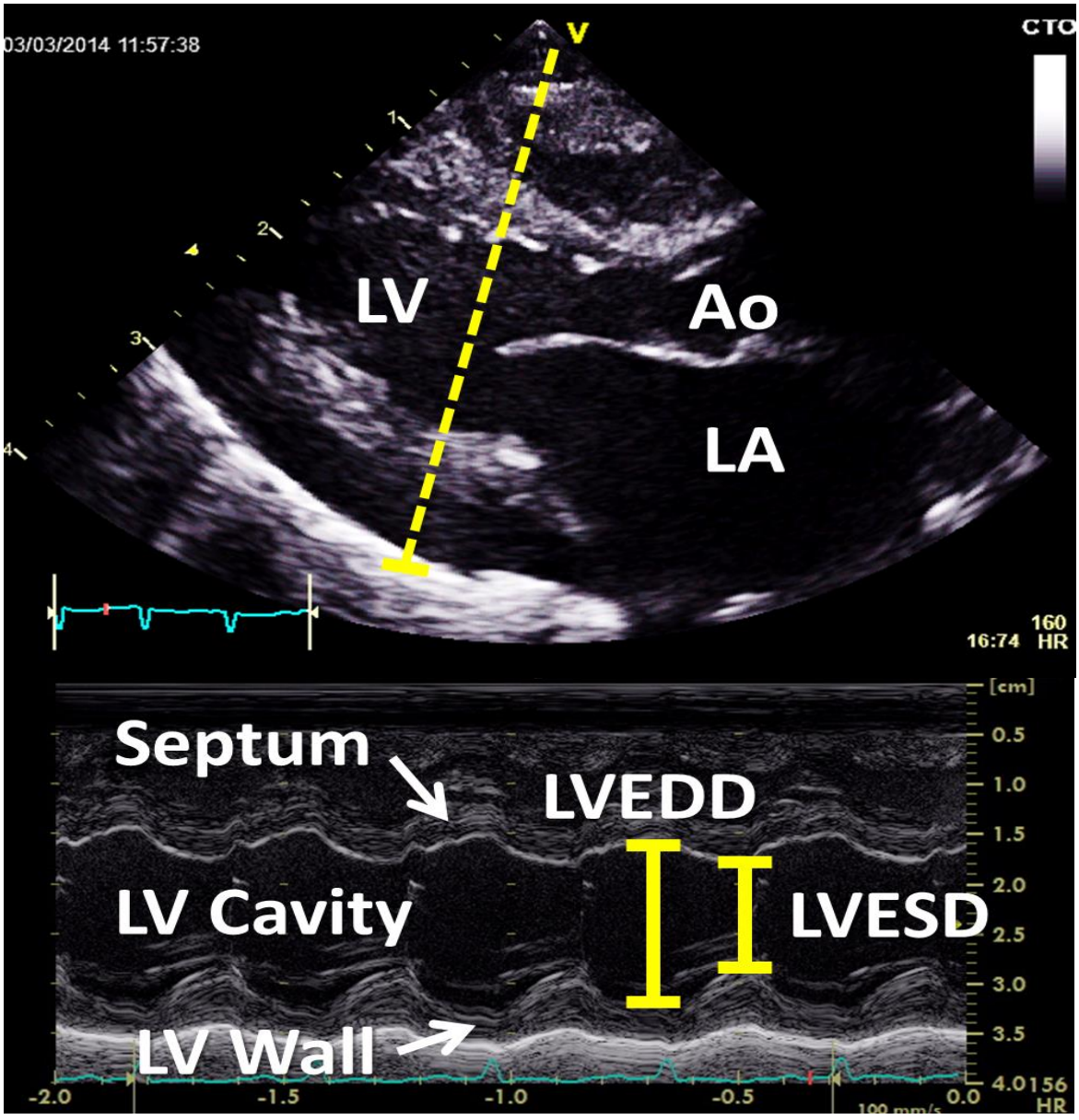

Figure 2.1 demonstrates the long axis view of the left ventricle with the yellow dotted line depicted the plane through which the corresponding M-Mode image is obtained. LV- Left ventricle; Ao- Aorta; LA- Left Atrium; LVEDD- Left ventricle end diastolic dimension; LVESD- Left ventricle end systolic dimension

Ejection fraction

Ejection fraction was calculated using the Simpsons biplane method using the LV 2-chamber and LV 4-chamber views (Mertens et al., 2011b). This measurement of systolic function becomes increasingly important when considering abnormal LV geometry or septal motion as it incorporates changes in volume size from diastole to systole in different planes. Area is traced around the endocardial border in both the 4 chamber and 2 chamber views at end systole and end diastole. The area is divided into disks and using software available in the echocardiography machine the ejection fraction is calculated by measuring the change in area from diastole to systole over the cardiac cycle (Mertens et al., 2011b), (Figure 2.2).

LV dimensions

LV dimensions were calculated from the 4 chamber view and the parasternal long axis view and include Left ventricular end diastolic diameter (LVEDD), LV internal diameter in diastole (LVID), and LV posterior wall diameter in diastole (LVPWD).

Figure 2.2: 4-chamber and 2-chamber views of the Left ventricle at end systole and end-diastole.

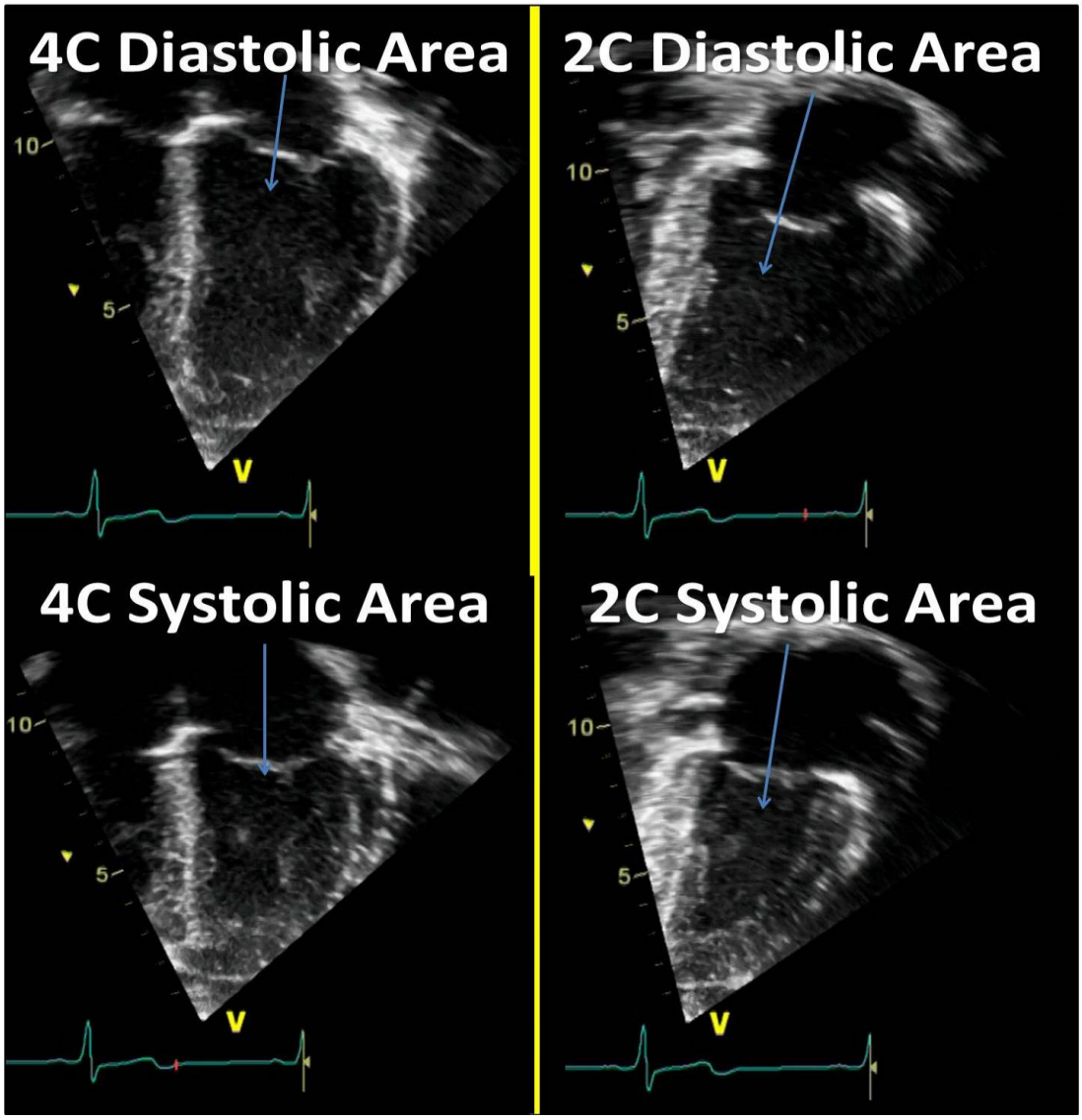

Figure 2.2 demonstrates the two views used to calculate ejection fraction using the Simpsons biplane method. 4C- 4 Chamber; 2C- 2 Chamber.

Left ventricular output (LVO)

The left ventricular output can be obtained by measuring the mean velocity of blood flow in the left ventricular outflow tract (LVOT) using pulsed wave Doppler and calculating the aortic diameter from the parasternal long axis view (Figure 2.3). Pulsed wave Doppler of the aorta during systole gives the velocity time integral (VTI), which is the distance travelled by blood during a given beat. The Left ventricular output can then be calculated by using the formula:

$$LVO = \pi \frac{D^2}{4} \times HR \times VTI \ /weight$$

where D is the aortic diameter, HR is the heart rate and VTI is the velocity time integral. LVO is expressed in ml/kg/min and the normal value ranges from 150 to 300ml/kg/min (Evans and Kluckow, 1996).

Figure 2.3: Pulsed wave Doppler of the Aortic Valve showing the Velocity Time Integral (VTI)

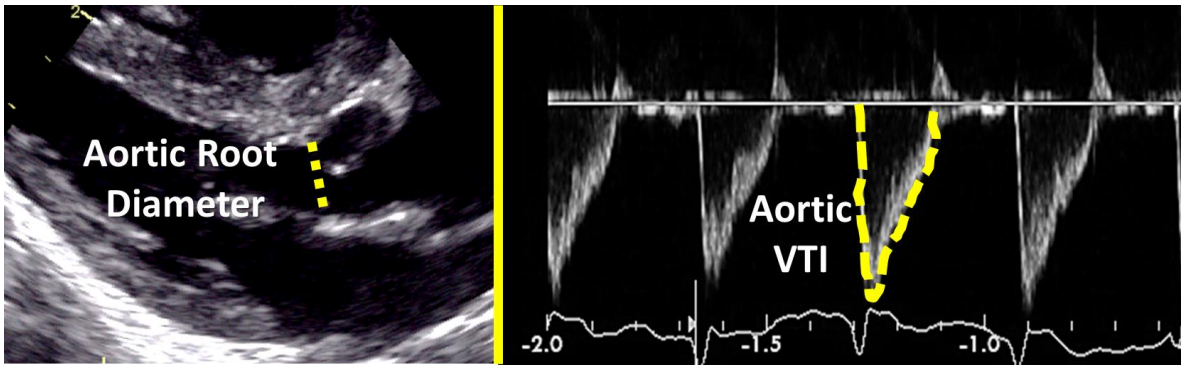

Aortic root diameter is measures from the parasternal long axis views. Pulsed Wave Doppler is performed through the left outflow tract to give the Doppler signal produced by the blood flow through the aortic valve. By tracing the Doppler wave for one beat, the velocity time integral (VTI) can be obtained from which the left ventricular output can be calculated.

Right ventricular output (RVO)

In a similar fashion to the LVO, the RVO can be calculated by measuring the velocity time integral of the pulmonary blood flow in the modified parasternal long axis view (Figure 2.4) and calculating the diameter of the pulmonary valve. The RVO can then be calculated using the formula

$$RVO = \pi \frac{D^2}{4} \times HR \times VTI \ /weight$$

Figure 2.4: Pulmonary valve and the Right ventricular outflow tract (RVOT) with corresponding pulsed wave Doppler signal of the RVOT

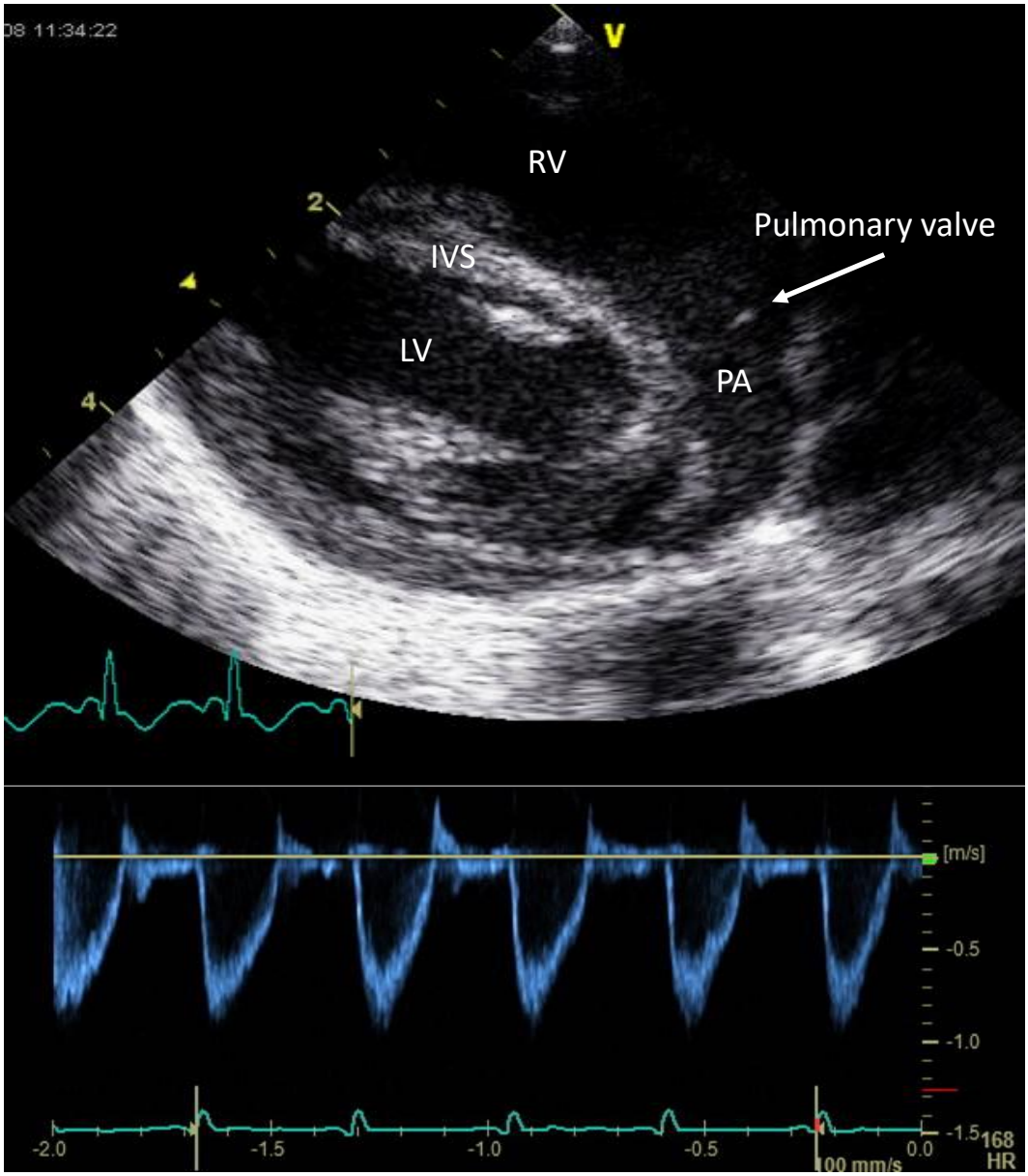

The RVOT can be viewed by the parasternal long axis view. Pulsed Wave Doppler signal is shown from the right outflow tract from which the velocity time integral (VTI) can be calculated. RV-Right ventricle; LV-Left ventricle; IVS-Intraventricular septum; PA-Pulmonary artery.

Colour flow and Colour Doppler

Assessment of flow across the atrioventricular valves (AV valves) can be achieved by using 2- dimensional imaging, colour flow and colour Doppler imaging at the level of these valves. Colour can be placed across the mitral valve to assess for mitral incompetence. Pulsed Doppler can be performed on the mitral valve and the waveform stored with the E and A wave pattern observed for normal mitral blood flow (Figure 2.5). The ratio of the E wave to the A wave (E:A ratio) can be used as a surrogate of LV diastolic function.

Figure 2.5: Mitral Doppler flow pattern.

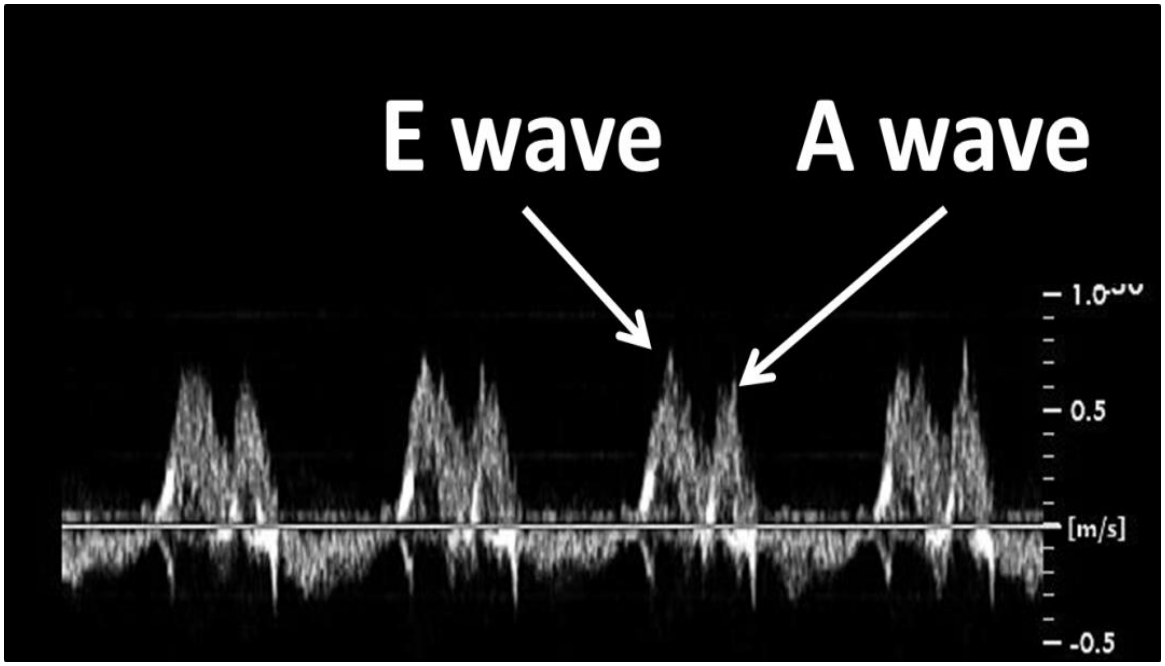

Pulsed wave Doppler signal through the mitral valve showing the typical dual peaked pattern. The Doppler pattern shows the early (E) and late (A) waveforms

Similarly colour flow can be placed across the tricuspid valve to assess for competency of the valve. Pulsed wave and continuous wave Doppler across the tricuspid valve can be performed to assess the blood flow across the tricuspid valve (Figure 2.6). Tricuspid regurgitation can also be assessed at this stage (Figure 2.11).

The pulmonary veins can be seen returning into the left atrium from the 4 chamber view. Pulsed wave Doppler velocities measurement of a pulmonary vein enables assessment of pulmonary venous return (Figure 2.7). The 4 chamber view of the heart can be viewed to quantify left ventricular (LV) and right ventricular (RV) size, assess the intraventricular septum for any defects such as a VSD and assess valve function (Figure 2.8).

Figure 2.6: Tricuspid Doppler flow pattern.

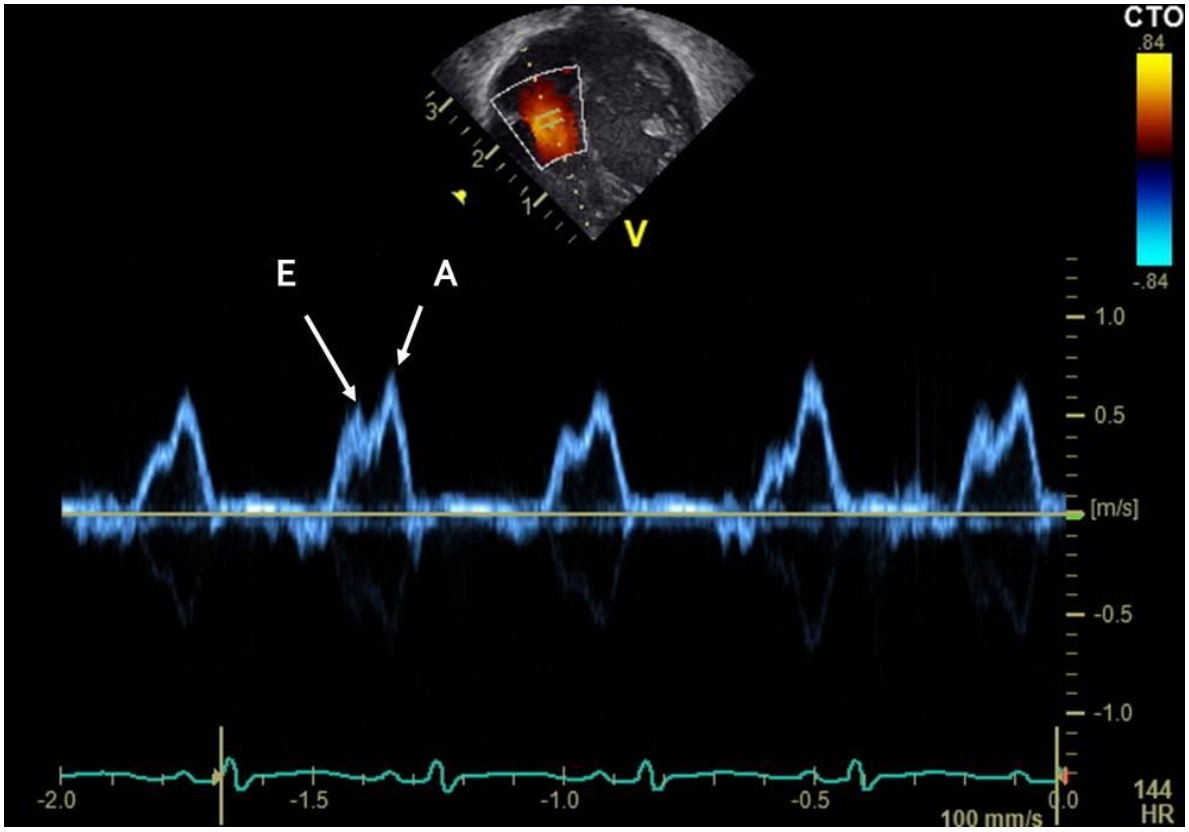

Pulsed wave Doppler signal through the tricuspid valve demonstrating the early (E) and late (A) waveforms of blood flow.

Figure 2.7: Pulmonary venous drainage to the Left Atrium.

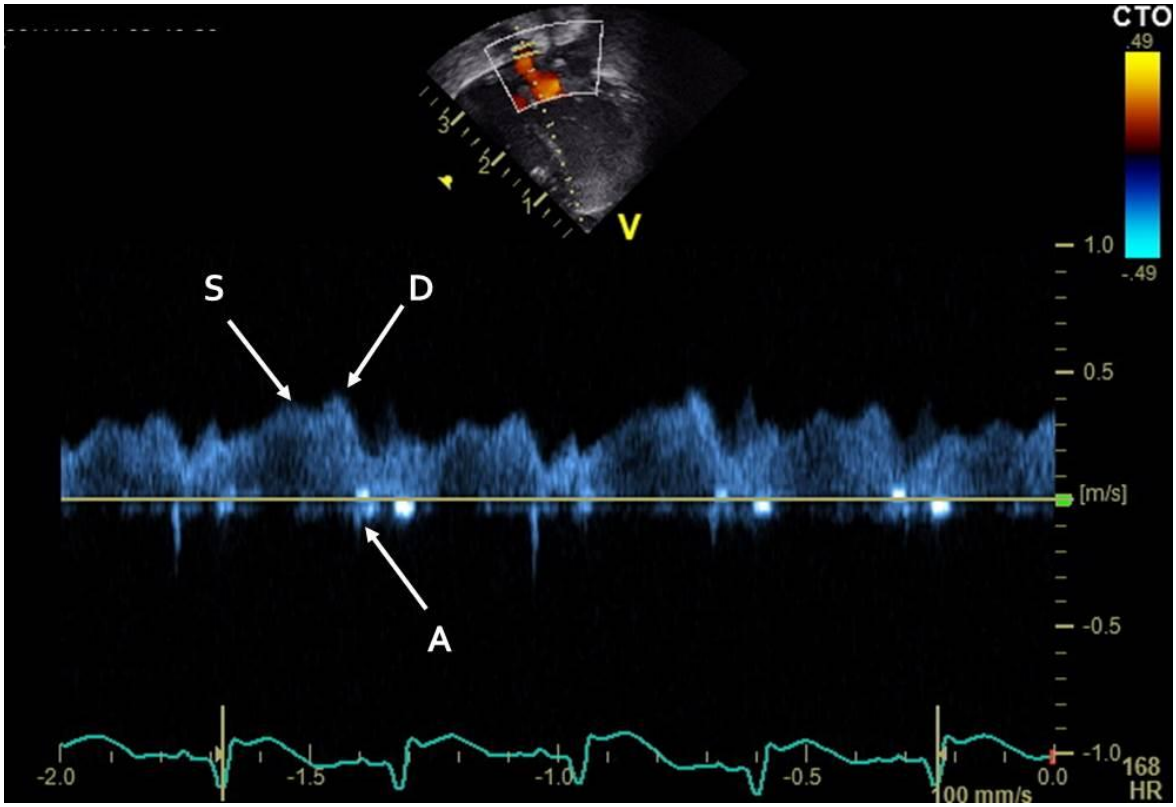

Figure 2.7 shows the pulsed wave doppler signal through one of the pulmonary veins as it enters the Left atrium. S- systolic velocity, D- diastolic velocity, A atrial contraction velocity

Figure 2.8 : Four chamber view of the heart.

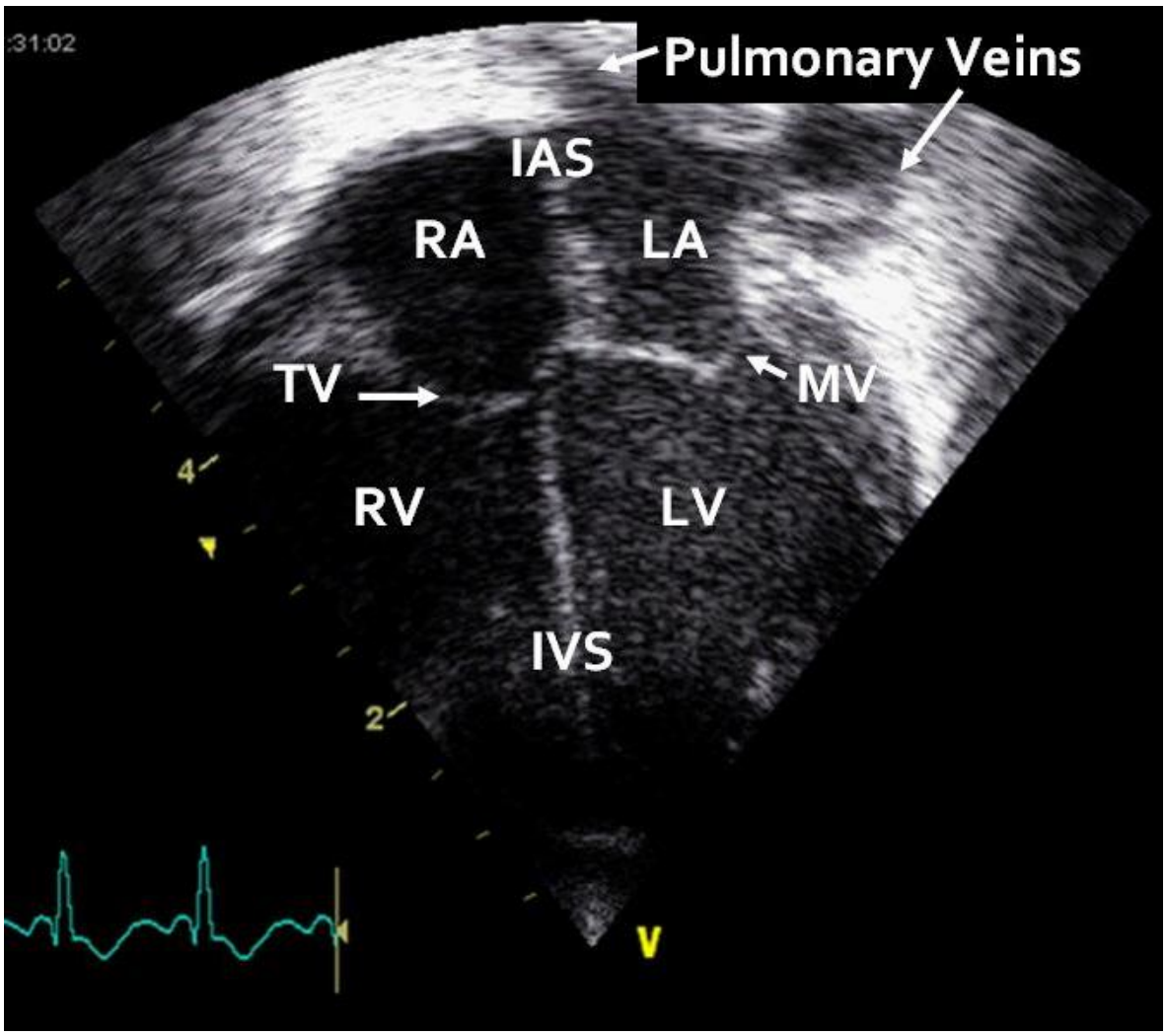

The 4-chamber view with its representative structures LV- Left Ventricle; RV-Right Ventricle; IVS-intraventricular septum; TV-Tricuspid valve; MV-Mitral valve; LA-Left atrium; RA-Right atrium; IAS-intra-atrial septum.

PDA size and flow

The PDA diameter was obtained from the ductal view at the suprasternal notch. The PDA diameter was seen by 2D imaging of the pulmonary end. Colour Doppler is then used to identify flow across the PDA. Continuous wave Doppler is performed and the flow wave of the PDA is documented. The peak and minimum velocity is recorded as well as the peak and mean pressure gradient. From this it is possible to determine if the PDA is restrictive, non-restrictive, bidirectional left to right flow or right to left flow (Figure 2.9).

Figure 2.9: Direction of flow across the Patent Ductus Arteriosus (PDA).

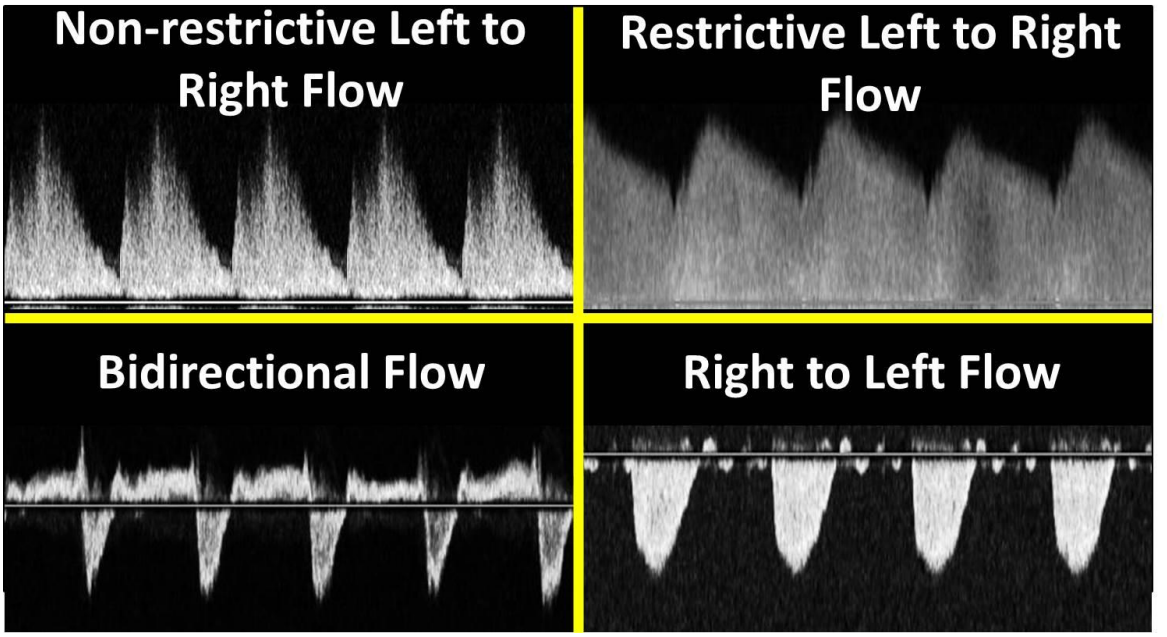

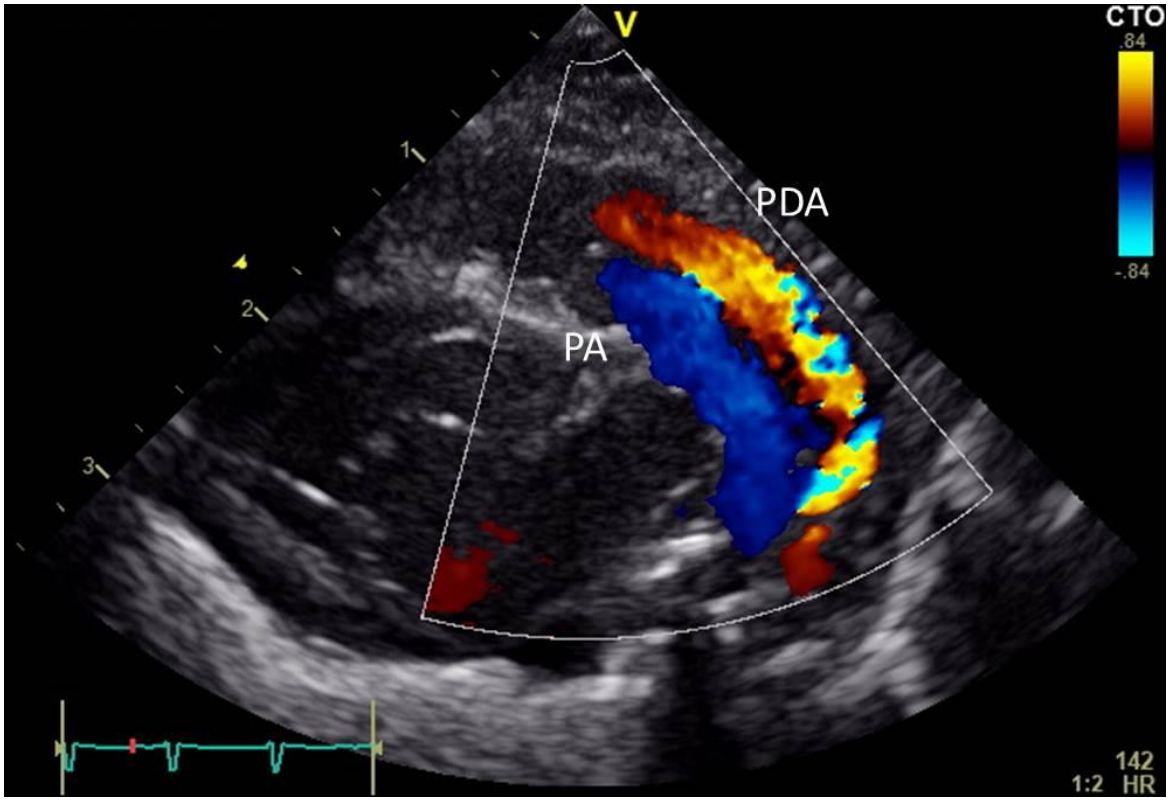

Figure 2.9 shows the colour flow of the Patent Ductus Arteriosus (PDA) (RED) relative to the Pulmonary Artery (PA) (BLUE).

Left atrial to aortic ratio (LA:Ao)

Left atrial to aortic ratio (LA:Ao), which is a marker of pulmonary over circulation can be measured from the parasternal long axis view. Using M-mode the cursor is placed perpendicular to the aortic wall at the level of the aortic valves as demonstrated in figure 2.10. From this the ratio of the aortic diameter can be measured to the corresponding left atrial diameter at this level. As the aorta has a relatively fixed measurement this can be used to evaluate left atrial volume overload that is often seen in premature infants most notably in those with a PDA. This is due to the increase in effective pulmonary blood flow from the left to right shunt across the PDA and subsequent increase in pulmonary venous return resulting in dilation of the left atrium. A LA:Ao ratio of greater than 1.4:1 is generally deemed to be an indication of a significant PDA (McNamara and Sehgal, 2007).

Figure 2.10: Left atrial to aortic ratio (LA:Ao) as measured from the parasternal long axis view

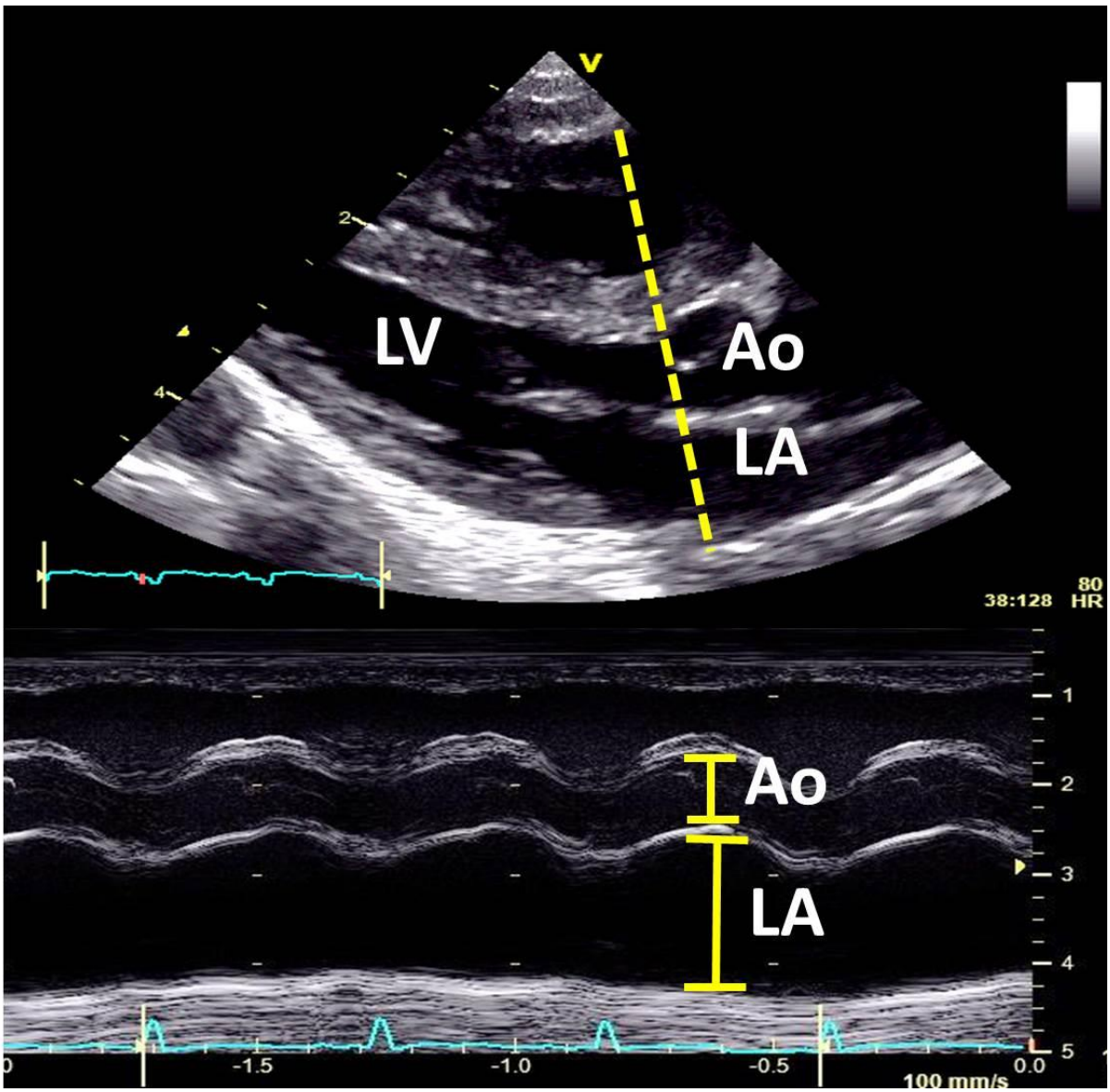

The cursor is placed through the aortic valve and the left atrium in the parasternal long axis view. M-Mode imaging is performed to calculate the left atrium to aortic ratio. Ao- Aorta; LA- Left atrium; LV- Left ventricle

Pulmonary Hypertension assessment

Pulmonary hypertension can be assessed by looking for a tricuspid regurgitant jet to estimate the RV pressure, by monitoring the direction of flow through the PDA or by defining the morphology and motion of the intraventricular septum during systole.

Pulsed wave Doppler can be used to assess tricuspid blood flow either from the 4 chamber view or the parasternal long axis view. Often Tricuspid regurgitation may be present due to increased pulmonary arterial pressure especially in the early postnatal period due to the delay in falling pulmonary vascular resistance. Tricuspid regurgitation can be measured using continuous wave (CW) colour Doppler. From this the peak velocity can be calculated (Figure 2.11) and RV systolic pressure (RVSp) estimated using the modified Bernoulli equation and assuming a right atrial pressure of 5mmHg (Hatle L, 1982). The Bernoulli equation states that

$$PAP = 4\ X\ (TR\ velocity)^2$$

where PAP is the Pulmonary arterial pressure and TR velocity is the tricuspid regurgitant velocity.

The RVSp is then estimated by adding the pulmonary arterial pressure and the right atrial pressure.

$$RVSp = PAP + 5mmHg$$

Figure 2.11: Colour Doppler through the tricuspid valve with tricuspid regurgitation.

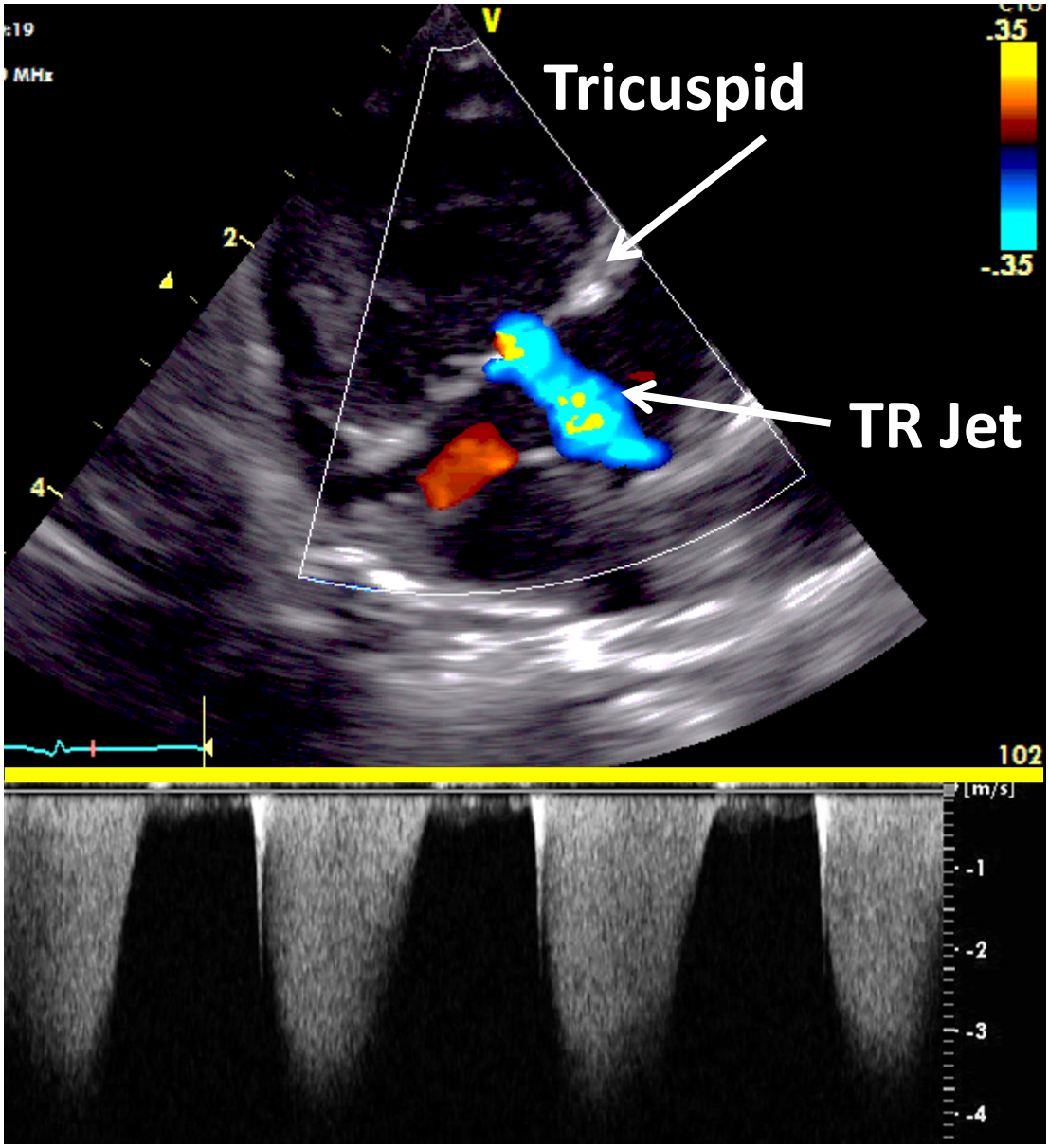

Figure 2.11 shows the tricuspid regurgitant jet (TR jet) through the tricuspid valve as seen in the parasternal long axis view. Continuous wave Doppler signal of this jet will allow calculation of the peak TR velocity from which estimation of the Right ventricle end systolic pressure can be calculated.

2.6.2 RV functional assessment

Tricuspid Annular Plane Systolic Excursion (TAPSE)

Tricuspid annular plane systolic excursion (TASPE) is a measure of movement of the tricuspid annulus from base to apex during systole and reflects global RV function. TAPSE was measured based on M-mode echocardiography through the tricuspid annulus. Both 2 dimensional TAPSE and tissue Doppler velocity imaging (TDI) TAPSE were performed. This is an easy measurement of RV systolic function which can be achieved by placing the cursor through the tricuspid annulus on the RV free wall in the RV focused 4-chamber view, as demonstrated in figure 2.12. Measurements are taken over 3 cardiac cycles and an average value is obtained.

Figure 2.12: Tricuspid annular plane systolic excursion (TAPSE).

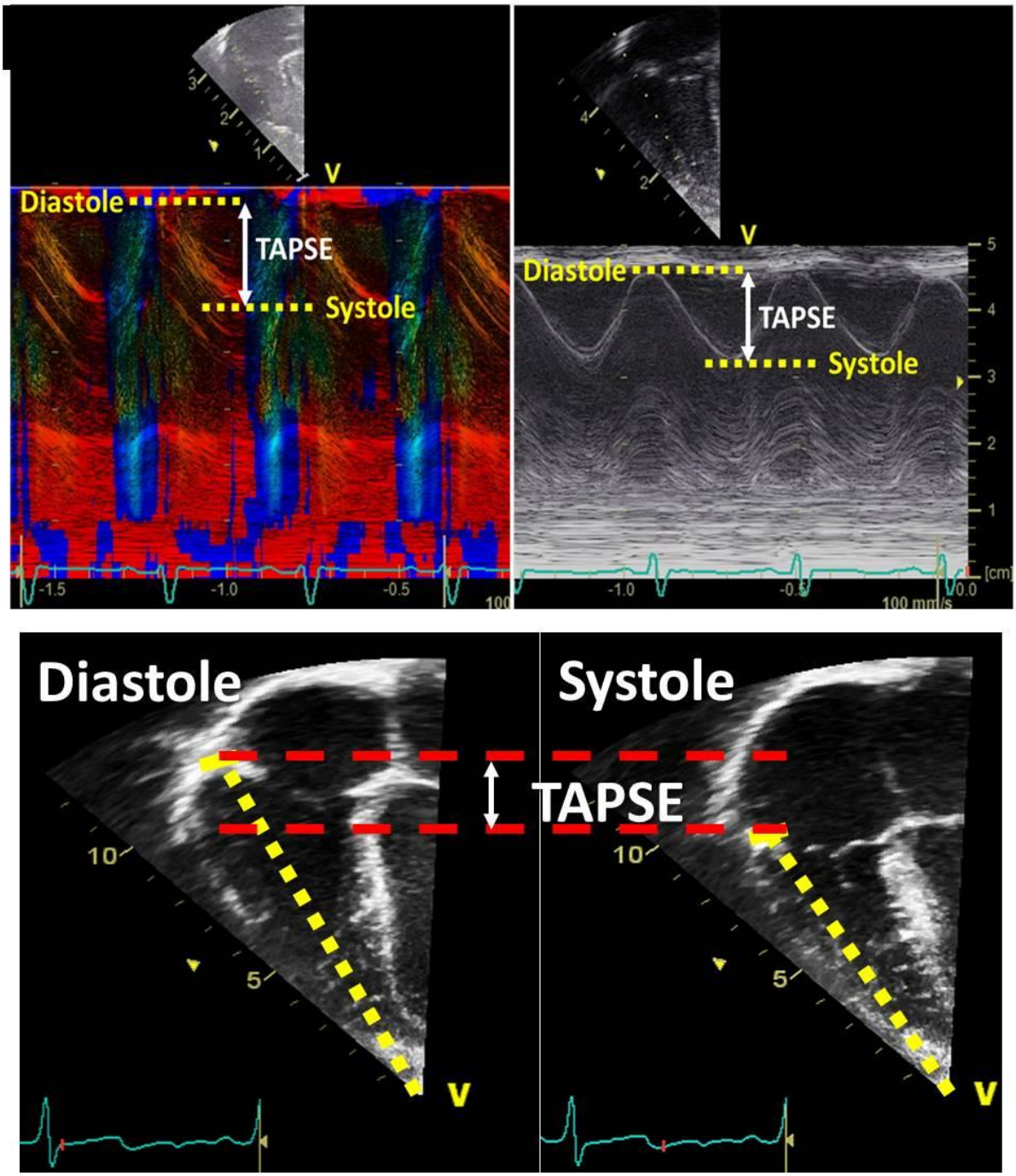

Figure 2.12 shows the movement in the tricuspid annulus from diastole to systole towards the apex with the difference noted as the TAPSE. The above image demonstrates the Tissue Doppler (TDI) and 2 dimensional M-Mode with slope calculation of the TAPSE being performed.

RV dimensions

RV dimensions were measured at end diastole from the apical 4-chamber view. Tricuspid valve annular (TVAD) diameter was measured as the distance between the two hinge points of the two visible valve leaflets. Basal diameter (RVBD) was measured as the maximal distance between the RV lateral wall and the septum parallel to the annular diameter. RV length (RVL) was measured from the midpoint of the annular diameter to the RV apex and finally, the RV mid cavity (RVMC) was measured as a line parallel to the basal diameter at the midpoint of the RV length (Figure 2.13a).

Figure 2.13: Right Ventricular Three-chamber view and Right Ventricular dimension measurement in the four chamber view.

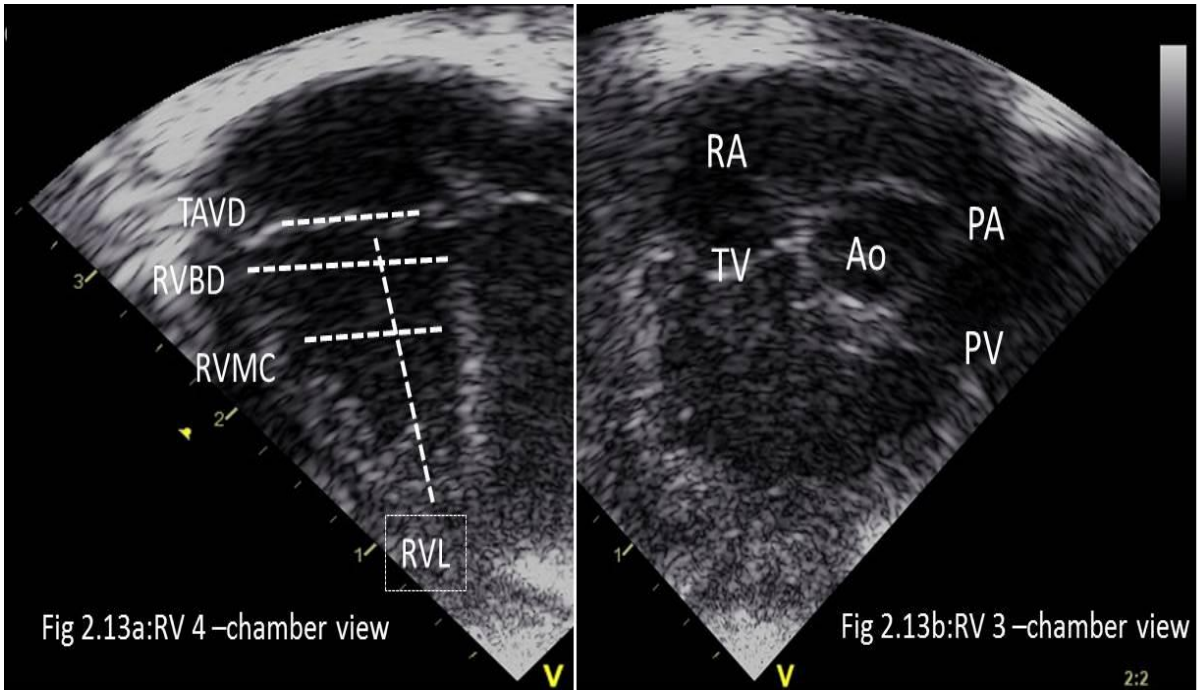

Figure 2.13a demonstrates the points at which the various aspects of RV four chamber dimensions during diastole were measured in the RV focused 4 chamber view. Figure 2.13b demonstrates the RV three-chamber view with all the identifiable structures. TV: tricuspid valve; RA: right atrium; Ao: aorta; PA: pulmonary artery; PV: pulmonary valve; TAVD: tricuspid valve annular diameter; RVBD: right ventricular basal diameter; RVMC: right ventricular mid cavity diameter; RVL: right ventricular length.

Fractional Area Change (FAC)

Global Fractional Area Change (FAC) is a measure of the change in RV cavity area from diastole to systole in two planes. This measurement is obtained by averaging FAC from the apical 4-chamber and 3-chamber views. The RV 3-chamber view is acquired by rotating the transducer anticlockwise from the standard apical 4-chamber view until the LV is no longer visible followed by anterior tilting of the probe. The RV inflow and outflow should both be visible along with a cross sectional view of the aorta between those two structures (Figure 2.13b).

The endocardial border is traced in a RV focussed 4 chamber view, including the RV trabeculations and the FAC is calculated from the formula:

$$4C\text{-}FAC = \frac{-4C\ RV\ area\ at\ end\ diastole - 4C\ RV\ area\ at\ end\ systole}{4C\ RV\ area\ at\ end\ diastole}\ X\ 100$$

Using RV 3-chamber view the 3C-FAC can be calculated using the same formula as the RV 4 chamber.

$$3C - FAC = \frac{3C\ RV\ area\ at\ end\ diastole - 3C\ RV\ area\ at\ end\ systole}{3C\ RV\ area\ at\ end\ diastole}\ X\ 100$$

2.6.3 Tissue Doppler Velocities

Tissue Doppler velocities were obtained from the apical 4-chamber view using a pulsed wave Doppler sample gate of 2 mm at the level of the annuli and the basal part of the intra-ventricular septum. We aligned the pulsed wave cursor with the longitudinal plane of motion at all times. On the tissue Doppler traces we measured peak systolic (s'), early diastolic (e') and late diastolic (a') velocities. If the e` and a` wave were fused, we measured the single wave as an a` wave. Isovolumic contraction and relaxation times and left ventricular systolic and diastolic times were also measured. The systolic to diastolic time ratio (SD ratio) was derived from the tissue Doppler traces. (Figure 2.14)

Figure 2.14: Tissue Doppler velocities of the Left Ventricle, Right ventricle and interventricular septum

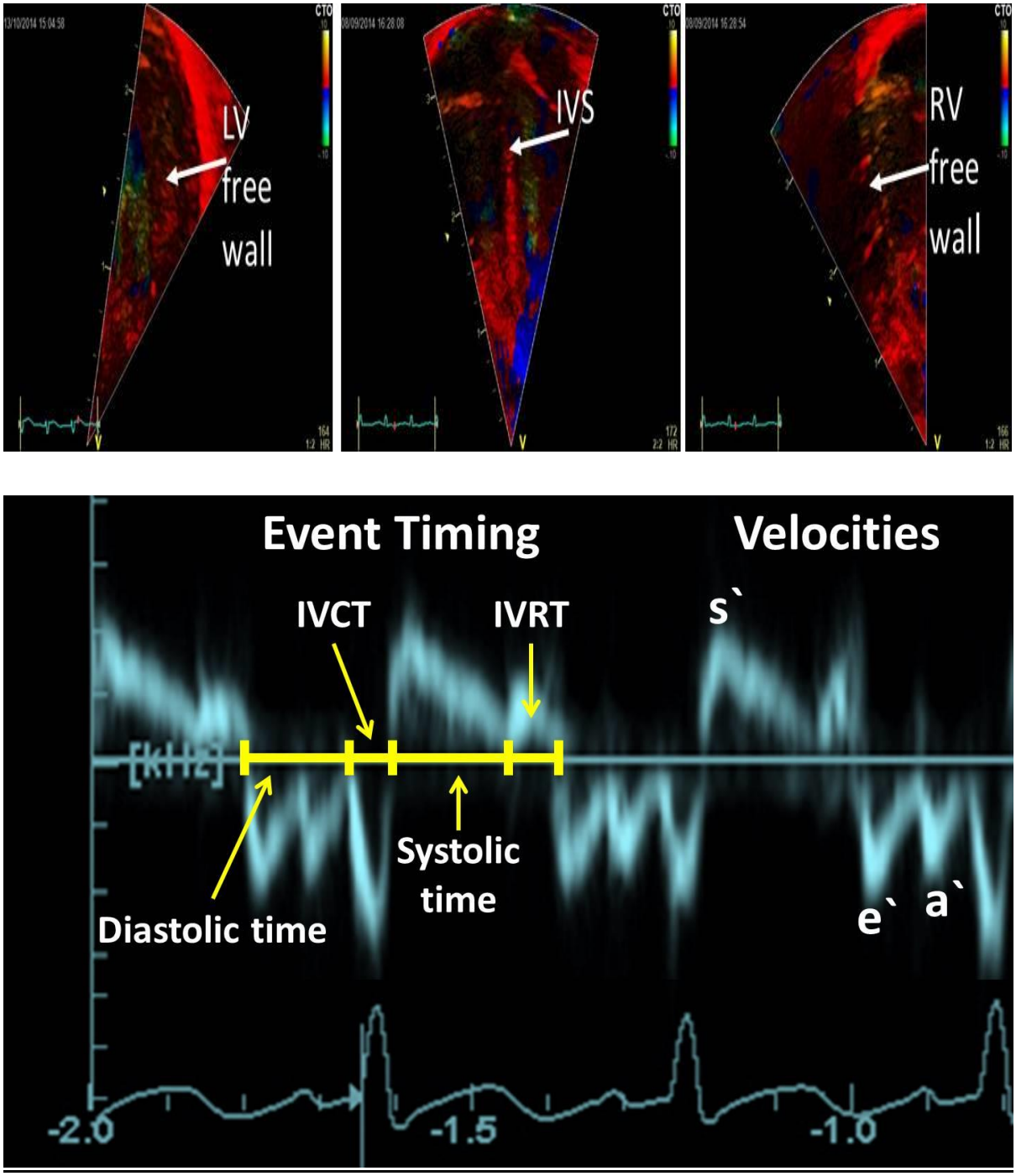

Figure 2.14 shows the focussed tissue Doppler imaging of the Left Ventricular (LV) free wall, the Intraventricular Septum (IVS) and the Right ventricular (RV) free wall. To optimise image quality and frame rate the sector width is narrowed. The bottom panel illustrates the different measurements obtained from tissue Doppler imaging.

2.7 Tissue Doppler-derived Strain and Strain Rate

The 4-chamber view was used to acquire colour-tissue Doppler images of the LV and RV free walls and the septum. Sector width was narrowed to maximally increase the frame rates. Offline analysis was performed to measure longitudinal peak systolic strain, peak systolic strain rate (SRS), early diastolic strain rate (SRE) and late diastolic strain rate (SRA) in the basal segments of the LV and RV free wall and the IVS. RV strain was obtained from the free wall following angling towards the RV to obtain a clearer image of the wall. Image quality was assessed visually prior to analysis and only images of sufficient 2-D quality were used. A single elliptical region of interest (ROI) was determined with a width of 2mm and length of 1mm. Strain length (the computational distance) was set at 6mm. Those settings have been demonstrated to be the most reliable in extremely premature infants (Poon et al., 2011). Linear drift compensation and 40 ms Gaussian smoothing was used. Event timing, including aortic and mitral valve opening and closure were determined using the electrocardiogram and pulsed wave Doppler of the flow across those valves. Strain, SR, SRE and SRA were manually determined by averaging the results of three cardiac cycles (Figure 2.15). Two cardiac cycles were used if measurement artefact was present in once cycle. If two cycles contained measurement artefact then the study was excluded from analysis. If E and A wave fusion was present in diastole then the single wave was reported as an A wave.

Figure 2.15: Tissue Doppler-derived measurement of strain and strain Rate.

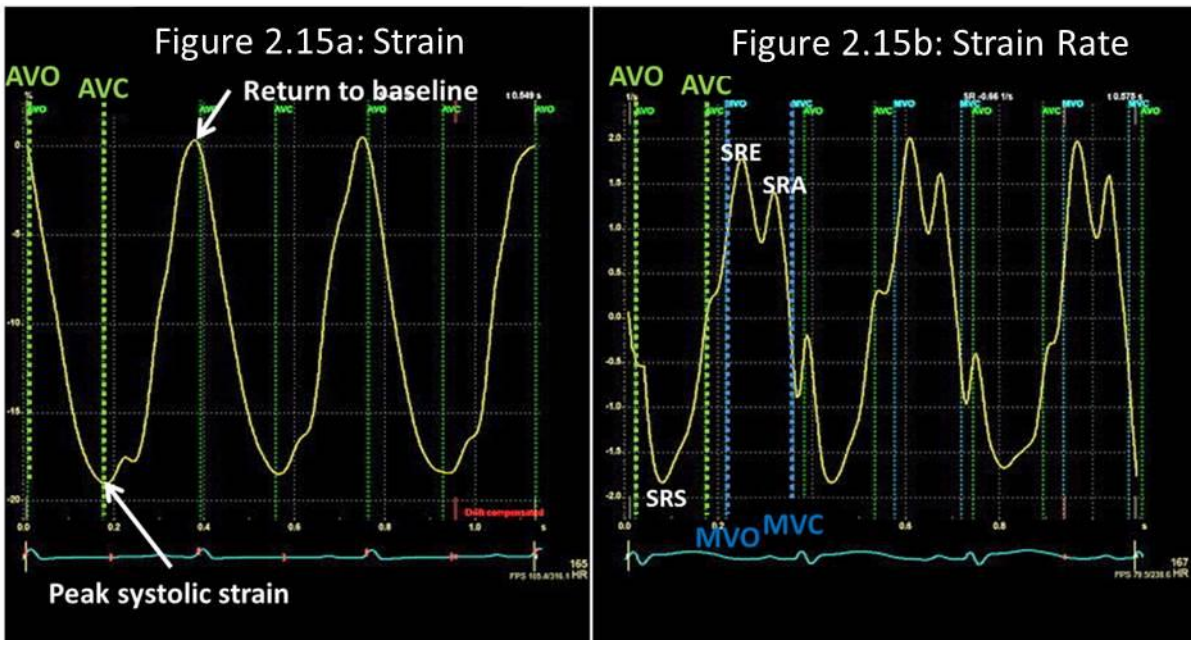

During aortic valve opening (AVO), the wall segment strain is at baseline as indicated in figure 2.15a. Peak systolic strain (figure 2.15a) is identified at the time of aortic valve closure (AVC). Figure 2.15b demonstrates peak systolic strain rate occurring in mid systole (SRS). Early (SRE) and late (SRA) diastolic strain rate occur between mitral valve opening (MVO) and mitral valve closure (MVC).

2.8 Rotational Mechanics

Left ventricular basal and apical rotation, twist, torsion, twist rate and untwist rate were measured using speckle tracking echocardiography of the parasternal short axis views of the LV base and apex (Figure 2.16). Rotation is defined as the circumferential clockwise or counter-clockwise movement of the apex and base along the long axis of the left ventricle occurring during systole (in degrees). Viewed from the apex, counter-clockwise rotation is displayed as positive and clockwise rotation is displayed as negative.

Twist was defined as the net difference between apical and basal rotation using the following formula: LV Twist (^{o}) = apical rotation (^{o}) – basal rotation (^{o}) (Figure2.17).

Left ventricular torsion is defined as twist normalized to LV end diastolic length and is calculated as follows: Torsion (^{o}/cm) = Twist (^{o}) ÷ LV end diastolic length (cm).

LV twist rate is the velocity at which twist occurs per unit time and is depicted as a positive (degrees/second). Untwisting is the motion opposite to the direction of twist occurring in diastole. LV untwist rate is the velocity of untwist during diastole per unit time and is depicted as negative (degrees/second).

The LV base and apex in short axis were obtained from the LV short axis parasternal view. The basal plane was defined as the image at the level of the mitral valve leaflets while ensuring that no left atrial tissue is visible. The apical plane was defined as the image distal to the papillary muscles. Three consecutive cardiac cycles were acquired and digitally stored as raw DICOM data for later offline analysis.

We aimed for frame rates between 120 to 130 frames per second (FPS) for all image loops to achieve a frame rate to heart rate ratio (FR/HR) of between 0.7 to 0.9. Recently,

Sanchez *et al* demonstrated that intra- and inter-observer reproducibility of measuring left and right ventricular longitudinal strain in preterm infants less than 29 weeks gestation using 2D STE was highest when the cine loops were acquired with frames rates ranging between 110 to 130 FPS and achieving a FR/HR between 0.7 to 0.9 (Sanchez et al., 2014).

Figure 2.16: Apical and Basal rotation of the Left Ventricle

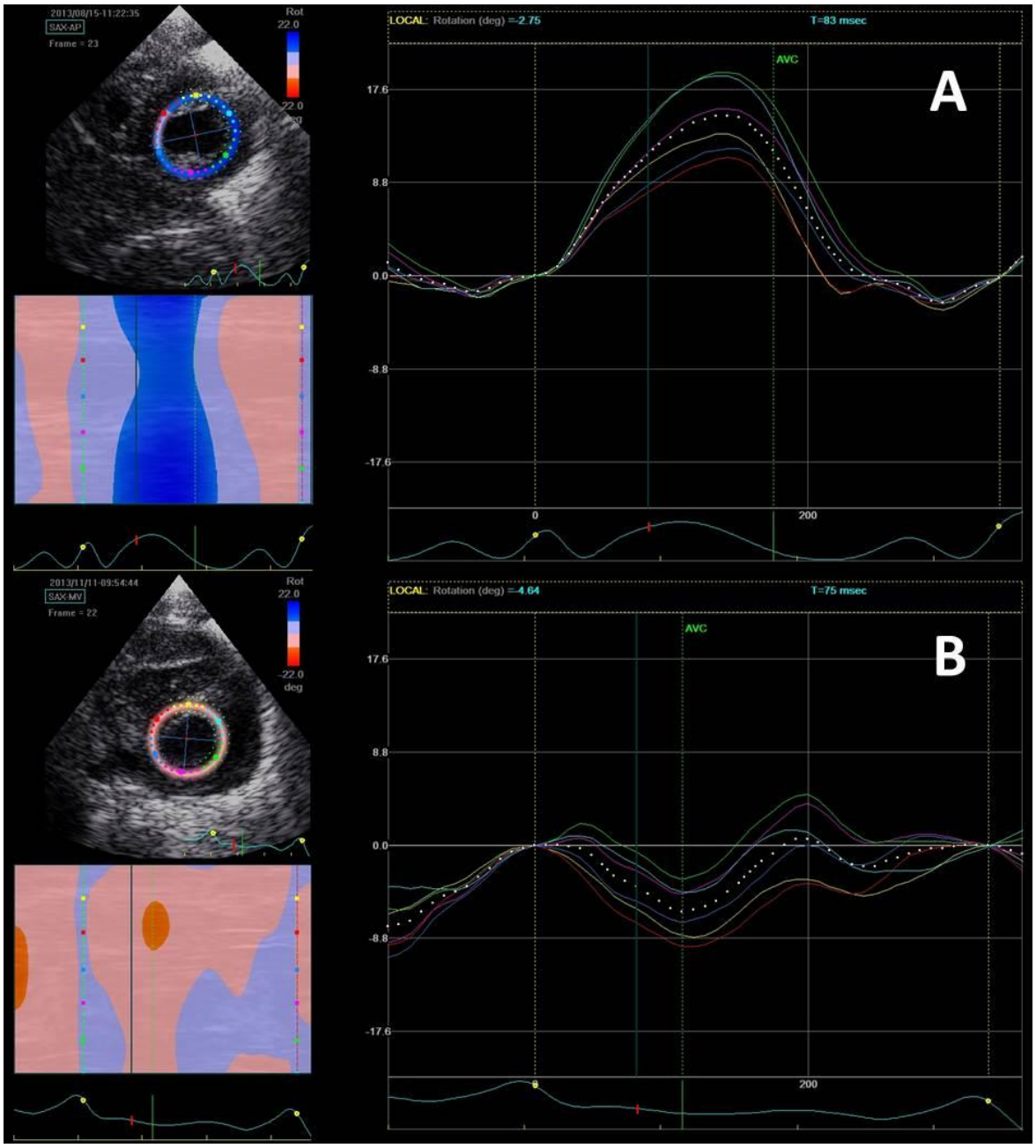

Figure2.16A depicts the rotational movement of the apex of the Left Ventricle using speckle tracking echocardiography with the positive deflection indicating counterclockwise rotation. Figure 2.16B depicts the rotational movement of the base of the Left Ventricle at the level of the mitral valve. The negative deflection indicates clockwise rotation.

Figure 2.17: Graphic representation of the Twist of the Left Ventricle.

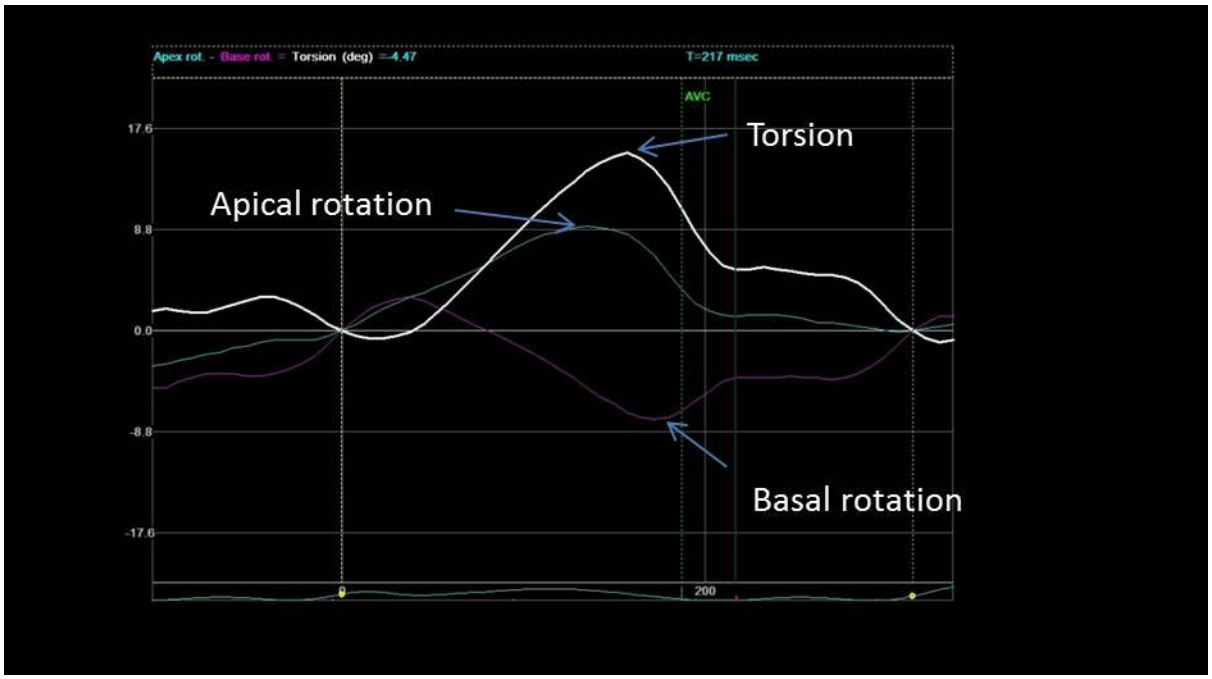

The blue line depicts the apical rotation in a counter-clockwise direction. The magenta line depicts the basal rotation in a clockwise direction. The white line depicts the resulting net twist of the left ventricle

Off line analysis

Data was stored for further offline analysis on a designated echocardiogram work station using the EchoPAC system (EchoPAC, General Electric, version 112 revision 1.3). All offline analysis was conducted by a single investigator ATJ.

2.9 Statistics

Continuous variables were presented as mean (standard deviation) if normally distributed or medians [inter-quartile range] if skewed. Categorical variables were presented as proportions (%). Serial data was tested using one or two way ANOVA with repeated measures as appropriate. Independent two group measurements were compared using independent student t-test or Mann-Whitney U test as appropriate. Correlations were assessed using Pearson's or Spearman's correlation coefficients as appropriate. Linear regression and logistic regression was carried out as appropriate to assess the independent effect of various variables on outcomes on interest. Reliability analysis was conducted using the intraclass correlation coefficient, Bland Altman Analysis and the coefficient of variation. The specific approach to statistical analysis to each chapter is described in detail. SPSS (IBM, Version 21) was used to conduct the analysis. A p value < 0.05 was considered significant.

Chapter 3 Feasibility and Reliability

3.1 Background

The use of those novel echocardiography markers in preterm infants is relatively new and as such little information is available on their feasibility and reliability in this population. Those parameters include tissue Doppler derived strain and strain rate, LV rotational mechanics, and RV – specific markers of function such as FAC and TAPSE. Recent studies have explored the feasibility and reliability of some of those markers of function in term infants with promising results. (Jain et al., 2014, Joshi et al., 2010, Takahashi et al., 2010). Based on this, as part of our protocol we aimed to assess the feasibility and reliability of using those measurements in the preterm population.

Our group has previously demonstrated the feasibility and reliability of myocardial deformation measured by STE and tissue Doppler velocities (El-Khuffash et al., 2012, Saleemi et al., 2013). This is in keeping with previous papers looking at reliability of both tissue Doppler and speckle tracking derived strain and strain rate in the preterm cohort (Poon et al., 2011, Helfer et al., 2013). Poon and his colleagues, as part of a study looking at deformation imaging assessed the reproducibility of using this technique in preterm infants and found that it was practical and reproducible especially at higher frame rates in the infants less than 34 weeks gestation. Helfer and his colleagues similarly quantified the reproducibility and reliability of tissue Doppler derived strain and strain rate in preterm infants less than 1500g and found that their results were comparable to older populations

(Helfer et al., 2013). Therefore, in this current section we aim to demonstrate the feasibility and reliability of the following parameters:

- LV, Septal and RV tissue Doppler-Derived strain and strain rate
- LV Rotational Mechanics
- RV fractional Area Change in 4 chamber, 3 chamber and global
- Tricuspid Valve Annular Plane Systolic Excursion in 2D and TDI
- RV dimension Parameters

3.2 Methods

Strain, Strain rate, RV function and dimensions

As described in the methods section the 4-chamber view was used to acquire the colour-tissue Doppler images of the LV and RV free wall and the septum for offline deformation imaging analysis. A region of interest width of 2mm and length of 2mm was used with a strain length of 6mm as this has previously been demonstrated to be the most reliable in extremely premature infants (Helfer et al., 2013, Poon et al., 2011).

RV dimensions were obtained from the RV focused 4 chamber view and the RV 3 chamber view. Fractional area change (FAC) was taken from the both the RV 3 and 4 chamber views by measuring the change in RV cavity area from diastole to systole and this was averaged to give the global FAC. Both 2D M-mode and Tissue Doppler Imaging TAPSE were obtained. TAPSE was taken for 3 consecutive cardiac cycles and an average was taken to give the TAPSE value.

Intra and inter-observer variability of strain, SR and the RV-specific function and dimension parameters were assessed using 30 randomly selected studies from the cohort. For intra-observer variability, one investigator (ATJ) performed two offline analyses 12 weeks apart to avoid recall bias while inter-observer variability was assessed by a second investigator (AK) who was blinded to the measurements of the first investigator. Intra- and inter-observer agreement was tested using Bland-Altman (BA) analysis and is presented as mean bias and 95% confidence intervals. In addition, the intra-class correlation coefficient (ICC version 2,1) was used to assess agreement.

Rotational Mechanics

Intra- and inter observer reproducibility of apical rotation, basal rotation, LV twist and torsion, LVTR and LVUTR were assessed by two observers. Twenty five studies from the cohort were randomly selected for analysis. We aimed for frame rates between 120 to 130 frames per second (FPS) for all image loops to achieve a frame rate to heart rate ratio (FR/HR) of between 0.7 to 0.9. Recently, Sanchez *et al* demonstrated that intra- and inter-

observer reproducibility of measuring left and right ventricular longitudinal strain in preterm infants less than 29 weeks gestation using 2D STE was highest when the cine loops were acquired with frames rates ranging between 110 to 130 FPS and achieving a FR/HR between 0.7 to 0.9 (Sanchez et al., 2014).

One investigator (AJ) assessed intra-observer variability by performing two offline analyses 4 weeks apart to avoid recall bias. A second investigator (AK) carried out an assessment blinded to the results of the first observer for inter-observer variability. Agreement was again assessed using the intra-class correlation coefficient version 2.1 (ICC) with agreement between investigators being further demonstrated using the Bland-Altman method by calculating the bias between the two repeated measurements (mean difference) and the 95% limits of agreement (1.96 standard deviations (SD) around the mean difference) (Bland and Altman, 1986).

3.3 Results

3.3.1 Tissue Doppler derived Strain and Strain rate and RV Function Parameters

One hundred and eight scans were carried out in fifty four infants whose median [IQR] gestation and weight at birth were 26.5 [25.8 – 28.0] weeks and 915 [758 – 1142] grams respectively. Thirty one infants (57%) were male. Twenty seven infants (50%) were singleton births with 9 (33%) twin pairs and 3 (17%) triplet sets. Forty five (83%) received a full course of antenatal steroids with 7 (13%) receiving one dose and 2 (4%) receiving none. Their median [IQR] 1 and 5 minute Apgar scores were 6 [5 – 8] and 9 [7 – 9] respectively.

The mean cord gas of the cohort was 7.33 (0.05). All infants received early surfactant prior to the first echo.

Strain measurement was feasible in the majority of infants except for ten LV (9%), 8 septal (7%) and 8 RV (7%) where images were deemed to be poor quality. Strain rate measurement was not possible in 16 LV (15%), 9 septal (8%) and 8 of RV (7%) basal segments. The mean (SD) frames rates used for image acquisition were 266 (43), 281 (43) and 279 (40) frames per second for the LV, septum and RV respectively. E/A wave fusion occurred in 28 LV (26%), 27 septal (25%) and 46 RV (43%) images. The intra- and inter-observer variability of strain and strain rate measurements are described in Table 3.1. LV free wall strain and LV SR parameters demonstrated the highest degree of intra and inter-observer variability. Septal and RV free wall strain and SR parameters were more reliable measurements. RV dimensions, TAPSE and global FAC were feasible in all studies. Overall most RV measurements are highly reproducible with the highest variability in FAC (Table 3.1 & Figure 3.1)

Figure 3.1: Intra- and Inter-observer variability of Left Ventricle, Septal and Right Ventricle Strain

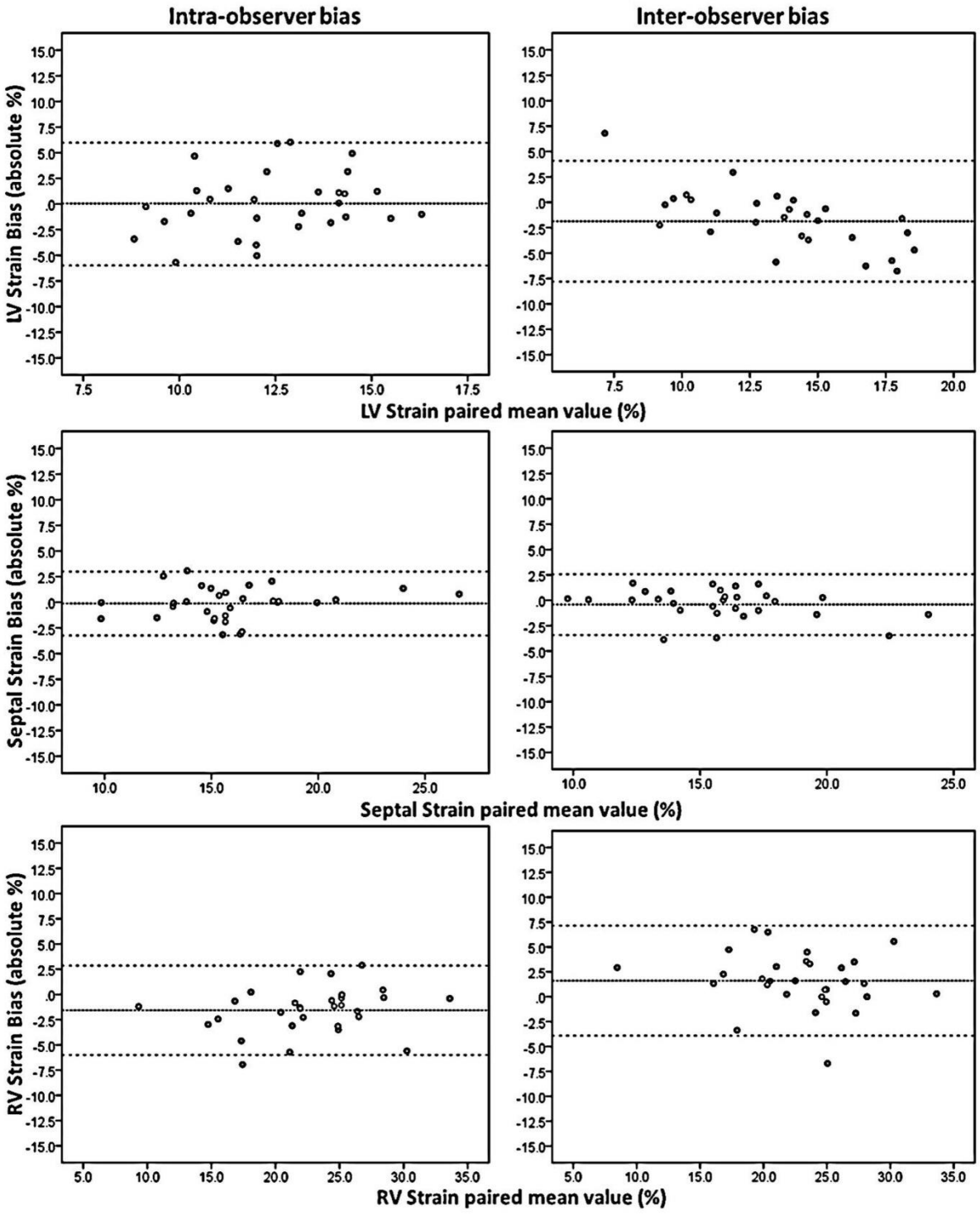

Graphs showing Bland Altman analysis of inter-observer and intra-observer variability of the strain measurements. The solid line represents the mean bias while the dotted line represents the 95% confidence intervals. RV: Right Ventricle. LV: Left Ventricle

Table 3.1: Reliability of parameters of left, septal and Right Ventricular function and dimensions

	Intra-observer variability		Inter-observer variability	
	Bias Mean (SD)	ICC (95% CI, p)	Bias Mean (SD)	ICC (95% CI, p)
Left Ventricle free wall				
Strain (%)	0.05 (3.02)	0.43(-0.23-0.73)	-1.87 (3.03)	0.69 (0.23-0.86)
Systolic Strain Rate (1/s)	0.05 (0.24)	0.93 (0.85-0.97)	-0.18 (0.49)	0.81 (0.59-0.91)
Diastolic E` strain rate (1/s)	-0.03 (0.50)	0.80 (0.49-0.92)	-0.17 (0.41)	0.78 (0.36-0.93)
Diastolic A` strain rate (1/s)	0.15 (0.85)	0.62 (0.18-0.82)	-0.25 (0.59)	0.85 (0.68-0.93)
Intraventricular Septum				
Strain (%)	-0.12 (1.59)	0.95 (0.90-0.98)	-0.42 (1.53)	0.97 (0.94-0.99)
Systolic Strain Rate (1/s)	0.00 (0.12)	0.92 (0.84-0.96)	0.02 (0.20)	0.89 (0.76-0.94)
Diastolic E` strain rate (1/s)	0.01 (0.20)	0.97 (0.93-0.99)	-0.05 (0.20)	0.98 (0.97-1.00)
Diastolic A` strain rate (1/s)	-0.01 (0.31)	0.95 (0.90-0.98)	-0.02 (0.40)	0.92 (0.84-0.96)
RV Function Parameters				
Strain (%)	-1.58 (2.26)	0.94 (0.82-0.98)	1.60 (2.82)	0.92 (0.82-0.97)
Systolic Strain Rate (1/s)	-0.13 (0.23)	0.93 (0.82-0.97)	-0.02 (0.36)	0.91 (0.81-0.96)
Diastolic E` Strain Rate (1/s)	-0.06 (0.45)	0.87 (0.60-0.96)	0.02 (0.27)	0.96 (0.89-0.99)
Diastolic A` Strain Rate (1/s)	0.26 (0.59)	0.92 (0.81-0.97)	0.40 (0.58)	0.92 (0.76-0.97)
M-mode TAPSE (mm)	0.08 (0.28)	0.98 (0.96-0.99)	-0.19 (0.38)	0.97 (0.93-0.99)
TD TAPSE (mm)	0.14 (0.41)	0.97 (0.93-0.99)	-0.27 (0.34)	0.97 (0.84-0.99)
3-Chamber FAC (%)	0.9 (6)	0.60 (0.11-0.81)	7.0 (6)	0.62 (-0.14-0.86)
4-Chamber FAC (%)	0.09 (6)	0.62 (0.26-0.81)	0.02 (6)	0.69 (0.35-0.85)
Global FAC (%)	0.5 (5.0)	0.77 (0.51-0.89)	5.0 (4.3)	0.78 (-0.47-0.93)
RV Dimension Parameters				
4C diastolic fractional area (cm^2)	0.01 (0.19)	0.90 (0.78-0.95)	0.11 (0.19)	0.83 (0.57-0.93)
3C diastolic fractional area (cm^2)	-0.07 (0.22)	0.90 (0.80-0.95)	-0.03 (0.21)	0.92 (0.83-0.96)
Annulus (mm)	-0.11 (0.47)	0.78 (0.53-0.89)	0.04 (0.54)	0.71 (0.38-0.86)
Base (mm)	0.21 (0.60)	0.92 (0.83-0.93)	0.69 (0.79)	0.81 (0.33-0.93)
Mid cavity (mm)	0.25 (0.61)	0.90 (0.78-0.96)	-0.90 (0.74)	0.89 (0.77-0.95)
RV length (mm)	-0.07 (0.97)	0.94 (0.87-0.97)	1.06 (1.06)	0.79 (0.16-0.93)

SD: Standard Deviation; ICC; infraclass correlation coefficient; 95% CI: 95% Confidence intervals; p: p values; TAPSE: Tricuspid annulus plane systolic excursion; FAC: fractional area change. 3C: three-chamber; 4C; four-chamber.

3.3.2 Feasibility and Reproducibility of Twist measurements

Fifty one infants with a mean (SD) gestation age of 26.8 weeks (1.5) and birth weight of 945 grams (233) respectively were included for reliability analysis. Thirty nine infants (77%) were delivered by cesarean section with a mean five minute Apgar score of 8 (2) and a cord pH of 7.34 (0.05). Twenty eight (55%) were male. There were 24 (47%) singleton births, 9 (35%) sets of twins and 3 (18%) sets of triplets.

Measurements of rotation, twist, torsion, LVTR and LVUTR were possible in 130 out of 153 scans (85%). In the remainder, the software was unable to track the walls due to poor image quality. The mean (SD) frame rates during the examinations were 127 (11) on Day 1, 125 (8) on Day 2 and 125 (9) on Day 5 – 7 (p=0.4). The mean (SD) FR/HR ratio was 0.83 (0.1) on Day 1, 0.76 (0.1) on Day 2 and 0.77 (0.1) on Day 5 – 7 (p=0.001). The results of the Bland-Altman analysis and intra-class correlation coefficient demonstrated better intra- and inter-observer reproducibility of apical rotation, basal rotation, twist and torsion when compared with LVTR and LVUTR (Table 3.2, Figure3.2).

Figure 3.2: Bland-Altman graphs for LV torsion twist and untwist.

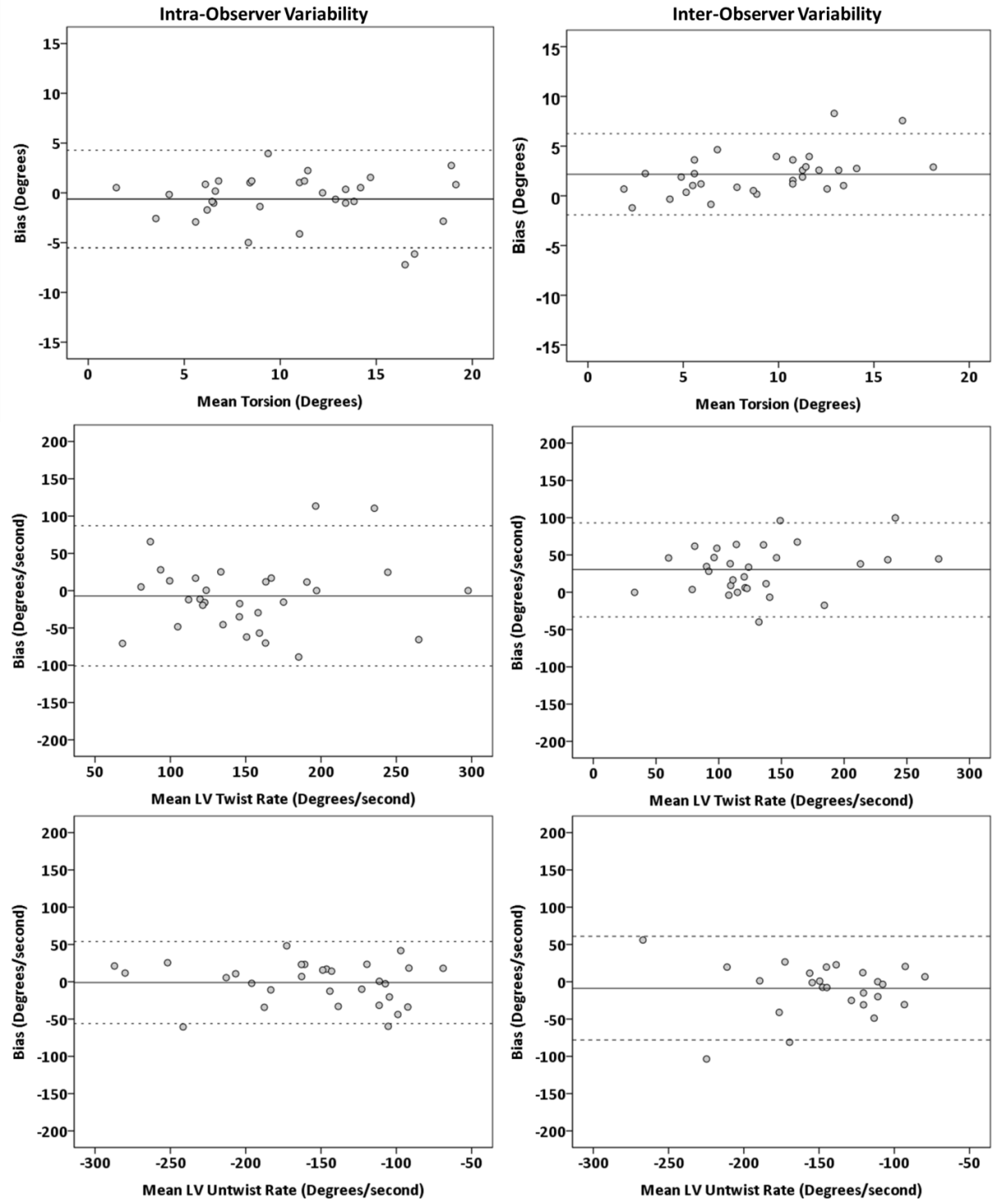

The solid black line represents the mean bias and the dotted lines represent the upper and lower limits of agreement. Torsion measurements demonstrated superior reproducibility compared with twist and untwist rates.

Table 3.2: Intra- and inter-obsevrver reliability data for the parameters.

	Intraobserver variability		Interobserver variability	
	ICC (95% CI)	**Bias (LOA)**	**ICC (95% CI)**	**Bias (LOA)**
Apical Rotation	0.96 (0.92 – 0.98)	0.04 (-1.51 – 1.59)	0.78 (0.50 – 0.90)	1.21 (-1.46 – 3.88)
Basal Rotation	0.93 (0.85 – 0.97)	0.11 (-3.77 – 3.99)	0.89 (0.78 – 0.94)	-0.21 (-2.8 – 2.34)
LV Twist	0.86 (0.74 – 0.93)	-0.13 (-2.89 – 2.63)	0.78 (0.18 – 0.92)	1.4 (-1.05 – 3.85)
LV Torsion	0.93 (0.86 – 0.97)	0.06 (-1.74 – 1.86)	0.93 (0.67 – 0.98)	0.61 (-0.85 – 2.07)
LV Twist Rate	0.83 (0.47 – 0.94)	-6 (-65 – 53)	0.70 (0.18 – 0.88)	21 (-28 – 70)
LV Untwist Rate	0.88 (0.74 – 0.94)	0 (-53 – 52)	0.73 (0.48 – 0.87)	-7 (-89 – 75)

ICC: Intraclass correlation coefficient; CI: confidence intervals; LOA: limits of agreement.
All ICC p values < 0.001.

3.4 Discussion

3.4.1 Feasibility and reproducibility of Tissue Doppler derived Strain and strain rate, RV dimensions and function

Tissue Doppler-derived strain and strain rate are newer echocardiography techniques that measure the degree of myocardial deformation (strain) and speed at which this deformation occurs (Strain rate). We chose to use the tissue Doppler-derived method for assessment of strain and strain rate in this population instead of speckle tracking due to the higher frame rates attainable with this method. The higher temporal resolution achievable with the tissue-Doppler derived method is of particular importance for the measurement of peak systolic and diastolic strain rates in this population. We demonstrated that measurement of longitudinal strain and strain rate along with RV specific function and dimension parameters is feasible in this population with the majority of the images suitable for analysis. The reproducibility of strain and SR in our study was comparable to those by Helfer et al (Helfer et al., 2013). Their group demonstrated the lowest variability to be present in the septum, and the highest variability in the left ventricular wall. We found a similar pattern in our cohort. Assessment of left ventricle free wall was less reliable with ICC values for LV strain, SRS, SRE and SRA ranging from 0.43 to 0.93. The poor reliability of LV free wall measurements is thought to relate to artifact produced by the left lung obstructing a clear view of the LV free wall. In addition, segmental FAC demonstrated moderate reliability with ICC values ranging from 0.60 to 0.69. However, global FAC showed stronger agreement of 0.77 to 0.78.

3.4.2 Feasibility and Reproducibility of LV Rotational Mechanics in Preterm Infants

Our reproducibility results for rotation, twist/torsion, and twisting rates were comparable with studies on twist in older populations (Laser et al., 2009, Zhang et al., 2010, Al-Naami, 2010, Takahashi et al., 2010). The superior reproducibility observed in the rotation and twist parameters when compared to the twist and untwist *rate* parameters (LVTR and LVUTR) may be explained by the frames rates used in our study. We obtained images with an average frame rate of 125 FPS which is slightly higher than the recommended frame rate for STE of 60-110 FPS (Biswas et al., 2013). Our use of those higher frame rates for 2D STE assessment of rotational mechanics is supported by a recent study which demonstrated superior reproducibility of LV and right ventricle deformation measurement in preterm infants when conducted using frame rates between 110 to 130 FPS and maintaining a frame rate to heart rate ratio between 0.7 to 0.9 (Sanchez et al., 2014). We attempted to strike a balance between spatial resolution (which can affect rotation and twist measurements) and temporal resolution (which can affect twist and untwist rate measurements). A relatively high frame rate may affect the software's ability to adequately track the speckles within the ROI thus compromising absolute rotation and twist measurements. Relatively lower frame rates run the risk of missing peak rotational rates thereby reducing the reproducibility of these values. Further studies are needed to determine the ideal frame rates needed to assess rotation, twist and twist / untwist rates in this population.

Rotational mechanics of the left ventricle offer novel insights into myocardial performance. Two dimensional STE is a relatively novel technique that can be applied to preterm infants at the bedside to measure those rotational mechanics. Demonstration of feasibility, reproducibility in addition to the examination of changes occurring in the first

week of life in cohort of haemodynamically stable preterm population may pave the way for the application of those parameters to infants with disease states and those with haemodynamic instability

3.5 Conclusion

Both Tissue Doppler derived strain and strain rate, RV functional parameters such as FAC and TAPSE and RV dimensions as well as rotational mechanics such as twist, untwist and torsion are feasible and reliable in preterm infants less than 29 weeks gestation. Establishing feasibility and reliability of these parameters is an important step before demonstrating reference ranges and longitudinal changes in this population.

Chapter 4: Longitudinal changes in strain and strain rate in preterm infants

4.1 Introduction

There has been a recent interest in characterising myocardial function in preterm infants using newer echocardiography methods of assessment such as tissue Doppler (TD) derived strain and strain rate (Helfer et al., 2013, Nestaas et al., 2009, Levy et al., 2015, Jain et al., 2014). TD-derived deformation measurement uses high frame rates to assess regional wall function and may help to provide more accurate information on systolic and diastolic function, particularly in preterm infants with high heart rates (Helfer et al., 2013). Longitudinal systolic strain, systolic and diastolic strain rate have proven to be valuable diagnostic tools in adults, children and term infants (Ersboll et al., 2013, Czernik et al., 2013, Kailin et al., 2012, Marcus et al., 2011a, Khoo et al., 2011). In addition, left ventricular (LV) and RV dimension assessment is becoming increasingly recognised as important components of a comprehensive functional assessment (Mertens et al., 2011b). In Chapter 3, we reported the feasibility and reproducibility of obtaining those measurements in infants less than 29 weeks gestation over the first 48 hours of age.

There remains a paucity of data on the longitudinal evolution of those markers over the first week of age (including the first 48 hours – the transitional period) and at 36 weeks post menstrual age (PMA). The influence of loading conditions during the transitional period, the effect of a patent ductus arteriosus, and the difference in those markers between infants with and without chronic lung disease (CLD) warrant further study. Those measurements could provide new insights into the post-natal adaptation of the preterm

heart in the face of various stressors. We aimed to describe the change in these functional parameters and dimensions over the first week of life and at 36 weeks PMA, examine the effect of early systemic vascular resistance (SVR), the influence of a haemodynamically significant patent ductus arteriosus (PDA), and the effect of chronic lung disease (CLD) on those parameters in infants less than 29 weeks gestation.

4.2 Methods

4.2.1 Study population

Infants less than 29 weeks gestation were prospectively recruited from the Neonatal Intensive care Unit at the Rotunda Hospital, Dublin, Ireland. Written informed consent was obtained from all participants before enrolment in the study and ethical approval was obtained from the Rotunda Hospital Research and Ethics Board. Infants were recruited between January 2013 and December 2014. Infants were excluded if they had a suspected or definite chromosomal abnormality or had congenital heart disease other than a PDA or a patent foramen ovale (PFO). Our unit currently adopts a conservative approach to PDA management. Medical and/or surgical treatment is only instituted beyond the second week of life in infants on prolonged invasive ventilation. Perinatal variables, baseline characteristics and outcome data were collected from the infants chart including chronic lung disease (defined as the need for oxygen or respiratory support at 36 weeks gestational age (Kinsella et al., 2006)), and death.

4.2.2 Echocardiography Assessment

Echocardiographic assessment is defined in more detail in Chapter 2 describing the methodology of this research study. Specifically with respect to Longitudinal Strain and strain rate, echocardiography was carried out at a median [interquartile range] of 10 hours [7 – 13] (Day 1), 43 hours [38 – 46] (Day 2), 143 hours [125 – 161] (Day 5 – 7) and at a corrected gestation of 36 weeks. Echocardiography was performed using the GE Vivid I or Vivid S6 ultrasound machines and a 10S or 12S probe (at a frequency of 8Mz) during the first week of age, and a 7S probe (at a frequency of 3 - 4 MHz) at 36 weeks PMA (Mertens et al., 2011b). Images were stored as raw DICOM data and archived for later offline analysis using the EchoPac software (GE, version 112, revision 1.3).

Conventional echocardiography measurements were obtained in the study infants including left ventricular output (LVO); PDA diameter in 2D measured at the pulmonary end; direction of flow and PDA shunt gradient; mitral valve inflow velocity time integral (MV VTI); and left atrial to aortic root ratio (LA:Ao) (Ramos et al., 2010). The presence of a patent foramen ovale and the shunting across it and the presence of tricuspid regurgitation (TR) were also noted. Systemic vascular resistance (SVR) was calculated using the formula: (mean systemic BP – mean tricuspid valve inflow pressure gradient estimated as 4 mmHg) / LVO (Noori et al., 2007a). Tissue Doppler velocities (TDI) was obtained as mentioned in the methodology section for the LV lateral wall, the intraventricular septum and the RV free wall.

Peak basal systolic longitudinal strain (BLS), peak basal systolic longitudinal strain rate (SRs), early diastolic longitudinal strain rate (SRe) and late diastolic strain rate (SRa) were measured at the basal segment of the LV lateral wall, the basal segment of the septal wall and the basal segment of the RV free wall all imaged from the apical four-chamber view

using Tissue Doppler derived deformation imaging as previously described. If SRe and SRa fusion occurred we labelled the single wave as an SRa wave (Voigt et al., 2015)

LV posterior wall thickness (LVPW), LV septal wall thickness (LVSW), and LV internal diameter (LVID) were all obtained using m-mode of the long axis parasternal view at the level of the mitral valve (MV) leaflet tips. MV annular diameter and LV length were obtained from the apical 4-chamber view. RV basal diameter, mid cavity diameter and length in addition to tricuspid valve annular diameter were all obtained from a RV-focussed four chamber view as we previously described in chapter 2. All dimension values were measured during the frame just before the MV completely closes at end-diastole (Voigt et al., 2015).

LV dimensions were obtained in diastole from the long axis parasternal view including LV septal wall thickness (LVSW), LV internal diameter (LVID), and LV posterior wall thickness (LVPW). RV dimensions were measured from a RV focused 4 chamber view during end diastole. For RV dimensions, the tricuspid valve annular diameter was measured as the distance between the two hinge points of the tricuspid valve leaflets. RV basal diameter was measured as the maximal distance between the RV free wall and the septum parallel to the annular diameter. The RV length was measured from the midpoint of annular diameter to the RV apex.

The influence of gestation, birthweight, heart rate and SVR on the measured parameters on Day 1 was assessed. In addition, the influence of a PDA > 1.5 mm on Day 5 – 7 was also examined. We defined a haemodynamically significant PDA as being one that is greater than 1.5mm in size(Zonnenberg and de Waal, 2012). The influence of a PDA > 1.5 mm was compared with markers of increased LV preload (pulmonary vein Diastolic wave, PVd) at 5-7days of age. This time-point was chosen as it was felt this would accurately

reflect those infants who have a persistent PDA. Finally the difference in the parameters in infants with and without CLD at 36 weeks PMA was assessed.

4.2.3 Statistical Analysis

Continuous variables were presented as mean (standard deviation) if normally distributed or medians [inter-quartile range] if skewed. Categorical variables were presented as proportions (%). Serial data were tested using one way ANOVA with repeated measures and values were compared to the previous measurement (Day 2 vs. Day 1, Day 3 vs. Day 2, and 36 weeks PMA vs, Day 3) using the Bonferroni adjustment. Independent two group measurements were compared using independent student t-test or Mann-Whitney U test as appropriate. Correlations were assessed using Pearson's or Spearman's correlation coefficients as appropriate. Linear regression was carried out to assess the independent effect of important perinatal variables and clinical characteristics (Gestation, SVR, gender, chorioamnionitis, pre-eclampsia, antepartum haemorrhage, prolonged rupture of membranes and 5 minutes Apgar score) on function during Day 1. In addition, linear regression was carried out to assess the independent effect of CLD on myocardial function while adjusting for gestation at birth and the use of antenatal steroids. SPSS (IBM, Version 21) was used to conduct the analysis. A p value < 0.05 was considered significant.

4.3 Results

One hundred and five infants with a median [IQR] gestation and birthweight of 27.1 [26.0 – 28.1] weeks and 965 [785 – 1153] grams respectively were studied. Sixty two (59%) were male and 74 (71%) were delivered by caesarean section. Ninety nine infants (94%) received at least one course of antenatal steroids. Their mean cord pH was 7.34 (0.07) and their median 5 minute Apgar score was 9 [7 – 9]. There was a relatively low rate of chorioamnionitis (n=9, 9%), pre-eclampsia (n=5, 5%), and antepartum haemorrhage (n=17, 16%). Thirty five infants (33%) had prolonged rupture of membranes prior to delivery. Thirteen infants (12%) had a weight less than the 10^{th} centile for gestation. Ten infants (10%) died prior to hospital discharge.

Complete studies were available for 102 infants (97%) on Day 1, 105 (100%) on Day 2 and 101 (96%) on Day 5 – 7. Fifty-eight infants were transferred to a peripheral hospital prior to 36 weeks PMA leaving 47 infants (45%) available for assessment at that time point. There was no difference in gestation, birthweight, 5 minute Apgar score, or cord pH between infants who were transferred and those who stayed until 36 weeks PMA (data not shown). The clinical characteristics and conventional echocardiography measurements during each time point are illustrated in Table 4.1. There was no difference in any of the conventional function values between infants invasively ventilated and those on CPAP during the first three time points. In addition, there was no correlation between mean airway pressure and any of the functional values.

Table 4.1: Clinical parameters at the time of the echocardiogram over the first week of life

	Day 1	Day 2	Day 5 – 7	p
Hours of Life	10 [7 – 13]	43 [38 – 46]*	142 [125 – 161]*	<0.001
Heart rate	155 (14)	163 (12)*	165 (13)*	<0.001
Systolic BP (mmHg)	46 (8)	53 (9)*	57 (9)*	<0.001
Diastolic BP (mmHg)	28 (7)	32 (8)*	32 (8)*	<0.001
Mean BP(mmHg)	35 (6)	40 (8)*	40 (7)*	<0.001
Mean Airway Pressure (cmH_2O)	8 (2)	8 (2)	8 (1)*	<0.001
Oxygen %	21 [21 – 60]	21 [21 – 65]	21 [21 – 49]	0.6
Invasive ventilation	56 (53%)	33 (31%)*	25 (24%)*	<0.001
Fluid Intake (ml/kg/day)	83 (8)	122 (23)*	171 (17)*	<0.001
pH	7.33 (0.06)	7.31 (0.07)*	7.30 (0.06)*	0.002

Hours of life and oxygen are presented as medians [inter-quartile range].The remainder of data are presented as means (standard deviation) or absolute values and (percentages). BP: blood pressure. Invasive ventilation refers to intermittent positive pressure ventilation. None of the infants were on high frequency oscillation. All non-invasively ventilated infants were on continuous positive pressure ventilation during the study period. * p value < 0.05 compared with baseline (one way ANOVA with repeated measures with Bonferroni adjustment)

Table 4.2: Conventional Echocardiography parameters and Markers of pulmonary vascular resistance

	Day 1 n=102	Day 2 n=105	Day 5 – 7 n=101	36 weeks n=47	p
LVO (mls/kg/min)	147 (60)	201 (72)*	229 (89)*	234 (49)*	<0.001
Shortening Fraction (%)	35 (6)	38 (5)*	41 (6)*	39 (7)	0.002
Ejection Fraction (%)	58 (7)	61 (7)*	62 (8)*	58 (6)	0.003
SVR	251 [196 – 338]	188 [146 – 288]*	188 [127 – 259]*	Not Calculated	<0.001
Number (%) PDA	99 (94%)	90 (95%)	69 (66%)	36 (77)	<0.001
PDA Diameter (mm)	2.4 [2.0 – 2.9]	2.8 [2.3 – 3.2]*	2.8 [2.2 – 3.2]*	2.8 [2.3 – 3.2]	0.04
Bidirectional shunt	38 (36%)	13 (12%)	5 (5%)	0	<0.001
PDA Diastolic Velocity (m/s)	1.26 [0.83 – 1.66]	1.42 [1.10 – 2.1]*	2.0 [1.45 – 2.7]*	2.7 [1.52 – 3.3]*	<0.001
PDA Systolic Velocity (m/s)	0.26 [-0.45 – 0.84]	0.46 [0.22 – 1.11]*	0.58 [0.25 – 1.36]*	0.79 [0.37 – 1.3]	<0.001
LA:Ao Ratio	1.32 (0.25)	1.46 (0.31)*	1.51 (0.37)*	1.47 (0.25)*	<0.001
PFO	75 (71%)	82 (78%)	66 (63%)	12 (26%)	<0.001
PFO Shunt (m/s)	0.41 [0.33 – 0.49]	0.56 [0.42 – 0.72]*	0.53 [0.41 – 0.71]*	0.70 [0.64 – 0.78]*	<0.001
PAAT (ms)	42 (9)	47 (11)*	52 (12)*	51 (11)*	<0.001
RVET (ms)	155 (21)	160 (26)	161 (31)	195 (20)*	<0.001

Data is presented as medians [inter-quartile range], means (standard deviation) or proportions (percentages). * p value < 0.05 compared with baseline (one way ANOVA with repeated measures with Bonferroni adjustment). LVO-Left ventricular output, SVR-systemic vascular resistence, PDA-Patent ductus arteriosus, PFO-patent foramen ovale, PAAT-Pulmonary artery acceleration time, RVET- Right ventricular ejection time

4.3.1 Image Quality and Measurement feasibility

On Day 1, deformation values were measurable in 92 (90%) LV lateral wall, 93 (91%) septal, and in 97 (95%) RV basal segments. SRe/SRa fusion occurred in 29 (28%) LV lateral wall, 18 (18%) septal and in 40 (39%) RV basal segments. The remainder of the time points during the first week of life demonstrated similar quality and feasibility characteristics. At 36 week PMA 39 (83%) of LV lateral wall images, and all of the septal and RV images were analysable.

4.3.2 Longitudinal Changes in Function and Dimensions

The change in LV, septum and RV function are illustrated in Table 4.3 and 4.4. These show that using Tissue Doppler imaging (TDI), TAPSE and RV FAC, there was a longitudinal increase in values up to 36 weeks PMA. Table 4.5 and Figure 4.1 show the changes in Tissue Doppler derived deformation parameters over the 4 time points up to 36 weeks PMA. LV, Septal and RV strain values significantly increased until 36 weeks PMA. Strain rate values however (with the exception of LV SRe and SRa which demonstrated no change) only increased over the first week of age (Table 4.5). LVSW and LVPW did not change over the first 2 days of age but were significantly higher on Day 5 – 7 and 36 weeks PMA. LV cavity dimensions demonstrated a change over the first two days and between Day 5 – 7 and 36 weeks PMA. Conversely, there was no change in RV dimensions over the first week of age with values only significantly higher than Day 5 – 7 at 36 weeks PMA (Table 4.6).

Table 4.3: LV and Septal Function values over the four time points

	Day 1 n=102	Day 2 n=105	Day 5 – 7 n=101	36 weeks n=47	p
LV TDI (cm/s)					
s`	2.7 (0.8)	3.2 (0.7)*	3.9 (1.0)*	4.6 (0.9)*	<0.001
e`	3.4 (1.4)	4.3 (1.3)*	4.3 (1.1)*	6.5 (1.9)*	<0.001
a`	4.0 (1.6)	4.9 (1.6)*	5.4 (1.8)*	6.9 (2.7)*	<0.001
Septal TDI (cm/s)					
s`	2.6 (0.6)	2.6 (0.6)	2.9 (0.6)*	3.8 (0.8)*	<0.001
e`	2.8 (0.8)	3.7 (1.2)*	3.7 (0.9)*	5.6 (1.3)*	<0.001
a`	3.8 (1.3)	4.9 (1.6)*	5.6 (1.4)*	7.8 (2.1)*	<0.001
LV event times and dimensions					
Heart Rate	155 (14)	163 (12)*	165 (13)*	154 (14)	<0.001
IVCT (ms)	58 (14)	48 (13)*	44 (13)*	48 (10)*	<0.001
IVRT (ms)	60 (13)	53 (12)*	51 (12)*	49 (12)*	<0.001
Systolic Time (ms)	140 (18)	148 (19)*	139 (16)	164 (15)*	<0.001
Diastolic Time (ms)	125 (22)	119 (22)	123 (20)	128 (27)	0.05
SD ratio	1.1 (0.2)	1.3 (0.2)*	1.1 (0.2)	1.3 (0.3)*	<0.001

* p value < 0.05 compared with baseline day 1 values (one way ANOVA with repeated measures with Bonferroni adjustment)

Table 4.4: RV Function values over the four time points

	Day 1 n=102	Day 2 n=105	Day 5 – 7 n=101	36 weeks n=47	p
RV TDI (cm/s)					
s`	3.6 (0.9)	4.6 (1.0)*	5.4 (0.9)*	7.3 (1.2)*	<0.001
e`	3.8 (1.2)	5.1 (1.5)*	5.5 (1.2)*	8.1 (2.5)†	<0.001
a`	7.1 (2.1)	8.6 (2.0)*	9.8 (2.3)*	12.9 (3.8)	<0.001
RV TAPSE and FAC					
TD TAPSE (mm)	4.8 (1.1)	6.0 (1.1)*	6.6 (1.0)*	11.1 (1.6)	<0.001
Normalised TD TAPSE (mm)	2.5 (0.6)	3.1 (0.5)*	3.4 (0.5)*	3.8 (0.6)*	<0.001
3-Chamber FAC (%)	38 (10)	46 (8)*	49 (7)*	51 (9)*	<0.001
4-Chamber FAC (%)	31 (10)	41 (8)*	44 (9)*	45 (8)*	<0.001
Global FAC (%)	34 (9)	43 (6)*	46 (7)*	48 (6)*	<0.001

† Only 8 infants without e:a fusion. * p value < 0.05 compared with baseline (one way ANOVA with repeated measures with Bonferroni adjustment)

Table 4.5: Longitudinal Changes in Deformation parameters

	Day 1 n=102	Day 2 n=105	Day 5 – 7 n=101	36 weeks n=47	p
Left Ventricle					
Strain (%)	-12.2 (2.8)	-12.8 (2.8)	-12.7 (2.2)	-15.0 (2.2)*	<0.001
Systolic SR (1/s)	-1.5 (0.5)	-1.7 (0.6)*	-1.7 (0.5)*	-1.8 (0.5)*	0.02
Early Diastolic SR (1/s)	1.6 (0.8)	2.1 (0.6)	2.1 (0.7)	2.1 (0.9)	0.2
Late Diastolic SR (1/s)	2.6 (0.8)	2.7 (1.0)	2.7 (0.9)	3.2 (1.2)	0.08
Septum					
Strain (%)	-15.5 (3.0)	-17.4 (3.5)*	-17.9 (3.1)*	-20.6 (3.6)*	<0.001
Systolic SR (1/s)	-1.6 (0.3)	-1.9 (0.4)*	-2.0 (0.4)*	-2.1 (0.4)*	<0.001
Early Diastolic SR (1/s)	1.7 (0.6)	2.1 (0.6)*	2.1 (0.7)*	2.0 (0.6)	0.001
Late Diastolic SR (1/s)	2.3 (0.8)	2.7 (1.0)*	2.7 (0.9)*	2.7 (1.0)*	0.03
Right Ventricle					
Strain (%)	-22.8 (4.8)	-24.3 (4.7)*	-25.1 (4.9)*	-28.0 (5.5)*	0.001
Systolic SR (1/s)	-2.1 (0.5)	-2.5 (0.7)*	-2.9 (0.7)*	-3.0 (0.7)*	<0.001
Early Diastolic SR (1/s)	2.4 (0.8)	2.6 (0.7)	2.7 (0.9)	2.9 (0.9)	0.4
Late Diastolic SR (1/s)	3.6 (1.0)*	4.4 (1.3)*	4.3 (1.3)*	4.6 (1.6)*	0.008

Values are presented as means (SD). * p value < 0.05 compared with baseline (one way ANOVA with repeated measures with Bonferroni adjustment)

Figure 4.1 Longitudinal strain of the Left ventricle (LV), septum and Right ventricle (RV)

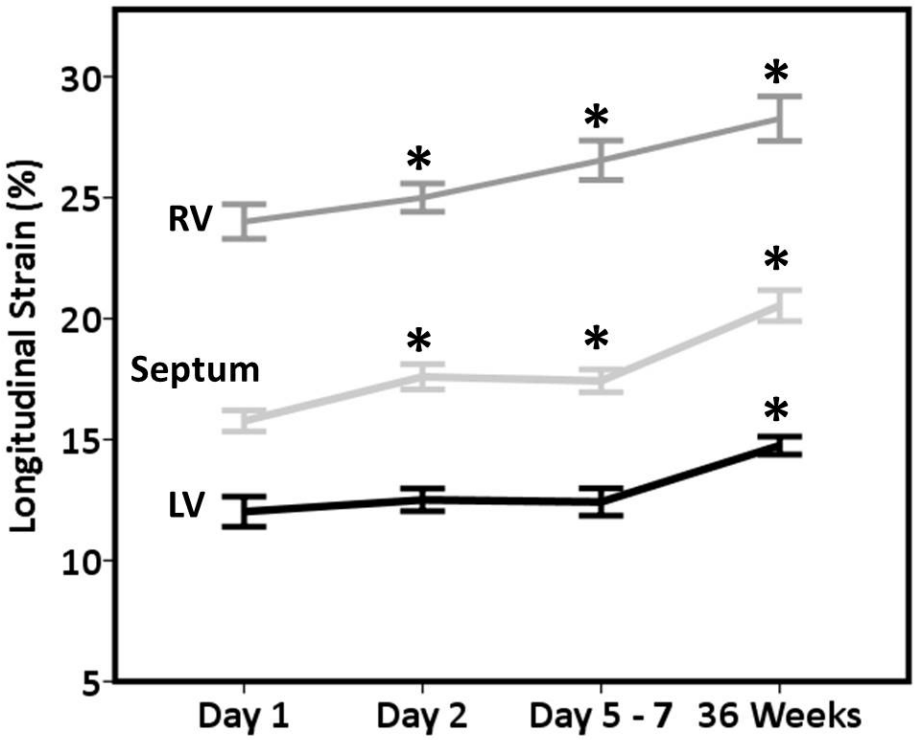

GraphicalG representation of absolute strain values of the Right Ventricle (RV), Septum and Left Ventricle (LV) from day 1 of life to 36 weeks postnatal gestation. Error bars represent ± 1 standard error. * p value < 0.05 compared with baseline (Day1).

Table 4.6: Longitudinal changes in dimension parameters

	Day 1	Day 2	Day 5 - 7	36 weeks	P
Left Ventricle					
Septal Wall Thickness (mm)	2.6 (0.6)	2.6 (0.6)	2.9 (0.6)*	3.8 (0.8)*	<0.001
Posterior wall thickness (mm)	2.5 (0.6)	2.6 (0.7)	2.9 (0.6)*	3.9 (0.7)*	<0.001
Internal Diameter (mm)	11.3 (2.0)	12.2 (2.0)	12.2 (2.1)	16.7 (1.9)*	<0.001
Mitral Annular Diameter (mm)	5.2 (0.9)	5.5 (0.7)*	5.9 (0.9)	7.9 (0.9)*	<0.001
Length (mm)	16.8 (2.6)	17.4 (1.9)*	18.0 (2.9)	24.9 (2.1)*	<0.001
Right Ventricle					
Tricuspid Annular Diameter (mm)	6.4 (0.9)	6.4 (0.8)	6.4 (0.7)	8.8 (1.2)*	<0.001
Basal Diameter (mm)	11.1 (1.3)	11.1 (1.5)	11.1 (1.4)	15.0 (2.0)*	<0.001
Mid Cavity Diameter (mm)	9.5 (1.3)	9.3 (1.5)	9.3 (1.5)	12.6 (1.5)*	<0.001
Length (mm)	18.9 (2.4)	19.1 (2.5)	19.6 (2.3)	29.0 (3.3)*	<0.001

Values are presented as means (SD). p values represents one way repeated measures ANOVA. * indicates a p value < 0.05 compared with previous value: Day 2 vs. Day 1, Day 3 vs. Day 2, and 36 weeks PMA vs, Day 3.

4.3.3 Influence of Gestation, Birthweight, Heart Rate and Systemic Vascular Resistence (SVR) on Day 1 Values

Table 4.7 shows the correlation between SVR on Day 1 and functional parameters. There was a weak but significant negative correlation between SVR and absolute LV BLS values ($r=-0.27$, $p=0.01$) indicating that a higher SVR is associated with BLS values closer to 0, SVR and LV SRe ($r=-0.4$, $p=0.001$) and SVR and absolute septal BLS values($r=-0.37$, $p=0.007$) also indicating that a higher SVR is associated with BLS values closer to 0. On multiple linear regression, SVR (standardised $\beta=-0.4$, $p=0.001$) and gestation (standardised $\beta=0.3$, $p=0.005$) had an independent effect on LV BLS when adjusting for other variables (gender, chorioamnionitis, pre-eclampsia, antepartum haemorrhage, prolonged rupture of membranes, 5 minute Apgar score). There was a similar association between SVR and gestation with septal BLS (SVR standardised $\beta=-0.5$, $p<0.001$; Gestation standardised $\beta=0.3$, $p=0.02$). LV, septal and RV tissue Doppler systolic velocities (s') had a stronger negative correlation with SVR when compared to deformation measurements (Table 4.7).

Table 4.7: Correlation between Systemic Vascular Resistance and functional parameters on day 1 of life

Parameter	r	P value
SF	-0.24	0.02
EF	-0.32	0.002
LV s`	-0.49	<0.001
Septal s`	-0.63	<0.001
RV s`	-0.51	<0.001
RV FAC	-0.54	<0.001
Normalised TAPSE	-0.53	<0.001
LV Strain	-0.27	0.01
LV Systolic Strain Rate	-0.18	0.1
Septal Strain	-0.37	<0.001
Septal Systolic Strain Rate	-0.17	0.1
RV Strain	-0.18	0.08
RV Systolic Strain Rate	-0.20	0.06

Table 4.7 describes the different functional echocardiographic parameters of the Left ventricle (LV), Septum and Right ventricle (RV) correlating them to SVR on Day 1 of life. SF-shortening fraction, EF-Ejection fraction, FAC- Fractional Area Change, TAPSE- Tricuspid Annular Plane Systolic Excursion,

There was no correlation between gestation or birthweight with any of the functional measurements during the Day 1 scan. There was a weak correlation between LV SRs and heart rate ($r=0.4$, $p<0.001$) and between RV SRs and heart rate ($r=0.3$, $p=0.01$). There was no correlation on Day 1 functional measurements and any of the antenatal factors (pre-eclampsia, antenatal steroids, septic risk factors, antepartum haemorrhage, use of $MgSO_4$), gender, mode of delivery or small for gestational age.

Comparing the functional parameters on day 2 of life to the presence of a PDA we found that there was no correlation with either the presence or absence of a PDA or with those that had a significant PDA defined as a PDA greater than 1.5mm in diameter.

4.3.4 Relationship between a PDA on Day 5 - 7 and Functional Measurements

On Day 5 – 7, 64 infants (61%) had a PDA with a diameter > 1.5 mm. There was no difference in gestation between those with and without a PDA > 1.5 mm [26.8 (1.3) vs. 26.3 (1.4) weeks, p=0.06]. Infants with a PDA > 1.5 mm had a larger LVID (12.7 (2.3) vs 11.1 (1.5) mm, p<0.001), but there was no difference in LVSW and LVPW. In addition, infants with a PDA > 1.5 mm had a higher LVO [264 (86) vs. 167 (42) ml/kg/min, p<0.001], a higher MV VTI [6.7 (1.8) vs. 5.3 (1.2), p<0.001] and a higher LA:Ao [1.6 (0.4) vs. 1.3 (0.2), p<0.001]. LV BLS was significantly higher in infants with a PDA > 1.5 mm [-13.0 (2.4) vs. -11.9 (1.9) %, p = 0.03]. There was a weak positive correlation between absolute LV BLS values and LVO (r=0.3, p=0.01), indicating that a higher LVO is associated with higher function. There was no correlation between LV BLS and LVID or with LA:Ao. There was no difference in any of the RV measurement between those with and without a PDA > 1.5mm (data not shown). Thirty seven infants (35%) received medical treatment for a persistent PDA beyond the second week of life, and 7 (7%) required surgical ligation.

4.3.5 Influence of CLD on LV and RV Function at 36 weeks PMA

Forty seven infants were assessed at 36 weeks PMA, 28 of which (60%) developed CLD. Infants with CLD had a significantly lower gestation than those without CLD [25.7 (1.4) vs. 27.5 (0.07) weeks, $p < 0.001$]. As a consequence, infants with CLD were scanned at 9.6 (2.1) weeks of age compared with those without CLD who were scanned at 7.0 (1.4) weeks of age ($p<0.001$). Infants with CLD had lower RV BLS [-26.4 (5.0) vs. -30.7 (5.5) %, p=0.0.1] and lower RV SRa [4.2 (1.3) vs. 5.3 (1.9) 1/s, p=0.04] (Figure 4.2). The association between CLD and low RV BLS (p=0.024) and low RV SRa (p=0.015) remained significant when adjusting for gestation and antenatal steroids on linear regression. There was no difference in RV dimensions between infants with and without CLD. In addition, there was no difference in LV or septal strain/strain rate values between infants with and without CLD.

Figure 4.2: Comparison of RV Longitudinal Strain (RV BLS) and RV late diastolic strain rate (RV SRa) in infants with and without Chronic Lung Disease (CLD)

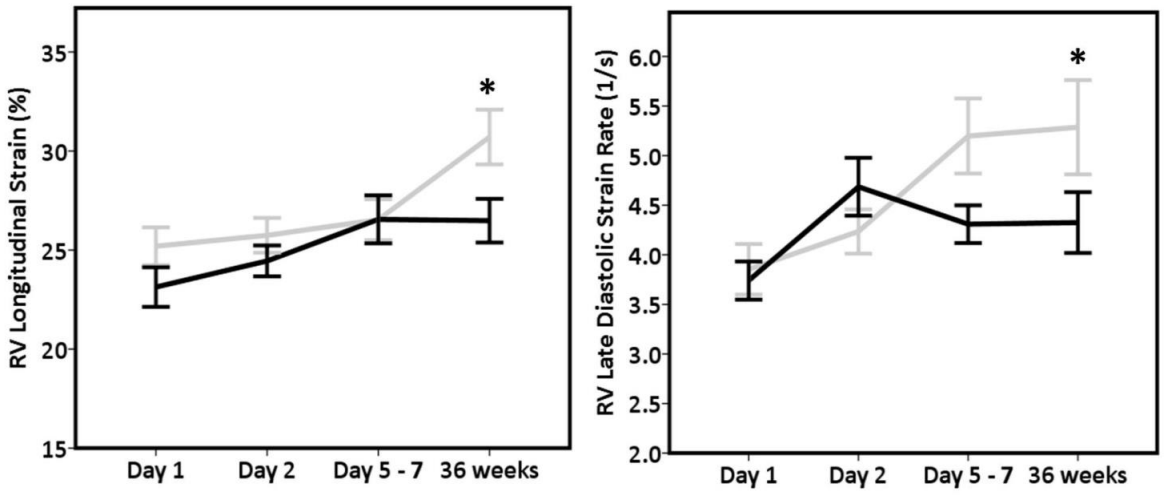

Absolute strain values are used for graphical representation. The black line depicts children with CLD and the grey line depicts children without CLD. Error bars represent ± 1 standard error. * p value < 0.05 compared with baseline (Day1).

4.4 Discussion

Deformation imaging has grown in popularity to become useful as a marker of global and regional myocardial function in the adult and paediatric populations (Sutherland et al., 2004, Abraham et al., 2007, Mori et al., 2007, Ganame et al., 2007b, El-Khuffash et al., 2012). As part of this research we have demonstrated the feasibility and reproducibility of using TDI derived deformation imaging in this population. We chose to use the tissue Doppler-derived method for assessment of deformation instead of speckle tracking echocardiography (STE) because this method is better suited for measurement of strain rate values as it employs a natural strain rate calculation method at much higher frame rates (de Waal et al., 2014). Specifically, measurement of diastolic strain rate values is more appropriate using this method, and prior to this study, has previously been unreported. Levy et al used STE to derive RV strain measures in a similar cohort of premature infants, and was only able to show reproducibility with strain and systolic strain rate (not with diastolic measures), further highlighting the novelty of this manuscript (Levy et al., 2013). However, it is worth noting that this method is highly angle dependent with a large angle of insonation (>20^{o}) resulting in a significant underestimation of values. This can be a particular technical issue in the LV free wall, especially with PDA-associated LV enlargement. In addition, strain values obtained with the tissue-Doppler derived method are not interchangeable with those obtained using STE as this method calculates Lagrangian rather than natural strain. This is particularly true if the extent of the deformation is large (Voigt et al., 2015).

We demonstrated an increase in the strain values of the septum and RV between Days 1 and 2 and between Day 5 – 7 and 36 weeks PMA. As strain represents deformation in particular plane with reference to baseline, the increase in those values cannot be

attributed to an increase in heart size occurring over the study period. Systolic and diastolic strain rate values on the other hand did not generally further increase beyond the first week of life. This may highlight that inherent contractility (represented by strain rate values, see below) becomes established early on during infancy and that strain continues to improve secondary to changes in loading conditions. LV free wall values on the other hand did not show a similar pattern of change, with only LV BLS showing a significant difference from Day 5 – 7 values at 36 weeks PMA. The lack of change in LV values may stem from the relatively lower reproducibility achieved with LV strain and strain rate values which we demonstrated in chapter 3. Helfer *et al,* also recently explored the use of TDI derived LV and RV (but not septal) strain and systolic strain rate in a smaller cohort of preterm infants (ranging between 23 and 32 weeks gestation) over the first 28 days of age. Although they demonstrated an increase in RV BLS and RV SRs in a similar fashion to our population, they failed to demonstrate a similar change in LV values. This may also reflect the lower reliability of LV free wall strain measurements using TDI in this population. The group did not report diastolic strain rate values.

We also explored the influence of echocardiography-measured SVR on those functional measurements on Day 1 of age. We used SVR as a surrogate of afterload. There was a weak negative correlation between SVR and absolute LV/septal BLS values but not strain rate. This indicates that higher SVR leads to lower BLS. On multiple linear regression controlling for many potentially important factors, SVR continues to have a negative impact on BLS while increasing gestation had an independent positive effect. This highlights the importance of taking gestation and afterload condition into account when assessing myocardial function using tissue-Doppler derived basal strain. Recent animal data demonstrate that strain is negatively influenced by increasing afterload and as a result, it

may not reflect intrinsic contractility (Ferferieva et al., 2012). Peak systolic strain rate on the other hand is less influenced by afterload and may be a better surrogate marker for contractility. Our data seem to support this. However, SVR calculations derived from echocardiography-measured LVO and BP become problematic in the context of a PDA as what the LV senses will be influenced by the pulmonary vascular resistance.

We used the presence of a PDA > 1.5 mm by Day 5 to 7 to explore the effect of increasing preload on strain measurements on Day 5 – 7. Infants with a PDA > 1.5 mm had a higher LA:Ao, a higher mitral valve VTI and a higher LVO indicating higher pulmonary venous return and higher preload. LV (but not septal or RV) BLS was marginally higher in those infants with a PDA, with weak positive correlations with LVO and no correlation with LA:Ao or LVID. This indicates the relative lack of influence of preload on those markers suggesting that they may be used to reflect myocardial performance during times of high preload. This supports animal data suggesting the lack of influence of preload on strain and strain rate values (Ferferieva et al., 2012).

We found that at 36 weeks PMA there was a significant difference in RV measurements between infants with and without chronic lung disease. CLD is associated with increased right pulmonary pressures and pulmonary hypertension which can cause an increase in the afterload of the right ventricle (Ryan et al., 2015). We were unable to demonstrate a difference in RV pressures between infants with and without CLD as none had a tricuspid regurgitant jet during that time point. However, the lower RV BLS and RV SRa observed in our patients with CLD supports the association between this condition and lower RV function observed in other studies (Helfer et al., 2014). This difference remained significant after adjusting for the gestational age at birth and antenatal steroid use. Helfer et al also demonstrated that CLD negatively impacted RV BLS measurements at 28 days (Helfer

et al., 2014). However, in the study by Helfer and in our cohort, LV tissue Doppler deformation values were unaffected by CLD suggesting that LV function may remain preserved in the setting of CLD. The same group also reported LV deformation values on the same cohort of infants using STE. Although they demonstrated differences in early global LV strain rate between infants with and without CLD, there were no differences in LV function at 30 days of life (Czernik et al., 2014). Our study differs in several aspects: the gestational age range is much narrower potentially eliminating effect of higher gestations on our results; we performed an echocardiogram at a later point at which CLD was more accurately defined.

Limitations

This study incorporated a large number of preterm infants with serial data looking at how deformation imaging can be used to monitor myocardial function however there was some limitations to this study. Our inclusion criteria of preterm infants less than 29 weeks gestation incorporates a very heterogeneous group with different pathologies. This may have impacted on the functional parameters which we were measuring. We attempted to account for this by incorporating a large cohort and using strict timing and conditions for each echocardiogram. A large number of patients were transferred to 2nd level neonatal units before the 36 corrected gestational age scan could be performed. This included around 50% of the patient population. As the rotunda Hospital is a tertiary referral center the clinical demand is high with bed availability being limited. For this reason patients are often transferred back to their referring hospital at around 34 weeks gestation when they

are stable. This could have introduced bias into those infants in whom we performed the 36 week scan as this may have reflected the sicker patients who were not stable enough to be transferred at this stage. It is also relevant that the long term of these infants is currently not known.

4.5 Conclusion

Tissue Doppler derived strain and strain rate is feasible in the preterm population and shows changes from day 1 to 36 weeks corrected gestational age. The loading conditions of the heart, specifically with the effect of the PDA appear to correlate with an increased LV systolic strain. Chronic lung disease appears to be negatively associated with RV functional parameters when these are measured at 36 weeks corrected gestational age.

Chapter 5 Rotational Mechanics

5.1 Introduction

Left ventricular (LV) twist describes the wringing motion of the LV during systole, and is the net result of the rotation of the apex and the base in opposite directions along the long axis of the left ventricle. LV torsion refers to twist normalized to LV length at end diastole (Mor-Avi et al., 2011) . This wringing motion improves the ejection of blood from the LV cavity during systole. LV untwist describes the recoil during early diastole thereby generating a suction force for LV filling. LV twist is facilitated by the helical arrangement of the subepicardial (left handed) and subendocardial (right handed) fibres and is influenced by contractile function and loading conditions (Buckberg et al., 2011). LV untwist contributes directly to early diastolic filling and is influenced by muscle fibre compliance and elastic recoil properties. These rotational parameters can add important information on myocardial performance (Burns et al., 2008, Buckberg et al., 2011, Russel et al., 2009, Huang and Orde, 2013).

LV rotational mechanics can be assessed by two-dimensional speckle tracking echocardiography (2D STE) at the bedside in an intensive care unit. This technique has been validated against both magnetic resonance imaging (MRI) tissue tagging and Doppler tissue imaging (DTI) (Notomi et al., 2005). 2D STE is also angle independent and is the selected modality for measuring LV rotation in older populations. Recent studies have established rotational mechanics values and patterns in healthy paediatric populations (Takahashi et al., 2010, Al-Naami, 2010, Kaku et al., 2014), the change in rotational mechanics following exercise in children (Boissiere et al., 2013, Di Maria et al., 2014) and in children with a variety of cardiopulmonary disease states (Laser et al., 2013, Cheung et al., 2011b, Cheung

et al., 2011a). Despite the growing application of 2D STE in children and neonates (Levy et al., 2013, Helfer et al., 2013, El-Khuffash et al., 2012), there is a lack of data on LV rotation and twist mechanics in preterm infants. The rotational mechanics of the LV could potentially be different in the preterm population due to differences in myocardial contractile properties, different loading conditions, and the interaction between the LV and the right ventricle (RV), especially during the transitional period.

Our primary aim was to assess the clinical feasibility and reproducibility of apical and basal rotation, LV twist and torsion, LV twist rate and untwist rate measurements in hemodynamically stable preterm infants less than 29 weeks gestation. The secondary aim was to assess the physiological adaptations of rotational and twist parameters across three time points during the first week of age. We hypothesised that the measurement of rotational mechanics in the preterm population is feasible and reproducible. In addition, we hypothesized that those parameters undergo important changes in the first week after delivery.

5.2 Methods

Clinical information regarding pregnancy, delivery and the postnatal period were collected. Three echocardiography assessments were performed during which the following cardio-respiratory parameters were collected: systolic and diastolic blood pressure, heart rate, mode of ventilation, mean airway pressure, oxygen requirement, arterial saturation, total fluid intake and pH.

5.2.1 Terminology

Left ventricular basal and apical rotation, twist, torsion, twist rate and untwist rate were measured using speckle tracking echocardiography of the parasternal short axis views of the LV base and apex. Rotation is defined as the circumferential clockwise or counter-clockwise movement of the apex and base along the long axis of the left ventricle occurring during systole (in degrees). Viewed from the apex, counter-clockwise rotation is displayed as positive and clockwise rotation is displayed as negative. Figure 5.1 demonstrates basal and apical rotation plotted against time during once cardiac cycle.

Figure 5.1: Graphical display of apical rotation (blue line), basal rotation (magenta line) and the resultant net torsion of the left ventricle (white line).

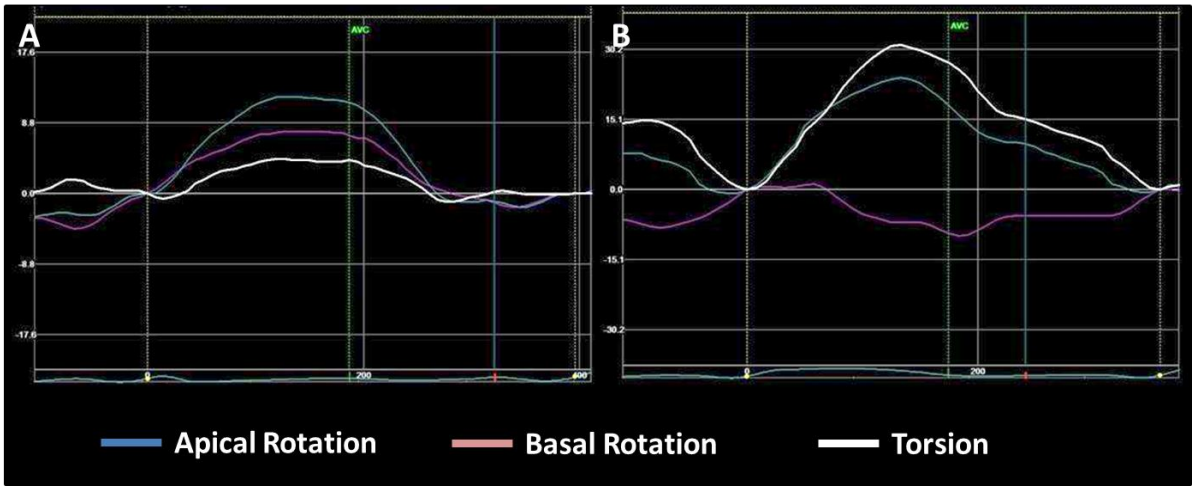

Figure 5.1A illustrates both the apex and base moving in a counter clockwise (positive) direction resulting in minimal torsion. Figure 5.1B illustrates the apex rotating in a counter clock wise (positive) direction and the base rotating in a clockwise (negative) direction resulting in greater net torsion.

Twist was defined as the net difference between apical and basal rotation using the following formula: LV Twist (^{o}) = apical rotation (^{o}) – basal rotation (^{o}).

Left ventricular torsion is defined as twist normalised to LV end diastolic length and is calculated as follows:

Torsion (^{o}/cm) = Twist (^{o}) ÷ LV end diastolic length (cm).

LV twist rate is the velocity at which twist occurs per unit time and is depicted as a positive (degrees/second). Untwisting is the motion opposite to the direction of twist occurring in diastole. LV untwist rate is the velocity of untwist during diastole per unit time and is depicted as negative (degrees/second).

5.2.2 Measurements of Twist, LV twist and untwist rates

The LV base and apex in short axis were obtained from the LV short axis parasternal view. The basal plane was defined as the image at the level of the mitral valve leaflets while ensuring that no left atrial tissue is visible. The apical plane was defined as the image distal to the papillary muscles. Image acquisition at the two planes of interest was carried out to ensure the LV cross section was as circular as possible. Three consecutive cardiac cycles were acquired and digitally stored as raw DICOM data for offline analysis.

We aimed for frame rates between 120 to 130 frames per second (FPS) for all image loops to achieve a frame rate to heart rate ratio (FR/HR) of between 0.7 to 0.9. Recently, Sanchez *et al* demonstrated that intra- and inter-observer reproducibility of measuring left and right ventricular longitudinal strain in preterm infants less than 29 weeks gestation

using 2D STE was highest when the cine loops were acquired with frames rates ranging between 110 to 130 FPS and achieving a FR/HR between 0.7 to 0.9 (Sanchez et al., 2014).

Data were analysed using the 2D STE software described above. A region of interest (ROI) was obtained manually by tracing around the endocardial border of the LV wall during end-systole. The software package divides the LV wall in short axis into six segments and measures the rotation based on the change in speckle movement within each segment. This produces six rotational curves and a global average. The quality of the tracings was assessed by the software and a visual assessment of tracking adequacy. We only accepted tracings where all six segments were adequately traced. The peak rotation of the apex and base, LV twist, LV twisting rate (LVTR) and LV untwisting rate (LVUTR) were determined. The peak rotation was defined as the maximal amount of rotation, positive or negative, during systole. Similarly the peak twisting rate was defined as the maximal amount of twist per unit time between these time points with the untwisting rate in the opposite direction during diastole (Figure 5.2).

Figure 5.2: Left ventricle (LV) twist and untwist rate.

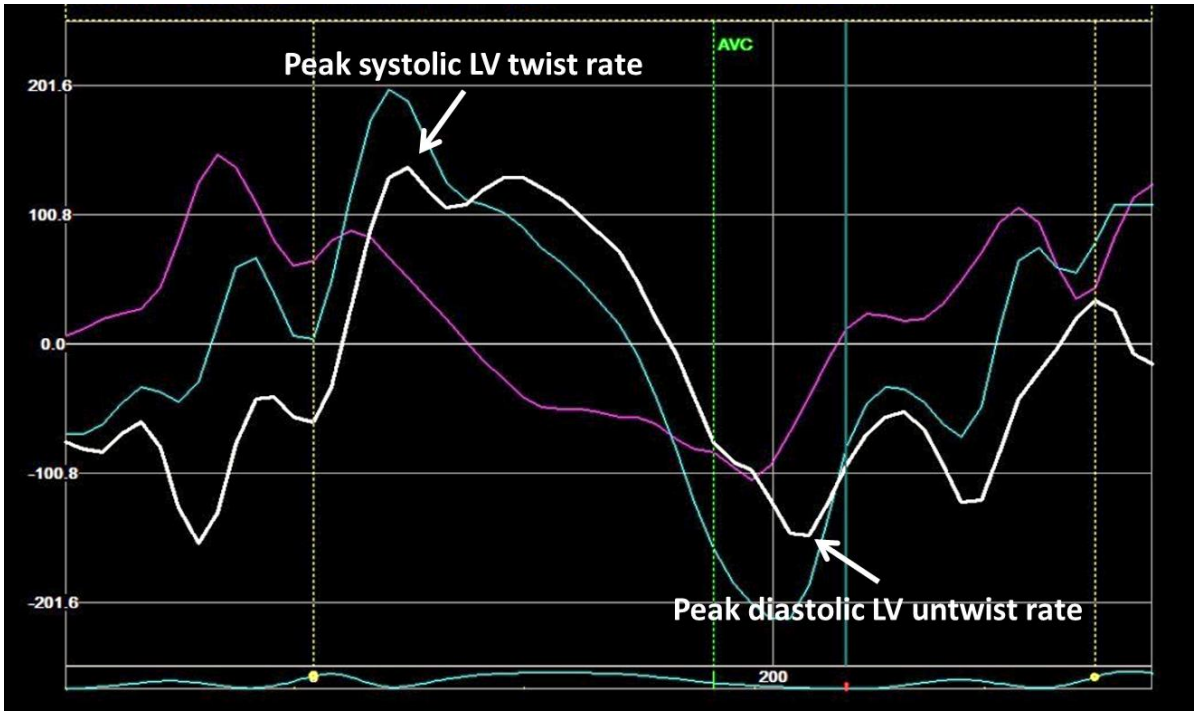

Twist rate occurs during systole while untwist rate occur in the opposite direction during early diastole. AVC: AV valve closure. Magenta- Basal twist rate, Purple- apical twist rate, White- Total twist rate

5.2.3 Statistical Analysis

Continuous variables were tested for normality using the Shapiro-Wilk test, and were presented as means (standard deviation, SD) or medians [inter-quartile range, IQR] as appropriate unless otherwise stated. Differences in the echocardiography values across the three time points were compared using a one-way ANOVA with repeated measures. The Greenhouse-Geisser adjusted p value was used if the assumption of sphericity was violated. Skewed data were compared using the Kruskal Wallis test. Categorical data were presented as proportions. Correlation between wall stress and the function parameters were assessed using Pearson's Correlation Coefficients for normally distributed data or Spearman's Correlation Coefficient for skewed data. In order to assess the systolic-diastolic relationship of the rotational mechanics, correlation between systolic torsion and LVUTR at each time point was carried out using Spearman's Correlation Coefficient. We accepted a p value of less than 0.05 as significant. The statistical analysis was performed using SPSS version 21.

5.3 Results

Seventy three infants less than 29 weeks gestation were considered for inclusion of assessment of rotational mechanics during the study period between January 2013 and December 2014. Seven were excluded due to investigator unavailability, 1 refused consent, 3 had weights less than the 10th centile, 4 received inotropes during the study period, 4 died in the first week of age, and in three infants, short axis views were not acquired during at least two time points. This patient group was a subset of the overall patient population described in Chapter 2 in the methods section for the specific period described above*. Fifty one infants with a mean (SD) gestation age of 26.8 weeks (1.5) and birth weight of 945 grams (233) respectively were included. Thirty nine infants (77%) were delivered by caesarean section with a mean five minute Apgar score of 8 (2) and a cord pH of 7.34 (0.05). Twenty eight (55%) were male. There were 24 (47%) singleton births, 9 (35%) sets of twins and 3 (18%) sets of triplets. All infants received surfactant prior to the first echocardiogram. None of the infants received inotropes during the first 7 days of age. During the first scan, 32 (63%) were invasively ventilated, this reduced to 19 (37%) on day 2 and 15 (29%) by days 5 to 7. All infants survived to hospital discharge. The remainder of the clinical characteristics are displayed in table 5.1. On Day 1, 48 (94%) infants had a PDA compared with 43 (84%) on Day 2 and 35 (69%) on Day 5 – 7. ($p = 0.003$). None of the infants received medical treatment for PDA in the first week of age. There was an increase in PDA maximum systolic velocity and a fall in the number of bidirectional PDA shunts across the three time points. There was a significant but not clinically relevant change in heart rate, LVEDD and LV length over the study period (Table 5.1).

Table 5.1: Cardiorespiratory characteristics of the infants across the three time points.

	Day 1	Day 2	Day 5 to 7	ANOVA p
Heart Rate	156 (13)	165 (13)	164 (12)	<0.001
Systolic BP (mmHg)	45 (8)	52 (9)	52 (8)	<0.001
Diastolic BP (mmHg)	29 (8)	31 (8)	30 (7)	0.07
Wall stress (g/cm^2)	22 [16 – 32]	28 [19 – 35]	20 [15 – 27]	0.01
Total fluid intake (ml/kg/day)	83 (8)	117 (25)	170 (18)	<0.001
FiO_2 (%)	21 [21 – 60]	21 [21 – 35]	21 [21 – 35]	0.2
Oxygen Saturation (%)	95 (2)	96 (3)	96 (3)	0.05
Mean airway pressue (cmH_2O)	8 (2)	8 (2)	7 (2)	0.009
pH	7.33 (0.06)	7.29 (0.06)	7.30 (0.06)	0.002

Values are presented as means (SD). Wall stress is presented as median [IQR] and FiO_2 is displayed as median [Range].

5.3.1 Feasibility and Reproducibility of Twist measurements

Measurements of rotation, twist, torsion, LVTR and LVUTR were possible in 130 out of 153 scans (85%). In the remainder, the software was unable to track the walls due to poor image quality. The mean (SD) frame rates during the examinations were 127 (11) on Day 1, 125 (8) on Day 2 and 125 (9) on Day 5 – 7 (p=0.4). The mean (SD) FR/HR ratio was 0.83 (0.1) on Day 1, 0.76 (0.1) on Day 2 and 0.77 (0.1) on Day 5 – 7 (p=0.001). The results of the Bland-Altman analysis and intraclass correlation coefficient demonstrated better intra- and inter-observer reproducibility of apical rotation, basal rotation, twist and torsion when compared with LVTR and LVUTR (Table 5.2, Figure 5.3).

5.3.2 Longitudinal Rotation, Twist, Torsion, Twist and Untwist values

Apical rotation remained constant over the first week in a positive counter clockwise fashion. However basal rotation changed from a positive counter clockwise rotation to a negative clockwise rotation, resulting in an overall net increase in twist and torsion across the three time points (Table 5.3, Figure 5.4). There was no change in LV twist rate over the first week of age (p=0.6). The LV untwist rate increased over the time period (Table 5.3, Figure 5.5).

Table 5.2: Intra- and inter-obsevrver reliability data for the parameters.

	Intraobserver variability		Interobserver variability	
	ICC (95% CI)	**Bias (LOA)**	**ICC (95% CI)**	**Bias (LOA)**
Apical Rotation	0.96 (0.92 – 0.98)	0.04 (-1.51 – 1.59)	0.78 (0.50 – 0.90)	1.21 (-1.46 – 3.88)
Basal Rotation	0.93 (0.85 – 0.97)	0.11 (-3.77 – 3.99)	0.89 (0.78 – 0.94)	-0.21 (-2.8 – 2.34)
LV Twist	0.86 (0.74 – 0.93)	-0.13 (-2.89 – 2.63)	0.78 (0.18 – 0.92)	1.4 (-1.05 – 3.85)
LV Twist Rate	0.83 (0.47 – 0.94)	-6 (-65 – 53)	0.70 (0.18 – 0.88)	21 (-28 – 70)
LV Untwist Rate	0.88 (0.74 – 0.94)	0 (-53 – 52)	0.73 (0.48 – 0.87)	-7 (-89 – 75)

ICC: Intraclass correlation coefficient; CI: confidence intervals; LOA: limits of agreement All p values < 0.001.

Table 5.3: Rotation, torsion, twist and untwist rate over the three time points.

	Day 1	Day 2	Day 5 to 7	ANOVA p
Apical Rotation (°)	11.4 (5.8)	11.1 (7.8)	11.0 (9.1)	0.96
Basal Rotation (°)	5.5 [-0.3 – 8.3]	4.0 [-4.7 – 7.2]	-4.5 [-5.8 - -2.3]	<0.001
Torsion (°)	8.5 (5.7)	9.3 (7.9)	12.9 (9.4)	0.01
Normalised Torsion (°/cm)	4.9 (3.3)	5.1 (4.7)	7.1 (4.5)	0.01
LV twist Rate	69 [55 – 92]	67 [55 – 107]	74 [56 – 123]	0.6
LV untwist Rate	-74 [-82 - -57]	-82 [-109 - -60]	- 95 [-128 - -63]	0.005

Values are presented as mean (standard deviation) or medians [interquartile range].

Figure 5.3: Bland-Altman graphs for LV torsion twist and untwist.

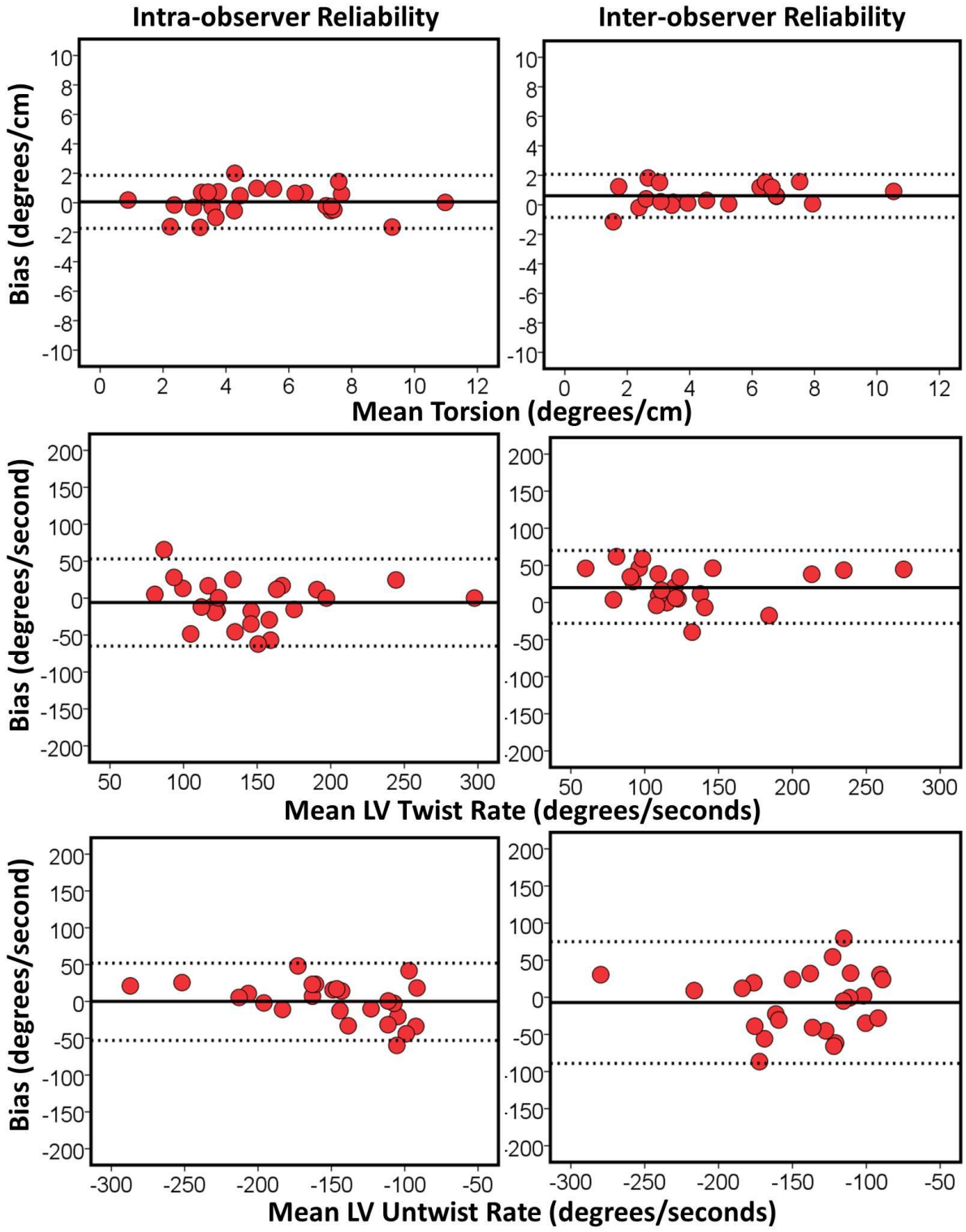

The solid black line represents the mean bias and the dotted lines represent the upper and lower limits of agreement.

Figure 5.4: Apical and Basal rotation and LV torsion over the three time points.

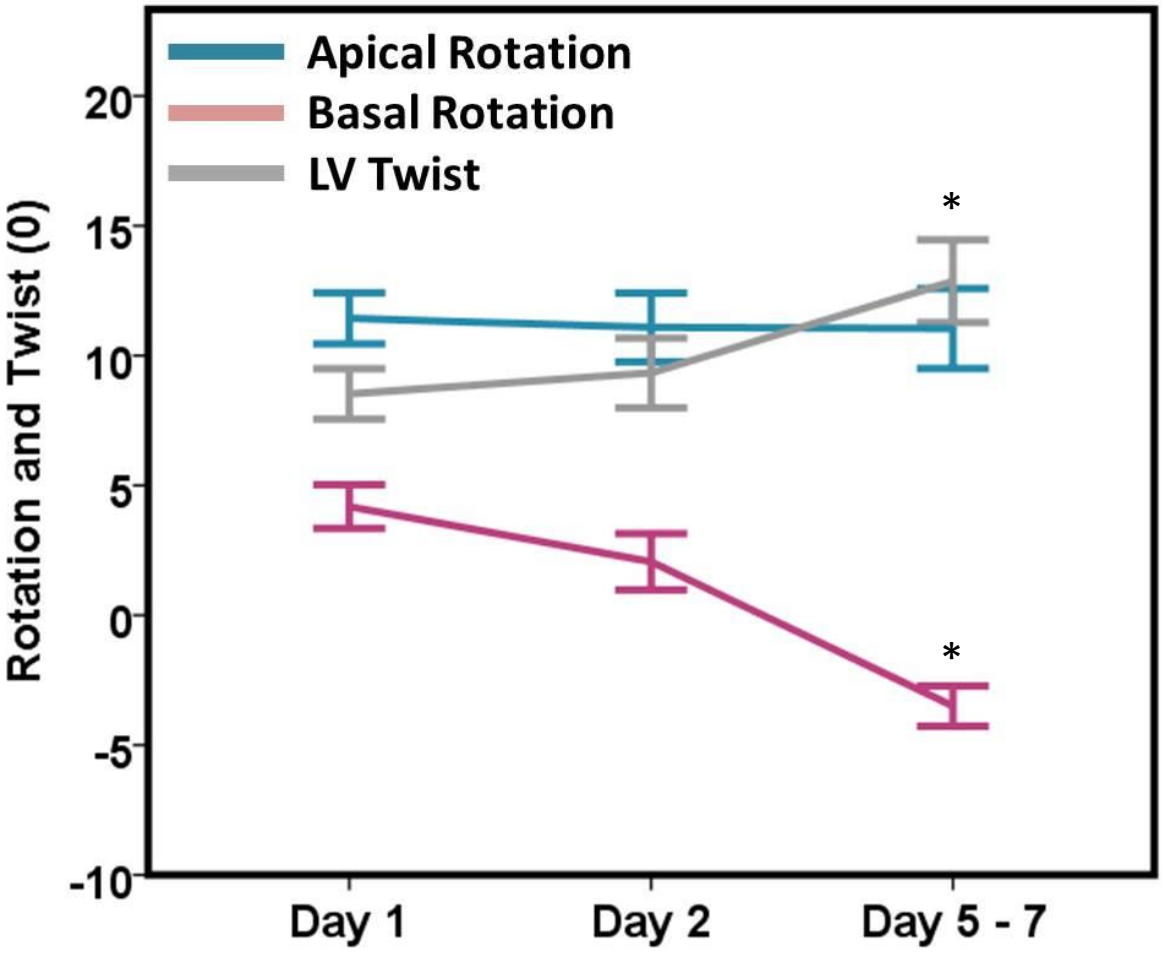

Values are presented as means. The error bars represent the standard error of the mean. There was a significant change in basal rotation across the three time points ($p < 0.001$) and a resultant increase in torsion ($p=0.01$) as represented by (*)

Figure 5.5: LV twist and untwist rate over the three time points.

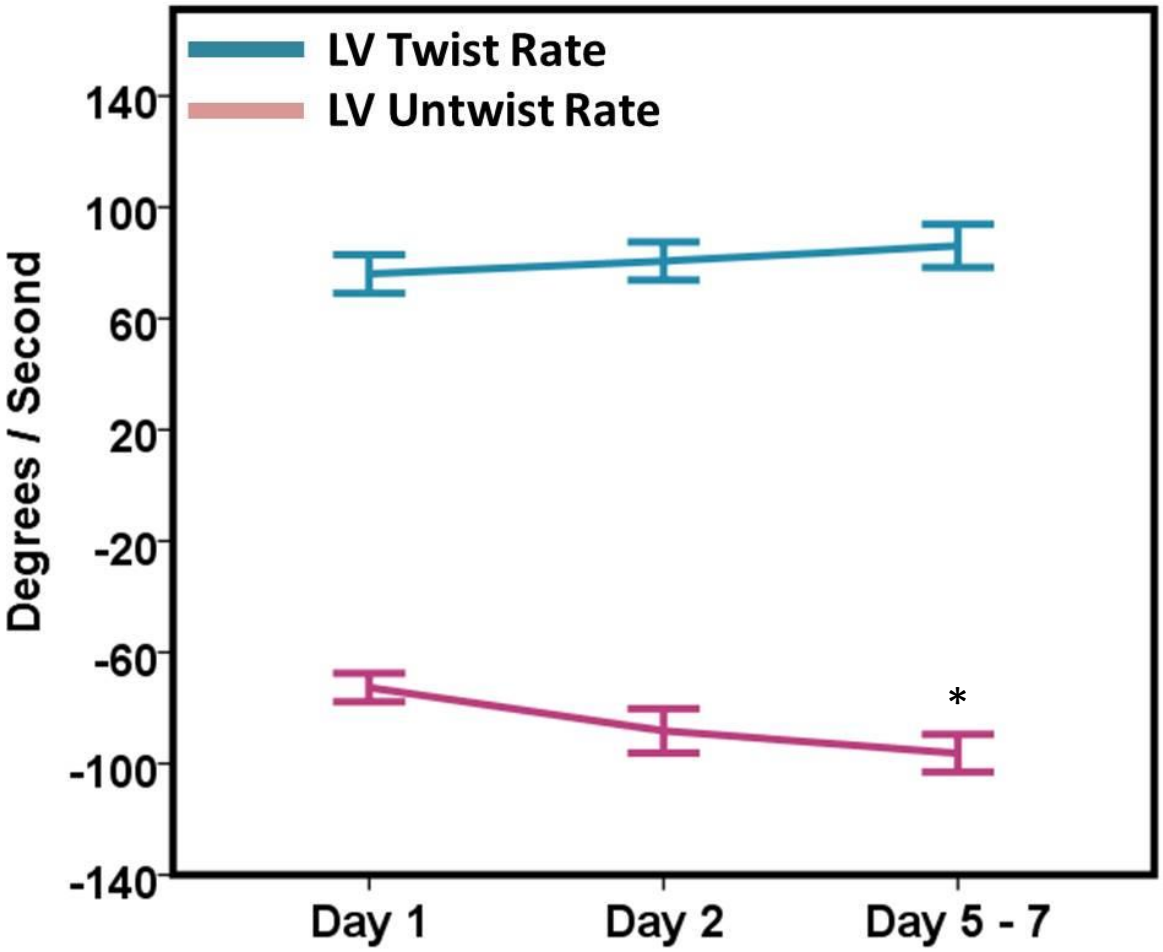

Values are presented as medians. The error bars represent the 95% confidence interval around the median. There was no change in LV twist rate (p=0.6). LV untwist rate increased over the three time points (p=0.005) as represented by *.

5.3.3 Effect of Clinical Parameters and Correlation between Torsion and LVUTR

During the Day 1 scan, there was a weak negative correlation between wall stress and torsion (r= -0.3, p=0.04), LVTR (r= -0.46, p=0.002), and LVUTR (r= 0.33, p=0.03). There were no significant correlations between wall stress and the remainder of the function parameters at any time point. There was no difference in LV twist, torsion, twist rate and untwist rate between infants with a PDA > 1.5 mm and those with a smaller or no PDAs across the time points (data not shown). There was a positive correlation between torsion and LVUTR across the three time points, with the association becoming stronger with increasing age (Figure 5.6).

Figure 5.6: Relationship between Systolic tosrion and diasotlic untwist rate across the three timepoints.

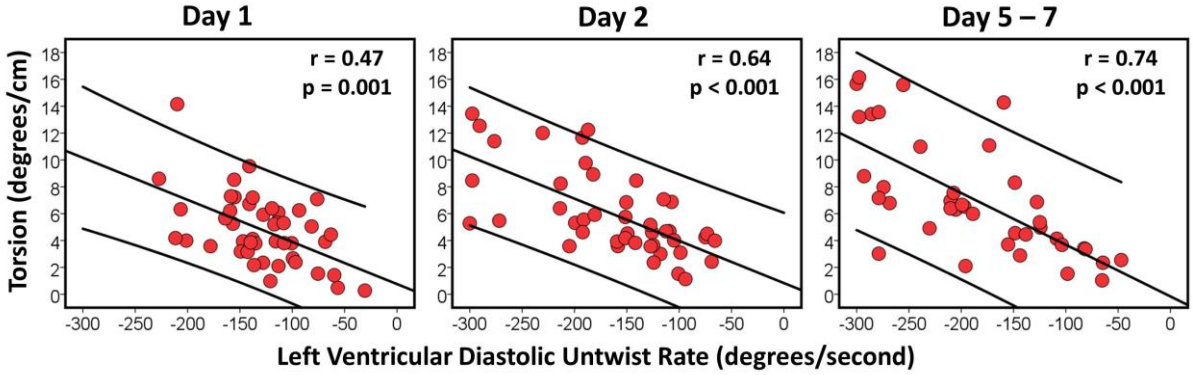

The graphs show thepositive correlation between Torsion and Left Ventricular Untwist rate with the correlation becoming increasingly stronger over the first week of age.

5.4 Discussion

We demonstrated that the assessment of apical / basal rotation, LV twist/torsion, LVTR and LVUTR is possible in a select group of hemodynamically stable preterm infants less than 29 weeks gestation with acceptable reproducibility. The reproducibility of assessing rotation and twist/torsion was higher than that for twist and untwist rates. There was an overall net increase in twist and torsion (twist normalised to LV end-diastolic length) over the first week after birth mainly due to the change in basal rotation from a positive counter clockwise direction to a negative clockwise direction. Apical rotation remained constant in a counter clockwise direction throughout the study period. A net increase in LV untwisting rate was also noted over the three time points. LVTR negatively correlated with LV wall stress with higher stress values resulting in lower LVTR. A significant PDA, and LV volume loading (assessed using LVEDD and LA:Ao) did not appear to have any influence on any of the parameters during the study period. There was a positive correlation between systolic torsion and diastolic LVUTR with the relationship becoming stronger by the end of the first week after birth.

5.4.1 Feasibility and Reproducibility of LV Rotational Mechanics in Preterm Infants

Our reproducibility results for rotation, twist/torsion, and twisting rates were comparable with studies on twist in older populations (Laser et al., 2009, Zhang et al., 2010, Al-Naami, 2010, Takahashi et al., 2010). The superior reproducibility observed in the rotation and twist parameters when compared to the twist and untwist *rate* parameters

(LVTR and LVUTR) may be explained by the frames rates used in our study. We obtained images with an average frame rate of 125 FPS which is slightly higher than the recommended frame rate for STE of 60-110 FPS (Biswas et al., 2013). Our use of those higher frame rates for 2D STE assessment of rotational mechanics is supported by a recent study which demonstrated superior reproducibility of LV and right ventricle deformation measurement in preterm infants when conducted using frame rates between 110 to 130 FPS and maintaining a frame rate to heart rate ratio between 0.7 to 0.9 (Sanchez et al., 2014). We attempted to strike a balance between spatial resolution (which can affect rotation and twist measurements) and temporal resolution (which can affect twist and untwist rate measurements). A relatively high frame rate may affect the software's ability to adequately track the speckles within the ROI thus compromising absolute rotation and twist measurements. Relatively lower frame rates run the risk of missing peak rotational rates thereby reducing the reproducibility of these values. Further studies are needed to determine the ideal frame rates needed to assess rotation, twist and twist / untwist rates in this population.

5.4.2 Comparison of Rotational Mechanics between Preterm and Older Populations

LV twist obtained in our cohort across the three time points was 2 to 4 fold higher than values obtained for infants in their first year of age (Al-Naami, 2010, Zhang et al., 2010, Takahashi et al., 2010). Normalizing twist to LV length (torsion) facilitates comparison of LV rotational mechanics across differing age groups and LV sizes. Interestingly, our cohort of preterm infants demonstrated much higher torsion values when compared to infants, children and adults (Table 5.4). Beyond the preterm period, values of apical/basal rotation and the resultant twist increase with increasing age. However once normalized for LV

length, torsion tends to peak during adulthood before beginning to fall in older individuals. Age related changes in LV twist are due to maturational changes in the myocardium. Twist (and torsion) results from a balance between the positive torsional deformation of the left handed subepicardial fibres and the negative torsional deformation of the right handed subendocardial fibres. The subepicardial force is dominant due to the larger radius leading to an overall positive torsional deformation which is usually attenuated by the opposing force of the subendocardial fibres (Ingels et al., 1989). Generally, subendocardial dysfunction develops with aging. This is coupled with increasing afterload and fibre stress associated with increasing age (MacGowan et al., 1996). This results in a decrease in subendocardial torsional deformation with an increase of epicardial torsional deformation resulting in an augmentation of the positive twist. Following preterm birth, there is a sudden increase in LV afterload due to the loss of the low pressure system of the placenta. The increase in torsion over the first week of life (resulting from a change in basal rotation) may be a result of the attenuation of the subendocardial fibres contraction due to their exposure to increase in afterload occurring after birth.

Table 5. 4: Comparison of Rotational Mechanics across different age groups.

Age group	**23 – 28 weeks**	**Term <28 days**	**3 – 9 years**	**33 – 40 years**	**> 65 years**
Study	James *et al*	Zhang *et al*	Takahashi *et al*	Takahashi et al	Zhang *et al*
Apical Rotation (°)	11.7 (8.3)	2.2 (1.3)	6.5 (2.3)	10.1 (1.9)	10.3 (1.5)
Basal Rotation (°)	-4.5 [-5.8 – -2.3]	1.1 (0.4)	-5.0 (2.0)	4.9 (2.0)	-7.21 (2.2)
Twist (°)	12.9 (9.4)	1.9 (1.2)	10.0 (3.3)	14.2 (3.1)	18.0 (1.8)
Torsion (°/cm)	7.0 (4.3)	1.4 (0.3)	1.7 (0.5)	1.8 (0.4)	1.5 (0.3)
Twist Rate (°/sec)	142 [107 – 213]	Not reported	85 (24)	74 (25)	Not Reported
Untwist Rate (°/sec)	-166 [-107 – -259]	-50 (12)	-105 (41)	-78 (23)	-88.7 (16.6)

Values are presented as mean (standard deviation) or medians [interquartile range]. Day 5 – 7 values were used for our preterm cohort population.

Diastolic LV untwist rate in our cohort was much higher when compared with older children and adults (Table 5.4). This unique pattern noted in preterm infants is interesting and may also be explained by the unique characteristics of the preterm myocardium and the transitional physiology. Studies examining the change in rotational mechanics in children and adults following exercise may help to explain this unique pattern. In children, LV systolic twist and diastolic twist rate increase during exercise but at a much lower rate than the increase observed in adults (Boissiere et al., 2013). Is it postulated that children possess higher myocardial intrinsic relaxation properties and are therefore rely less on untwisting to facilitate LV filling during early diastole. Furthermore, diastolic untwisting is highly dependent on systolic twist as the potential energy stored in the helical fibres during systole is released in early diastole. Indeed, the relationship between systolic twist and diastolic untwist rate appears linear in adults and children. As adults have higher twist values compared with children, the resultant untwist rate is also higher. Due to immaturity of the calcium handling metabolism, early relaxation in preterm infants is significantly slower than in children and adults as we demonstrated in our initial analysis. This could potentially be compensated by a higher elasticity of the myocardial fibres. Faster elastic recoil may serve as a compensatory mechanism for the slower early active relaxation. The systolic-diastolic relationship between twist and untwist rates in the preterm cohort is also present and becomes stronger during the first week. Higher twist values in the preterm population may also be responsible for the higher untwist rates. Our findings suggest that assessing LVUTR could potentially help in better understanding diastolic function and could be a reproducible

and useful marker of diastolic function in this population (Burns et al., 2009, Burns et al., 2008, Notomi et al., 2006a).

5.4.3 Effect of Loading Conditions on LV Twist in Preterm Infants

Interestingly, we demonstrated that the longitudinal increase in LV twist over the first week of age was secondary to the change in basal rotation over the same period. Recently Ramani et al in a study of adult patients demonstrated that pulmonary arterial hypertension (PAH) significantly reduces basal LV rotation, with higher negative values seen in controls without PAH (-5.76 degrees in controls versus -2.03 degrees in PH patients, p= 0.001). In their study, PAH had no effect on LV apical rotation (5.30 degrees versus 4.54 degrees; p = 0.6) (Ramani et al., 2009). Although direct comparisons are not possible, the change in basal rotation in our population from positive on Day 1 to negative on Day 5 – 7 may be a result of the fall in pulmonary vascular resistance (PVR) that occurs during the early neonatal period. We demonstrated this fall in PVR by a reduction in the number of bidirectional shunts and an increase in the peak systolic velocity across the PDAs over the study period. This increase in peak velocity across the PDA occurred without a clinically relevant change in PDA diameter indicating that the increased velocity was likely to be a result of falling PVR (Hamrick and Hansmann, 2010).

The effect of loading conditions on LV twist, twist and untwist rates remains an area of interest. Increased afterload appears to decrease LV twist and twist rates in experimental animal models (mongrel dogs) and human adults (Burns et al., 2010, MacGowan et al., 1996). This is supported by our data indicating that higher wall stress is associated with lower torsion, LVTR and LVUTR on Day 1. However, we were not able to demonstrate an association between wall stress and any of the rotational parameters on Day 2 and Day 5 –

7. In our study, wall stress appeared to increase during the second scan and fall again during the third scan. Factors contributing to this pattern of change in wall stress appear to be multiple as there were changes in the mean BP and LV posterior wall thickness. We used mean blood pressure as an estimate of end systolic BP and this may not be a true representation of the end systolic blood wall stress. Laser et al demonstrated that twist increased in children with pressure loaded LVs as a consequence of aortic stenosis and coarctation of the aorta (Laser et al., 2009). They demonstrated that twist values decrease following the intervention and speculated that the increase in twist was compensatory mechanism for the increased afterload.

We compared the impact of PDA on torsion by comparing those with a small PDA (<1.5mm) to those with a larger PDA (>1.5mm). No significant difference was seen between these two groups over the first week of age. A significant duct would increase the preload by increasing pulmonary venous return(Halliday et al., 1979). Previous studies examined the effect of preload on torsion and found that preload has very little effect on maximal torsion (Moon et al., 1994, Kaku et al., 2014). Our findings would concur with this suggesting that the absence or presence of a PDA does not impact on the torsion of the LV. Although the infants' fluid intake more than doubled over the one week period, this represents their normal fluid maintenance requirements as the increased urine output and insensible losses in those infants considerably increase their fluid requirements. Further studies examining the effect of loading conditions on twist parameters in the preterm population are needed.

5.4.4 Clinical Implications

Rotational mechanics of the left ventricle offer novel insights into myocardial performance. Two dimensional STE is a relatively novel technique that can be applied to preterm infants at the bedside to measure those rotational mechanics. Demonstration of feasibility, reproducibility in addition to the examination of changes occurring in the first week of life in cohort of hemodynamically stable preterm population may pave the way for the application of those parameters to infants with disease states and those with haemodynamic instability (Kaku et al., 2014).

5.5 Limitations

There are important limitations to our study. The reproducibility of the parameters were assessed with a limited range of frame rates with heart rate variability affecting frame rates used, and further studies need to be conducted using different frame rates in an attempt to optimize reproducibility, particularly of LVTR and LVUTR measurements. The changes of twist, LVTR and LVUTR may have been influenced by unexamined confounders both antenatally and in the immediate post natal period and due to the relatively small number of infants, we were unable to assess the effect of those variables. The selective nature of our population should be taken into account when applying these reproducibility data in preterm infants.

5.6 Conclusion

Measurement of twist, rotation, twist and untwist rate in preterm infants is feasible and demonstrates acceptable reproducibility. The changes in those parameters over the first week after birth may represent important changes in both systolic and diastolic function.

Those parameters appear to be influenced by loading conditions in both ventricles occurring during the transitional period. Further studies in preterm infants are required to confirm those findings and investigate those parameters in different disease states.

Chapter 6 Clinical Utility of Right Ventricular Fractional Area Change in Preterm Infants

6.1 Introduction

Assessment of right ventricular (RV) performance in preterm infants is gaining considerable interest with an increasing realisation that RV function has important prognostic implications in various disease states and populations (Moenkemeyer and Patel, 2014, Lewandowski et al., 2013, Rajagopal et al., 2014). Several studies have recently emerged describing various methods of objective RV functional assessment in preterm infants using a variety of methods including tissue Doppler imaging, tricuspid area plane systolic excursion (TAPSE), RV deformation imaging and RV fractional area change (de Waal et al., 2014, Levy et al., 2015, Koestenberger et al., 2011, Murase et al., 2015b, Levy et al., 2013). However, the clinical relevance of those markers in the preterm population and how they relate to disease states warrants further study.

Right ventricular fractional area change (RV FAC) describes the change in the RV cavity area from diastole to systole in the four chamber view and provides the dominant contribution to RV ejection fraction (Levy et al., 2015). There is a strong correlation between RV FAC and RV ejection fraction determined by MRI (Anavekar et al., 2007). RV FAC appears to be uninfluenced by significant intra-atrial shunts in adults (Kowalik et al., 2011) and therefore may reflect blood returning from the upper and lower circulation. Recently, the feasibility, reproducibility and reference values of RV FAC in preterm infants have been established in Chapter 3 and by others (Levy et al., 2015). However no current data is available on the relationship between RV FAC measured during the first week of life and

perinatal characteristics, peri/intraventricular haemorrhage (P/IVH), and patent ductus arteriosus (PDA). Evaluating the role of RV FAC in the first week of life in relationship to common morbidities to demonstrate the validity of this measure in premature infants is of paramount importance.

In this study, we hypothesise that RV FAC has important associations with perinatal factors, P/IVH and haemodynamically significant PDAs in preterm infants less than 29 weeks gestation. The aims of this study are to assess the relationship between RV FAC and gestational age/birthweight, assess the ability of a low RV FAC on day one of age to predict the later evolution of P/IVH, and the assess the influence of a persistent PDA on RV FAC during the first week of age.

6.2 Methods

This was a prospective observational cohort study carried out over a two year period in the neonatal intensive care unit of the Rotunda Hospital, Dublin, Ireland, between January 2013 and December 2014. Infants born less than 29 weeks gestation were included in the study. Prior to enrolment, all infants underwent a cranial ultrasound examination on the first day of age to rule out early P/IVH. Infants were excluded if there was evidence of a congenital or chromosomal abnormality at birth, congenital heart disease (other than a PDA or a PFO) identified antenatally or during the first echocardiogram, a P/IVH (IVH grades 2 or higher) identified on day one of age based on the Papile system of classification (Papile et al., 1978), or death within the first week of age. We currently adopt a conservative approach to PDA treatment. Prophylactic indomethacin is not used at this institution and medical treatment of the PDA with non-steroidal anti-inflammatory drugs is not provided in the first

7 days of life. The echocardiography assessments conducted for this study were not revealed to the clinical team caring for the infant unless there was a clinical reason (other than a PDA) to do so. Written parental informed consent was obtained from all parents and ethical approval was obtained from the Hospital's local Research Ethics Committee.

6.2.1 Clinical Demographics

Along with antenatal, birth, and clinical cardiorespiratory characteristics, obtained from the hospital records, the following clinical outcomes were also obtained: culture proven sepsis, necrotizing enterocolitis (NEC) with radiological evidence of pneumatosis; chronic lung disease (CLD) defined as the need for oxygen at 36 weeks corrected gestation; treated retinopathy of prematurity; length of hospital stay; P/IVH assessed on day 7 of age and classified according to Papile Classification (Papile et al., 1978); death before discharge.

6.2.2 Echocardiography

Echocardiography was carried out according to the protocol described in the methodology chapter. Data were stored as raw DICOM images in an archiving system (EchoPac, General Electric, version 112 revision 1.3) and analysis of all the echocardiography parameters was carried out by an investigator who was blinded to the results of the cranial ultrasounds.

To measure RV FAC, two dimensional images were obtained from a RV-focussed apical four-chamber view (Figure 6.1). During offline analysis RV cavity end diastolic area (RVEDA) was identified as the frame just after tricuspid valve closure and RV cavity end systolic area (RVESA) was identified as the frame just before tricuspid valve opening. The

area of the cavity was manually traced during those two time-points within the cardiac cycle as illustrated in Figure 6.1. RV trabeculations were included in the trace. RV FAC was then calculated using the following formula:

$$\text{RV FAC (\%)} = [\text{RVEDA}(cm^2) - \text{RVESA}\ (cm^2)] \div \text{RVEDA}(cm^2).$$

The following echocardiography parameters were also measured using previously described methods (El-Khuffash and McNamara, 2011b): LVO (ml/kg/min); PDA diameter (mm) measured in 2D at the pulmonary end; diastolic and systolic flow velocity across the PDA; the presence of a patent foramen ovale (PFO) and the velocity of the shunt across the PFO; left atrial to aortic root ratio (LA:Ao); celiac artery and descending aortic end diastolic velocity; tricuspid regurgitant jet velocity (TRv) if present and right ventricular systolic pressure (RVSp) measured using Bernoulli's equation as follows: $\text{RVSp} = 4 \times TRv^2$. Peak systolic to diastolic flow velocity ratio across the PDA was calculated on Day 5 – 7 to determine the flow pattern across the duct (Smith et al., 2015). Systemic vascular resistance (SVR) was calculated by using the following formula: (mean systemic BP – mean tricuspid valve inflow pressure gradient) ÷ LVO (Noori et al., 2007b).

Figure 6.1: Measurement of right ventricular fractional area change.

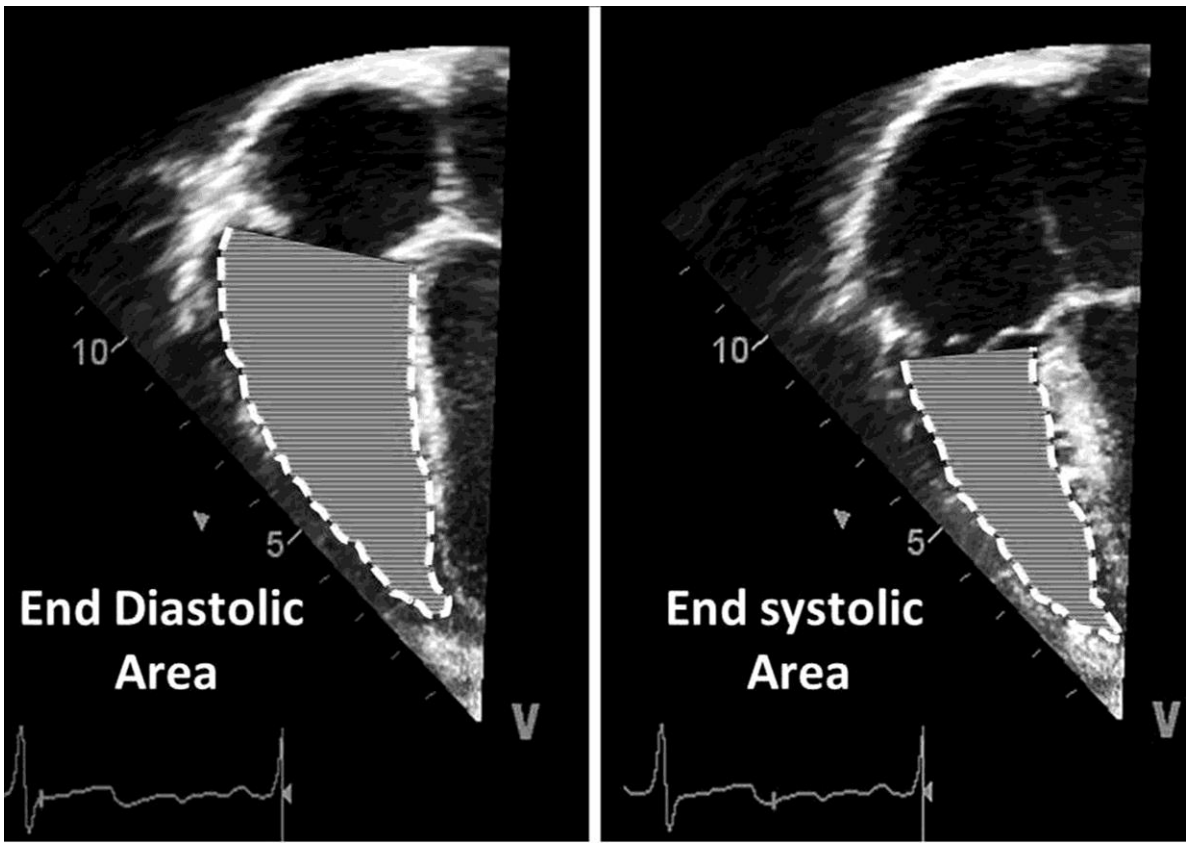

RV cavity end diastolic area (RVEDA) and RV cavity end systolic area (RVESA) are manually traced. RV FAC was then calculated using the following formula:
RV FAC (%) = [RVEDA(cm^2) – RVESA (cm^2)] ÷ RVEDA(cm^2).

6.2.3 Statistical Analysis

The cohort was divided into two groups based on whether or not they developed P/IVH by day 5 – 7 of age. Another two group analysis was also carried out based on the presence of absence of a PDA on the Day 5 – 7 scan. Continuous data was tested for normality using the Shapiro-Wilk test and a histogram representation and presented as mean (standard deviation) if normally distributed or median [inter-quartile range] if skewed. For two group analysis, normally distributed data were compared using the student t-test and skewed data were compared using the Mann-Whitney U test. Categorical variables were presented using count (percent) and compared using Chi Square or Fisher Exact tests as appropriate. Serial data across the two groups were compared using a two way ANOVA with repeated measures. Correlations between measured variables were compared with Pearson's correlation coefficient if normally distributed or Spearman correlation coefficient if skewed. Logistic regression was used to assess the independent association between Day 1 RV FAC and P/IVH while controlling for gestational age and antenatal steroid administration. A receiver operating characteristics curve was constructed to assess the ability of Day 1 RV FAC to predict P/IVH. A value < 0.05 was considered significant. SPSS (IBM version 22) was used to conduct the statistical analysis.

6.3 Results

One hundred and twenty five infants were considered for inclusion during the study period. Three infants died during the first week of age; five infants developed a P/IVH on Day 1 of age; seven were missed due to investigator unavailability for at least two time points; six parents refused consent; three infants were excluded due to congenital heart disease (total anomalous pulmonary venous drainage; transposition of the great arteries; large atrial septal defect). One hundred and one infants with a mean gestation of 26.5 (1.4) weeks and a birthweight of 983 (240) grams were enrolled in the study (Table 6.1). Echocardiography scans were available for 98 infants on Day 1 and all infants on Days 2 and 5 – 7.

6.3.1 Relationship between RV FAC and Perinatal Characteristics

There was a positive correlation between RVEDA and RVESA with birthweight on Day 1; however, there was no relationship between RV FAC and birthweight (Figure 6.2). There was a positive correlation between RV FAC and LVO ($r=0.52$, $p<0.001$) and a negative correlation between RV FAC and echo-measured SVR ($r=0.57$, $p<0.001$, Figure 6.2). On Day 1, 50 infants had a visible tricuspid regurgitant jet with a median right ventricular systolic pressure (RVSp) of 26 mmHg [21 – 34]. There was no relationship between RV FAC and RVSp ($r=-0.1$, $p=0.3$). Similarly, 33 infants had a bidirectional shunt across the PDA. There was no difference in RV FAC between those with and without a bidirectional shunt (31% vs. 31%, $p=1.0$). There was no correlation between RV FAC and any other perinatal characteristics including gestational age. Perinatal characteristics are listed in Table 6.1.

On Day 2, RV FAC was only influenced by RVSp and the presence of a bidirectional shunt. Forty infants had a visible tricuspid regurgitant jet on Day 2. There a negative correlation between RV FAC and RVSp ($r=-0.42$, $p=0.008$). Infants with a bidirectional shunt on Day 2 (n= 13/86, 15%) had a lower RV FAC [31 (9) vs. 42 (8), $p<0.001$]. There was no relationship between RV FAC and SVR on Day 2 ($r=-0.07$, $p=0.5$).

Figure 6.2: Correlation between RVEDA/RVESA/RV FAC and birthweight and between RV FAC and SVR during the first day of age.

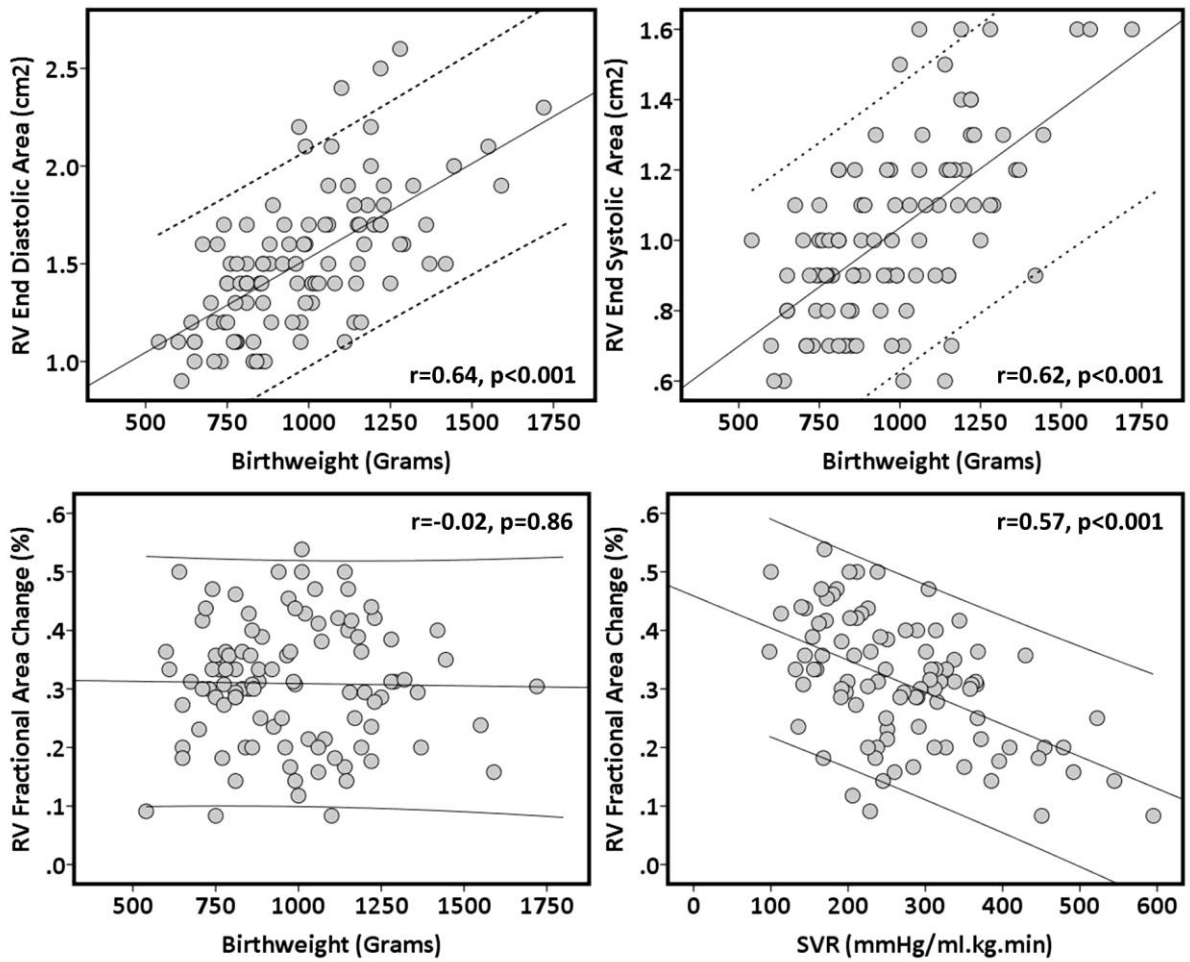

RVEDA: right ventricle end diastolic area; RVESA: right ventricle end systolic area; RV FAC: right ventricle fractional area change; SVR: systemic vascular resistance.

6.3.2 Relationship between RV FAC and P/IVH

Twenty one infants (21%) developed a P/IVH by Day 5 – 7. Table 6.1 demonstrates their demographics, antenatal characteristics and clinical outcomes. On Day 1, RV FAC was lower in infants who developed a P/IVH (24% [18 – 34] vs. 31% [25 – 40], p=0.04). This relationship remained significant when controlling for gestation and antenatal steroid use using logistic regression (RV FAC β = -7.2, p=0.01; Gestation β = -0.29, p=0.16; Antenatal steroids β=-0.67, p=0.4). There was no difference in RV FAC between those with and without a P/IVH during the two other time points (Figure 6.3A). However, the increase in RV FAC from Day 1 to 2 between the groups was much higher in the P/IVH group (12 [6 – 20] vs. 6 [1 – 14] %, p=0.01). Day 1 RV FAC has an area under the curve of 0.7 (95% CI 0.5 – 0.8, p=0.01) for the ability to predict later P/IVH with a RV FAC cut off value of 30% giving a sensitivity of 70% and a specificity of 60%.

6.3.3 Relationship between RV FAC and a persistent PDA

During Day 1, 95 (95%) infants had a PDA with a mean diameter of 2.5 (0.6) mm and mean maximum velocity of 1.2 (0.6) m/s suggesting a low volume shunt. The number of infants with a PDA reduced to 86 (85%) on Day 2 and to 69 (68%) on Day 5 – 7. There was a significant increase in the maximum velocity across the PDA between Day 2 and Day 5 – 7 [1.7 (0.6) and 2.0 (0.8) m/s respectively, ANOVA p <0.001] without a change in the PDA diameter [2.7 (0.6) vs. 2.7 (0.7), p=0.88] with median peak systolic to diastolic flow ratio across the duct of 2.8 [1.8 – 4.7] on Day 5 – 7 suggesting an increase in shunt volume and an unrestrictive flow pattern during that time period. Infants with a PDA on Day 5 – 7 had a higher LVO [256 (88) vs. 168 (45) ml/kg/min], a larger LA:Ao ratio [1.6 (0.4) vs. 1.3 (0.2)], a lower celiac artery end diastolic velocity [0.04 (0.10) vs. 0.17 (0.10) m/s] and reversed end

diastolic flow in the descending aorta [-0.06 (0.10) vs. 0.08 (0.04) m/s] (all p values < 0.001). This suggests that a PDA on Day 5 – 7 has a significant haemodynamic impact. There was no difference in RV FAC between infants with and without a PDA on Days 1 and 2. However, on Day 5 – 7 infants with a PDA had a lower RV FAC compared with those without [42 (7) vs. 49 (9) %, p<0.001, Figure 6.3B]. There was a positive correlation between RV FAC and celiac artery end diastolic velocity (r=0.3, p=0.004) and with descending aorta end diastolic velocity (r=0.3, p<0.001). There was no correlation between RV FAC and shunt velocity across the PFO at any time point.

Table 6.1: Infants Perinatal Characteristics and Outcomes divided by the presence or absence of peri- intraventricular haemorrhage.

	No P/IVH Group (n=80)	P/IVH Group (n=21)	p
Gestation (weeks)	27.1 ± 1.3	26.5 ± 1.5	0.11
Birth weight (grams)	994 ± 250	941 ± 198	0.38
Male	43 (54%)	16 (72%)	0.08
Antenatal Steroids (Completed Course)	64 (80%)	13 (62%)	0.02
PPROM	29 (36%)	5 (24%)	0.32
Chorioamnionitis	6 (8%)	2 (10%)	0.67
Caesarean Delivery	58 (73%)	12 (57%)	0.16
Apgar at 5 minutes	9 [8 – 9]	8 [7 – 9]	0.04
Cord pH	7.33 (0.07)	7.36 (0.05)	0.10
PDA at Days 5 – 7	54 (68%)	15 (71%)	0.80
NEC	11 (14%)	6 (29%)	0.19
CLD	36 (47%)	11 (61%)	0.43
Culture Proven Sepsis	15 (19%)	7 (33%)	0.23
Treated ROP	8 (11%)	1 (6%)	1.0
Hospital Length of Stay (Days)	70 [52 – 87]	77 [64 – 107]	0.11
Survival to Discharge	76 (95%)	18 (86%)	0.16

Data are presented as means ± standard deviation, count (%), or medians [interquartile range]. NEC: Necrotising Enterocolitis, CLD: Chronic Lung Disease, PPROM: Preterm prolonged rupture of Membranes, PDA: Patent Ductus Arteriosus, ROP: Retinopathy of Prematurity

Figure 6.3: RV FAC in infants with and without P/IVH (A) and infants with and without a PDA on Day 5 – 7 (B).

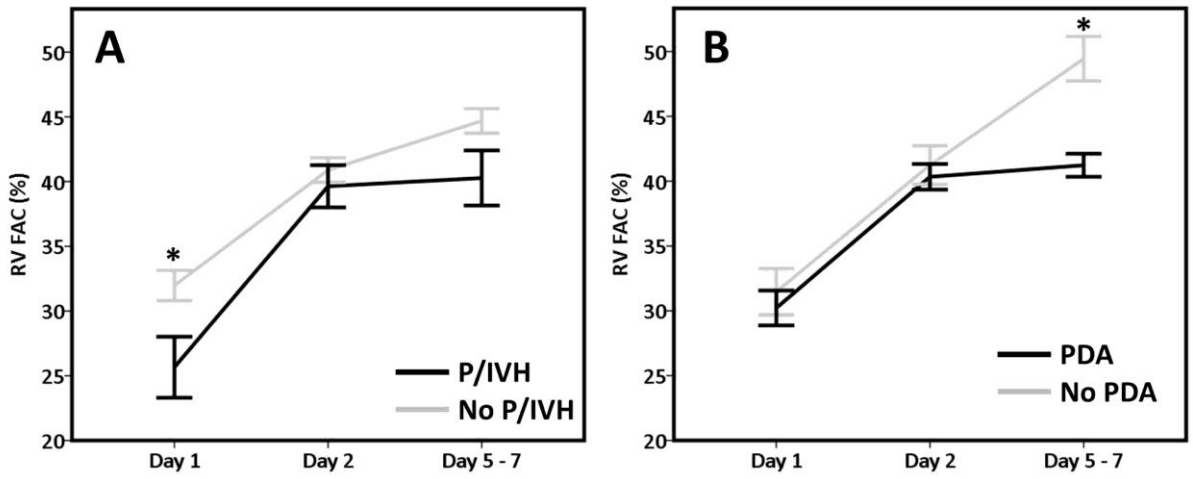

Error bars represent standard error of the mean. * indicates a p value < 0.05. P/IVH: peri/intraventricular haemorrhage; PDA: patent ductus arteriosus; RV FAC: right ventricle fractional area change.

6.4 Discussion

In this study, we demonstrated that SVR has a dominant effect on right ventricular fractional area change on Day 1, while on Day 2, pulmonary vascular resistance (PVR) has a more dominant effect. Although there was a positive correlation between RVEDA/RVESA and birthweight, this did not translate to an association between RV FAC and birthweight. A low RV FAC on Day 1 of age is associated with the evolution of P/IVH in preterm infants by Day 5 – 7. In addition, a PDA with significant left to right shunting results in a lower RV FAC when compared to those without a PDA on Day 5 – 7. A PFO does not appear to increase RV FAC during the first week of life.

Recently, our group and that of Levy *et al*, demonstrated the feasibility and reproducibility of measuring RV FAC in preterm infants, and presented reference data for this population from birth to 36 week post menstrual age (Levy et al., 2015). Those studies reported a low coefficient of variation of 8 – 11%, and an intra- and inter-observer intraclass correlation coefficient of up to 0.94. MRI studies in the adult population assessing the correlation between MRI-measured RV ejection fraction and echocardiography-measured RV FAC demonstrated a very strong correlation between the two methods ($r=0.80$, $p<0.001$) (Anavekar et al., 2007). In addition, RV FAC appears to be uninfluenced by shunting across the PFO in both adult studies (Kowalik et al., 2011) and in our population. There is no current data looking at MRI –measured RV function in the preterm neonate but future studies may be able to elicit this with correlation of normative RV FAC by echocardiography.

Other emerging methods of RV assessment, such as TAPSE and Tissue Doppler velocities require indexing to infant size or RV length in order to make them comparable across differing infant sizes as we described earlier. Although RVEDA and RVESA were positively correlated with birthweight, RV FAC had no relationship with birthweight or

gestation. This is due to the fact that is a measure of relative change in cavity area from baseline. Therefore, this parameter can be used to compare function across a range of weights and gestations.

The negative relationship between SVR and RV FAC on Day 1 is interesting. A high SVR in the presence of an open ductus arteriosus may result in RV exposure to the high resistance of the systemic circulation. Lower RV FAC in the face of higher SVR may highlight the inability of the preterm myocardium to adequately function in the face of high afterload. There was no association between PVR and RV FAC on Day 1. This may indicate that SVR rather than PVR has a dominant effect on the right ventricle during the immediate transitional period. In addition, the positive correlation between RV FAC and LVO suggests that this parameter is also influenced by systemic blood flow (and systemic venous return, preload) during the early transitional period. The relationship between RV FAC and SVR was no longer present on Day 2. SVR calculations using echocardiography become problematic in the context of a PDA of increasing significance as what the RV senses will be also influenced by the pulmonary vascular resistance. Indeed, on Day 2, infants with a persistently high PVR (indicated by the presence of a bidirectional shunt) have a lower RV FAC. RV FAC is therefore like to be negatively influenced by high afterload.

We studied the association between P/IVH evolution and RV FAC. Both groups demonstrated an increase in RV FAC over the first two days and a smaller increase between Day 2 and Day 5 – 7. However, the P/IVH group had a significantly lower Day 1 value and demonstrated a larger increase between Days 1 and 2. This association was independent of gestational age and antenatal steroids. Our findings are similar to those of Noori *et al,* who used LVO measurements over the first 76 hours of life to assess the association between the changes in LVO and the evolution of IVH. In their study, infants with a P/IVH had a lower

LVO initially and demonstrated a higher rate of rise preceding the bleed (Noori et al., 2014a). This adds further evidence that the evolution of late IVH (occurring beyond the second day of age) is at least in part related to myocardial function in the immediate neonatal period. As RV FAC is likely influenced by both RV preload (which is determined by systemic blood flow) and RV afterload, this add to the theory that a low blood flow state in the early neonatal period followed by a surge in blood flow in the subsequent 24 to 48 hours predisposes infants to P/IVH. This theory was originally raised by Kluckow et al in their early studies on SVC flow (Kluckow and Evans, 2000).

The presence of a patent ductus arteriosus, particularly if persisting during the first week of age, is associated with systemic hypoperfusion despite a rising LVO (El-Khuffash and McNamara, 2011b, Broadhouse et al., 2013). The study by Levy et al did not show a relationship between RV FAC and PDA diameter at 72 hours of life (Levy et al., 2015). This may highlight that that haemodynamic impact of a PDA may not be overtly established within the first 72 hours of life. In our study, we found no relationship between a PDA and RV FAC during the Day 1 and Day 2 scans. However, the impact on the systemic circulation is likely to become more apparent as pulmonary vascular resistance continues to fall by the end of the first week of age thereby increasing the pressure gradient and the shunt volume between the systemic and pulmonary circulations. In our cohort, we demonstrated an increasing shunt velocity in infants with a persistent PDA without a change in PDA diameters across the three time-points. We demonstrated a median peak systolic to diastolic flow velocity of 2.7 indicating a non-restrictive flow pattern across those PDAs. This indicates that the increase in shunt velocity was a result of an increase in shunt volume rather than a constriction of PDA diameter. In addition, we demonstrated that all infants with a PDA on Day 5 – 7 had a higher LVO and LA:Ao suggesting increased pulmonary blood flow and lower

celiac artery and descending aortic velocities suggesting reduced systemic perfusion. Those features in combination highlight the significant haemodynamic impact a PDA has on the preterm circulation. RV FAC was significantly lower in the PDA group compared to controls on Days 5 – 7, with a positive correlation with celiac artery and descending aorta end diastolic velocities (indicating the reduced systemic perfusion is associated with a low RV FAC). This suggests that RV FAC may identify reduced systemic blood flow associated with a PDA and is therefore also affected by preload. It could be a valuable tool to assist in the evaluation of the haemodynamic impact of the PDA.

6.5 Clinical Implications and Conclusion

The properties of RV FAC illustrated above all suggest that this relatively novel and reproducible measurement in preterm infants is influenced by both RV preload (and systemic blood flow) and RV afterload. It appears uninfluenced by gestational age or birthweight making it a suitable method for assessing function across varying gestations and infant sizes. The relationship between a low RV FAC and P/IVH is similar to other measures of flow in this population including LVO and SVC flow. Due to its predictive properties and its association with disease states such as a PDA, it may be a useful addition to the haemodynamic assessment of preterm infants during the first week of age.

Chapter 7: PDA Severity Score

7.1 Introduction

Treatment of a patent ductus arteriosus (PDA) in extremely low birth weight preterm infants is a controversial topic (Evans, 2015). Randomized controlled studies of PDA treatment have failed to demonstrate a reduction in PDA-associated morbidities which include intraventricular haemorrhage (IVH), necrotizing enterocolitis (NEC), chronic lung disease (CLD), death, and poor neurodevelopmental outcome (Cooke et al., 2003, El-Khuffash et al., 2011, Cunha et al., 2005, Shortland et al., 1990, Van, 2007, Brooks et al., 2005, El-Khuffash et al., 2008). Those trials demonstrate an overall failure to physiologically categorise PDA severity with weaknesses arising from using poorly validated clinical signs, treating the PDA as an all or none phenomenon or using echocardiography such as PDA diameter. Haemodynamic significance relates to the volume of the shunt from the systemic to the pulmonary circulation. The resultant flow across the shunt will lead to increased pulmonary blood flow (pulmonary over-circulation) at the expense of systemic blood flow (systemic hypoperfusion). The magnitude of this shunt (and how the heart handles it) may explain the association between a PDA and the above-mentioned morbidities. Despite these flaws the haemodynamically significant PDA remains clinically significant with a high burden on the patient, family and society with both short and long term morbidity and mortality leading to a need for a more robust assessment of the significance of a PDA. Therefore, a more comprehensive appraisal of those physiological features in the presence of a PDA using echocardiography may improve our understanding of haemodynamic significance.

Recently, the relationship between the severity and duration of the ductal shunt and the evolution of CLD in preterm infants has been further highlighted (Schena et al., 2015).

The presence of significant early shunting leading to increased pulmonary blood flow reduces lung compliance and may expedite the inflammatory process leading to CLD evolution (Chang et al., 2008). However, defining haemodynamic significance in the early neonatal period remains a challenge with several methods being employed using clinical criteria, echocardiography, or both (Zonnenberg and de Waal, 2012). There is further scope to accurately define early haemodynamic significance, determine the optimum time of assessment and relating that to important outcomes such as CLD. The aim of this study was to identify PDA characteristics associated with CLD or death and devise a PDA severity score at an optimal time point during the first week of life that can predict CLD or death before discharge

7.2 Methods

7.2.1 Study Design, Setting and Patient Population

This was a multicentre prospective observational cohort study conducted in tertiary neonatal intensive care units (NICU) in Ireland, Canada, and Australia. Institutional research ethics board approval was obtained at all participating sites. All admitted preterm neonates with a gestational age less than 29 weeks to NICU were considered eligible for inclusion. Parents of all eligible infants were provided with an information sheet and fully informed written consent was obtained prior to enrolment. Infants with major congenital abnormalities and cardiac lesions other than PDA were excluded from this study. Neither prophylactic indomethacin nor medical treatment of the PDA with non-steroidal anti-inflammatory drugs was used during the first 7 days of life in enrolled patients. Treatment beyond the first week of life was done at the discretion of the attending neonatologist and was primarily driven by dependence on invasive ventilator support and clinical evaluation. Management of hypotension during the study period was based on local hospital guidelines employing a combination of fluid resuscitation and inotropes. Echocardiograms were performed for the assessment and management of hypotension were not part of this study and no PDA management was instituted to reverse hypotension. The approach to pulmonary haemorrhage management was fluid and red blood cell resuscitation and increasing mean airway pressure. All cases of pulmonary haemorrhage in this cohort were relatively mild requiring minimal resuscitation. Frusemide was not used during the study period (first week of life). All frusemide use occurred beyond the first two weeks of age either during blood transfusions or to improve clinical symptoms of evolving CLD.

Continuous frusemide infusions were not used in the patient cohort. The results of the echocardiograms were not communicated to the medical team caring for the infants unless they specifically requested a clinically indicated echocardiography assessment or if congenital heart disease was identified.

7.2.2 Clinical Data Collection

Antenatal, birth, and clinical characteristics were collected including gestational age and birthweight at delivery, gender, mode of delivery, 5 minute Apgar score, cord pH, the use of antenatal steroids, magnesium sulphate ($MgSO_4$) administration, the presence of pre-eclampsia and chorioamnionitis. The following clinical outcomes were also obtained: culture proven sepsis, inotrope and frusemide use, postnatal steroids administration, PDA treatment beyond day 7 of age (including PDA ligation), necrotizing enterocolitis (NEC) with radiological evidence of pneumatosis intestinalis; intraventricular haemorrhage assessed on day 7 of age and classified according to Papile Classification (Papile et al., 1978), chronic lung disease (CLD) defined as the need for oxygen at 36 weeks post menstrual age (PMA); treated retinopathy of prematurity; length of hospital stay; death before discharge.

7.2.3 Echocardiography assessment

Echocardiography scans were performed at three time periods: a median [interquartile range] of 10 hours [7 – 12] (Day 1), 43 hours [38 – 47] (Day 2) and 144 hours [125 – 164] (Day 5 – 7). Evaluations were performed using the Vivid (GE Medical, Milwaukee) or Phillips (Andover, MA) echocardiography systems in accordance with recent published guidelines (Mertens et al., 2011b). A comprehensive anatomic assessment was conducted for the first echocardiogram of each infant to rule out congenital heart disease,

other than a PDA or a patent foramen ovale (PFO). All scans were stored in an offline archiving system for later offline measurements.

A comprehensive echocardiography assessment of PDA characteristics, markers of pulmonary overcirculation and systemic hypoperfusion, and LV function was performed. The following echocardiography measurements were obtained during each assessment [description of the methodology used to obtain those measurements are detailed elsewhere]Chapter 2, (Mertens et al., 2011b, El-Khuffash and McNamara, 2011a): narrowest PDA diameter (mm) measured using 2D methods at the pulmonary end (colour Doppler was not used to assess PDA diameter); maximum shunt velocity across the PDA (Vmax in m/s); left ventricular output (LVO in ml/kg/min); mitral valve inflow E wave, A wave, and E:A ratio; pulmonary vein diastolic velocity (PVd in m/s); left atrial to aortic root ratio (LA:Ao); descending aortic, celiac artery and middle cerebral artery (MCA) end diastolic flow (EDF in m/s). Tissue Doppler imaging (TDI) of the apical 4-chamber view was used to obtain LV systolic (s`) early diastolic (e`) and late diastolic (a`) velocities using a pulsed wave Doppler sample gate of 2 mm at the level of the lateral mitral valve annulus. If the e` and a` wave were fused, we measured the single wave as an a` wave. Measurement technique was standardized across all hospitals. Specifically, left ventricular output was measured as follows: the aortic root diameter was measured at the hinges of the aortic valve leaflets from the long axis parasternal view used to calculate the aortic cross sectional area (AoCSA). The velocity time index (VTI) of the ascending aorta was obtained from measuring the pulsed wave Doppler from the apical 5-chamber view. The cursor was aligned to become parallel to the direction of flow. No angle correction was used and an average of three consecutive Doppler wave forms was used to estimate the VTI. Left ventricular output (ml/kg/min) was determined using this formula: (AoCSA × VTI × Heart rate) ÷ Weight.

7.2.4 Statistical Analysis

The cohort was divided into two groups based on the presence of the primary outcome defined as a composite of CLD and death before discharge (CLD/Death). We investigated longitudinal trends in echocardiography parameters, measured across the three time points, between infants with and without CLD/Death. This analysis was performed to identify the ideal time point for creating the PDA severity score to predict CLD/Death. Univariate analysis was conducted on all the measured echocardiography parameters comparing infants with and without CLD/Death. Continuous variables were tested for normality using the Shapiro-Wilk test and presented as as means (standard deviation) or median [inter-quartile range] as appropriate. Two group analyses were conducted using a student t test or a Mann Whitney U test as appropriate. A two way repeated measures ANOVA was used to assess the difference in the echocardiography parameters between infants with and without CLD/Death across the three time points. Pair wise comparisons with Bonferroni adjustment were conducted if ANOVA was significant. Categorical variables were presented as proportions, and compared using the Chi squared or Fisher exact test as appropriate. We accepted a p value of < 0.05 as significant. SPSS (version 21) was used to perform the statistical analysis.

7.2.5 Developing the PDA Severity Score

Parameters from the Day 2 scan were used to devise the PDA severity score (PDAsc). During this time point, several echocardiography markers were significantly different between those with and without the primary outcome (a composite of CLD and/or death before discharge). On Day 1, the echocardiography markers were more homogenous in the entire cohort with less difference between the two groups observed (see figure 7.1 later).

We decided a priori not to interrogate the predictive value of the Day 5 – 7 scan as it would delay the identification of a clinically significant PDA. In addition, clinical signs of a PDA would be more overt by the first week of life.

All echocardiography variables of pulmonary over-circulation and systemic hypoperfusion were considered for inclusion in the multivariate logistic regression model used to devise the PDA severity score. In addition, we included functional parameters of the left ventricle measured using TDI. Gestation at delivery expressed in whole weeks and days (as two decimal points) was included *a priori* in the model as it is an important determinant of CLD/Death evolution in this population. Echocardiography parameters were entered into the model and retained if their association with CLD/Death remained significant. Variables that were highly correlated with others (collinearity) and those with no predictive value (p value > 0.10) were removed from the final model. Four echocardiography parameters were included in the final model: PDA diameter (mm), maximum velocity across the PDA shunt (m/s), left ventricular output (ml/kg/min), and left ventricular diastolic function (LV free wall), measured as an a` wave using TDI (cm/s). The variables in the final model were tested for collinearity. All the variance inflation factor (VIF) values were less than 1.5.

We also examined the effect of including cardiorespiratory characteristics measured at the time of the scan in the model (mean airway pressure, inspired oxygen, oxygen saturation and systolic/diastolic blood pressure) in addition to gestation and the four chosen echocardiography markers to assess whether this would improve its predictability. Although there was a statistically significant difference in those parameters between the two groups during the Day 2 scan, those differences were very small in magnitude and were not clinically relevant (Table 7.1). There was a significant positive correlation between

gestational age and all of those parameters. None of those parameters improved the ability of the model to predict the outcome of interest.

A weighted scoring system based on the beta coefficients of the significant predictors was used to derive the PDA severity score (Harrell et al., 1996). The following equation was used to derive the risk score for each infant: (Gestation *in weeks* × -1.304) + (PDA diameter *in mm* × 0.781) + (Left ventricular output *in ml/kg/min* × 0.008) + (maximum PDA velocity *in m/s* × -1.065) + (LV a` wave *in cm/s* × -0.470) + 41, where 41 is the constant of the formula. This score ranges between 0 (low risk) and 13 (high risk). The predicted probability for each infant to develop CLD/Death was also derived from the model. Infants without a PDA at the time of the scan were assigned a risk of 0 as a severity score cannot be derived from infants without a PDA diameter or maximum PDA velocity measurement.

We compared the ability of the PDAsc to predict CLD/death against the predictive value of gestational age alone or PDA diameter (measured on Day 2) alone. In addition, we compared the PDAsc with another score derived from a combination of five clinical characteristics using the same methodology described above: Gestation; use of antenatal steroids; days on invasive ventilation; late onset sepsis; and necrotizing enterocolitis. A receiver operating characteristics (ROC) curve was constructed to assess the ability of the derived PDA severity score to predict CLD/Death compared with gestation, PDA diameter and the clinical parameters. In addition, we also assessed the association between the PDAsc and two components of the composite outcome separately, in addition to NEC.

Table 7.1: Demographics and antenatal details in the two groups.

	No CLD/Death (n=62)	CLD/Death (n=79)	p
Gestation (weeks)	27.7 (1.1)	26.1 (1.3)	<0.001
Birth weight (g)	1128 (211)	813 (143)	<0.001
Male	34 (55%)	52 (66%)	0.2
Caesarean Section	39 (63)	51 (65)	0.9
5 minute Apgar Score	9 [7 – 9]	8 [6 – 9]	0.01
Cord pH	7.33 (0.06)	7.30 (0.10)	0.2
Chorioamnionitis	5 (8%)	7 (9%)	1.0
Pre-Eclampsia	0 (0%)	7 (9%)	0.02
$MgSO_4$	45 (73%)	58 (73%)	1.0
Any Surfactant Use	47 (76%)	75 (95%)	0.001
Antenatal Steroids			
None	6 (10%)	14 (18%)	
One Dose	19 (31%)	11 (14%)	0.04
Two Doses	37 (60%)	54 (68%)	
Cardio-respiratory Characteristics*			
Mechanical Ventilation	10 (16%)	51 (65%)	<0.001
MAP (mmHg)	8 (2)	9 (2)	<0.001
FiO2 (%) †	21 [21 – 42]	21 [21 – 65]	<0.001
O2 Saturations (%)	96 (3)	94 (3)	<0.001
pH	7.32 (0.06)	7.28 (0.07)	0.003
TFI (ml/kg/day)	120 [100 – 125]	120 [100 – 140]	0.24
Systolic BP (mmHg)	52 [47 – 60]	50 [44 – 54]	0.03
Diastolic BP (mmHg)	31 [27 – 36]	28 [24 – 39]	0.01

Values are presented as means (standard deviation), median [inter-quartile range] and count (%). $MgSO_4$: Magnesium Sulphate, BP: Blood Pressure, TFI: Total Fluid Intake, MAP: Mean Airway Pressure, FiO2: Inspired Oxygen. ***** During Day 2 echocardiogram. † presented as median [range].

7.3 Results

One hundred and forty one infants were enrolled in the study. The mean (SD) gestational age and weight at birth of the cohort were 26.8 (1.4) weeks and 952 (235) grams respectively. Echocardiography scans were available for 134 infants (95%) on Day 1, 141 infants (100%) on Day 2 and 123 infants (87%) on Day 5 – 7 (the attrition was due to investigator unavailability). A PDA was present in 130 infants (97%) on Day 1, 118 (84%) on Day 2 and 84 (68%) on Day 5 – 7. Seventy nine infants (56%) developed the primary outcome of interest (CLD/Death), of which 65 developing CLD and 15 died before discharge. The causes of death are as follows: withdrawal of life sustaining treatment for severe IVH (n=6); gram negative sepsis (n=2); severe NEC (n=3); severe respiratory failure (n=3), one of which also attained the diagnosis of CLD prior to death) and one with a volvulus. Table 7.1 illustrates the differences in demographics, antenatal details, and the cardiorespiratory characteristics between the two groups. Infants with CLD/Death had lower gestational age and weight at birth and a lower 5 minute Apgar score. In addition, there was a higher incidence of pre-eclampsia and a slightly lower use of antenatal steroids in the CLD/Death group (Table 7.1). Infants with CLD/Death also had a marginally lower mean airway pressure, oxygen saturations, pH and blood pressure. Those differences however, were not clinically relevant (Table 7.1). Table 7.2 demonstrates the distribution of other important outcomes between the two groups. Infants with CLD/Death had a longer duration of mechanical ventilation, and a higher incidence of inotrope, frusemide and postnatal steroid use. PDA treatment beyond the first week of life and culture proven late onset sepsis were also more common in the CLD/Death group (Table 7.2). None of the infants received PDA treatment over the first week of life. PDA treatment beyond this period was left to the discretion of the local centre and is outlined in Table 7.2.

Table 7.2: Distribution of other outcomes between the two groups.

	CLD/Death (n=79)	No CLD/Death (n=62)	p
Grade 3 or 4 IVH by Day 7	11 (14%)	4 (7%)	0.2
Pulmonary Haemorrhage	8 (10%)	2 (3%)	0.2
NEC	16 (20%)	7 (11.3%)	0.2
Clinical Suspicion	3	2	0.6
Radiological Diagnosis	5	3	
Surgical Treatment	8	2	
Use of Frusemide	53 (72%)	13 (22%)	<0.001
Postnatal Steroids	23 (29%)	1 (2%)	<0.001
PDA treatment (beyond day 7)	49 (62%)	8 (13%)	<0.001
Ibuprofen	38 (48%)	8 (13%)	<0.001
Paracetamol	19 (24%)	1 (2%)	<0.001
Surgical Ligation	9 (11%)	1 (2%)	0.04
Culture-Proven Sepsis	35 (44%)	5 (8%)	<0.001
PVL (in survivors)	10 (15%)	3 (5)	0.07

Values are presented as count (%). PVL: Periventricular Leukomalacia, NEC: Necrotising Enterocolitis, PDA: Patent ductus arteriosus.

7.3.1 Univariate Analysis of the Echocardiography Parameters

Echocardiography parameters measured across the three time points were compared between infants with and without CLD/Death. Figure 7.1 illustrates the change in those parameters between the two groups across the three time points. The three PDA related echocardiography markers used in the regression model are in the first row of the figure. LVO was higher and PDA Vmax was lower in the CLD/Death group across the three time points. PDA diameter was significantly larger in the CLD/Death group on Days 2 and 5 – 7 ($p< 0.05$ on ANOVA). The differences in the remainder of the echocardiographic markers across the two groups with respect to time were not significant (two way ANOVA $p>0.05$) (Figure 7.1). There was a significant increase in LV a` over the first week of age in the entire cohort: 4.4 (1.9) vs. 5.3 (1.9) vs. 5.8 (2.0) m/s (one way ANOVA <0.001). There was no difference in LV a` between the two groups at any time point. During the Day 2 scan, wave fusion occurred in 31 infants (22%).

Figure 7.1: Echocardiography parameters measured across the three time points between the two groups.

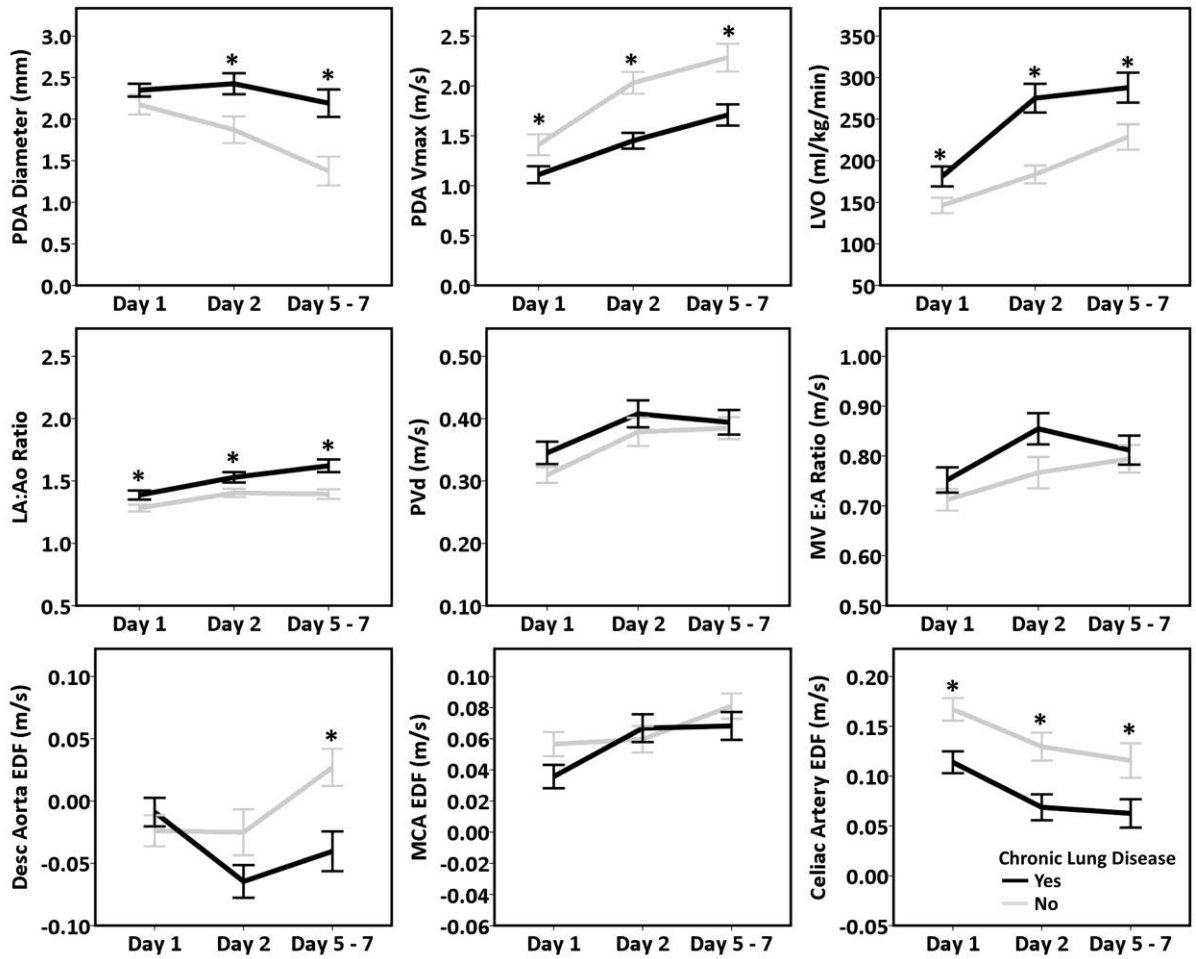

Values are presented as means. The black line represents Chronic Lung disease/Death while the grey line represents no Chronic Lung Disease/Death. The error bars represent the standard error of the mean. Two way repeated measures ANOVA was used to compare the two groups across the three time points. * indicates a p value < 0.05. PDA: Patent ductus arteriosus; Vmax: Maximum flow velocity; LVO: Left ventricular output; LA:Ao: Left atrial to aortic root ratio; PVd: Pulmonary vein diastolic flow velocity; MV: Mitral valve; EDF: end diastolic flow; MCA: Middle cerebral artery.

7.3.2 PDA Severity Score

Five variables were included in the final logistic regression model devised to predict the primary outcome, CLD/Death: Gestation (weeks), PDA diameter (mm), Vmax (m/s), LVO (ml/kg/min) and LV a` (cm/s). The four echocardiography parameters included in the model were obtained from the Day 2 scan which was performed at a median 43 hours [38 – 47]. Table 7.3 illustrates the unstandardized beta coefficients of the variables which were used to devise the PDA severity score, the standardised beta coefficients which demonstrate the relative importance of each variable in the model, and the significance of each variable. The regression formula used to devise the score is also presented in Table 7.3. A PDA severity score ranging from 0 (low risk) to 13 (high risk) was obtained. The mean (SD) risk score in the population was 6.0 (2.5). Infants with CLD/Death had a higher score than those without CLD/Death [7.3 (1.8) vs. 3.8 (2.0), $p<0.001$, Figure 7.2A]. There was a strong correlation between the predicted probability of developing CLD/Death based on the model and the PDA severity score (Figure 7.2B).

Table 7.3: Results of the regression model used to devise the PDA severity score.

Predictor Variable	Unstandardized β	Standardized β	p
Gestation	-1.304	-0.398	<0.01
PDA Diameter	0.781	0.079	0.07
LVO	0.008	0.272	0.03
PDA Vmax	-1.065	-0.163	0.02
LV a`	-0.470	-0.236	0.01

The unstandardized beta coefficients were used to devise the risk score by using the following formula: (Gestation × -1.304) + (PDA diameter × 0.781) + (LVO × 0.008) + (Vmax × -1.065) + (LV a` × -0.470) + 41, where 41 is the constant of the formula. Negative β coefficients indicate that higher variable values ae associated with a decrease in the risk of developing the outcome. Positive β coefficients indicate that higher variable values are associated with an increase in the risk of developing the disease.

Figure 7.2: Difference in the PDA severity score between infants with and without CLD/Death (A) and the relationship between the score and the predicted probability of CLD/Death in the entire cohort (B).

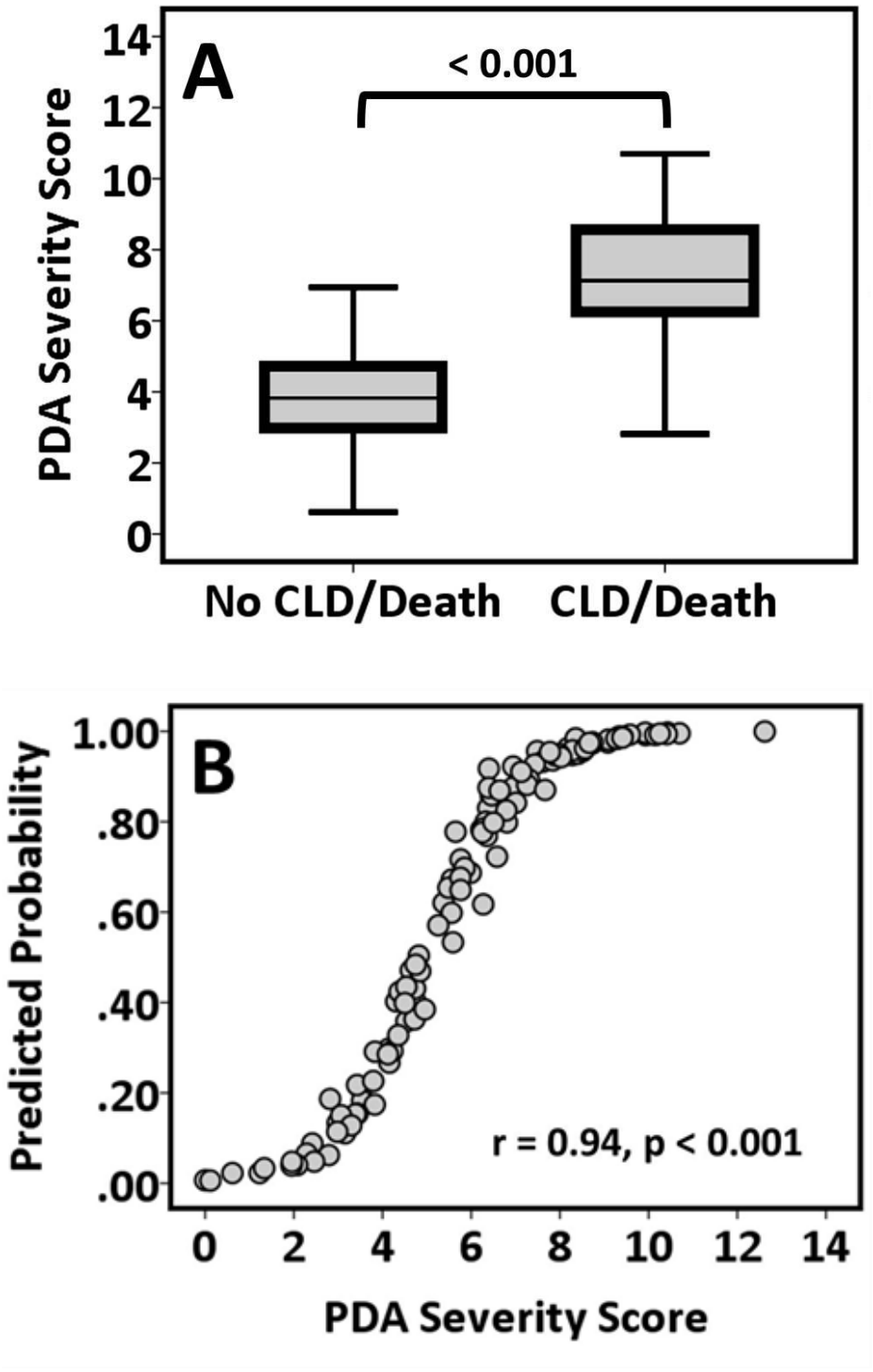

A ROC curve, constructed to assess the ability of the score to predict CLD/Death in the population, yielded an area under the curve (AUC) of 0.92 (95% CI 0.86 – 0.97, p<0.001). This compared favourably with comparator predictive models based on a combination of clinical characteristics (Gestation, antenatal steroids, late onset sepsis, NEC and ventilation days) (AUC 0.84, p=0.04), gestation alone (AUC 0.80, p=0.04) and PDA diameter alone which had very poor predictability (AUC 0.59, p=0.06) (Figure 7.3). A cut off of 5 had a sensitivity of 92%, a specificity of 87%, a positive predictive value of 92%, and a negative predictive value of 82%. In this cohort, 73 infants (52%) had a score of 5 or greater.

The relationship between the PDA severity score and CLD/Death was further examined by controlling for important outcomes presented in table 2 that were associated with CLD/Death on univariate analysis. The relationship between the PDA severity score and CLD/Death remained significant (Adjusted odds ratio 2.1 [95%CI 1.5 – 3.1], p<0.001) when controlling for other potential predictors of CLD: PDA ligation, late onset sepsis, post-natal steroid use, and frusemide use, none of which remained significantly associated with CLD/Death in this model. In addition we examined the difference in the score between infants with and without CLD alone, Death alone before discharge and NEC. Infants with CLD had a significantly higher score [7.2 (1.9) vs. 3.8 (2.0), p < 0.001]. Similarly, infants that died before discharge has a higher score [7.7 (1.7) vs. 5.7 (2.5), p = 0.01]. Finally, infants with NEC had a higher PDA severity score than those without NEC [7.5 (2.3) vs. 5.6 (2.4), p < 0.003]. The PDAsc had an AUC of 0.70 (95% 0.57 – 0.81, p=0.007) for the ability to predict NEC.

Figure 7.3: Receiver operating characteristics curve of the ability of PDAsc to predict CLD/death.

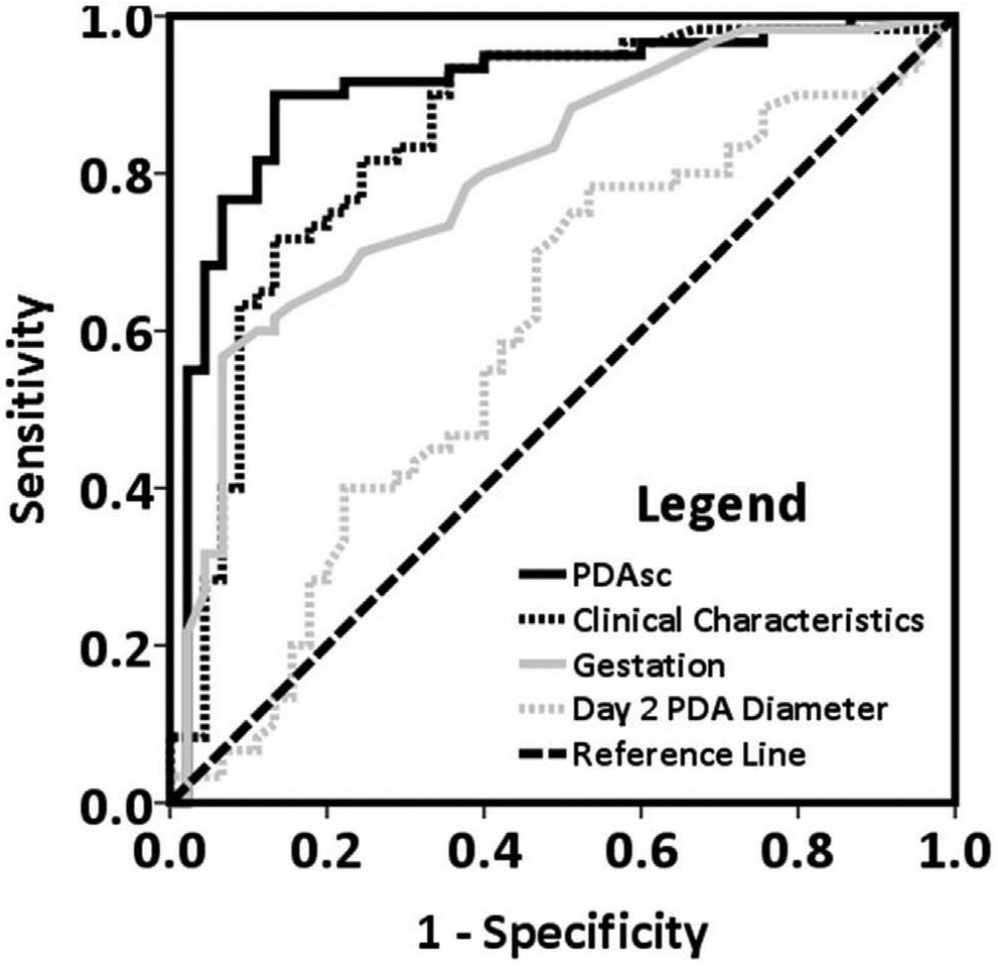

The PDAsc was compared with a combination of clinical characteristics, gestation and PDA diameter.

7.4 Discussion

In this study, we demonstrated that there are early differences in characteristics of the PDA during the first week of life between infants who develop CLD or die before discharge and those who do not develop those outcomes, with increasing divergence of those characteristics over the first week of life. The phenotypic features of these higher risk patients include larger PDA diameter, lower maximum velocity across the PDA (indicating a lack of ductal constriction and an unrestricted flow pattern in the absence of significant pulmonary hypertension) and increased pulmonary blood flow (indicated by a higher LVO). In addition, a PDA severity score derived on day 2 of age using gestation along with echocardiography markers of PDA characteristics and LV diastolic function can predict the later occurrence of chronic lung disease or death in a group of preterm infants less than 29 weeks gestation.

There has been a recent reemphasis to derive a better definition of PDA "haemodynamic significance" which resulted from the failure of all randomised controlled trials of pre-symptomatic PDA treatment to yield an improvement in short- and long-term PDA associated morbidities (Cooke et al., 2003, Schmidt et al., 2006). All of these studies however, treated the PDA as an all-or-none phenomenon, with no quantification of the impact the PDA has on pulmonary or systemic blood flow. Those trials relied almost solely on PDA diameter to determine significance. This over-simplification ignores the effect of shunt volume in determining PDA significance. Despite this a haemodynamically significant PDA remains a large burden on the infant which continues to be something which needs to be better defined. The PDA in the premature infant's early life should be regarded as a

continuum from being physiologic, and potentially beneficial to being pathological (when pulmonary vascular resistance drops) leading to systemic hypoperfusion and pulmonary congestion. There are several challenges with defining haemodynamic significance associated with a PDA. A variety of definitions for haemodynamic significance have been employed which incorporate clinical and echocardiography parameters without clear validation and justification (Zonnenberg and de Waal, 2012). In addition, the cut offs at which echocardiography PDA characteristics are assigned significance are often allocated based on whether infants received treatment or not rather than associating them with morbidity(McNamara and Sehgal, 2007, Youn et al., 2013), or are based on the short-term occurrence of clinical features of a PDA such as bounding pulses, a murmur and an active precordium (Alagarsamy et al., 2005).

There have been recent attempts to relate early PDA features to the later evolution of PDA-associated morbidities, particular respiratory morbidities such as CLD. In the premature newborn baboons model, exposure to a PDA with an increased pulmonary blood flow leads to impaired pulmonary function and arrested alveolar development and surface area. Pharmacologic closure of the PDA in this animal model reduces the detrimental effects of preterm delivery on pulmonary function and surface area (Chang et al., 2008). In preterm infants, Sehgal and McNamara demonstrated that a composite score of PDA significance based on echocardiography criteria measured at the time of PDA treatment (at a median of 7 day) is associated with CLD (Sehgal et al., 2012b). Although this study strengthens the evidence of the association between a PDA and CLD, applying a staging system for ductal diseases severity at an earlier time point may facilitate better targeted treatment. Sellmer *et al*, demonstrated that large PDAs assessed on day 3 of age are associated with IVH, CLD and mortality, although causality may not be directly extrapolated (Sellmer et al., 2013). More

recently, Schena *et al* demonstrated that infants exposed to a more severe PDA (based on a scoring system proposed by McNamara and Sehgal (McNamara and Sehgal, 2007)) for a longer period during their hospital stay are more likely to develop CLD. Interestingly, after adjusting for PDA severity, PDA ligation was no longer associated with CLD in their cohort (Schena et al., 2015). The lack of association between PDA ligation and CLD when PDA severity is accounted for is gaining an increased recognition (Weisz et al., 2014, El-Khuffash et al., 2015). Whilst none of these temporal studies prove a cause and effect relationship between a PDA and CLD, the evidence is strengthening for a select population with increased shunt volume.

There exists a need for a *discriminative and predictive* score to measure the degree of hemodynamic significance of a PDA in the first 48 hours of life (Guyatt et al., 1992), and associate this score with the development of morbidities associated with a PDA. As gestational age plays an independent role in the evolution of important morbidities it should be included in devising the score. This score should also include markers of shunt size (PDA diameter and Vmax) and shunt volume (LVO). A larger PDA diameter with unrestrictive low velocity flow will lead to increased pulmonary blood flow identified by an increased LVO. The effect of increased pulmonary blood flow on the preterm neonatal lung may be similar to that of the baboon model described above.

In addition consideration should be given to left heart diastolic function as this plays a key role in handling the increased blood volume returning to the heart. LV diastolic function may be an important determinant of how the heart can accommodate the increased preload resultant from the shunt. Compromised diastolic function may contribute to increased pulmonary venous pressure, thereby worsening the effect of increased pulmonary blood flow. Preterm infants have impaired diastolic function due to their stiffer

myocardium and are therefore heavily reliant on the late diastolic phase of atrial contraction for ventricular filling. Impaired diastolic function in the setting of increased pulmonary venous return will lead to increased left atrial pressure and eventual pulmonary venous congestion (Dokainish, 2015). Therefore, devising a score of haemodynamic significance applied during the early neonatal period using echocardiography markers that incorporate diastolic function of the LV may lead to a better characterisation of the pathological nature of the PDA. The PDA severity score derived in this study encompasses all the components mentioned above. This score was highly predictive of the composite outcome (CLD/Death). As CLD and death were predominantly mutually exclusive outcomes in this study, the score was also significantly higher in infants with the individual components of the outcome. In addition, a higher score was observed in infants with PDA associated morbidities such as NEC. The score was also predictive of NEC with an AUC of 0.70. Interestingly, PDA ligation was no longer associated with CLD when the score was taken into account. These data further emphasise the increasing realisation that PDA severity and haemodynamic impact rather than the ligation *per se,* is likely to have a causal effect. The cut off of 5 yielded the best sensitivity and specificity. More importantly, it yielded the best positive and negative predictive value which is more generalizable to other populations. This cut off could therefore be used to further validate the predictability of this score in a different population or to determine selection for treatment in a randomised controlled setting.

It is worth noting that markers for systemic hypoperfusion (such as descending aortic EDF) were not included as a component of the score due to collinearity with the markers for pulmonary over- circulation. The relative influence of each variable in the score was illustrated by the standardized beta coefficient in Table 7.3. Although gestation had the

biggest influence (with the largest standardised beta value), LVO and LV a` had values of almost similar magnitude emphasising their importance in predicting the outcome of interest. The relatively lower standardised beta coefficient value for PDA diameter illustrate that PDA size in isolation is a poor surrogate for haemodynamic significance as the pressure gradient across the PDA, rather than the size, is the major determinant of shunt volume during the early period.

The PDAsc compared favourably with a score based on a combination of important clinical characteristics to predict CLD/Death. These clinical characteristics were chosen for comparison as they are all strongly associated with CLD and/or death: gestational age, use of antenatal steroids, sepsis, NEC and duration of invasive ventilation. Although a clinical score based on a combination of clinical characteristics had a relatively good predictive ability with an AUC of 0.85, their utility for early targeted PDA treatment is questionable as the majority of thresholds in this risk score are only attained beyond the first two weeks of life. Similarly, the PDAsc performed better than gestation alone, or PDA diameter alone highlighting the benefit of a more comprehensive assessment of PDA significance during the early neonatal period. The addition of cardiorespiratory parameters to the regression model, particularly mean airway pressure, did not improve the predictability of the PDAsc. We found that gestational age had a large influence on these clinical characteristics; therefore as such, including gestational age in the model was likely to account for the impact of these characteristics. In addition, using mean airway pressure may be problematic as variation in clinical practise across centres (rather than the clinical status of the infant) is a major determinant of the level of respiratory support those infants receive.

7.5 Limitations

Although a relatively large number of infants were included in this study, the observational nature of this study may have introduced selection bias to the patient cohort. In addition, although a standardised protocol for PDA assessments was used in all participating centres, inter-observer variability during image acquisition and/or offline measurement analysis could have influenced the results. In particular, TDI measurements require equipment and expertise that may not be present in all units. Furthermore the treatment of the PDA after 7 days of life is at the discretion of the physician which may vary between institutions affecting some of the outcome measurements. However we were most interested in the effects of early shunting on important neonatal outcomes. We used a simple definition of CLD (need for oxygen at 36 weeks corrected) without taking into account the severity of the condition. This was performed to have a dichotomous outcome for the purposes of the regression model and to facilitate generalizability of the score. Our sample size did not support further outcome stratification into a more complex end point. This approach may have missed milder forms of the disease. We did not test the utility of the score in another cohort and therefore, the generalizability of this score is unproven.

7.6 Conclusion

The ability to accurately predict PDA associated morbidities such as CLD/Death using a PDA severity score can pave the way for a more targeted treatment. The cut off used in this cohort places about 50% of infants under 29 weeks gestation in the high risk category

thereby limiting the number of infants exposed to PDA treatment. This PDA severity score should be validated in a similar cohort of preterm infants in a prospective manner, and may be used to devise a randomised controlled trial of targeted PDA treatment.

Chapter 8: Magnesium Sulphate and its influence on haemodynamics during the transitioning period

8.1 Introduction

The use of antenatal magnesium sulphate ($MgSO_4$) prior to premature birth for neuroprotection is now well established (Doyle et al., 2009). A recent Cochrane study reviewed all trials examining antenatal magnesium sulphate administration to preterm infants and its effects on neurological outcomes. They found based on this by analysing over 6000 infants that the use of $MgSO_4$ substantially reduced the risk of cerebral palsy in these children (relative risk 0.68) and also significantly reduced the rate of substantial gross motor dysfunction (relative risk 0.61). Based on these and other findings, the use of $MgSO_4$ for threatened preterm birth has become the standard of care in most institutions alongside the use of antenatal steroids. However, the impact of antenatal $MgSO_4$ administration on the haemodynamic status of preterm infants during the first 48 hours of age is poorly understood. One study sought to establish the effect of antenatal $MgSO_4$ on systemic blood flow in the first 24 hours of life by assessing the superior vena cava blood flow and right ventricular output. By comparing 48 infants who received antenatal $MgSO_4$ to placebo control infants, they found there was no consistent cardiovascular effect of $MgSO_4$ in the first 24 hours (Paradisis et al., 2012).

Recent studies have demonstrated inconsistent results of the effect of $MgSO_4$ on cerebral blood flow using Doppler flow measurements (Imamoglu et al., 2014, Shokry et al., 2010). Further studies are required to assess the impact of $MgSO_4$ on left myocardial

performance, systemic blood flow, LV loading conditions, and systemic vascular resistance in the first few hours of life.

We have demonstrated the feasibility and reproducibility of left ventricular (LV) longitudinal strain measured using tissue Doppler deformation imaging, and LV rotational mechanics (LV apical and basal rotation, LV twist, and LV untwist rate) in extremely preterm infants. LV longitudinal strain has the advantage of detecting early myocardial dysfunction in different diseases (El-Khuffash et al., 2014, Sehgal et al., 2013). Similarly, LV rotational mechanics can be assessed using STE to measure LV twist (the wringing motion of the LV during systole) and LV untwist rate (the recoil of the LV during early diastole thereby generating a suction force for LV filling). The application of those novel echocardiography parameters and their relationship to loading conditions and SVR in preterm infants warrants further study.

We hypothesize that preterm infants exposed to antenatal $MgSO_4$ for the purposes of neuroprotection have a lower LV afterload and SVR, and a higher myocardial performance measured using STE. The primary aim was to assess the effect of $MgSO_4$ administration on LV functional parameters, systemic blood flow and loading conditions when compared with infants who did not receive $MgSO_4$.

8.2 Methods

Within our cohort of 105 infants between January 2013 and December 2014, infants who did not receive antenatal $MgSO_4$ (Control group) were matched for gestation (± 2 days), birthweight (± 100 grams) and mode of delivery with infants who were in receipt of $MgSO_4$ prior to delivery ($MgSO_4$ group). The investigator performing the matching was blinded to all other infants' characteristics and outcome measures. Written parental informed consent

was obtained from all participants and ethical approval was obtained from the Hospital Ethics Committee.

In the Rotunda Hospital, mothers with pregnancies less than 32 weeks gestation who are likely to deliver within 12 – 24 hours are given a 4g loading dose of $MgSO_4$ over a 20 minute period for foetal neuroprotection. No subsequent infusion of $MgSO_4$ is given. Mothers also receive a course of antenatal steroids prior to delivery where possible (Two doses of Beclomethasone 12mg, 12 hours apart). The main reason for not receiving $MgSO_4$ is the lack of time available between presentation and delivery, or an unexpected preterm delivery.

8.2.1 Clinical Demographics

Antenatal, birth and neonatal characteristics were obtained from the database. In addition clinical cardio-respiratory characteristics during the two echocardiography assessments were collected and included: systolic and diastolic blood pressure, heart rate, mean airway pressure, oxygen requirements, oxygen saturation, invasive ventilation, and pH. The following clinical outcomes were also obtained: intraventricular hemorrhage (IVH) assessed on day 7 of age and classified according to Papile Classification (10); pulmonary hemorrhage; necrotizing enterocolitis (NEC) with radiological evidence of pneumatosis; and chronic lung disease (CLD) defined as the need for oxygen at 36 weeks corrected gestation; death before discharge.

8.2.2 Echocardiography Assessment

Echocardiography was performed on day one of life at a median [interquartile range] of 11 hours [9 – 13] (Day 1) and at day two of life at a median of 40 hours [37 – 46] (Day 2)

All studies were conducted using a the standardized functional protocol as discussed in the Methods chapter. The scans were all stored as raw data in an archiving system (EchoPac, General Electric, version 112 revision 1.3) for later offline analysis. All offline analysis was carried out by a single investigator who was blinded to the $MgSO_4$ status of the infants.

The following echocardiography parameters were obtained on all infants. The methods for obtaining those parameters, their feasibility and reproducibility, and their reference ranges for this population are described in detail elsewhere: Patent ductus arteriosus (PDA) diameter; Ejection fraction (EF) measured by Simpson's biplane method; Left ventricular output (LVO); LV longitudinal strain (LS); LV basal and apical rotation defined as the circumferential clockwise or counter-clockwise movement of the apex and base along the long axis of the left ventricle occurring during systole (in degrees); LV twist fined as the net difference between apical and basal rotation; LV untwist rate (LVUTR) defined as the velocity of untwist during diastole per unit time(degrees/second); Global right ventricle (RV) Fractional Area Change (RV FAC) defined as the measure of the change in RV cavity area from diastole to systole in two planes (four- and three-chamber views). LV wall stress (g/cm^2) was calculated as: [1.35 x (mean arterial pressure) x (LVESD)]/[4 x (LVPWT) x (1 + LVPWT/LVESD)], where 1.35 is the conversion factor from millimetres of mercury to grams per square centimetre, LVESD is the LV cavity end systolic diameter and LVPWT is the LV posterior wall thickness at end systole. Systemic vascular resistance (SVR) was calculated by using the following formula: (mean systemic BP – mean tricuspid valve inflow pressure gradient) / LVO (Noori et al., 2007a).

8.2.3 Statistical Analysis

The cohort was divided into two groups based on whether or not they received antenatal $MgSO_4$. Continuous data were checked for normality using the Shapiro-Wilk test and a histogram representation and presented as mean (standard deviation) if normally distributed or median [inter-quartile range] if skewed. Normally distributed data were compared using the student t-test and skewed data were compared using the Mann-Whitney U test. Categorical variables were presented using count (percent) and compared using Chi Square or Fisher Exact tests as appropriate. Logistic regression was used to assess the independent effects of $MgSO_4$ and antenatal steroids on CLD. Linear regression was used to assess the independent effect of $MgSO_4$ and antenatal steroids on the echocardiography functional parameters. A p value < 0.05 was considered significant. SPSS (IBM version 22) was used to conduct the statistical analysis.

8.3 Results

Nineteen infants less than 29 weeks gestation did not receive antenatal $MgSO_4$ over a two year period out of a total of 105 infants (18%). Those infants were matched from the same cohort with 19 infants who were in receipt of $MgSO_4$. All infants in the $MgSO_4$ group received the drug within 4 hours of delivery. There was no difference in gestation, birthweight, gender, mode of delivery or other antenatal characteristics between the two groups (Table 8.1). There was a trend towards more antenatal steroid use in the $MgSO_4$ group ($p = 0.05$, Table 8.1). Infants in the $MgSO_4$ Group had a higher rate of CLD compared

with the Control Group (Table 8.1). There was no difference between the groups in any of the other outcome parameters.

Table 8.1: Infant Characteristics and Clinical Outcomes.

	Control	$MgSO_4$	P
Gestation (weeks)	27.4 [25.5 – 28.0]	27.8 [26.1 – 28.5]	0.5
Birthweight (g)	980 [921 – 1143]	880 [810 – 1220]	0.7
Male	12 (63)	12 (63)	1.0
Caesarean Section	10 (53)	10 (53)	1.0
Preterm prolonged rupture of membranes	6 (32)	6 (32)	1.0
Antepartum Haemorrhage	4 (21)	3 (16)	1.0
Chorioamnionitis	0	1 (5)	1.0
Pre-eclampsia	0	0	NA
Small for Gestational Age	1 (5)	1 (5)	1.0
5 minute Apgar Score	8 [6 – 9]	9 [8 – 9]	0.3
Cord pH	7.33 [7.28 – 7.38]	7.36 [7.35 – 7.38]	0.2
Full Course of Antenatal Steroids	7 (37)	14 (74)	0.05
Grades III and IV IVH	5 (26)	1 (5)	0.2
Inotropes Use (1st week of age)	3 (16)	4 (21)	1.0
Pulmonary Haemorrhage	4 (21)	0	0.1
Necrotizing Enterocolitis	4 (21)	1 (5)	0.3
Chronic Lung Disease (in survivors)	5 (31)	13 (68)	0.04
Death before Discharge	3 (16)	0	0.2

Data are presented as medians [inter-quartile range] or count (percent). IVH: Intraventricular haemorrhage.

On Day 1, infants in the $MgSO_4$ Group had a lower systolic blood pressure [43 (5) vs. 50 (11), p=0.03] and a slightly higher pH [7.35 (0.04) vs. 7.31 (0.06), p=0.01] when compared with the Control Group. There was no difference in any of the other clinical cardio-respiratory characteristics between the groups (Table 8.2)**.** On Day 1, infants in the $MgSO_4$ group had a significantly lower SVR and a significantly higher EF, LV longitudinal strain, basal rotation, twist, LVUTR and RV FAC. There was a trend towards a lower LV wall stress in the $MgSO_4$ Group (p=0.06) (Table 8.2). All infants had a PDA with no difference in PDA diameter between the groups. On Day 2, there were no differences in any of the clinical or echocardiography parameters between the two groups with the exception of a clinically irrelevant difference in oxygen saturations. Seventeen infants in each group had a PDA with no difference in the diameter between the groups (Table 8.2).

On logistic regression, the association between $MgSO_4$ and CLD became a trend when controlling for antenatal steroids (p=0.06). On linear regression, the association between $MgSO_4$ and EF, LV longitudinal strain, basal rotation, twist and RV FAC remained significant when controlling for antenatal steroids (Table 8.3). Antenatal steroids did not have an independent effect on any of the outcome parameters of interest.

Table 8.2: Difference in cardiorespiratory characteristics and echocardiography parameters between infants with and without $MgSO_4$ on days 1 and 2.

	Control	$MgSO_4$	p	Control	$MgSO_4$
Cardiorespiratory					
FiO_2	21 [21 – 47]	21 [21 – 25]	0.39	21 [21 – 60]	21 [21 – 29]
MAP (cm H_2O)	9 (3)	8 (2)	0.18	9 (3)	8 (2)
Oxygen Saturations (%)	95 (3)	95 (2)	0.83	97 (3)	95 (2)
Invasive Ventilation	9 (47)	10 (53)	1.0	8 (42)	7 (37)
Heart Rate	155 (13)	154 (17)	0.75	166 (10)	168 (14)
Systolic BP (mmHg)	50 (11)	43 (5)	0.03	53 (9)	52 (8)
Diastolic BP (mmHg)	29 (9)	27 (5)	0.59	29 (6)	32 (7)
pH	7.31 (0.06)	7.35 (0.04)	0.01	7.32 (0.06)	7.31 (0.06)
Echocardiography					
PDA diameter (mm)	2.4 (0.6)	2.4 (0.4)	0.76	2.7 (0.6)	2.5 (0.9)
Ejection Fraction (%)	55 (8)	60 (6)	0.03	61 (9)	61 (8)
LVO (ml/kg/min)	138 (70)	155 (50)	0.41	200 (83)	213 (81)
SVR (mmHg/ml.kg.min)	293 [211 – 479]	238 [170 – 282]	0.03	203 [151 – 287]	173 [134 – 296]
Wall Stress (g/cm^2)	23 (9)	18 (7)	0.06	23 (11)	22 (9)
LV Longitudinal strain (%)	-12.7 (5.3)	-17.4 (3.6)	0.04	-19.6 (2.2)	-20.1 (8.1)
LV Basal Rotation (^{o})	5.6 (7.5)	-1.1 (4.7)	0.03	0.5 (8.1)	-1.0 (8.8)
LV Apical Rotation (^{o})	9.9 (7.4)	9.6 (3.5)	0.9	11.4 (2.5)	10.2 (2.9)
LV Twist ($_o$)	4.1 (2.7)	8.8 (3.2)	0.01	8.5 (1.4)	7.9 (5.1)
LV untwist rate (^{o}/s)	-55 (27)	-110 (59)	0.02	-105 (21)	-73 (55)
RV FAC (%)	29 [24 – 39]	39 [30 – 45]	<0.01	39 [36 – 46]	44 [40 – 50]

Data is presented as means (standard deviation), medians [inter-quartile ranges] or count (%). MAP: Mean Airway Pressure; FiO_2: fractional inspired oxygen; BP: blood pressure; SVR: systemic vascular resistance; LV: left ventricle; RV: right ventricle; FAC: fractional area change.

Table 8.3: Independent effect of $MgSO_4$ and antenatal steroids on outcome parameters using logistic and linear regression.

	$MgSO_4$		Antenatal Steroids	
Outcome	**β coefficient**	**p**	**β coefficient**	**p**
Chronic Lung Disease	1.4	0.06	0.3	0.67
Ejection Fraction	5.5	0.04	-0.5	0.87
SVR	-82.7	0.06	-46.2	0.29
LV Longitudinal Strain	4.6	0.04	-0.7	0.75
Basal Rotation	-6.7	0.02	5.1	0.07
LV Twist	4.5	0.02	-1.9	0.26
LV untwist Rate	-57.8	0.06	-13.8	0.63
RV FAC	0.1	0.03	0.03	0.24

Logistic regression was used for chronic lung disease and linear regression for the remainder of the outcomes. β coefficients are unstandardized. SVR: systemic vascular resistance; LV: left ventricle; RV: right ventricle; FAC: fractional area change.

8.4 Discussion

In this matched cohort analysis, we demonstrated that exposure to antenatal $MgSO_4$ in preterm infants less than 29 weeks gestation is associated with a lower systolic BP and SVR on day 1 of age when compared to infants who did not receive $MgSO_4$. Consequently, those infants had better LV function illustrated by higher LV longitudinal strain, twist and untwist rate, and higher systemic blood flow illustrated by higher LV ejection fraction and RV fractional area change, although LVO was no different between the groups. Most of those associations remained significant when controlling for antenatal steroid administration which was understandably more prevalent in the $MgSO_4$ group. There was no difference in any of the parameters between $MgSO_4$ exposed infants and controls on Day 2 of age. A trend was seen between $MgSO_4$ and CLD when correcting for antenatal steroid use. This was an unexpected finding in the setting of $MgSO_4$ having anti-inflammatory properties but may be reflective of the fact that antenatal $MGSO_4$ was used in a sicker population who delivered at an earlier gestational age.

The effect of $MgSO_4$ on the haemodynamic status of preterm infants remains an area of active research. This is the first to assess the impact of antenatal $MgSO_4$ administration on novel echocardiography parameters in the preterm neonatal setting. LV longitudinal strain measured using speckle tracking techniques may be a more sensitive marker of myocardial performance than conventional measures (such as shortening fraction). Animal studies have demonstrated that strain measurements are highly dependent on afterload (Ferferieva et al., 2012). We recently demonstrated that LV longitudinal strain in preterm infants is negatively influenced by increasing afterload in the post PDA ligation model (El-Khuffash et al., 2012, El-Khuffash et al., 2014). Similarly in this

study, we illustrated that $MgSO_4$ administration results in lower blood pressure and SVR (and possibly lower LV wall stress) which leads to a higher LV longitudinal strain. The lower blood pressure in this cohort did not translate to an increased use of inotropes. The BP lowering effect of $MgSO_4$ in this setting was previously demonstrated by others (Rantonen et al., 2001).

The use of LV rotational mechanics in preterm infants is gaining interest and this is an example of their application in a clinical setting to further delineate the haemodynamic effects of a therapeutic interventionThese rotational parameters can add important information on myocardial performance (Buckberg et al., 2011). Increased afterload appears to decrease LV twist and untwist rate in experimental animal models (mongrel dogs) and human adults (Burns et al., 2010). This is supported by our data demonstrating higher basal rotation, twist and untwist values in infants in receipt of $MgSO_4$ and exposed to lower LV afterload.

The effect of $MgSO_4$ on systemic blood flow remains unclear. In a randomized controlled trial of antenatal $MgSO_4$ administration, Paradisis *et al,* could not demonstrate consistent effects of $MgSO_4$ on systemic blood flow measured using right ventricular output (RVO) and superior vena cava (SVC) flow (Paradisis et al., 2012). The apparent lack of effect of $MgSO_4$ on systemic blood flow may have stemmed from the poor reproducibility of those methods in determining blood flow (Lee et al., 2010, Ficial et al., 2013). In our cohort, we demonstrated higher EF (indicating higher left ventricular output and pulmonary circulation) and a higher RV FAC (indicating higher RV ejection fraction and systemic blood flow) in infants receiving $MgSO_4$. We have demonstrated these methods to be reliable and reproducible in preterm infants. This may indicate that a lower SVR and higher myocardial performance translated to an increase in systemic blood flow in those infants. However,

further studies are needed to confirm this association. The administration of $MgSO_4$ does not appear to have an influence on PDA diameter or closure rates in the first two days of age in this study population.

The clinical relevance of those findings is yet to be determined. In our cohort, with the exception of chronic lung disease (which may have been an effect of antenatal steroids), there was no significant difference in any of the other outcome parameters between the two groups. It is worthy of note however, that only one infant in the $MgSO_4$ group developed a severe IVH (and no deaths) compared with 5 cases of severe IVH in the controls (and three deaths). Previous studies have demonstrated that a stable cardiac output in the first few days of life is protective against severe IVH (Noori et al., 2014b).

This study has important limitations. Although, the two groups with the exception of antenatal steroids were well matched, there may have been unknown confounders that have resulted in the difference in the outcome parameters. Similarly, the sample size was relatively small and any differences between the groups may have been a result of a type 1 error.

8.5 Conclusion

The antenatal administration of $MgSO_4$ to preterm infants results in important haemodynamic effects during the first day of age characterised by a lower blood pressure and systemic vascular resistance and higher myocardial functional parameters. This may translate to an improved systemic blood flow state. The application of novel echocardiography parameters in preterm infants can help delineate differences in myocardial performance of preterm infants exposed to different therapeutic interventions.

Chapter 9: Conclusion

9.1 Introduction

The use of echocardiography in the haemodynamic assessment of the preterm infant has gained in popularity over recent years. Conventionally, shortening fraction, ejection fraction in addition to subjective assessment were used for functional assessment, but these methods showed poor reliability. With the advance of technology and echocardiographic machines, techniques such as strain, strain rate, Tissue Doppler, torsion, fractional area change amongst other techniques have been used to further assess the function of the heart. These techniques over the last number of years have grown in popularity, been shown to be feasible and reliable in clinical use and now are being used in mainstream clinical practice both in adults, paediatrics and neonatal populations.

9.2 Reliability

The echocardiographic methods used in this research is novel and has not been studied in great detail in the preterm population. We initially undertook to test the feasibility and reliability of these markers in 54 infants before applying them to certain disease states. We looked at the feasibility and reliability of both tissue Doppler derived strain and strain rate as well as the twist and torsion of the left ventricle and RV FAC. Based on this, we demonstrated that measurement of longitudinal strain and strain rate along with RV specific function and dimension parameters is feasible in this population with the majority of the images suitable for analysis. The least reliable measurement was found in the LV free wall, most likely due to artefact caused by the left lung obstructing a clear view of the LV free wall.

Similarly LV rotational mechanics looking at LV rotation, twist, untwist and torsion showed good reproducibility with results similar to that of older populations. Our methodology was based on previous published guidelines in older populations (Sanchez et al., 2014) with higher frame rates and is the first study showing the feasibility and reproducibility of the novel technique in the preterm population less than 29 weeks gestation.

9.3 Longitudinal changes

Assessment was carried out on the longitudinal changes of these echocardiographic parameters over the first week of life and at 36 weeks corrected gestational age. We chose the time points of day 1, day 2, day 5-7 and 36 weeks CGA as there is a vast change in the haemodynamics of the preterm heart in the first week as the pulmonary vascular resistance drops, the PDA plays a role and the child is exposed to different extra-utero adaptations. 36

weeks was chosen as this best reflects the time point at which chronic lung disease is defined (Kinsella et al., 2006).

Using Tissue Doppler imaging (TDI), TAPSE and RV FAC, there was a longitudinal increase in values up to 36 weeks post menstrual age. LV, Septal and RV strain values also significantly increased until 36 weeks post menstrual age. Strain rate values however (with the exception of LV SRe and SRa which demonstrated no change) only increased over the first week of age which may represent the early inherent increase in contractility in the first week of life while the increase in strain represents the continued effect of loading conditions on the myocardium.

We looked at the effect of Systemic Vascular Resistance (SVR), a surrogate of afterload, on the functional measurements on day 1 of life and found that SVR had a negative correlation with basal longitudinal strain showing the importance of loading conditions on this parameter.

We found that at 36 weeks post menstrual age there was a significant difference in RV measurements between infants with and without chronic lung disease. The increased afterload seen in infants with chronic lung disease due to high pulmonary pressures and pulmonary hypertension may be influential in why these patients showed a lower RV BLS and RV Sra, reflecting lower RV function when compared to infants without chronic lung disease.

9.4 Rotation

When the left ventricle contracts there is also a wringing motion of the heart which aids in expulsion of the blood during systole as well as relaxation and filling of the heart during diastole. Recently speckle tracking echocardiography has been used to analyse this twisting motion of the heart but this process has never been applied to the preterm heart. After confirming its feasibility and reliability we looked at this marker over the first week of life.

There was an overall net increase in twist and torsion (twist normalised to LV end-diastolic length) over the first week after birth mainly due to the change in basal rotation from a positive counter clockwise direction to a negative clockwise direction. This increase was greater than that seen in older populations which may be due to the vast changes in afterload conditions that the neonate experiences after birth. A net increase in LV untwisting rate was also noted over the three time points. This again may be reflective of the unique myocardial physiology and transitional haemodynamics that the preterm possesses.

9.5 Patent Ductus Arteriosus (PDA)

A patent ductus arteriosus is associated with morbidity and mortality in the preterm population and very little data is available on predicting which clinical factors and myocardial function analysis are associated with the long term outcomes of a PDA. We used a PDA predictive score (PDAsc) using some of the novel techniques described in our research in assessing myocardial function to evaluate the predictability of this tool in those infants who will develop chronic lung disease (CLD) or death.

Five variables were included in the final logistic regression model devised to predict the primary outcome, CLD/Death: Gestation (weeks), PDA diameter (mm), Vmax (m/s), LVO (ml/kg/min) and LV a` (cm/s). The four echocardiography parameters included in the model were obtained from the Day 2 scan. An ROC curve using the PDAsc to predict CLD/death showed an area under the curve of 0.92 with a score of 5 showing a high sensitivity and specificity. This score uses markers of LV diastolic function which may play an important role in infants with a PDA as they are subject to an increase in preload from the shunt through the duct and pulmonary venous return.

The ability to accurately predict PDA associated morbidities such as CLD/Death using a PDA severity score can pave the way for a more targeted treatment.

9.6 Magnesium Sulphate

The use of antenatal magnesium sulphate ($MgSO_4$) prior to premature birth for neuroprotection has been established. We measured the effect of $MgSO_4$ administration on LV functional parameters, systemic blood flow and loading conditions when compared with infants who did not receive $MgSO_4$. On Day 1, infants in the $MgSO_4$ group had a significantly lower SVR and a significantly higher EF, LV longitudinal strain, basal rotation, twist, LV untwist rate and RV FAC. These parameters remained significant when controlling for antenatal steroid use. A trend was noted between $MgSO_4$ and CLD in our population. These findings may indicate that a lower SVR and higher myocardial performance translated to an increase in systemic blood flow in those infants who receive $MgSO_4$ which may be part of its neuroprotective effect.

9.7 Fractional Area Change and Systemic blood flow

The assessment of systemic blood flow (SBF) in preterm infants is challenging with current methods providing difficulties and limitations. Right ventricular fractional area change (RV FAC) describes the change in the Right Ventricle cavity area from diastole to systole in the four chamber view and provides the dominant contribution to RV ejection fraction.

We assessed the correlation between RV FAC and left ventricular output (LVO) on Day 1 when shunting across the PDA is not thought to be significant due to the raised pulmonary vascular resistance and found there was a positive correlation between RV FAC and LVO and a negative correlation between RV FAC and echo measured systemic vascular resistance (SVR) suggesting that it may reflect systemic blood flow.

We also assessed the relationship between RV FAC on Day 1 and the evolution of P/IVH by Day 5 – 7 with the knowledge that low blood flow states in the first week is associated with the development of P/IVH. On Day 1, RV FAC was lower in infants who developed a P/IVH remaining significant when controlling for gestation.

Finally we assessed the relationship between a persistent PDA on Day 5 – 7 and RV FAC with the hypothesis that a PDA will be associated with a low RV FAC due to its negative impact on SBF. We found that a PDA with significant left to right shunting results in a lower RV FAC when compared to those without a PDA on Day 5 – 7 suggesting that RV FAC can identify reduced systemic blood flow associated with a PDA.

9.8 Future Direction

We have established normative data for novel echocardiographic methods in preterm infants which has not previously been published. We also have looked at how these markers apply to various disease states to see if their applicability can be used to help to prognosticate certain outcomes. We hope that we have established that these can be valuable tools for both the neonatologist and cardiologist. Further studies are needed to validate these findings amongst other centres.

Future work by our group will further assess the association between those novel echocardiography markers and important disease states in the neonatal population, Namely: Trisomy 21, monochorionic diamniotic twins, and infants with neonatal encephalopathy undergoing therapeutic hypothermia.

With the advancement in technology and use of echocardiography in clinical practice we feel that these novel markers will become less of a research tool and more of a clinical tool in preterm infants. This has already been established in adult and paediatricpediatric echocardiography where deformation imaging and RV functional parameters have been included in echocardiographic guidelines. The increased ability of the neonatologist to perform echocardiography will allow real time assessment of cardiac function and haemodynamic assessment allowing better informed clinical management.

9.9 Summary

From our research we have shown that myocardial function assessment using tissue Doppler derived strain, strain rate, torsion and fractional area change is both feasible and reliable. We applied these novel echocardiographic markers to assess certain disease states

and found that they may be a useful tool as part of a comprehensive functional myocardial assessment in the preterm population. With the advancement in echocardiography and the continued widespread use for the assessment of the preterm infant these tools may pave the way forward for its clinical use in aiding the diagnosis and management of pathological conditions of preterm infants to improve both morbidity and mortality.

References

A, E. L.-K., MCNAMARA, P. J., LAPOINTE, A. & JAIN, A. 2013. Adrenal function in preterm infants undergoing patent ductus arteriosus ligation. *Neonatology,* 104**,** 28-33.

ABRAHAM, T. P., DIMAANO, V. L. & LIANG, H. Y. 2007. Role of tissue Doppler and strain echocardiography in current clinical practice. *Circulation,* 116**,** 2597-2609.

AL-NAAMI, G. H. 2010. Torsion of young hearts: a speckle tracking study of normal infants, children, and adolescents. *Eur J Echocardiogr,* 11**,** 853-62.

ALAGARSAMY, S., CHHABRA, M., GUDAVALLI, M., NADROO, A. M., SUTIJA, V. G. & YUGRAKH, D. 2005. Comparison of clinical criteria with echocardiographic findings in diagnosing PDA in preterm infants. *J.Perinat.Med.,* 33**,** 161-164.

ALDERLIESTEN, T., LEMMERS, P. M., VAN HAASTERT, I. C., DE VRIES, L. S., BONESTROO, H. J., BAERTS, W. & VAN BEL, F. 2014. Hypotension in preterm neonates: low blood pressure alone does not affect neurodevelopmental outcome. *J Pediatr,* 164**,** 986-91.

AMOOZGAR, H., FARHANI, N. & KARIMI, M. 2011. Early echocardiographic findings in beta-thalassemia intermedia patients using standard and tissue Doppler methods. *Pediatr Cardiol,* 32**,** 154-9.

AMUNDSEN, B. H., HELLE-VALLE, T., EDVARDSEN, T., TORP, H., CROSBY, J., LYSEGGEN, E., STOYLEN, A., IHLEN, H., LIMA, J. A., SMISETH, O. A. & SLORDAHL, S. A. 2006. Noninvasive myocardial strain measurement by speckle tracking echocardiography: validation against sonomicrometry and tagged magnetic resonance imaging. *J Am Coll Cardiol,* 47**,** 789-93.

ANAVEKAR, N. S., GERSON, D., SKALI, H., KWONG, R. Y., YUCEL, E. K. & SOLOMON, S. D. 2007. Two-dimensional assessment of right ventricular function: an echocardiographic-MRI correlative study. *Echocardiography,* 24**,** 452-456.

ARNOLD, R., GOEBEL, B., ULMER, H. E., GORENFLO, M. & POERNER, T. C. 2007. An exercise tissue Doppler and strain rate imaging study of diastolic myocardial dysfunction after Kawasaki syndrome in childhood. *Cardiol.Young.,* 17**,** 478-486.

BANCALARI, E. & CLAURE, N. 2006. Definitions and diagnostic criteria for bronchopulmonary dysplasia. *Semin.Perinatol.,* 30**,** 164-170.

BEARD, N. A., LAVER, D. R. & DULHUNTY, A. F. 2004. Calsequestrin and the calcium release channel of skeletal and cardiac muscle. *Prog Biophys Mol Biol,* 85**,** 33-69.

BELL, M. J. 1978. Neonatal necrotizing enterocolitis. *N.Engl.J.Med.,* 298**,** 281-282.

BISWAS, M., SUDHAKAR, S., NANDA, N. C., BUCKBERG, G., PRADHAN, M., ROOMI, A. U., GORISSEN, W. & HOULE, H. 2013. Two- and three-dimensional speckle tracking echocardiography: clinical applications and future directions. *Echocardiography,* 30**,** 88-105.

BLAND, J. M. & ALTMAN, D. G. 1986. Statistical methods for assessing agreement between two methods of clinical measurement. *Lancet,* 1**,** 307-310.

BOISSIERE, J., MAUFRAIS, C., BAQUET, G., SCHUSTER, I., DAUZAT, M., DOUCENDE, G., OBERT, P., BERTHOIN, S. & NOTTIN, S. 2013. Specific left ventricular twist-untwist mechanics during exercise in children. *J Am Soc Echocardiogr,* 26**,** 1298-305.

BROADHOUSE, K. M., FINNEMORE, A. E., PRICE, A. N., DURIGHEL, G., COX, D. J., EDWARDS, A. D., HAJNAL, J. V. & GROVES, A. M. 2014. Cardiovascular magnetic resonance of cardiac function and myocardial mass in preterm infants: a preliminary study of the impact of patent ductus arteriosus. *J Cardiovasc Magn Reson,* 16**,** 54.

BROADHOUSE, K. M., PRICE, A. N., DURIGHEL, G., COX, D. J., FINNEMORE, A. E., EDWARDS, A. D., HAJNAL, J. V. & GROVES, A. M. 2013. Assessment of PDA shunt and systemic blood flow in newborns using cardiac MRI. *NMR Biomed,* 26**,** 1135-1141.

BROOKS, J. M., TRAVADI, J. N., PATOLE, S. K., DOHERTY, D. A. & SIMMER, K. 2005. Is surgical ligation of patent ductus arteriosus necessary? The Western Australian experience of conservative management. *Arch.Dis.Child Fetal Neonatal Ed,* 90**,** F235-F239.

BUCKBERG, G., HOFFMAN, J. I., NANDA, N. C., COGHLAN, C., SALEH, S. & ATHANASULEAS, C. 2011. Ventricular torsion and untwisting: further insights into mechanics and timing interdependence: a viewpoint. *Echocardiography.,* 28**,** 782-804.

BURNS, A. T., LA GERCHE, A., PRIOR, D. L. & MACISAAC, A. I. 2009. Left ventricular untwisting is an important determinant of early diastolic function. *JACC Cardiovasc Imaging,* 2**,** 709-16.

BURNS, A. T., LA GERCHE, A., PRIOR, D. L. & MACISAAC, A. I. 2010. Left ventricular torsion parameters are affected by acute changes in load. *Echocardiography,* 27**,** 407-14.

BURNS, A. T., MCDONALD, I. G., THOMAS, J. D., MACISAAC, A. & PRIOR, D. 2008. Doin' the twist: new tools for an old concept of myocardial function. *Heart,* 94**,** 978-83.

BUTT, W. W. & WHYTE, H. 1984. Blood pressure monitoring in neonates: comparison of umbilical and peripheral artery catheter measurements. *J.Pediatr.,* 105**,** 630-632.

CHANG, L. Y., MCCURNIN, D., YODER, B., SHAUL, P. W. & CLYMAN, R. I. 2008. Ductus arteriosus ligation and alveolar growth in preterm baboons with a patent ductus arteriosus. *Pediatr.Res.,* 63**,** 299-302.

CHARLES S. KLEINMAN, I. S. 2012. *Hemodynamics and Cardiology: Neonatology Questions and Controversies,* Philedelphia, Elsevier Health Sciences.

CHEUNG, Y. F., LI, S. N., CHAN, G. C., WONG, S. J. & HA, S. Y. 2011a. Left ventricular twisting and untwisting motion in childhood cancer survivors. *Echocardiography,* 28**,** 738-45.

CHEUNG, Y. F., WONG, S. J., LIANG, X. C. & CHEUNG, E. W. 2011b. Torsional mechanics of the left ventricle in patients after surgical repair of tetralogy of Fallot. *Circ J,* 75**,** 1735-41.

COOKE, L., STEER, P. & WOODGATE, P. 2003. Indomethacin for asymptomatic patent ductus arteriosus in preterm infants. *Cochrane.Database.Syst.Rev.***,** CD003745.

CUNHA, G. S., MEZZACAPPA-FILHO, F. & RIBEIRO, J. D. 2005. Risk factors for bronchopulmonary dysplasia in very low birth weight newborns treated with mechanical ventilation in the first week of life. *J.Trop.Pediatr.,* 51**,** 334-340.

CZERNIK, C., RHODE, S., HELFER, S., SCHMALISCH, G. & BUHRER, C. 2013. Left ventricular longitudinal strain and strain rate measured by 2-D speckle tracking echocardiography in neonates during whole-body hypothermia. *Ultrasound Med Biol,* 39**,** 1343-9.

CZERNIK, C., RHODE, S., HELFER, S., SCHMALISCH, G., BUHRER, C. & SCHMITZ, L. 2014. Development of left ventricular longitudinal speckle tracking echocardiography in very low birth weight infants with and without bronchopulmonary dysplasia during the neonatal period. *PLoS One,* 9**,** e106504.

DANHAIVE, O., MARGOSSIAN, R., GEVA, T. & KOUREMBANAS, S. 2005. Pulmonary hypertension and right ventricular dysfunction in growth-restricted, extremely low birth weight neonates. *J.Perinatol.,* 25**,** 495-499.

DE BOODE, W. P. 2010. Clinical monitoring of systemic hemodynamics in critically ill newborns. *Early Hum Dev,* 86**,** 137-41.

DE WAAL, K., LAKKUNDI, A. & OTHMAN, F. 2014. Speckle tracking echocardiography in very preterm infants: feasibility and reference values. *Early Hum Dev,* 90**,** 275-9.

DEMPSEY, E. M. & BARRINGTON, K. J. 2006. Diagnostic criteria and therapeutic interventions for the hypotensive very low birth weight infant. *J.Perinatol.,* 26**,** 677-681.

DEMPSEY, E. M. & BARRINGTON, K. J. 2009. Evaluation and treatment of hypotension in the preterm infant. *Clin.Perinatol.,* 36**,** 75-85.

DI MARIA, M. V., CARACCIOLO, G., PRASHKER, S., SENGUPTA, P. P. & BANERJEE, A. 2014. Left Ventricular Rotational Mechanics before and after Exercise in Children. *J Am Soc Echocardiogr,* 27**,** 1336-43.

DOKAINISH, H. 2015. Left ventricular diastolic function and dysfunction: Central role of echocardiography. *Global Cardiology Science and Practice,* 2015**,** 3.

DOYLE, L. W., CROWTHER, C. A., MIDDLETON, P., MARRET, S. & ROUSE, D. 2009. Magnesium sulphate for women at risk of preterm birth for neuroprotection of the fetus. *Cochrane Database Syst Rev***,** Cd004661.

EDVARDSEN, T., GERBER, B. L., GAROT, J., BLUEMKE, D. A., LIMA, J. A. & SMISETH, O. A. 2002. Quantitative assessment of intrinsic regional myocardial deformation by Doppler strain rate echocardiography in humans: validation against three-dimensional tagged magnetic resonance imaging. *Circulation,* 106**,** 50-6.

EGAN, M. J., HUSAIN, N., STINES, J. R., MOIDUDDIN, N., STEIN, M. A., NELIN, L. D. & CUA, C. L. 2012. Mid-term differences in right ventricular function in patients with congenital diaphragmatic hernia compared with controls. *World J Pediatr,* 8**,** 350-4.

EL-KHUFFASH, A., BARRY, D., WALSH, K., DAVIS, P. G. & MOLLOY, E. J. 2008. Biochemical markers may identify preterm infants with a patent ductus arteriosus at high risk of death or severe intraventricular haemorrhage. *Arch.Dis.Child Fetal Neonatal Ed,* 93**,** F407-F412.

EL-KHUFFASH, A., HERBOZO, C., JAIN, A., LAPOINTE, A. & MCNAMARA, P. J. 2013a. Targeted neonatal echocardiography (TnECHO) service in a Canadian neonatal intensive care unit: a 4-year experience. *J.Perinatol.*

EL-KHUFFASH, A., JAMES, A. T., CLEARY, A., SEMBEROVA, J., FRANKLIN, O. & MILETIN, J. 2015. Late medical therapy of patent ductus arteriosus using intravenous paracetamol. *Arch Dis Child Fetal Neonatal Ed,* 100**,** F253-6.

EL-KHUFFASH, A. F., JAIN, A., DRAGULESCU, A., MCNAMARA, P. J. & MERTENS, L. 2012. Acute changes in myocardial systolic function in preterm infants undergoing patent ductus arteriosus ligation: a tissue Doppler and myocardial deformation study. *J Am Soc Echocardiogr,* 25**,** 1058-67.

EL-KHUFFASH, A. F., JAIN, A. & MCNAMARA, P. J. 2013b. Ligation of the Patent Ductus Arteriosus in Preterm Infants: Understanding the Physiology. *J.Pediatr.*

EL-KHUFFASH, A. F., JAIN, A., WEISZ, D., MERTENS, L. & MCNAMARA, P. J. 2014. Assessment and treatment of post patent ductus arteriosus ligation syndrome. *J Pediatr,* 165**,** 46-52 e1.

EL-KHUFFASH, A. F. & MCNAMARA, P. J. 2011a. Neonatologist-performed functional echocardiography in the neonatal intensive care unit. *Semin Fetal Neonatal Med,* 16**,** 50-60.

EL-KHUFFASH, A. F. & MCNAMARA, P. J. 2011b. Neonatologist-performed functional echocardiography in the neonatal intensive care unit. *Semin. Fetal Neonatal Med,* 16**,** 50-60.

EL-KHUFFASH, A. F., SLEVIN, M., MCNAMARA, P. J. & MOLLOY, E. J. 2011. Troponin T, N-terminal pro natriuretic peptide and a patent ductus arteriosus scoring system predict death before discharge or neurodevelopmental outcome at 2 years in preterm infants. *Arch.Dis.Child Fetal Neonatal Ed,* 96**,** F133-F137.

ELKIRAN, O., KARAKURT, C., KOCAK, G. & KARADAG, A. 2013. Tissue Doppler, strain, and strain rate measurements assessed by two-dimensional speckle-tracking echocardiography in healthy newborns and infants. *Cardiol Young***,** 1-11.

ERIKSEN, B. H., NESTAAS, E., HOLE, T., LIESTOL, K., STOYLEN, A. & FUGELSETH, D. 2013a. Longitudinal assessment of atrioventricular annulus excursion by grey-scale m-mode and colour tissue Doppler imaging in premature infants. *Early Hum Dev*.

ERIKSEN, B. H., NESTAAS, E., HOLE, T., LIESTOL, K., STOYLEN, A. & FUGELSETH, D. 2013b. Myocardial function in premature infants: a longitudinal observational study. *BMJ Open,* 3.

ERSBOLL, M., VALEUR, N., ANDERSEN, M. J., MOGENSEN, U. M., VINTHER, M., SVENDSEN, J. H., MOLLER, J. E., KISSLO, J., VELAZQUEZ, E. J., HASSAGER, C., SOGAARD, P. & KOBER, L. 2013. Early echocardiographic deformation analysis for the prediction of sudden cardiac death and life-threatening arrhythmias after myocardial infarction. *JACC Cardiovasc Imaging,* 6**,** 851-60.

EVANS, J. R., LOU, S. B., VAN, M. K. & CHERYL, S. H. 2006. Cardiovascular support in preterm infants. *Clin.Ther.,* 28**,** 1366-1384.

EVANS, N. 2015. Preterm patent ductus arteriosus: A continuing conundrum for the neonatologist? *Semin Fetal Neonatal Med,* 20**,** 272-7.

EVANS, N. & KLUCKOW, M. 1996. Early determinants of right and left ventricular output in ventilated preterm infants. *Arch.Dis.Child Fetal Neonatal Ed,* 74**,** F88-F94.

FERFERIEVA, V., VAN DEN BERGH, A., CLAUS, P., JASAITYTE, R., VEULEMANS, P., PELLENS, M., LA GERCHE, A., RADEMAKERS, F., HERIJGERS, P. & D'HOOGE, J. 2012. The relative value of strain and strain rate for defining intrinsic myocardial function. *Am J Physiol Heart Circ Physiol,* 302**,** H188-95.

FICIAL, B., FINNEMORE, A. E., COX, D. J., BROADHOUSE, K. M., PRICE, A. N., DURIGHEL, G., EKITZIDOU, G., HAJNAL, J. V., EDWARDS, A. D. & GROVES, A. M. 2013. Validation study of the accuracy of echocardiographic measurements of systemic blood flow volume in newborn infants. *J Am Soc Echocardiogr,* 26**,** 1365-71.

FROMMELT, P. C., BALLWEG, J. A., WHITSTONE, B. N. & FROMMELT, M. A. 2002. Usefulness of Doppler tissue imaging analysis of tricuspid annular motion for determination of right ventricular function in normal infants and children. *Am.J.Cardiol.,* 89**,** 610-613.

GANAME, J., CLAUS, P., EYSKENS, B., UYTTEBROECK, A., RENARD, M., D'HOOGE, J., GEWILLIG, M., BIJNENS, B., SUTHERLAND, G. R. & MERTENS, L. 2007a. Acute cardiac functional and morphological changes after Anthracycline infusions in children. *Am.J.Cardiol.,* 99**,** 974-977.

GANAME, J., MERTENS, L., EIDEM, B. W., CLAUS, P., D'HOOGE, J., HAVEMANN, L. M., MCMAHON, C. J., ELAYDA, M. A., VAUGHN, W. K., TOWBIN, J. A., AYRES, N. A. & PIGNATELLI, R. H. 2007b. Regional myocardial deformation in children with hypertrophic cardiomyopathy: morphological and clinical correlations. *Eur.Heart J.,* 28**,** 2886-2894.

GEBAUER, C. M., KNUEPFER, M., ROBEL-TILLIG, E., PULZER, F. & VOGTMANN, C. 2006. Hemodynamics among neonates with hypoxic-ischemic encephalopathy during whole-body hypothermia and passive rewarming. *Pediatrics,* 117**,** 843-850.

GROVES, A. M., KUSCHEL, C. A., KNIGHT, D. B. & SKINNER, J. R. 2008. Echocardiographic assessment of blood flow volume in the superior vena cava and descending aorta in the newborn infant. *Arch.Dis.Child Fetal Neonatal Ed,* 93**,** F24-F28.

GUPTA, S., KHAN, F., SHAPIRO, M., WEEKS, S. G., LITWIN, S. E. & MICHAELS, A. D. 2008. The associations between tricuspid annular plane systolic excursion (TAPSE), ventricular dyssynchrony, and ventricular interaction in heart failure patients. *Eur J Echocardiogr,* 9**,** 766-71.

GUYATT, G. H., KIRSHNER, B. & JAESCHKE, R. 1992. Measuring health status: what are the necessary measurement properties? *J.Clin.Epidemiol.,* 45**,** 1341-1345.

HALL, R. W., KRONSBERG, S. S., BARTON, B. A., KAISER, J. R. & ANAND, K. J. 2005. Morphine, hypotension, and adverse outcomes among preterm neonates: who's to blame? Secondary results from the NEOPAIN trial. *Pediatrics,* 115**,** 1351-1359.

HALLIDAY, H. L., HIRATA, T. & BRADY, J. P. 1979. Echocardiographic findings of large patent ductus arteriosus in the very low birthweight infant before and after treatment with indomethacin. *Arch Dis Child,* 54**,** 744-9.

HAMRICK, S. E. & HANSMANN, G. 2010. Patent ductus arteriosus of the preterm infant. *Pediatrics,* 125**,** 1020-30.

HARRELL, F. E., JR., LEE, K. L. & MARK, D. B. 1996. Multivariable prognostic models: issues in developing models, evaluating assumptions and adequacy, and measuring and reducing errors. *Stat.Med.,* 15**,** 361-387.

HATLE L, A. B. 1982. *Doppler Ultrasound in Cardiology: Physical Principles and Clinical Applications,* Philadelphia, Lea & Febiger.

HELFER, S., SCHMITZ, L., BUHRER, C. & CZERNIK, C. 2013. Reproducibility and optimization of analysis parameters of tissue Doppler-derived strain and strain rate measurements for very low birth weight infants. *Echocardiography,* 30**,** 1219-26.

HELFER, S., SCHMITZ, L., BUHRER, C. & CZERNIK, C. 2014. Tissue Doppler-derived strain and strain rate during the first 28 days of life in very low birth weight infants. *Echocardiography,* 31**,** 765-72.

HERBOTS, L., MAES, F., D'HOOGE, J., CLAUS, P., DYMARKOWSKI, S., MERTENS, P., MORTELMANS, L., BIJNENS, B., BOGAERT, J., RADEMAKERS, F. E. & SUTHERLAND, G. R. 2004. Quantifying myocardial deformation throughout the cardiac cycle: a comparison of ultrasound strain rate, grey-scale M-mode and magnetic resonance imaging. *Ultrasound Med Biol,* 30**,** 591-8.

HIARADA, K., ORINO, T., YASUOKA, K., TAMURA, M. & TAKADA, G. 2000. Tissue doppler imaging of left and right ventricles in normal children. *Tohoku J.Exp.Med.,* 191**,** 21-29.

HOFFMAN, T. M., WERNOVSKY, G., ATZ, A. M., KULIK, T. J., NELSON, D. P., CHANG, A. C., BAILEY, J. M., AKBARY, A., KOCSIS, J. F., KACZMAREK, R., SPRAY, T. L. & WESSEL, D. L. 2003. Efficacy and safety of milrinone in preventing low cardiac output syndrome in infants and children after corrective surgery for congenital heart disease. *Circulation,* 107**,** 996-1002.

HOLZMAN, C., LIN, X., SENAGORE, P. & CHUNG, H. 2007. Histologic Chorioamnionitis and Preterm Delivery. *Am.J.Epidemiol.*

HUANG, S. J. & ORDE, S. 2013. From speckle tracking echocardiography to torsion: research tool today, clinical practice tomorrow. *Curr Opin Crit Care,* 19**,** 250-7.

HUNT, R. W., EVANS, N., RIEGER, I. & KLUCKOW, M. 2004. Low superior vena cava flow and neurodevelopment at 3 years in very preterm infants. *J.Pediatr.,* 145**,** 588-592.

IGARASHI, H., SHIRAISHI, H., ENDOH, H. & YANAGISAWA, M. 1994. Left ventricular contractile state in preterm infants: relation between wall stress and velocity of circumferential fiber shortening. *Am.Heart J.,* 127**,** 1336-1340.

IMAMOGLU, E. Y., GURSOY, T., KARATEKIN, G. & OVALI, F. 2014. Effects of antenatal magnesium sulfate treatment on cerebral blood flow velocities in preterm neonates. *J Perinatol,* 34**,** 192-6.

INDER, T. E. & VOLPE, J. J. 2000. Mechanisms of perinatal brain injury. *Semin.Neonatol.,* 5**,** 3-16.

INGELS, N. B., JR., HANSEN, D. E., DAUGHTERS, G. T., 2ND, STINSON, E. B., ALDERMAN, E. L. & MILLER, D. C. 1989. Relation between longitudinal, circumferential, and oblique shortening and torsional deformation in the left ventricle of the transplanted human heart. *Circ Res,* 64**,** 915-27.

ISALM, Z. S., DILEEP, D. & MUNIM, S. 2015. Prognostic value of obstetric Doppler ultrasound in fetuses with fetal growth restriction: an observational study in a tertiary care hospital. *J Matern Fetal Neonatal Med,* 28**,** 12-5.

JAIN, A., MOHAMED, A., EL-KHUFFASH, A., CONNELLY, K. A., DALLAIRE, F., JANKOV, R. P., MCNAMARA, P. J. & MERTENS, L. 2014. A comprehensive echocardiographic protocol for assessing neonatal right ventricular dimensions and function in the transitional period: normative data and z scores. *J Am Soc Echocardiogr,* 27**,** 1293-304.

JOSHI, S., EDWARDS, J. M., WILSON, D. G., WONG, J. K., KOTECHA, S. & FRASER, A. G. 2010. Reproducibility of myocardial velocity and deformation imaging in term and preterm infants. *Eur.J.Echocardiogr.,* 11**,** 44-50.

KAILIN, J. A., MIYAMOTO, S. D., YOUNOSZAI, A. K. & LANDECK, B. F. 2012. Longitudinal myocardial deformation is selectively decreased after pediatric cardiac transplantation: a comparison of children 1 year after transplantation with normal subjects using velocity vector imaging. *Pediatr Cardiol,* 33**,** 749-56.

KAKU, K., TAKEUCHI, M., TSANG, W., TAKIGIKU, K., YASUKOCHI, S., PATEL, A. R., MOR-AVI, V., LANG, R. M. & OTSUJI, Y. 2014. Age-related normal range of left ventricular strain and torsion using three-dimensional speckle-tracking echocardiography. *J Am Soc Echocardiogr,* 27**,** 55-64.

KHOO, N. S., SMALLHORN, J. F., KANEKO, S., MYERS, K., KUTTY, S. & THAM, E. B. 2011. Novel insights into RV adaptation and function in hypoplastic left heart syndrome between the first 2 stages of surgical palliation. *JACC Cardiovasc Imaging,* 4**,** 128-37.

KINSELLA, J. P., GREENOUGH, A. & ABMAN, S. H. 2006. Bronchopulmonary dysplasia. *Lancet,* 367**,** 1421-31.

KLUCKOW, M. 2005. Low systemic blood flow and pathophysiology of the preterm transitional circulation. *Early Hum.Dev.,* 81**,** 429-437.

KLUCKOW, M. & EVANS, N. 2000. Low superior vena cava flow and intraventricular haemorrhage in preterm infants. *Arch.Dis.Child Fetal Neonatal Ed,* 82**,** F188-F194.

KLUCKOW, M. & EVANS, N. 2001. Low systemic blood flow in the preterm infant. *Semin.Neonatol.,* 6**,** 75-84.

KOESTENBERGER, M., NAGEL, B., RAVEKES, W., URLESBERGER, B., RAITH, W., AVIAN, A., HALB, V., CVIRN, G., FRITSCH, P. & GAMILLSCHEG, A. 2011. Systolic right ventricular function in preterm and term neonates: reference values of the tricuspid annular plane systolic excursion (TAPSE) in 258 patients and calculation of Z-score values. *Neonatology,* 100**,** 85-92.

KOREN, G., JAMES, A. & PERLMAN, M. 1985. A simple method for the estimation of glomerular filtration rate by gentamicin pharmacokinetics during routine drug monitoring in the newborn. *Clin Pharmacol Ther,* 38**,** 680-5.

KORINEK, J., WANG, J., SENGUPTA, P. P., MIYAZAKI, C., KJAERGAARD, J., MCMAHON, E., ABRAHAM, T. P. & BELOHLAVEK, M. 2005. Two-dimensional strain--a Doppler-independent ultrasound method for quantitation of regional deformation: validation in vitro and in vivo. *J.Am.Soc.Echocardiogr.,* 18**,** 1247-1253.

KOWALIK, E., KOWALSKI, M. & HOFFMAN, P. 2011. Is right ventricular myocardial deformation affected by degree of interatrial shunt in adults? *Eur. J Echocardiogr,* 12**,** 400-405.

LANG, R. M., BIERIG, M., DEVEREUX, R. B., FLACHSKAMPF, F. A., FOSTER, E., PELLIKKA, P. A., PICARD, M. H., ROMAN, M. J., SEWARD, J., SHANEWISE, J. S., SOLOMON, S. D., SPENCER, K. T., SUTTON, M. S. & STEWART, W. J. 2005. Recommendations for chamber quantification: a report from the American Society of Echocardiography's Guidelines and Standards Committee and the Chamber Quantification Writing Group, developed in conjunction with the European Association of Echocardiography, a branch of the European Society of Cardiology. *J Am Soc Echocardiogr,* 18**,** 1440-63.

LASER, K. T., HAAS, N. A., FISCHER, M., HABASH, S., DEGENER, F., PRINZ, C., KORPERICH, H., SANDICA, E. & KECECIOGLU, D. 2013. Left ventricular rotation and right-left ventricular interaction in congenital heart disease: the acute effects of interventional closure of patent arterial ducts and atrial septal defects. *Cardiol Young***,** 1-14.

LASER, K. T., HAAS, N. A., JANSEN, N., SCHAFFLER, R., PALACIOS ARGUETA, J. R., ZITTERMANN, A., PETERS, B., KORPERICH, H. & KECECIOGLU, D. 2009. Is torsion a suitable echocardiographic parameter to detect acute changes in left ventricular afterload in children? *J Am Soc Echocardiogr,* 22**,** 1121-8.

LEE, A., LIESTOL, K., NESTAAS, E., BRUNVAND, L., LINDEMANN, R. & FUGELSETH, D. 2010. Superior vena cava flow: feasibility and reliability of the off-line analyses. *Arch Dis Child Fetal Neonatal Ed,* 95**,** F121-5.

LEE, L. A., KIMBALL, T. R., DANIELS, S. R., KHOURY, P. & MEYER, R. A. 1992. Left ventricular mechanics in the preterm infant and their effect on the measurement of cardiac performance. *J.Pediatr.,* 120**,** 114-119.

LEVY, P. T., DIONEDA, B., HOLLAND, M. R., SEKARSKI, T. J., LEE, C. K., MATHUR, A., CADE, W. T., CAHILL, A. G., HAMVAS, A. & SINGH, G. K. 2015. Right ventricular function in preterm and term neonates: reference values for right ventricle areas and fractional area of change. *J Am Soc Echocardiogr,* 28**,** 559-69.

LEVY, P. T., HOLLAND, M. R., SEKARSKI, T. J., HAMVAS, A. & SINGH, G. K. 2013. Feasibility and reproducibility of systolic right ventricular strain measurement by speckle-tracking echocardiography in premature infants. *J Am Soc Echocardiogr,* 26**,** 1201-13.

LEWANDOWSKI, A. J., BRADLOW, W. M., AUGUSTINE, D., DAVIS, E. F., FRANCIS, J., SINGHAL, A., LUCAS, A., NEUBAUER, S., MCCORMICK, K. & LEESON, P. 2013. Right ventricular systolic dysfunction in young adults born preterm. *Circulation,* 128**,** 713-720.

LOBOS, A. T., LEE, S. & MENON, K. 2012. Capillary refill time and cardiac output in children undergoing cardiac catheterization. *Pediatr Crit Care Med,* 13**,** 136-40.

LOPEZ, L., COLAN, S. D., FROMMELT, P. C., ENSING, G. J., KENDALL, K., YOUNOSZAI, A. K., LAI, W. W. & GEVA, T. 2010. Recommendations for quantification methods during the performance of a pediatric echocardiogram: a report from the Pediatric Measurements Writing Group of the American Society of Echocardiography Pediatric and Congenital Heart Disease Council. *J Am Soc Echocardiogr,* 23**,** 465-95; quiz 576-7.

MACGOWAN, G. A., BURKHOFF, D., ROGERS, W. J., SALVADOR, D., AZHARI, H., HEES, P. S., ZWEIER, J. L., HALPERIN, H. R., SIU, C. O., LIMA, J. A., WEISS, J. L. & SHAPIRO, E. P. 1996. Effects of afterload on regional left ventricular torsion. *Cardiovasc Res,* 31**,** 917-25.

MARCUS, K. A., BARENDS, M., MORAVA-KOZICZ, E., FEUTH, T., DE KORTE, C. L. & KAPUSTA, L. 2011a. Early detection of myocardial dysfunction in children with mitochondrial disease: An ultrasound and two-dimensional strain echocardiography study. *Mitochondrion,* 11**,** 405-12.

MARCUS, K. A., MAVINKURVE-GROOTHUIS, A. M., BARENDS, M., VAN, D. A., FEUTH, T., DE, K. C. & KAPUSTA, L. 2011b. Reference values for myocardial two-dimensional strain echocardiography in a healthy pediatric and young adult cohort. *J.Am.Soc.Echocardiogr.,* 24**,** 625-636.

MARTENS, S. E., RIJKEN, M., STOELHORST, G. M., VAN ZWIETEN, P. H., ZWINDERMAN, A. H., WIT, J. M., HADDERS-ALGRA, M. & VEEN, S. 2003. Is hypotension a major risk factor for neurological morbidity at term age in very preterm infants? *Early Hum.Dev.,* 75**,** 79-89.

MCNAMARA, P. J. & SEHGAL, A. 2007. Towards rational management of the patent ductus arteriosus: the need for disease staging. *Arch Dis Child Fetal Neonatal Ed,* 92**,** F424-7.

MERTENS, L., GANAME, J., CLAUS, P., GOEMANS, N., THIJS, D., EYSKENS, B., VAN, L. D., BIJNENS, B., D'HOOGE, J., SUTHERLAND, G. R. & BUYSE, G. 2008. Early regional myocardial dysfunction in young patients with Duchenne muscular dystrophy. *J.Am.Soc.Echocardiogr.,* 21**,** 1049-1054.

MERTENS, L., SERI, I., MAREK, J., ARLETTAZ, R., BARKER, P., MCNAMARA, P., MOON-GRADY, A. J., COON, P. D., NOORI, S., SIMPSON, J. & LAI, W. W. 2011a. Targeted neonatal echocardiography in the neonatal intensive care unit: practice guidelines and recommendations for training. *Eur J Echocardiogr,* 12**,** 715-36.

MERTENS, L., SERI, I., MAREK, J., ARLETTAZ, R., BARKER, P., MCNAMARA, P., MOON-GRADY, A. J., COON, P. D., NOORI, S., SIMPSON, J. & LAI, W. W. 2011b. Targeted Neonatal Echocardiography in the Neonatal Intensive Care Unit: Practice Guidelines and Recommendations for Training Writing group of the American Society of Echocardiography (ASE) in collaboration with the European Association of Echocardiography (EAE) and the Association for European Pediatric Cardiologists (AEPC). *J.Am.Soc.Echocardiogr.,* 24**,** 1057-1078.

MEYER, S., GORTNER, L., BROWN, K. & ABDUL-KHALIQ, H. 2011. The role of milrinone in children with cardiovascular compromise: review of the literature. *Wien Med Wochenschr,* 161**,** 184-91.

MOENKEMEYER, F. & PATEL, N. 2014. Right ventricular diastolic function measured by tissue Doppler imaging predicts early outcome in congenital diaphragmatic hernia. *Pediatr. Crit Care Med,* 15**,** 49-55.

MOHAMMED, A., MERTENS, L. & FRIEDBERG, M. K. 2009. Relations between systolic and diastolic function in children with dilated and hypertrophic cardiomyopathy as assessed by tissue Doppler imaging. *J.Am.Soc.Echocardiogr.,* 22**,** 145-151.

MOON, M. R., INGELS, N. B., JR., DAUGHTERS, G. T., 2ND, STINSON, E. B., HANSEN, D. E. & MILLER, D. C. 1994. Alterations in left ventricular twist mechanics with inotropic stimulation and volume loading in human subjects. *Circulation,* 89**,** 142-50.

MOR-AVI, V., LANG, R. M., BADANO, L. P., BELOHLAVEK, M., CARDIM, N. M., DERUMEAUX, G., GALDERISI, M., MARWICK, T., NAGUEH, S. F., SENGUPTA, P. P., SICARI, R., SMISETH, O. A., SMULEVITZ, B., TAKEUCHI, M., THOMAS, J. D., VANNAN, M., VOIGT, J. U. & ZAMORANO, J. L. 2011. Current and evolving echocardiographic techniques for the quantitative evaluation of

cardiac mechanics: ASE/EAE consensus statement on methodology and indications endorsed by the Japanese Society of Echocardiography. *J Am Soc Echocardiogr,* 24**,** 277-313.
MORI, K., HAYABUCHI, Y., INOUE, M., SUZUKI, M., SAKATA, M., NAKAGAWA, R., KAGAMI, S., TATARA, K., HIRAYAMA, Y. & ABE, Y. 2007. Myocardial strain imaging for early detection of cardiac involvement in patients with Duchenne's progressive muscular dystrophy. *Echocardiography.,* 24**,** 598-608.
MOSS, T. J. 2006. Respiratory consequences of preterm birth. *Clin.Exp.Pharmacol.Physiol,* 33**,** 280-284.
MOTOJI, Y., TANAKA, H., FUKUDA, Y., RYO, K., EMOTO, N., KAWAI, H. & HIRATA, K. 2013. Efficacy of right ventricular free-wall longitudinal speckle-tracking strain for predicting long-term outcome in patients with pulmonary hypertension. *Circ J,* 77**,** 756-63.
MURASE, M. & ISHIDA, A. 2006. Echocardiographic assessment of early circulatory status in preterm infants with suspected intrauterine infection. *Arch Dis Child Fetal Neonatal Ed,* 91**,** F105-10.
MURASE, M., MORISAWA, T. & ISHIDA, A. 2013. Serial assessment of left-ventricular function using tissue Doppler imaging in premature infants within 7 days of life. *Pediatr Cardiol,* 34**,** 1491-8.
MURASE, M., MORISAWA, T. & ISHIDA, A. 2015a. Serial assessment of right ventricular function using tissue Doppler imaging in preterm infants within 7 days of life. *Early Hum Dev,* 91**,** 125-30.
MURASE, M., MORISAWA, T. & ISHIDA, A. 2015b. Serial assessment of right ventricular function using tissue Doppler imaging in preterm infants within 7 days of life. *Early Hum. Dev,* 91**,** 125-130.
NAGUEH, S. F., MIDDLETON, K. J., KOPELEN, H. A., ZOGHBI, W. A. & QUINONES, M. A. 1997. Doppler tissue imaging: a noninvasive technique for evaluation of left ventricular relaxation and estimation of filling pressures. *J.Am.Coll.Cardiol.,* 30**,** 1527-1533.
NESTAAS, E., STØYLEN, A., BRUNVAND, L. & FUGELSETH, D. 2009. Tissue Doppler derived longitudinal strain and strain rate during the first 3 days of life in healthy term neonates. *Pediatr Res,* 65**,** 357-62.
NIKITIN, N. P., WITTE, K. K., THACKRAY, S. D., DE, S. R., CLARK, A. L. & CLELAND, J. G. 2003. Longitudinal ventricular function: normal values of atrioventricular annular and myocardial velocities measured with quantitative two-dimensional color Doppler tissue imaging. *J.Am.Soc.Echocardiogr.,* 16**,** 906-921.
NOORI, S., FRIEDLICH, P., SERI, I. & WONG, P. 2007a. Changes in myocardial function and hemodynamics after ligation of the ductus arteriosus in preterm infants. *J.Pediatr.,* 150**,** 597-602.
NOORI, S., FRIEDLICH, P., SERI, I. & WONG, P. 2007b. Changes in myocardial function and hemodynamics after ligation of the ductus arteriosus in preterm infants. *J. Pediatr,* 150**,** 597-602.
NOORI, S., MCCOY, M., ANDERSON, M. P., RAMJI, F. & SERI, I. 2014a. Changes in cardiac function and cerebral blood flow in relation to peri/intraventricular hemorrhage in extremely preterm infants. *J Pediatr,* 164**,** 264-270.
NOORI, S., MCCOY, M., ANDERSON, M. P., RAMJI, F. & SERI, I. 2014b. Changes in cardiac function and cerebral blood flow in relation to peri/intraventricular hemorrhage in extremely preterm infants. *J Pediatr,* 164**,** 264-70.e1-3.
NOORI, S. & SERI, I. 2005. Pathophysiology of newborn hypotension outside the transitional period. *Early Hum.Dev.,* 81**,** 399-404.
NOTOMI, Y., LYSYANSKY, P., SETSER, R. M., SHIOTA, T., POPOVIC, Z. B., MARTIN-MIKLOVIC, M. G., WEAVER, J. A., ORYSZAK, S. J., GREENBERG, N. L., WHITE, R. D. & THOMAS, J. D. 2005. Measurement of ventricular torsion by two-dimensional ultrasound speckle tracking imaging. *J Am Coll Cardiol,* 45**,** 2034-41.
NOTOMI, Y., MARTIN-MIKLOVIC, M. G., ORYSZAK, S. J., SHIOTA, T., DESERRANNO, D., POPOVIC, Z. B., GARCIA, M. J., GREENBERG, N. L. & THOMAS, J. D. 2006a. Enhanced ventricular untwisting

during exercise: a mechanistic manifestation of elastic recoil described by Doppler tissue imaging. *Circulation,* 113**,** 2524-33.
NOTOMI, Y., SRINATH, G., SHIOTA, T., MARTIN-MIKLOVIC, M. G., BEACHLER, L., HOWELL, K., ORYSZAK, S. J., DESERRANNO, D. G., FREED, A. D., GREENBERG, N. L., YOUNOSZAI, A. & THOMAS, J. D. 2006b. Maturational and adaptive modulation of left ventricular torsional biomechanics: Doppler tissue imaging observation from infancy to adulthood. *Circulation,* 113**,** 2534-41.
NUNTNARUMIT, P., YANG, W. & BADA-ELLZEY, H. S. 1999. Blood pressure measurements in the newborn. *Clin Perinatol,* 26**,** 981-96, x.
OSBORN, D., EVANS, N. & KLUCKOW, M. 2002. Randomized trial of dobutamine versus dopamine in preterm infants with low systemic blood flow. *J.Pediatr.,* 140**,** 183-191.
OSBORN, D. A., EVANS, N. & KLUCKOW, M. 2004. Clinical detection of low upper body blood flow in very premature infants using blood pressure, capillary refill time, and central-peripheral temperature difference. *Arch.Dis.Child Fetal Neonatal Ed,* 89**,** F168-F173.
PAPILE, L. A., BURSTEIN, J., BURSTEIN, R. & KOFFLER, H. 1978. Incidence and evolution of subependymal and intraventricular hemorrhage: a study of infants with birth weights less than 1,500 gm. *J.Pediatr.,* 92**,** 529-534.
PARADISIS, M., OSBORN, D. A., EVANS, N. & KLUCKOW, M. 2012. Randomized controlled trial of magnesium sulfate in women at risk of preterm delivery-neonatal cardiovascular effects. *J Perinatol,* 32**,** 665-70.
PATEL, N. 2012. Use of milrinone to treat cardiac dysfunction in infants with pulmonary hypertension secondary to congenital diaphragmatic hernia: a review of six patients. *Neonatology,* 102**,** 130-6.
PAULIKS, L. 2013. Tissue doppler myocardial velocity imaging in infants and children--a window into developmental changes of myocardial mechanics. *Echocardiography,* 30**,** 439-46.
PICKARD, A., KARLEN, W. & ANSERMINO, J. M. 2011. Capillary refill time: is it still a useful clinical sign? *Anesth Analg,* 113**,** 120-3.
POON, C. Y., EDWARDS, J. M., JOSHI, S., KOTECHA, S. & FRASER, A. G. 2011. Optimization of myocardial deformation imaging in term and preterm infants. *Eur.J.Echocardiogr.,* 12**,** 247-254.
RAJAGOPAL, S., FORSHA, D. E., RISUM, N., HORNIK, C. P., POMS, A. D., FORTIN, T. A., TAPSON, V. F., VELAZQUEZ, E. J., KISSLO, J. & SAMAD, Z. 2014. Comprehensive assessment of right ventricular function in patients with pulmonary hypertension with global longitudinal peak systolic strain derived from multiple right ventricular views. *J Am Soc Echocardiogr,* 27**,** 657-665.
RAMANI, G. V., BAZAZ, R., EDELMAN, K. & LOPEZ-CANDALES, A. 2009. Pulmonary hypertension affects left ventricular basal twist: a novel use for speckle-tracking imaging. *Echocardiography,* 26**,** 44-51.
RAMOS, F. G., ROSENFELD, C. R., ROY, L., KOCH, J. & RAMACIOTTI, C. 2010. Echocardiographic predictors of symptomatic patent ductus arteriosus in extremely-low-birth-weight preterm neonates. *J Perinatol,* 30**,** 535-9.
RANTONEN, T., KAAPA, P., GRONLUND, J., EKBLAD, U., HELENIUS, H., KERO, P. & VALIMAKI, I. 2001. Maternal magnesium sulfate treatment is associated with reduced brain-blood flow perfusion in preterm infants. *Crit Care Med,* 29**,** 1460-5.
REDMAN, C. W. & JEFFERIES, M. 1988. Revised definition of pre-eclampsia. *Lancet,* 1**,** 809-12.
ROWLAND, D. G. & GUTGESELL, H. P. 1995. Noninvasive assessment of myocardial contractility, preload, and afterload in healthy newborn infants. *Am.J.Cardiol.,* 75**,** 818-821.
RUSSEL, I. K., GOTTE, M. J., BRONZWAER, J. G., KNAAPEN, P., PAULUS, W. J. & VAN ROSSUM, A. C. 2009. Left ventricular torsion: an expanding role in the analysis of myocardial dysfunction. *JACC Cardiovasc Imaging,* 2**,** 648-55.

RYAN, J. J., HUSTON, J., KUTTY, S., HATTON, N. D., BOWMAN, L., TIAN, L., HERR, J. E., JOHRI, A. M. & ARCHER, S. L. 2015. Right ventricular adaptation and failure in pulmonary arterial hypertension. *Can J Cardiol,* 31**,** 391-406.

SALEEMI, M. S., BRUTON, K., EL-KHUFFASH, A., KIRKHAM, C., FRANKLIN, O. & CORCORAN, J. D. 2013. Myocardial assessment using tissue doppler imaging in preterm very low-birth weight infants before and after red blood cell transfusion. *J Perinatol*.

SANCHEZ, A. A., LEVY, P. T., SEKARSKI, T. J., HAMVAS, A., HOLLAND, M. R. & SINGH, G. K. 2014. Effects of Frame Rate on Two-Dimensional Speckle Tracking-Derived Measurements of Myocardial Deformation in Premature Infants. *Echocardiography*.

SCHENA, F., FRANCESCATO, G., CAPPELLERI, A., PICCIOLLI, I., MAYER, A., MOSCA, F. & FUMAGALLI, M. 2015. Association between Hemodynamically Significant Patent Ductus Arteriosus and Bronchopulmonary Dysplasia. *J Pediatr*.

SCHMIDT, B., ROBERTS, R. S., FANAROFF, A., DAVIS, P., KIRPALANI, H. M., NWAESEI, C. & VINCER, M. 2006. Indomethacin prophylaxis, patent ductus arteriosus, and the risk of bronchopulmonary dysplasia: further analyses from the Trial of Indomethacin Prophylaxis in Preterms (TIPP). *J.Pediatr.,* 148**,** 730-734.

SEHGAL, A., FRANCIS, J. V. & LEWIS, A. I. 2011. Use of milrinone in the management of haemodynamic instability following duct ligation. *Eur J Pediatr,* 170**,** 115-9.

SEHGAL, A. & MCNAMARA, P. J. 2008. Does point-of-care functional echocardiography enhance cardiovascular care in the NICU? *J.Perinatol.,* 28**,** 729-735.

SEHGAL, A., OSBORN, D. & MCNAMARA, P. J. 2012a. Cardiovascular support in preterm infants: a survey of practices in Australia and New Zealand. *J Paediatr Child Health,* 48**,** 317-23.

SEHGAL, A., PAUL, E. & MENAHEM, S. 2012b. Functional echocardiography in staging for ductal disease severity. *European Journal of Pediatrics,* 172**,** 179-184.

SEHGAL, A., WONG, F. & MENAHEM, S. 2013. Speckle tracking derived strain in infants with severe perinatal asphyxia: a comparative case control study. *Cardiovasc Ultrasound,* 11**,** 34.

SELLMER, A., BJERRE, J. V., SCHMIDT, M. R., MCNAMARA, P. J., HJORTDAL, V. E., HOST, B., BECH, B. H. & HENRIKSEN, T. B. 2013. Morbidity and mortality in preterm neonates with patent ductus arteriosus on day 3. *Arch Dis Child Fetal Neonatal Ed,* 98**,** F505-10.

SERI, I. & EVANS, J. 2001. Controversies in the diagnosis and management of hypotension in the newborn infant. *Curr.Opin.Pediatr.,* 13**,** 116-123.

SERI, I. & NOORI, S. 2005. Diagnosis and treatment of neonatal hypotension outside the transitional period. *Early Hum.Dev.,* 81**,** 405-411.

SHOKRY, M., ELSEDFY, G. O., BASSIOUNY, M. M., ANMIN, M. & ABOZID, H. 2010. Effects of antenatal magnesium sulfate therapy on cerebral and systemic hemodynamics in preterm newborns. *Acta Obstet Gynecol Scand,* 89**,** 801-6.

SHORTLAND, D. B., GIBSON, N. A., LEVENE, M. I., ARCHER, L. N., EVANS, D. H. & SHAW, D. E. 1990. Patent ductus arteriosus and cerebral circulation in preterm infants. *Dev.Med.Child Neurol.,* 32**,** 386-393.

SMITH, A., MAGUIRE, M., LIVINGSTONE, V. & DEMPSEY, E. M. 2015. Peak systolic to end diastolic flow velocity ratio is associated with ductal patency in infants below 32 weeks of gestation. *Arch. Dis. Child Fetal Neonatal Ed,* 100**,** F132-F136.

SUTHERLAND, G. R., DI, S. G., CLAUS, P., D'HOOGE, J. & BIJNENS, B. 2004. Strain and strain rate imaging: a new clinical approach to quantifying regional myocardial function. *J.Am.Soc.Echocardiogr.,* 17**,** 788-802.

TAKAHASHI, K., AL NAAMI, G., THOMPSON, R., INAGE, A., MACKIE, A. S. & SMALLHORN, J. F. 2010. Normal rotational, torsion and untwisting data in children, adolescents and young adults. *J Am Soc Echocardiogr,* 23**,** 286-93.

TEE, M., NOBLE, J. A. & BLUEMKE, D. A. 2013. Imaging techniques for cardiac strain and deformation: comparison of echocardiography, cardiac magnetic resonance and cardiac computed tomography. *Expert Rev Cardiovasc Ther,* 11**,** 221-31.

TESKE, A. J., DE BOECK, B. W., MELMAN, P. G., SIESWERDA, G. T., DOEVENDANS, P. A. & CRAMER, M. J. 2007. Echocardiographic quantification of myocardial function using tissue deformation imaging, a guide to image acquisition and analysis using tissue Doppler and speckle tracking. *Cardiovasc.Ultrasound,* 5**,** 27.

VAN DALEN, B. M., BOSCH, J. G., KAUER, F., SOLIMAN, O. I., VLETTER, W. B., TEN CATE, F. J. & GELEIJNSE, M. L. 2009. Assessment of mitral annular velocities by speckle tracking echocardiography versus tissue Doppler imaging: validation, feasibility, and reproducibility. *J Am Soc Echocardiogr,* 22**,** 1302-8.

VAN, O. B. 2007. Patent ductus arteriosus: how aggressive should we be? *Neonatology.,* 91**,** 318.

VILLAFANE, J., FEINSTEIN, J. A., JENKINS, K. J., VINCENT, R. N., WALSH, E. P., DUBIN, A. M., GEVA, T., TOWBIN, J. A., COHEN, M. S., FRASER, C., DEARANI, J., ROSENTHAL, D., KAUFMAN, B. & GRAHAM, T. P., JR. 2013. Hot topics in tetralogy of Fallot. *J Am Coll Cardiol,* 62**,** 2155-66.

VOELKEL, N. F., QUAIFE, R. A., LEINWAND, L. A., BARST, R. J., MCGOON, M. D., MELDRUM, D. R., DUPUIS, J., LONG, C. S., RUBIN, L. J., SMART, F. W., SUZUKI, Y. J., GLADWIN, M., DENHOLM, E. M., GAIL, D. B., NATIONAL HEART, L., BLOOD INSTITUTE WORKING GROUP ON, C. & MOLECULAR MECHANISMS OF RIGHT HEART, F. 2006. Right ventricular function and failure: report of a National Heart, Lung, and Blood Institute working group on cellular and molecular mechanisms of right heart failure. *Circulation,* 114**,** 1883-91.

VOIGT, J. U., PEDRIZZETTI, G., LYSYANSKY, P., MARWICK, T. H., HOULE, H., BAUMANN, R., PEDRI, S., ITO, Y., ABE, Y., METZ, S., SONG, J. H., HAMILTON, J., SENGUPTA, P. P., KOLIAS, T. J., D'HOOGE, J., AURIGEMMA, G. P., THOMAS, J. D. & BADANO, L. P. 2015. Definitions for a common standard for 2D speckle tracking echocardiography: consensus document of the EACVI/ASE/Industry Task Force to standardize deformation imaging. *J Am Soc Echocardiogr,* 28**,** 183-93.

WEIDEMANN, F., EYSKENS, B., MERTENS, L., DOMMKE, C., KOWALSKI, M., SIMMONS, L., CLAUS, P., BIJNENS, B., GEWILLIG, M., HATLE, L. & SUTHERLAND, G. R. 2002. Quantification of regional right and left ventricular function by ultrasonic strain rate and strain indexes after surgical repair of tetralogy of Fallot. *Am.J.Cardiol.,* 90**,** 133-138.

WEISZ, D. E., MORE, K., MCNAMARA, P. J. & SHAH, P. S. 2014. PDA ligation and health outcomes: a meta-analysis. *Pediatrics,* 133**,** e1024-46.

YATES, A. R., WELTY, S. E., GEST, A. L. & CUA, C. L. 2008. Myocardial tissue Doppler changes in patients with bronchopulmonary dysplasia. *J Pediatr,* 152**,** 766-70, 770 e1.

YOUN, Y., LEE, J.-Y., LEE, J. H., KIM, S.-Y., SUNG, I. K. & LEE, J. Y. 2013. Impact of patient selection on outcomes of PDA in very low birth weight infants. *Early Human Development,* 89**,** 175-179.

ZHANG, Y., ZHOU, Q. C., PU, D. R., ZOU, L. & TAN, Y. 2010. Differences in left ventricular twist related to age: speckle tracking echocardiographic data for healthy volunteers from neonate to age 70 years. *Echocardiography,* 27**,** 1205-10.

ZONNENBERG, I. & DE WAAL, K. 2012. The definition of a haemodynamic significant duct in randomized controlled trials: a systematic literature review. *Acta Paediatr,* 101**,** 247-51.